

10-1-2019 3:15 PM

## A Comprehensive Study of Sequential Simulated Moving Bed: Purification of Xylo-oligosaccharides and fructose-glucose

Yan Li, *The University of Western Ontario*

Supervisor: Ray, Ajay K., *The University of Western Ontario*

A thesis submitted in partial fulfillment of the requirements for the Doctor of Philosophy degree  
in Chemical and Biochemical Engineering

© Yan Li 2019

Follow this and additional works at: <https://ir.lib.uwo.ca/etd>

 Part of the [Other Chemical Engineering Commons](#)

---

### Recommended Citation

Li, Yan, "A Comprehensive Study of Sequential Simulated Moving Bed: Purification of Xylo-oligosaccharides and fructose-glucose" (2019). *Electronic Thesis and Dissertation Repository*. 6547.  
<https://ir.lib.uwo.ca/etd/6547>

This Dissertation/Thesis is brought to you for free and open access by Scholarship@Western. It has been accepted for inclusion in Electronic Thesis and Dissertation Repository by an authorized administrator of Scholarship@Western. For more information, please contact [wlsadmin@uwo.ca](mailto:wlsadmin@uwo.ca).

## Abstract

Chromatographic separation is a promising alternative for separation and purification of sugars in industry. Simulated moving bed (SMB) technique has been proven as an efficient chromatographic separation method due to its enhanced productivity and purity, reduced solvent consumption, convenient operating control, and improved separation performance for some systems with low resolution and selectivity. The sequential simulated moving bed (SSMB) is a modification of the conventional SMB process, which currently has some applications for sugar separation due to its low solvent consumption. This work mainly investigates the design strategy of the innovative SSMB process and explore its advantages and disadvantages over the SMB process based on the xylo-oligosaccharides (XOSs) and fructose-glucose systems.

SSMB separation of XOSs, a functional food additive in the form of a oligomeric saccharide, was firstly conducted. DOWEX MONOSPHERE™ 99/310 resin ionized with  $K^+$ , which has better selectivity compared with  $Ca^{2+}$  and  $Na^+$  was used as the stationary phase. Breakthrough experiments showed that XOSs and the two major industrial impurities, xylose and arabinose, all exhibit linear isotherms. Transport-dispersive (TD) model parameters were determined by pulse experiments carried out at various flowrates. Finally, both the averaged and individual parameters of XOSs and XOS2-XOS7 were obtained. Lab-scale SSMB experiments and the corresponding simulations were carried out to validate the acquired TD model parameters and adsorption isotherms. After that, in order to investigate the optimal operating conditions of this process, the multi-objective optimizations were carried out for three cases with various objectives and constraints. It was found that, for a given SSMB unit, there exist a pareto curve for simultaneous maximization of purity and unit throughput. The flowrate ratios ( $m$  values), however, exhibit some trends that are different from those of conventional SMB and cannot be explained by the direct use of Triangle Theory with averaged  $m$  values.

According to the literature, the fructose-glucose system is representative and have linear isotherms over a wide concentration range, which makes it an excellent example system to conduct some basic analysis and performance prediction. Therefore, the multi-objective optimization of SMB and SSMB processes was conducted and compared based on the

fructose-glucose system. The results show that the solvent consumption of SSMB is always less than that of SMB unit.

### **Keywords:**

Simulated moving bed; sequential simulated moving bed; xylo-oligosaccharides; transport-dispersive model; equilibrium-dispersive model; adsorption isotherms; multi-objective optimization; Non-dominated sorting genetic algorithm; pareto curve; Fortran.

## Summary for Lay Audience

Simulated moving bed (SMB) chromatography, a well-developed continuous liquid chromatographic method, is widely used in petro-chemical industry, food industry, and pharmaceutical and biotechnological field. A typical 4-zone SMB unit consists of several packed chromatographic columns which are series-connected and form a closed loop. The mechanism of this separation process is the counter-current movement between the liquid and solid phases, which is achieved by periodically and simultaneously switching the inlet and outlet ports in the direction of the fluid flow. The sequential simulated moving bed (SSMB) is a modification of SMB process, which divides one switch in SMB into three steps with different flow patterns. Actually, SSMB technique is a preferential choice for some large-scale separation processes in industry due to its low solvent consumption. However, there is on one reported this SSMB process and explored its application in industry. Therefore, a comprehensive study of this SSMB technique was mainly conducted in this thesis.

Xylo-oligosaccharides (XOS), produced by hydrolysis of xylan-rich hemicelluloses, is a kind of oligosaccharides with prebiotic effect. Due to the nature of the enzyme hydrolysis reaction of XOS synthesis, the industrial produced XOS syrup generally contains 70% XOS, 22% unreacted xylose, and 8% by-product arabinose. To our knowledge, there is only one study on XOS purification by using SMB which does not contain the detailed modeling and optimization works. In this work, XOS was purified by using an economic SSMB process, and the optimal operating conditions were selected by using multi-objective optimization corresponding to different industrial requirements.

The multi-objective optimization was conducted based on XOS and fructose-glucose systems by using both SMB and SSMB processes in this work. The purpose of this method is to search several groups of equally good solutions (called a pareto set) for a certain problem. A pareto set means in which when we go from any one point to another, at least one objective function becomes better and at least one worsens. Therefore, any one solution in a pareto set is optimal and acceptable.

## Co-Authorship Statement

This PhD thesis contains materials that are published or “under review” for publication in peer reviewed journals as listed below.

### **Chapter 3:**

**Title of the paper:** Equilibrium and kinetic differences of XOS2-XOS7 in xylo-oligosaccharides and their effects on the design of simulated moving bed purification process.

**Authors:** Yan Li, Weifang Yu, Ziyuan Ding, Jin Xu, Yi Tong, and Ajay K. Ray.

**Status:** published.

**Journal:** Separation and Purification Technology

**Individual contributions:** The experiments were designed and conducted by the author under supervision of Dr. Xu, Dr. Yu, and Dr. Ray. The manuscript was written by the author and revised by Dr. Xu, and Dr. Ray. And the experimental set-up and chemicals were provided by Dr. Ding, and Yi Tong.

**Reference:** Li, Y., Yu, W.F., Ding, Z.Y., Xu, J., Tong, Y., Ray, A.K.. Equilibrium and kinetic differences of XOS2-XOS7 in xylo-oligosaccharides and their effects on the design of simulated moving bed purification process [J]. Separation and Purification Technology, 2019, (215): 360-367.

### **Chapter 4:**

**Title of the paper:** Multi-objective optimization of sequential simulated moving bed for the purification of xylo-oligosaccharides using averaged parameters.

**Authors:** Yan Li, Jin Xu, Weifang Yu, and Ajay K. Ray.

**Status:** under review.

**Journal:** Chemical engineering science

**Individual contributions:** The multi-objective optimization cases were designed by the author under supervision of Dr. Xu and Dr. Ray. The calculation works of optimization and the analysis were completed by the author. The manuscript was written by the author and revised by Dr. Xu, Dr. Yu, and Dr. Ray.

### **Chapter 5:**

**Title of the paper:** A comparison between SMB and SSMB for fructose-glucose separation based on multi-objective optimization.

**Authors:** Yan Li, Jin Xu, Weifang Yu, and Ajay K. Ray.

**Status:** submitted.

**Journal:** Chemical engineering science

**Individual contributions:** The multi-objective optimization cases were designed by the author under supervision of Dr. Xu and Dr. Ray. The calculation works of optimization were completed by the author with the help of Dr. Yu and Dr. Xu's research group. The optimization results were summarized and analyzed by the author. The manuscript was written by the author and revised by Dr. Xu and Dr. Ray.

To my parents, grandparents and friends for the endless  
support and love

## Acknowledgments

First, I wish to express my sincere gratitude to my research supervisor Dr. Ajay K. Ray, for his enthusiasm, encouragement, patience and suggestions, and for giving me the continuous support throughout the whole research project.

I also would like to thank my co-supervisor Dr. Jin Xu, and Dr. Weifang Yu from college of chemistry and materials engineering, Wenzhou University, China, for their invaluable guidance, suggestions, and encouragement.

I would also like to extend my gratitude to the graduate students Xiaoxiao Jiang and Jian Wang, for their help with my simulation works. I am thankful to Yongtao Chen, for his useful experiences of sequential simulated moving bed experiment. Thanks also to Yumei Wu and Fangyuan Wang, who made my stay in Wenzhou very enjoyable. I thank all my lab-mates and friends , who have enriched my life personally and professionally.

I sincerely acknowledge the China National Cereals, Oils and Foodstuffs Corporation (COFCO), for their lab support and corporation. The research scholarship from the Western university is also gratefully acknowledged.

I would like to extend special thanks to my parents and my grandparents for their endless love and extreme support and patience throughout the years of my graduate study.



# Table of Contents

Abstract.....	ii
Summary for Lay Audience.....	iv
Co-Authorship Statement.....	v
Acknowledgments.....	viii
List of Tables.....	xiii
List of Figures.....	xiv
List of Appendices.....	xvii
Nomenclature.....	xviii
Chapter 1 .....	1
1. Introduction.....	1
1.1. Background.....	1
1.2. Research objective.....	3
1.3. Thesis organization.....	5
1.4. Contribution.....	6
1.5. References.....	7
Chapter 2 .....	11
2. Literature review.....	11
2.1 Description of simulated moving bed (SMB) technology.....	11
2.1.1 Introduction to chromatography.....	11
2.1.2 Continuous counter-current chromatography.....	12
2.1.3 True moving bed (TMB).....	13
2.1.4 Simulated moving bed (SMB).....	15
2.2 SMB with variable conditions.....	22
2.2.1 Varicol system.....	22

2.2.2 SMB with variable flow rates.....	25
2.2.3 Gradient SMB system.....	25
2.2.4 Sequential simulated moving bed (SSMB).....	27
2.3 Application of SMB systems.....	28
2.4 Design strategies of SMB process.....	46
2.4.1 Triangle theory.....	46
2.4.2 Standing wave concept.....	50
2.4.3 Separation volume analysis.....	52
2.5 References.....	54
Chapter 3 .....	68
3. Equilibrium and kinetic differences of XOS2-XOS7 in xylo-oligosaccharides and their effects on the design of simulated moving bed purification process.....	68
3.1 Introduction.....	68
3.2 Theoretical.....	70
3.2.1 Transport dispersive (TD) chromatography model and parameters.....	70
3.2.2 Numerical scheme.....	71
3.2.3 Operation modes of sequential simulated moving bed (SSMB).....	73
3.3 Experimental.....	74
3.3.1 Chemicals and materials.....	74
3.3.2 Instruments.....	74
3.3.3 Procedures.....	75
3.4 Results and discussion.....	76
3.4.1 Screening of ion form of adsorbent.....	76
3.4.2 Frontal analysis.....	77
3.4.3 TD model parameters by linear pulse experiments.....	79
3.4.4 SSMB simulation and experiments.....	86

3.5 Conclusions.....	91
3.6 References.....	92
Chapter 4 .....	97
4. Multi-objective optimization of sequential simulated moving bed for the purification of xylo-oligosaccharides using averaged parameters.....	97
4.1 Introduction.....	97
4.2 SSMB modeling.....	99
4.2.1 Model description.....	99
4.2.2 Numerical scheme for the solution of TD model.....	100
4.2.3 Model parameters.....	101
4.3 Variables and objectives of a binary SSMB system.....	102
4.4 Results and discussions.....	106
4.4.1 Case 1: simultaneous maximization of Pur and UT.....	106
4.4.2 Case 2: maximization of unit throughput and minimization of water consumption at different XOS's purities.....	115
4.4.3 Case 3: maximization of XOS's recovery and minimization of water consumption at fixed unit throughput values.....	117
4.5 Conclusion.....	119
4.6 References.....	121
Chapter 5 .....	126
5. A comparison between SMB and SSMB for fructose-glucose separation based on multi-objective optimization.....	126
5.1 Introduction.....	126
5.2 Mathematical model.....	129
5.2.1 Model description.....	129
5.2.2 Numerical scheme.....	129
5.2.3 Model parameters.....	131
5.3 Multi-objective optimization problems.....	132

5.3.1 Variables and objectives of SMB.....	132
5.3.2 SSMB process.....	134
5.3.3 Configurations of optimization problems for both processes.....	136
5.4 Results and discussions.....	137
5.4.1 Case 1: simultaneous maximization of $Pur_{glu}$ and UT.....	137
5.4.2 Case 2: maximization of $Pur_{glu}$ and minimization of WCR.....	144
5.4.3 Case 3: maximization of $Pur_{glu}$ and minimization of WCR with fixed UT.....	148
5.4.4 Case 4 and case 5: maximization of $Rec_{glu}$ and minimization of water consumption ratio.....	151
5.5 Conclusions and Remarks.....	153
5.6 References.....	155
Chapter 6 .....	161
6. Conclusions and recommendations.....	161
6.1 Major conclusions based on XOS system.....	161
6.2 Major conclusions based on fructose-glucose system.....	163
6.3 Recommendations for future work.....	163
Appendices.....	165
Curriculum Vitae .....	182

## List of Tables

Table 2-1 Summary of applications of SMB technology in recent 10 years.....	30
Table 3-1 Characteristics of resins with different ionic forms.....	77
Table 3-2 Pulse experiments for xylose, ARS and XOS.....	81
Table 3-3 Pulse experiments for XOS2-XOS6.....	85
Table 3-4 Experiment data and simulation results by using different schemes.....	90
Table 4-1 Model parameters.....	102
Table 4-2 Dimensional operating parameters of SSMB.....	103
Table 4-3 Summary of optimization formulations and bounds of variables.....	106
Table 4-4 Optimized $m$ values for SSMB and SMB.....	108
Table 4-5 The averaged mass flow values of three different cases.....	113
Table 5-1 Model parameters.....	132
Table 5-2 Dimensional operating parameters of SSMB.....	135
Table 5-3 Summary of optimization formulations and bounds of variables.....	137
Table 5-4 Results of three simulations .....	141
Table 5-5 Representative points from the solution curves for maximized $Pur_{glu}$ and minimized WCR.....	146

## List of Figures

Figure 2-1 Analogy for elution chromatography [103].....	12
Figure 2-2 Analogy for countercurrent elution chromatography [103].....	13
Figure 2-3 Typical configuration of the true moving bed.....	14
Figure 2-4 (a) Typical configuration of the simulated moving bed.....	15
Figure 2-4 (b) Detailed description of valves and pumps in SMB process.....	15
Figure 2-5 Example of a 6-column SMB and Varicol configuration: switching of the lines over a period.....	24
Figure 2-6 Schematic diagram of SSMB process.....	28
Figure 2-7 Complete separation region and SMB operating regimes on (a) ( $m_{II}$ , $m_{III}$ ) plane and (b) ( $m_I$ , $m_{IV}$ ) plane for the binary separation of species A and B, with linear adsorption isotherm.....	48
Figure 2-8 Complete separation region and SMB operating regimes on the ( $m_{II}$ , $m_{III}$ ) plane for the binary separation with Langmuir adsorption isotherm.....	50
Figure 2-9 Effect of the feed concentration on the complete separation region in the ( $m_{II}$ , $m_{III}$ ) plane [103].....	50
Figure 2-10 Standing wave in a linear TMB system [108].....	51
Figure 3-1 Schematic diagram of SSMB process.....	74
Figure 3-2 Frontal analysis (FA) experiments. a: typical breakthrough curves (total concentration=60 g/L); b: isotherms acquired by FA. Preparative column; concentration range: 30-270 g/L; flowrate 5ml/min.....	78
Figure 3-3 Linear pulse experiments. a: Typical elution profiles (flowrate: 6ml/min); b: plot of $\tau$ against $L/u$ for the estimation of $H$ ; c: plot of $1/N$ against $\lambda u$ and the fits of Eq. (3-8) with	

constant $N_L$ for Xylose, ARS, and XOS. Preparative column (1m×2.5cm I.D); concentration: 100 g/L; sample size 5 mL; flowrate range: 4-12 ml/min.....	80
Figure 3-4 Comparison of elution profiles on the preparative column (30cm×1cm I.D). Sample size:1mL. Flowrate: 1 ml/min. Concentration: 5 g/L XOS; 1.79, 1.655, 0.905, 0.47, 0.135 g/L XOS2 to XOS6, respectively.....	82
Figure 3-5 Plot $1/N$ vs. $\lambda u$ for XOS2-XOS6 and the fits of Eq (3-8) with constant $N_L$ .....	84
Figure 3-6 $r_i$ as a function of flowrate for each component.....	87
Figure 3-7 Comparison of SSMB simulation results obtained by three schemes.....	89
Figure 4-1 Schematic diagrams of SMB and SSMB.....	103
Figure 4-2 Simultaneous maximization of unit throughput and purity. a: pareto, circle and triangle points are for Cases 1.1 and 1.2, respectively; b: corresponding optimized $m$ values; c: $t_1$ (min) and $Q_f$ (ml/min) derived from the $m$ values.....	107
Figure 4-3 Internal concentration profiles for 95.2% purity. a: XOS; b: impurity. Corresponding $m$ values: $m_I=0.73$ , $m_{II}=0.25$ , $m_{III}=0.46$ , $m_{IV}=0.079$ .....	110
Figure 4-4 MF plot for three representative purities. Black for XOS, gray for impurity; solid, dash and dot curves are for purities of 92.6% ( $m_I=0.73$ , $m_{II}=0.18$ , $m_{III}=0.47$ , $m_{IV}=0.075$ ), 95.2% ( $m_I=0.73$ , $m_{II}=0.25$ , $m_{III}=0.46$ , $m_{IV}=0.079$ ) and 98.1% ( $m_I=0.89$ , $m_{II}=0.28$ , $m_{III}=0.33$ , $m_{IV}=0.099$ ), respectively.....	112
Figure 4-5 Decision variables for Case 1.2.....	115
Figure 4-6 Simultaneous maximization of unit throughput and minimization of solvent consumption at various purity requirements. a: pareto, circle, triangle, and square are for purity constraints of 90%, 95% and 97%; b: corresponding optimized $m$ values of purity>90%; c: derived $t_1$ , $t_3$ , and $Q_f$ .....	116
Figure 4-7 Simultaneous maximization of XOS recovery and minimization of solvent consumption at various equipment capacities. a: pareto, circle, triangle, and square are for UT of 2, 3 and 4 ml/min; b: corresponding optimized $m$ values of UT=2 ml/min.....	119

Figure 5-1 Schematic diagrams of regular 4-zone SMB and SSMB.....	127
Figure 5-2 Comparison between pareto solutions for SMB and SSMB: Case 1.....	138
Figure 5-3 Optimal $m$ values corresponding to the pareto solutions in Figure 5-2. a: SMB; b: SSMB.....	139
Figure 5-4 MF plots of the three simulations in Table 5-4.....	142
Figure 5-5 Internal concentration profiles of glucose for SMB and SSMB with maximum UT at $Pur_{glu}=95.5\%$ .....	143
Figure 5-6 Internal concentration profiles of fructose for SMB and SSMB with maximum UT at $Pur_{glu}=95.5\%$ .....	144
Figure 5-7 Comparison between pareto solutions for SMB and SSMB: case 2.....	145
Figure 5-8 MF plots of the four solution points in Table 5-5.....	147
Figure 5-9 Optimal $m$ values of SMB and SSMB for Case 2. a: $m_I$ ; b: $m_{II}$ , c: $m_{III}$ ; d: $m_{IV}$ ..	148
Figure 5-10 Comparison between pareto solutions for SMB and SSMB: case 3.....	149
Figure 5-11 Optimal $m$ values of SMB and SSMB for Case 3. a: $m_I$ ; b: $m_{II}$ , c: $m_{III}$ ; d: $m_{IV}$	150
Figure 5-12 Comparison between pareto solutions for SMB and SSMB: case 4.....	152
Figure 5-13 Comparison between pareto solutions for SMB and SSMB: case 5.....	153



## List of Appendices

Appendix A : Supplementary information of Chapter 3 .....	165
Appendix B : Supplementary information of Chapter 4.....	169
Appendix C : Supplementary information of Chapter 5.....	176

## Nomenclature

$c$	concentration in liquid phase (mg/ml)
$d$	diameter (cm)
$D_{ap}$	apparent diffusivity ( $\text{cm}^2/\text{min}$ )
$D_L$	axial dispersion coefficient in TD model ( $\text{cm}^2/\text{min}$ )
$f$	function of the adsorption isotherm (dimensionless)
$H$	Henry's constant (dimensionless)
$k_m$	mass transfer coefficient in TD model ( $\text{min}^{-1}$ )
$L$	column length (cm)
$m$	flowrate ratio (dimensionless)
$N$	number of equivalent theoretical plates (dimensionless)
$N_L$	TD model parameter ( $\text{cm}^2/\text{min}$ )
$P_{ur}$	purity (%)
$P_{ro}$	productivity (%)
$q, q^*$	adsorbed concentration in stationary phase (mg/ml)
$Q$	flowrate (ml/min)
$Rec$	recovery (%)
$t$	time (min)
$t_s$	switching time (min)
$T$	temperature ( $^{\circ}\text{C}$ )

$u$	interstitial mobile phase velocity in the packed column (cm/min)
$V$	geometric column volume (mL)
$V_D$	dead volume (mL)
$z$	axial coordination (cm)

***Greek letters***

$\alpha$	selectivity between Xylose and XOS
$\beta$	fraction of flowrate
$\epsilon_t$	total column voidage
$\phi$	phase ratio
$\lambda$	constant defined in Eq. (8) ( $\text{cm}^{-1}$ )
$\rho$	density

***Subscripts***

ap	apparent
cal	calculation
e	equilibrium
ext	the external stream to an inlet port
exp	experimental data
jpre	the adjacent upstream column
i, j	indices of components, columns, and SSMB operating zones
D	desorbent port

E extract port

eluent eluent phase

F feed port

loop loop phase

R raffinate port

s switching

T total

opt optimization

### ***Abbreviations***

AMF averaged mass flow

ARS arabinose

ED equilibrium-dispersive

FOS fructo-oligosaccharides

GOS galacto-oligosaccharides

MF mass flows

MOO multi-objective optimization

NSGA-II non-dominated sorting genetic algorithm

SMB sequential simulated moving bed

SSMB sequential simulated moving bed

SWD standing wave design

TD transport-dispersive

UT unit throughput

WC water consumption

WCR water consumption ratio

XOS Xylo-oligosaccharides

XOSN XOS with various degrees of polymerization, N form 1 to 7, N=67 for the combination of XOS6 and XOS7

# Chapter 1

## 1. Introduction

### 1.1. Background

Chromatography is a widely used separation method based on the different adsorption affinity to the solid adsorbent of each component involved in a system. A conventional batch mode chromatographic process always shows low productivity, high desorbent consumption, and low operating efficiency. In order to overcome these disadvantages, the simulated moving bed (SMB) process was developed and first applied by Broughton and Gerhold in 1961 [1]. Unlike the traditional separation processes, a continuous counter-current movement of solid phase towards the fluid phase is achieved by the simultaneous switch of four inlet and outlet ports of SMB unit [2]. Therefore, the problems associated with the movement of solid phase can be solved, such as the particle attrition, the bed voidage variation, the unstable flow rate, and the bed expansion. In addition, the high productivity and purity, and the simple operation control can be accomplished due to the continuous operating mode. The current industrial applications of SMB mainly include extraction of p-xylene [3, 4], corn wet milling [5], and fructose/glucose separation [6]. Recently, its applications has been extended to the separation of fine and complicated chemicals, such as chiral drugs and biological components [7-9].

A typical 4-zone SMB system consists of several packed chromatographic columns which are series-connected and form a closed loop. The basic mechanism of SMB process is the counter-current movement between the liquid and solid phase. Each zone in a SMB unit owns its specific function: the separation takes place in zone II and zone III; zone I and zone IV are functioned for the solid and solvent regenerations, respectively.

Recently, SMB chromatography with variable conditions has been developed and reported in the literature in order to offer a larger potential for industrial production. These new formulations and techniques such as Varicol, SMB with variable flow rates, gradient SMB (i.e., temperature gradient, pressure gradient and solvent gradient SMB

processes), and sequential SMB (SSMB) are all based on the conventional SMB method but conducted at different procedures and operating conditions [10-12].

Among these methods, SSMB technique is a preferential choice for some large-scale separation processes in industry due to its low solvent consumption. Different from the SMB process, one switch in SSMB is divided into three steps with different flow patterns. In the 1st step, the mobile phase is circulated in the whole system, forming a closed loop; in the 2nd step, section IV is isolated and an external solvent stream is introduced at the desorbent port to purge the less adsorbed species to raffinate port; in the 3rd step, section II is also isolated and another feed stream is introduced such that preferentially and less adsorbed species are simultaneously collected at extract and raffinate ports, respectively. Due to the first step in SSMB, the solvent consumption is significantly reduced.

At first, we mainly studied sequential simulated moving bed (SSMB) technique for the separation and purification of xylo-oligosaccharides (XOS) syrup, with XOS being the desired product widely used in food industry. During last decades, most researchers only focused on SMB method, there is no reported literature on SSMB system and its simulation or optimization works. In the field of purification of oligosaccharides by using SMB, Jiang et al. [13-16] investigated and discussed the application of SMB system in fructo-oligosaccharides (FOS) and galacto-oligosaccharides (GOS) [17-19]. To our knowledge, the only study about XOS purification by SMB was reported by Meng et al. [20] who enriched XOS from 69% to 91% by using several groups of trial and error experiments. Therefore, it is essential to design an optimum and efficient SSMB separation process for XOS system. In addition, in order to investigate the differences between SMB and SSMB processes, some optimization works based on the fructose-glucose system corresponding to diverse industrial requirements were conducted and compared in this work.

There are generally multiple factors affecting the final products' purity, recovery, and solvent consumption of a certain SSMB process and always take effect in conflict with each other. Therefore, simple empirical design and optimization need a large number of experiments which seems impractical and uneconomical. For this reason, systematic

multi-objective optimization (MOO) of SSMB separation is necessary and developed in our research.

As proved, MOO could provide a much better description of the optimization problem and more precise screening on the optimal operating conditions [21-25]. The purpose of MOO method is to search several groups of equally good solutions (called a pareto set) for a certain problem. A pareto set means in which when we go from any one point to another, at least one objective function becomes better and at least one worsens. Therefore, any one solution in a pareto set is optimal and acceptable [21-25].

Genetic algorithm (GA) is a popular search and optimization method to solve MOO problems. It mimics the principles of genetics and the natural selection in Darwinian principle [26]. Non-dominated sorting genetic algorithm (NSGA) and NSGA-II are improved methods based on GA. Considering the faster convergence of NSGA-II, we used this method in our programming process. Actually, a lot of researchers successfully applied this method to multi-objective optimization problems (MOO). Kasat et al. [27] optimized the industrial FCC units with NSGA-II and the same procedure could be developed to other industrial FCC processes. Tarafder et al. studied the industrial styrene monomer manufacturing process and carried out the MOO of this system by using NSGA-II. Finally, the styrene selectivity was maximized and the required heat duty was minimized [25]. In Lee et al.'s [28] research, they reported the NSGA-II's application in MOO of an industrial penicillin V bioreactor train. In addition, Zhang et. al. extended the application of NSGA-II to chiral drug separation area [9]. The MOO of SMB and Varicol processes for enantio-separation of racemic pindolol was completed in their project. These various reviews motivated us to optimize the SSMB separation of XOS for multiple objectives by employing the NSGA-II.

## 1.2. Research objective

The major research objectives of this thesis: (i) conduct a comprehensive study for the sequential simulated moving bed (SSMB) process and explore its possibility in industrial



application; (ii) investigate the differences between SMB and SSMB processes. The research works were specifically divided into three parts as below.

### **Separation and purification of XOS system by using SSMB**

- (1) Screening the stationary phase;
- (2) Measuring and determining column parameters, column model parameters, and adsorption isotherm model parameters;
- (3) Separating XOS from the impurities by using SSMB process and validating the above parameters by experiment and simulation results.

### **Multi-objective optimization of SSMB process based on XOS system**

- (1) Simultaneous maximization of purity and unit throughput of XOS by using different groups of variables;
- (2) Maximization of unit throughput and minimization of water consumption with different XOS purity constraints;
- (3) Maximization of XOS recovery and minimization of water consumption at different fixed unit throughput values.

### **A comparison between SMB and SSMB processes for fructose-glucose separation based on multi-objective optimization**

- (1) Simultaneous maximization of purity of glucose and unit throughput for both SMB and SSMB processes;
- (2) Maximization of purity of glucose and minimization of water consumption ratio for both processes;
- (3) Maximization of recovery of glucose and minimization of water consumption ratio for both processes;

- (4) Maximization of purity of glucose and minimization of water consumption ratio with a fixed unit throughput for both processes;
- (5) Maximization of recovery of glucose and minimization of water consumption ratio with a fixed unit throughput for both processes.

### 1.3. Thesis organization

This thesis is organized based on the article-integrated format and is composed of 6 main chapters.

Chapter 1 gives a brief introduction of this thesis and followed by a comprehensive literature review for the background of simulated moving bed technology. The development, different kinds of SMB methods, basic design and optimization strategies, and the recent applications of SMB were reviewed in chapter 2.

In chapter 3, several column parameters were firstly measured, such as selectivity, bed voidage, and column efficiency. After that the adsorption isotherm and kinetic parameters of XOS, xylose, arabinose, and the individual xylobiose, xylotriose, xylotetraose, xylopentaose, xylohexaose, and xyloheptaose (XOS2-XOS7) were determined by using the frontal analysis method and the preparative pulse experiment. Furthermore, all these parameters obtained above were applied to conduct a series of SSMB experiments and simulations. A comparison between the simulation results of using the average parameters and the individual parameters was completed, which provided the future researchers an improved and innovative idea to design the SSMB separation process for the oligosaccharides systems.

In chapter 4, in order to obtain the optimal operating conditions of a SSMB process, the multi-objective optimization for separating XOS from the impurities (xylose and arabinose) was conducted. For this objective, various optimization formulations aimed at improving purity and recovery of XOS and unit throughput or reducing the solvent consumption were proposed. At first, simultaneous maximization of XOS's purity (raffinate purity) and unit throughput by using two different groups of variables was

conducted. After that, maximization of unit throughput and minimization of water consumption at different XOS's purity requirements was completed. Maximizing XOS's recovery and minimizing water consumption for several given unit throughput values was finally carried out. All the calculations of simulation and optimization works were programmed in FORTRAN codes, and non-dominated sorting genetic algorithm (NSGA-II) was applied to obtain the pareto solutions.

In chapter 5, in order to investigate the differences between SMB and SSMB processes, diverse multi-objective optimization cases contain different objectives and constraints were conducted. At first, simultaneous maximization of glucose's purity (raffinate purity) and unit throughput for SMB and SSMB was completed. After that, maximization of glucose's purity and minimization of water consumption ratio was conducted. Next, maximizing glucose's recovery and minimizing water consumption ratio was carried out. Finally, case 2 and 3 were repeated with a fixed unit throughput value for both processes. All the calculations of simulation and optimization works were programmed in FORTRAN codes, and non-dominated sorting genetic algorithm (NSGA-II) was applied to obtain the pareto solutions.

Finally, chapter 6 summarizes all the inferences and conclusions drawn from the previous chapters. The recommendations for future work are also included in this chapter.

## 1.4. Contribution

The major contribution of this project is successfully providing a comprehensive introduction, design, and optimization for a SSMB separation process for the first time. All the methods used in this work, such as parameters determination methods, design strategy for a SSMB experiment, multi-objective optimization approach, could be applied to other SSMB separation processes. In addition, all the conclusions obtained proved the advantage of SSMB in industrial production due to the reduced water consumption and the flexible operating pattern. Therefore, it is essential and significant to extend the application of SSMB technique in the future.

Secondly, to our knowledge, separation and purification of XOS system by using SSMB method has not been reported in the literature. Furthermore, this is the first time to investigate and compare the properties of XOS2-XOS7 and the averaged property of XOS system, and then explore the influence of these differences on a SSMB separation process. All the results corresponding to XOS system in this work could provide useful and applicable references for the industrial XOS production.

In addition, the comparison between SSMB and SMB processes is of great significance and shows the potential of SSMB in industry due to the reduced solvent consumption. Especially for some sugar separation and purification processes, the solvent consumption is a very important issue of concern.

## 1.5. References

- [1] Broughton, D.B., and Gerhold, C.G.. Continuous sorption process employing fixed bed of sorbent and moving inlets and outlets. US Patent 2 985 589. 1961.
- [2] Rajendran, A., Paredes, G., and Mazzotti, M.. Simulated moving bed chromatography for the separation of enantiomers. *Journal of Chromatography A*, 2009, (1216): 709-738.
- [3] Minceva, M., and Rodrigues, A.E.. Modeling and simulation of a simulated moving bed for the separation of p-xylene. *Ind. Eng. Chem. Res.*, 2002, (41): 3454-3461.
- [4] Minceva, M., and Rodrigues, A.E.. Two-level optimization of an existing SMB for p-xylene separation. *Computers and Chemical Engineering*, 2005, (29): 2215-2228.
- [5] Pynnonen, B.. Simulated moving bed processing: escape from the high-cost box. *Journal of Chromatography A*, 1998, (827): 143-160.
- [6] Azevedo, D.C.S., and Rodrigues, A.E.. Fructose-glucose separation in a SMB pilot unit: modeling, simulation, design, and operation. *AIChE J*, 2001, (9): 2042-2051.
- [7] Ribeiro, A.E., Gomes, P.S., Pais, L.S., and Rodrigues, A.E.. Chiral separation of ketoprofen enantiomers by preparative and simulated moving bed chromatography. *Separation Science and Technology*, 2011, (46): 1726-1739.

- [8] Faria, R.P.V. and Rodrigues, A.E.. Instrumental aspects of simulated moving bed chromatography. *Journal of Chromatography A*, 2015, (1421): 82-102.
- [9] Zhang, Y., Hidajata, K., and Ray, A.K.. Multi-objective optimization of simulated moving bed and Varicol processes for enantio-separation of racemic pindolol. *Separation and Purification Technology*, 2009, (65): 311-321.
- [10] Schmidt-Traub, H.. *Preparative Chromatography*. Germany: WILEY-VCH, 2005.
- [11] Jiang, X.X., Zhu, L., Yu, B., Su, Q., Xu, J., Yu, W.F.. Analyses of simulated moving bed with internal temperature gradients for binary separation of ketoprofen enantiomers using multi-objective optimization: Linear equilibria. *Journal of Chromatography A*, 2018, (1531): 131-142.
- [12] Pais, L.S., and Rodrigues, A.E.. Design of simulated moving bed and Varicol processes for preparative separations with a low number of columns. *Journal of Chromatography A*, 2003, (1006): 33-44.
- [13] Jiang, B., Wang, Z., Yang, R. J., Tang, L., Lamia, L.. Production of fructo-oligosaccharides with high purity. *China Food Additives*, 1999, (3): 1-7.
- [14] Nobre, C., Castro, C.C., Hantson, A.L., Teixeira, J.A., Rodrigues, L.R., Weireld, G.D.. Strategies for the production of high-content fructo-oligosaccharides through the removal of small saccharides by co-culture or successive fermentation with yeast. *Carbohydrate Polymers*, 2016, (136): 274-281.
- [15] Nobre, C., Teixeira, J.A., and Rodrigues, L.R.. New trends and technological challenges in the industrial production and purification of fructo-oligosaccharides. *Critical Reviews in Food Science and Nutrition*, 2013, (55): 1444-1455.
- [16] Nobre, C.. *Fructo-oligosaccharides recovery from fermentation processes*. Portugal: Universidade do Minho, 2011.
- [17] Liu, Z.L., Wang, N.Q., W, M.Z., W, C.M., and Y H.J.. Application of simulated moving bed chromatography in production of functional oligosaccharides. *China food*

additives, 2012, (3): 200-204.

[18] Valero, J.I.. Production of Galacto-Oligosaccharides from Lactose by Immobilized  $\beta$ -Galactosidase and Posterior Chromatographic Separation. The united states: The Ohio State University, 2009.

[19] Wiśniewski, L., Antošová, M., and Polakovič, M.. Simulated moving bed chromatography separation of galacto-oligosaccharides. *Acta Chimica Slovaca*, 2013, (2): 206-210.

[20] Meng, N., Feng, X.Y., Wang, C.F., Lu, F.P.. Study on separation of xylooligosaccharides by simulated moving bed chromatography. *Science and Technology of Food Industry*, 2011, (10): 310-313.

[21] Bhaskar, V., Gupta, S.K., and Ray, A.K.. Multi-objective optimization of an industrial wiped film poly (ethylene terephthalate) reactor: some further insights. *Computers and Chemical Engineering*, 2001, (25): 391-407.

[22] Tarafder, A., Rangaiah, G.P., Ray, A.K.. Multi-objective optimization of an industrial styrene monomer manufacturing process. *Chemical Engineering Science*, 2005, (60): 347-363.

[23] Bhutani, N., Ray, A.K., and Rangaiah, G.P.. Modeling, simulation, and multi-objective optimization of an industrial hydrocracking unit. *Ind. Eng. Chem. Res.*, 2006, (45): 1354-1372.

[24] Yu, W.F., Hariprasad, J.S., Zhang, Z.Y., Hidajat, K., and Ray, A.K.. Application of multi-objective optimization in the design of SMB in chemical process industry. *J. Chin. Inst. Chem. Engrs.*, 2004, (1): 1-8.

[25] Tarafder, A., Rangaiah, G.P., and Ray, A.K.. A study of finding many desirable solutions in multi-objective optimization of chemical processes. *Computers and Chemical Engineering*, 2007, (31): 1257-1271.

[26] Agrawal, N., Rangaiah, G.P., Ray, A.K., and Gupta, S.K.. Multi-objective

optimization of the operation of an industrial low-density polyethylene tubular reactor using genetic algorithm and its jumping gene adaptations. Ind. Eng. Chem. Res., 2006, (45): 3182-3199.

[27] Kasat, R.B., Kunzru, D., Saraf, D.N., and Gupta, S.K.. Multiobjective Optimization of Industrial FCC Units Using Elitist Nondominated Sorting Genetic Algorithm. Ind. Eng. Chem. Res., 2002, (41): 4765-4776.

[28] Lee, F.C., Rangaiah, G.P., and Ray, A.K.. Multi-objective optimization of an industrial penicillin V bioreactor train using non-dominated sorting genetic algorithm. Biotechnology and Bioengineering, 2007, (3): 586-598.

## Chapter 2

### 2. Literature review

#### 2.1 Description of simulated moving bed (SMB) technology

##### 2.1.1 Introduction to chromatography

In order to obtain the desired product with high purity and recovery, an effective separation technology is important and indispensable for nearly every chemical engineering process. Some traditional separation methods, such as crystallization, extraction, membrane separation, and distillation, are frequently used in research and practical industrial works. However, when the target system contains complex composition or chemically similar components (e.g. amino acids, chiral drugs, oligosacchides, and proteins), the separation consequently becomes extremely difficult and all the methods above are not applicable. In this condition, chromatography provides an alternative separation approach which is helpful in dealing with such difficult separations.

Chromatography is a separation method based on the different adsorption affinity to the solid adsorbent of each component involved in a system. Mikhail Tswett, who conducted the separation of plant pigments by using glass columns packed with calcium carbonate, first discovered and defined the chromatography method. Compared to other separation technologies, chromatography owns high selectivity, high separation efficiency, high purity of products, and low operation and energy cost. Thus, it is a suitable and optimal choice for most separation applications.

Figure 2-1 shows the basic principle of chromatography. The convey belt is considered as the solid adsorbent (stationary phase). The triangles A and B are the two different components in a system, and obviously triangle A has higher adsorption affinity to the stationary phase. The desorbent (mobile phase) flows with the same direction to the convey belt and the triangle B will be completely separated with A and firstly washed out of the convey belt. In this way, A and B were successfully separated [1, 2].



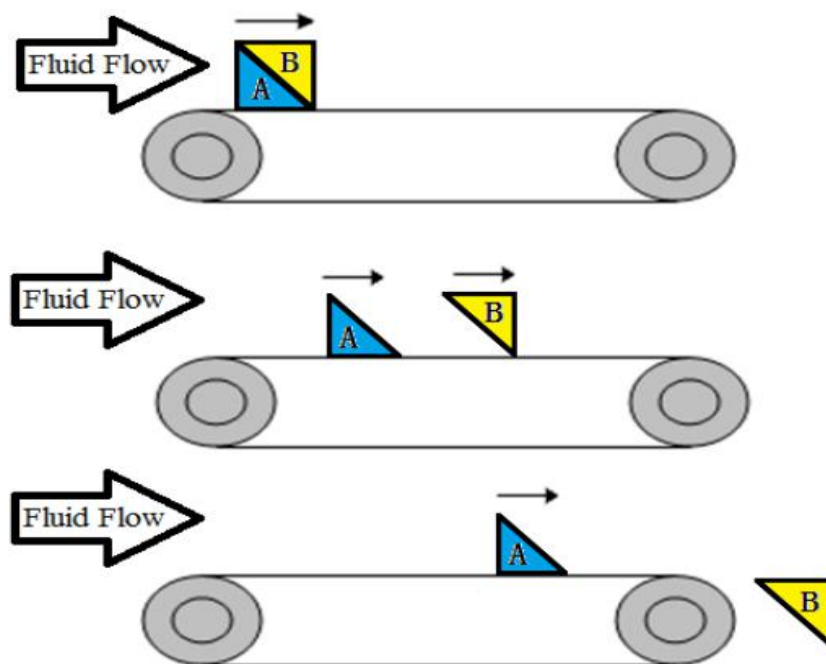


**Figure 2-1 Analogy for elution chromatography [103]**

### 2.1.2 Continuous counter-current chromatography

When the moving direction of mobile phase and the stationary phase is opposite, it is called continuous counter-current chromatography. As illustrated in figure 2-2, similar to figure 2-1, the triangle A and B are respectively defined as the more and less retained substances in the system. The fluid flows in the opposite direction of convey belt.

Therefore, according to different flow rate of convey belt, there will be three different conditions. If the moving velocity of convey belt is larger than that of A and less than that of B, the net velocity of two directions will lead to a completely separation of A and B. The component A can be collected at left side and B is purged to the right side. On the other hand, if convey belt's velocity is larger than B or less than A, the net velocity will push both A and B together to the right or left port, as shown in figure 2-2.

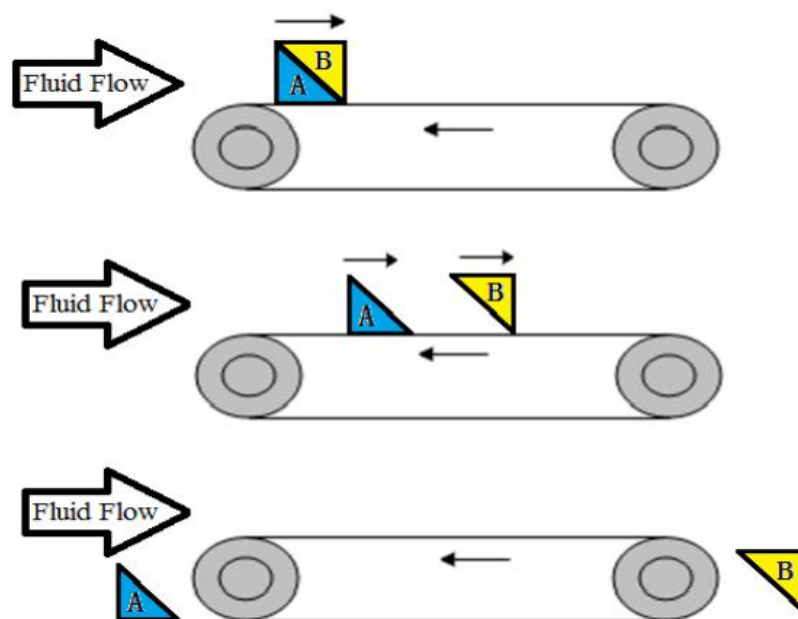


**Figure 2-2 Analogy for countercurrent elution chromatography [103]**

Based on the above principle of continuous counter-current chromatography, it is simple to understand the design strategy of this method. The adsorption performance of each component on one given stationary phase should be firstly investigated and then the moving velocity can be determined. According to these information, it is easy to choose an intermediate velocity, which can achieve the complete separation purpose.

### 2.1.3 True moving bed (TMB)

True moving bed (TMB) is actually an ideal counter-current system, which involves a circulation of solid phase with the constant moving velocity. As shown in figure 2-3, the solid phase enters at the top of the column and naturally moves downward with gravity as the driven force, while the desorbent enters the system through the bottom of the column and then moves upward [1]. In order to specifically illustrate the separation mechanism, a conventional binary separation process was chosen to investigate which contains component A and B. The column is divided into four sections by two outlet and two inlet streams. The feed solution, contains two components A and B, is continuously introduced to the column between section 2 and 3. With the counter-current movement of mobile

phase and stationary phase, A and B will be separated. The more retained substance A, could be collected at the extract port in section 1, meanwhile, the less retained substance B is purged to the raffinate part in section 3.

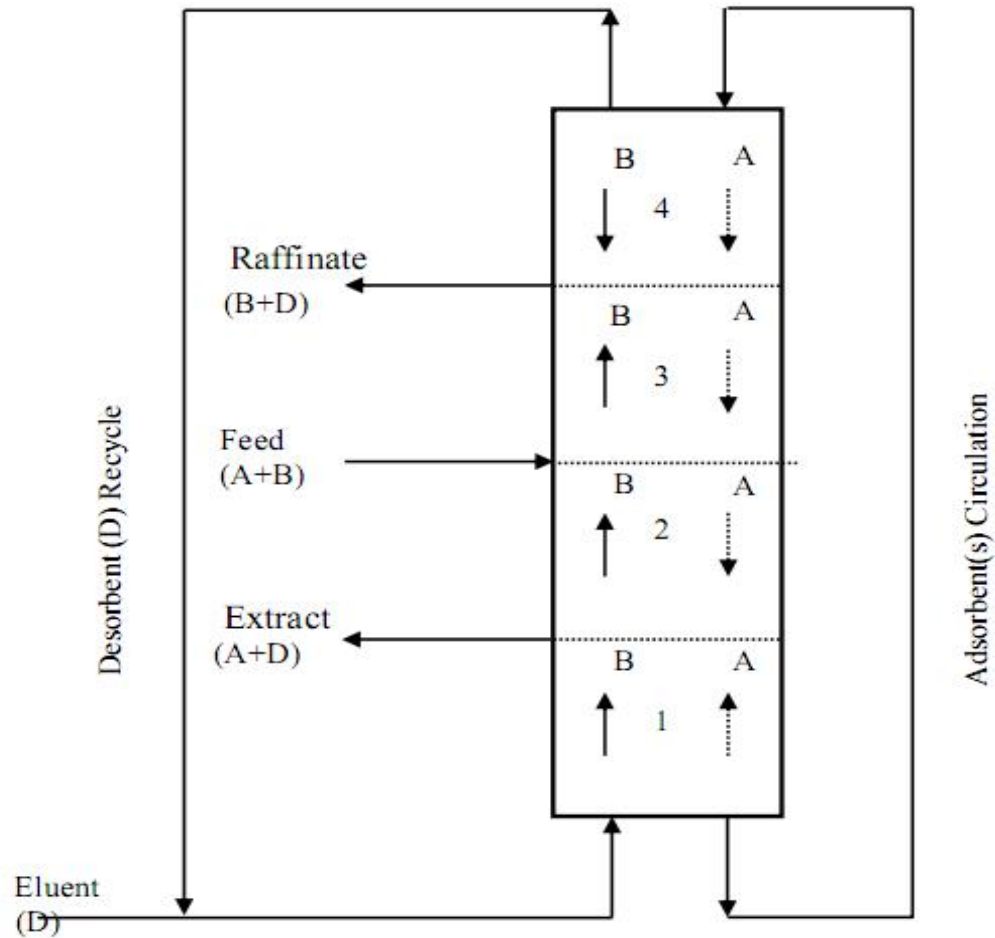


**Figure 2-3 Typical configuration of the true moving bed**

In conclusion, the different specific roles of each section in TMB can be determined. Section 1 and section 4 are used to respectively regenerate the solid phase and the mobile phase. The function of section 2 is desorbing the less retained component to guarantee the purity of final raffinate product. Section 3 works to adsorb the more retained component and carried it to the extract stream. The key point for this process is to choose appropriate flow rates in all sections to ensure each section functions well. For example, component A should move downward with solid in section 2-4, while move upward with fluid in section 1. For several cycles, component A with higher affinity can be successfully

recovered and collected in the extraction port. As the same principle is applicable for component B, a completely separation process could be achieved.

However, TMB works in an ideal condition, the constant movement of solid phase is technically impossible due to diverse practical problems. The simulated moving bed (SMB) technology was developed based on TMB and overcame all these deficiencies.

#### 2.1.4 Simulated moving bed (SMB)

A simulated moving bed system generally involves several fixed-bed chromatographic columns and is divided into four sections by four inlet and outlet ports (feed, raffinate, desorbent, and extract). An illustration of SMB process is shown in figure 2-4 (a).

Different from the TMB process, the counter-current movement of solid phase towards the fluid phase is achieved by the simultaneous switch of four streams [1, 3, 4]. Therefore, the problems associated with the movement of solid phase can be solved, such as the particle attrition, the bed voidage variation, the unstable flow rate, and the bed expansion. Despite these improvement, the high product quality and simple operation control can be effectively accomplished.

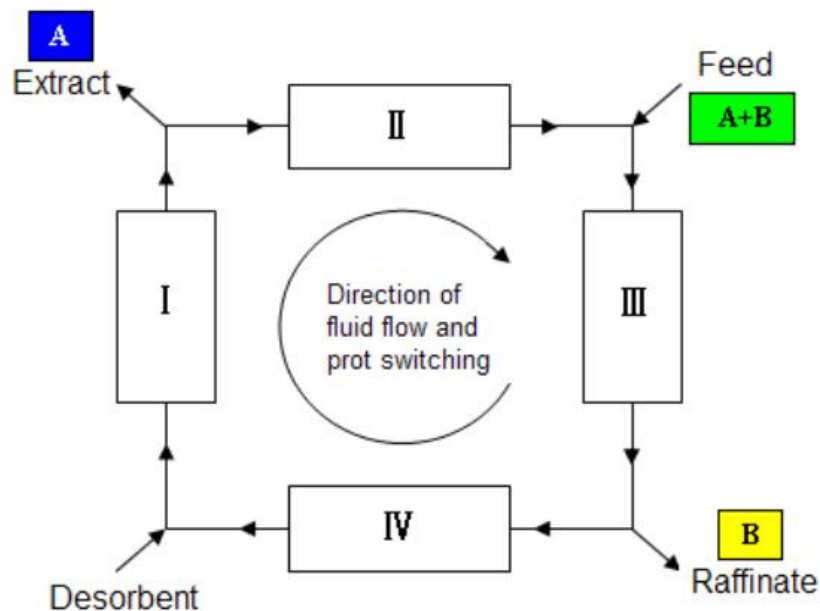


**Figure 2-4 (a) Typical configuration of the simulated moving bed**

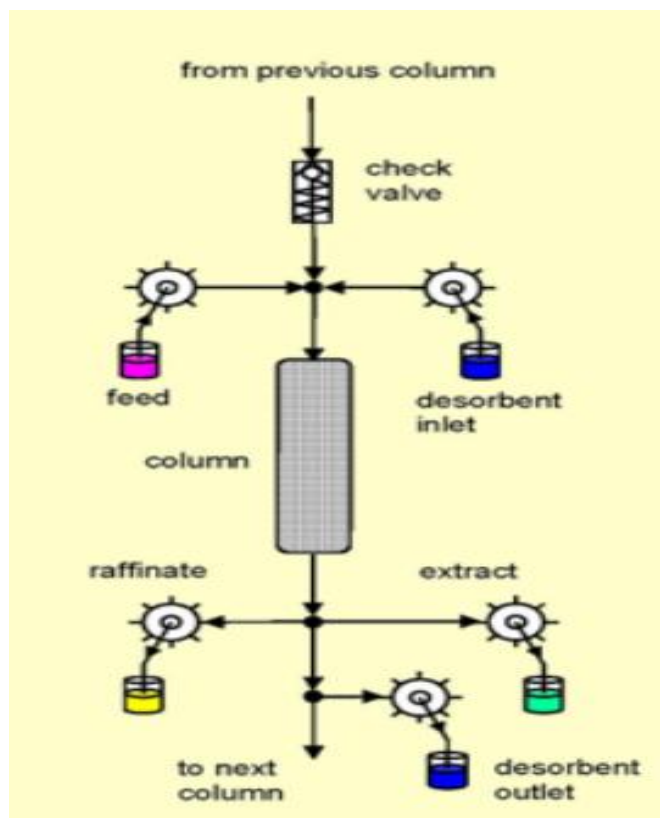


**Figure 2-4 (b) Detailed description of valves and pumps in SMB process**

Each section in a SMB unit owns its specific function: the separation takes place in section 2 and section 3; section 1 and section 4 are functioned for the solid and solvent regeneration, respectively. In Universal Oil Product's patent in 1960s, SMB was firstly reported and applied in separation and purification of bulk chemicals [5]. After that, the major application of SMB was extended to petrochemical industry and sugar industry. Until 1990, SMB was successfully used in pharmaceutical industry to purify the chiral drugs with high economic value. The detailed development of SMB applications will be discussed in section 2.3.

#### 2.1.4.1 Column models

Most classical chromatographic column models consider two or more effects below in calculation process [6].

- Convection

- Dispersion
- Adsorbent particle's mass transfer
- Pore diffusion
- Surface diffusion
- Adsorption equilibrium

In addition, in the modeling process, following assumption is taken into account.

- The column packing is homogeneous
- Isothermal process
- Fluid's properties are constant, e.g. flow rate, and viscosity.
- The axial dispersion coefficient is constant.
- No convection inside the particles.
- Size exclusion effect is negligible.

All the column models introduced in this section were comprehensively summarized by Guiochon et al., Ruthven, and Seidel-Morgenstern et al. [7-10].

### **(1) Ideal equilibrium model**

This is the simplest model in chromatography, which is built only based on the convection between solid and liquid phases and the thermodynamics. The axial dispersion and the kinetic effects are neglected due to it is an ideal case. The column mass balance equation is shown as below:

$$\frac{\partial c_{ij}}{\partial t} + \frac{1-\varepsilon}{\varepsilon} \cdot \frac{\partial q_{ij}}{\partial t} + u \cdot \frac{\partial c_{ij}}{\partial z} = 0 \quad (i = A, B) \quad (2-1)$$

Where  $c$  and  $q$  are the concentrations of the solute in the mobile phase and the stationary

phase, respectively. The subscript j stands for different sections.  $\varepsilon$  is the bed voidage, t is time, z is the space coordinate, and u is the interstitial fluid velocity. This model was firstly reported by Wicke for the elution of a single component in 1939 [6]. After that, several researchers, such as Lapidus and Amundson, Van Deemter et al., and Glueckauf applied this model in analyzing the cases of linear and nonlinear systems [6, 11, 12].

## (2) Equilibrium dispersive (ED) model

Based on the ideal model, the axial dispersion term is considered in the mass balance calculation process. The dispersion coefficient is assumed always constant through the whole column and the whole process. After adding a lumped apparent dispersion coefficient, the ED model can be described as:

$$\frac{\partial c_{ij}}{\partial t} + \frac{1-\varepsilon}{\varepsilon} \cdot \frac{\partial q_{ij}}{\partial t} + u \cdot \frac{\partial c_{ij}}{\partial z} = D_a \cdot \frac{\partial^2 c_{ij}}{\partial z^2} \quad (i = A, B) \quad (2-2)$$

This model was successfully used by researchers to design diverse chromatographic systems [13-15].

## (3) Transport dispersive (TD) model

The TD model adds both the axial dispersion and mass transfer effects in its modeling expression. As the mass transfer term is defined by the linear driving force approach, one frequently used consideration is the mass transfer is dominated by the resistance of solid phase. Therefore, TD model is generally written as:

$$\frac{\partial c_{ij}}{\partial t} + \frac{1-\varepsilon}{\varepsilon} \cdot \frac{\partial q_{ij}}{\partial t} + u \frac{\partial c_{ij}}{\partial z} = D_a \cdot \frac{\partial^2 c_{ij}}{\partial z^2} \quad (i = A, B) \quad (2-3)$$

$$\frac{\partial q_{ij}}{\partial t} = k_m (q_{ij}^* - q_{ij}) \quad (2-4)$$

Where  $D_a$  is the dispersion coefficient,  $k_m$  is the mass transfer coefficient,  $q^*$  is the adsorbed amount of each component in the solid phase which is equilibrated with the mobile phase.

This model has been used by a lot of authors in chromatographic simulation and optimization works which performs well in describing the mass transfer behavior [16-19].

## 2.1.4.2 Adsorption isotherm models

### (1) Linear isotherm

If the working region of chromatography has low mobile phase concentration and the retention time always keeps constant, the adsorption isotherm is in a linear range. The relationship between the mobile and the stationary phase's concentration is expressed as:

$$q_i = H_i c_i \quad (2-5)$$

Where  $q$  and  $c$  are the equilibrium concentrations of each component in stationary phase and mobile phase, respectively.  $H$  is the Henry's constant.

As reported by a lot of researchers, most sugars follow the linear isotherm models, such as fructose, glucose, xylose, and some oligosaccharides. In Long et al.'s work, frontal analysis was applied to determine the isotherm parameters of D-psicose and D-fructose. It turned out that the adsorption behaviour was in linear range [20]. Vankova et al. respectively measured the linear adsorption isotherms of fructooligosaccharides, glucose, fructose, and sucrose on a Ca-Form Cation Exchanger by using the frontal analysis method in 2010 [21]. Vankova et al. and Wisniewski et al. all successfully applied the linear adsorption model in SMB simulation and optimization works for separating the fructooligosaccharides and galacto-oligosaccharides [22-24].

### (2) Langmuir isotherm

For some systems, the adsorption isotherms of each component cannot be appropriately described by the simple linear model. The interference between each component and the adsorbent cannot be neglected. In order to solve this problem, an extension of linear isotherm, Langmuir isotherm which take the interference into account, was developed.



$$q_i^* = \frac{q_s b_i c_i}{1 + \sum b_i c_i} \quad (i = A, B) \quad (2-6)$$

where  $q_s$  is the monolayer capacity for the stationary phase,  $b$  is the ratio of the rate constant. This kind of model is widely used in describing some chiral drugs' adsorption behavior. (R,S)-mandelic acid is a typical chiral system contains two enantiomers and was studied by a lot of researchers in recent years. Mao et al. and Jandera et al. used Langmuir isotherm to model the adsorption isotherm of mandelic acid through different methods and finally achieved a good agreement with the experimental results [16, 25]. Skavrada et al. applied this model to determine the adsorption isotherm of 1,1-bis(2-naphthol) on CHIRIS AD1 and CHIRIS AD2 columns [26]. In Wang and Ching's work, the Langmuir model perform well to describe the adsorption isotherm of nadolol enantiomers [27]. Da Silva et al. studied the chromatographic separation parameters of ketamine enantiomers, and the isotherms were also adjusted satisfactorily to the Langmuir model [28].

### (3) Bi-Langmuir isotherm

Different from the Langmuir model, the bi-Langmuir isotherm model assumes that

the surface of the stationary phase contains two different types of binding sites, the non-selective and the selective sites. All the components have the same affinity to the non-selective site, while different components show different adsorption affinity to the selective site. This model is generally written as:

$$q_i^* = \frac{q_{1s} b_{1,i} c_i}{1 + b_{1,A} c_A + b_{1,B} c_B} + \frac{q_{2s} b_{2,i} c_i}{1 + b_{2,A} c_A + b_{2,B} c_B} \quad (i = A, B) \quad (2-7)$$

where  $q_{1s}$  and  $q_{2s}$  are the saturation capacities of the two sites;  $b_{1,i}$  and  $b_{2,i}$  are the equilibrium constants of the two sites for two components. This adsorption isotherm model is widely used in chiral drugs' simulation works in order to accurately describe the competitive retention mechanism of chiral molecules. In Zhang et al.'s research, pindolol enantiomers's adsorption isotherm on  $\alpha_1$ -acid glycoprotein chiral stationary phase was fitted to bi-Langmuir model, and the results were validated by using different

measurements [29]. Xu et al. successfully determined the five parameters of bi-Langmuir model for adsorption of ketoprofen on a Chiralpak AD column by using the inverse method [30]. Felinger et al. used and tested several kinds of isotherm models to define the adsorption behaviour of 1-indanol enantiomers, and the best-fit model was the bi-Langmuir model [31].

### 2.1.4.3 Performance parameters

In order to evaluate the separation performance of a SMB process, several important parameters introduced and calculated.

#### (1) Purity

As B is the less retained component, the purity of product B ( $Pur_B$ ) and A ( $Pur_A$ ) are defined as below:

$$Pur_B = \frac{\int_{t_0}^{t_s} c_{B,Raf} Q_R dt}{\int_{t_0}^{t_s} (c_{B,Raf} + c_{A,Raf}) Q_R dt} \quad (2-8)$$

$$Pur_A = \frac{\int_{t_0}^{t_s} c_{A,Ex} Q_E dt}{\int_{t_0}^{t_s} (c_{A,Ex} + c_{B,Ex}) Q_E dt} \quad (2-9)$$

Where  $c_{i,Raf}$  and  $c_{i,Ex}$  are the concentrations of the solute in the raffinate and extract products, respectively.

#### (2) Recovery

The recovery of component B ( $Rec_B$ ) is defined as the the ratio of the amount of B produced from the raffinate port to the amount of B fed into the system. Similar to B,  $Rec_A$  is determined in the same way.

$$Rec_B = \frac{\int_{t_0}^{t_s} c_{B,Raf} Q_R dt}{c_{B,feed} Q_{feed} t_s} \quad (2-10)$$

$$Re c_A = \frac{\int_{t_0}^{t_s} c_{A,Ex} Q_E dt}{c_{A,feed} Q_{feed} t_s} \quad (2-11)$$

### (3) Desorbent consumption

Desorbent consumption is one of the most serious problems we should concern in industrial applications. With the increased final products' quality, the solvent consumption amount should be controlled to a applicable and economic value. This parameter can be written as:

$$Dc = Q_D * t_s \quad (2-12)$$

### (4) Productivity

This parameter, Pro, is described by the ratio of the mass of feed to that of the stationary phase.

$$Pro = \frac{Q_F c_{T,F}}{(1 - \varepsilon) \rho_s V_T} \quad (2-13)$$

$c_{T,F}$  is the overall concentration of feed mixture,  $\rho_s$  is the density of the stationary phase.

## 2.2 SMB with variable conditions

Based on the standard SMB process, several modified technologies were developed with the improved product's quality and the reduced desorbent consumption. In this section, some typical systems are introduced.

### 2.2.1 Varicol system

Varicol as a novel chromatographic process was firstly reported by Ludemann-Hombourger et al. in 2000 [32]. It was modified by introducing a non-synchronous switch of the inlet and outlet ports during a global switching period. Varicol shows several advantages over the SMB technique due to the increased flexibility in column

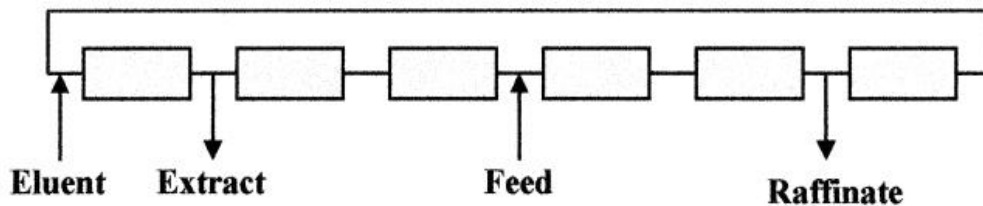
configurations at different sub-time intervals. The operation mechanism of varicol will be illustrated in details in this section.

In order to have a good understanding for Varicol, a conventional 6-column SMB set-up is introduced to make a comparison. As shown in figure 2-5 (a), section 1 and 4 have one column, while section 2 and 3 possess two columns, respectively. During one switching time  $t_s$ , the main differences between SMB and Varicol was exhibited in figure 2-5 (b) and (c). In a Varicol process:

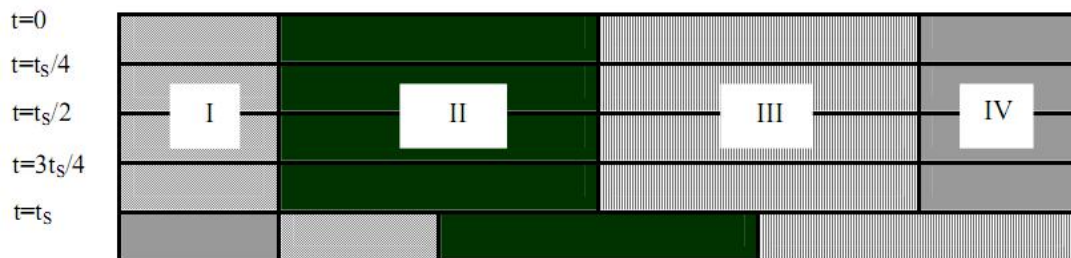
- The number of columns in each section is not constant, which means, the column configuration is not constant.
- The inlet and outlet ports are not shifted equally and simultaneously.
- The solid flow rate of the equivalent Varicol process is not constant with respect to the inlet and outlet ports.

In this way, Varicol process possesses higher flexibility than the simple SMB process, especially for some systems with a low number of columns.

**(a) 6-column set-up for SMB or Varical**



**(b) SMB configuration**



(c) Varicol configuration

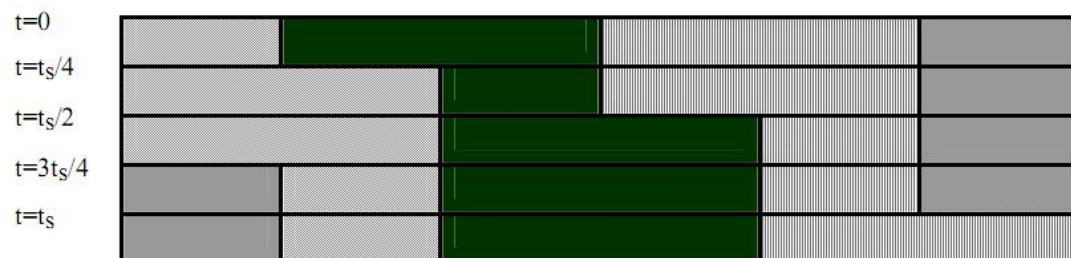


**Figure 2-5 Example of a 6-column SMB and Varicol configuration: switching of the lines over a period**

There are some works focus on Varicol system were published in the open literature. Zhang et al. conducted the multiobjective optimization of SMB and Varicol process for chiral separation, and they concluded that the performance of a Varicol was superior to that of SMB in terms of dealing with more feed solution while using less desorbent [33]. Subramani et al. completed a comprehensive optimization work for both SMB and Varicol system in separating the fructose from a mixture of glucose and fructose solution in 2003 [34]. In Pais et al.'s research paper, the separation performance of SMB and Varicol with a low number of columns (i.e. four, five. And six) was compared [35]. Yu et al. optimized the hydrolysis of methyl acetate by using SMBR and reactive Varicol, and the Varicol system performed better [36]. During recent years, Yao et al. investigated the switching strategies for achieving one certain average configuration of a Varicol system. Then, the improved strategies were applied on the optimization of the Varicol enantioseparation for 1,1-bi-2-naphthol and finally reduced the desorbent consumption by 17% comparing with SMB [37]. The feasibility and efficiency for the separation and purification of guaifenesin by using SMB and Varicol technologies were evaluated by

Gong et al. in 2014 [38].

### 2.2.2 SMB with variable flow rates

SMB with variable flow rates was firstly presented by Kloppenburg and Gilles in 1999 [39]. In this kind of process, the flow rates of four inlet/outlet ports ( $Q_F$ ,  $Q_R$ ,  $Q_D$ ,  $Q_E$ ) varied with time within one switching interval. Therefore, the internal flow rate of the whole system changed, which would lead to the different distribution of the solutes in the fluid and solid phase. The advantage of this method is to save the solvent consumption by varying the flow rates within one switching period. Nevertheless, the variable flow rates SMB was not widely applied due to the increased operation cost and design complexity.

### 2.2.3 Gradient SMB system

Conventional SMB units are operated under isothermal and isocratic conditions, and the selectivity between two components is constant in all sections. According to different roles of four sections in a SMB process, weak adsorption strength in section 1 and 2 and strong adsorption strength in section 3 and 4 are favorable. Therefore, if the separation of the components is difficult or a separation under conventional conditions is impossible, it is necessary to introduce the gradient SMB, which can effectively improve the separation performance by using temperature gradient, pressure gradient and solvent gradient.

#### **(1) Solvent-gradient SMB chromatography**

The most adopted way to achieve the solvent-gradient is introducing a desorbent with high elution strength, meanwhile, the feed stream is brought into the system with a lower solvent strength. In this way, the power of desorption in section 1 and 2 and the adsorption in section 3 and 4 is successfully improved. Consequently, the separation performance of SMB chromatography is improved in terms of productivity, solvent consumption, and product's quality.

In addition, selecting a suitable and desirable solvent is very important for this solvent-gradient SMB. There are diverse influence factors we should consider in this procedure,

such as the viscosity, diffusivity, and the heat generation during the mixing process [6].

In Antos and Seidel-Morgenstern's work, the two-step solvent gradient SMB process was analyzed numerically for linear equilibria. The results proved the great potential for this method [40]. Ziomek et al. focused on designing of the solvent gradient SMB by using a random search strategy and do the sensitivity analysis for SMB under gradient and isocratic conditions. Finally, the performance of gradient operation was superior [41]. Nam et al. successfully separated the two amino acids, phenylalanine and tryptophan, by using the solvent-gradient SMB process in 2012 [42]. Jiang et al.'s research work was proposed to separate two medium retained solutes (capsaicin and dihydrocapsaicin) from a quaternary mixture by using a three-zone SMB with solvent gradient in 2014 [43].

## **(2) Supercritical fluid SMB chromatography**

Supercritical fluid chromatography (SFC) always works above the critical temperature and pressure. Carbon dioxide (CO<sub>2</sub>) is widely used as the main component of the mobile phase in this system (the critical point is 31°C and 74 bar). The use of supercritical CO<sub>2</sub> offers the advantages of reduction in solvent cost, high flow rate, short equilibration time, high efficiency, non-toxic and non-flammable.

Clavier et al. is the first one combined the SFC with SMB and applied it to the separation of g-linolenic ethyl ester (GAL) and docosahex-aenoic ethyl ester (DHA) in 1996 [44]. The major advantages of SF-SMB contain easily obtaining concentrated product by evaporation of CO<sub>2</sub>, conducting pressure gradient SMB by setting different pressures in different sections, and adjusting the solvent powder by pressure. After the publication of Clavier et al.'s work, researchers from the TUHH (Hamburg University of Technology), ETH (Swiss Federal Institute of Technology) and Daicel Co. applied the supercritical fluid SMB to the separation of stereoisomers and enantiomers [45-48].

Recently, Cristancho et al. Extended the application of SF-SMB to the separation of ethyl linoleate and ethyl oleate on silica gel using supercritical carbon dioxide under linear conditions [49]. Some researchers have successfully used SF-SMB for the separation of bioactive compounds from natural resources. Liang et al. And Lin et al.

Completed the extraction of triterpenoids and lignans by using supercritical SMB, respectively [50, 51].

The variation of adsorption properties of this system increases the research complexity, and the solubility of most pharmaceutical components in pure CO<sub>2</sub> is limited. All these drawbacks can be solved by introducing a modifier, such as an alcohol or ether.

### **(3) Temperature-gradient SMB chromatography**

Except for the solvent gradient and pressure gradient, adsorption strength can also be adjusted by the variation of temperature. Temperature gradient can be controlled via direct and indirect mode [19]. The direct mode is achieved by using jackets of the column to modulate the column temperature. The indirect mode adjusts temperature of each individual column by inter-column heat exchangers. Another indirect mode works through the difference between feed and desorbent temperatures. One obvious limitation of this process is the non-instantaneous change of temperature, which has to be considered when a column switches and its temperature has to be changed.

Several research works have been reported to investigate the feasibility of temperature gradient SMB chromatography. Migliorini et al. assumed the temperature of four sections in SMB could be independently changed and then put forward the design strategy of non-isothermal SMB process [52]. Kim et al. and Jin et al. studied thermal four-zone SMB for the separation of toluene-xylene using simulations which were established by Aspen Chromatography v12.1 [53, 54]. Xu et al. successfully extended the temperature gradient SMB technique to a SMB reactor for the synthesis of methyl acetate. The results shown that the nonisothermal operations could effectively improve the SMBR's productivity [55]. Recently, Xu et al. investigated the feasibility of an internal temperature gradient established through a difference between feed and desorbent temperatures for ketoprofen enantiomers separation by using multi-objective optimization [19].

### **2.2.4 Sequential simulated moving bed (SSMB)**

Sequential simulated moving bed (SSMB) that has been already applied for the



commercial separation of fructose and glucose in industry, where solvent consumption is a major concern, introduces operational flexibility by dividing a switch into three steps with different flow patterns. As shown in Figure 2-6, in the 1<sup>st</sup> step, the mobile phase is circulated in the whole system, forming a closed loop; in the 2<sup>nd</sup> step, section IV is isolated and an external solvent stream is introduced at the desorbent port to purge the less adsorbed species to raffinate port; in the 3<sup>rd</sup> step, section II is also isolated and another feed stream is introduced such that preferentially and less adsorbed species are simultaneously collected at extract and raffinate ports, respectively.

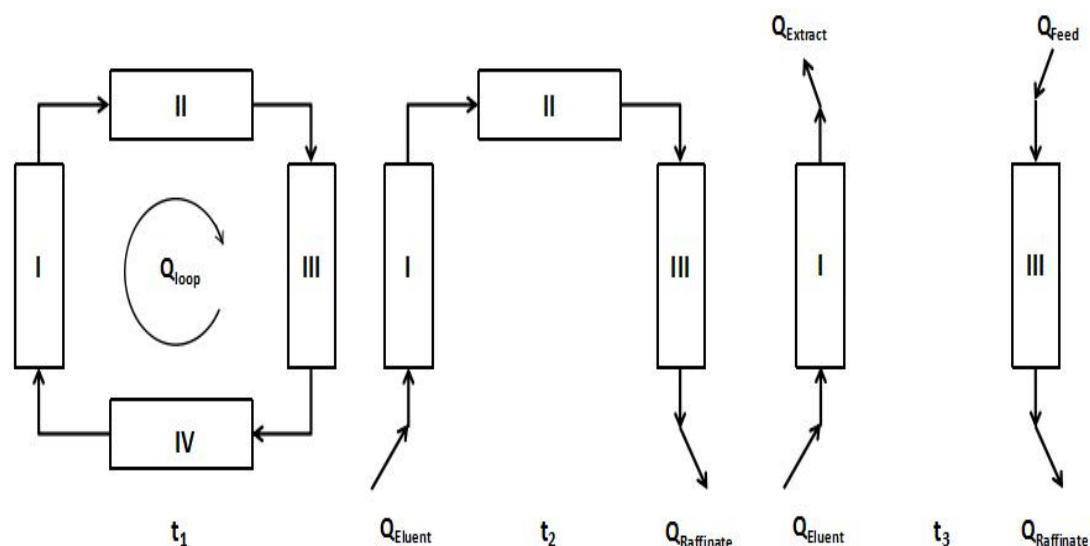


**Figure 2-6 Schematic diagram of SSMB process**

During last decades, there is no literature reported SSMB system and its simulation or optimization works. Actually, SSMB technique is a preferential choice for some large-scale separation processes in industry due to its low solvent consumption and flexible operation. In our work, we will mainly focus on this SSMB technique for the separation of xylo-oligosaccharides (XOS) syrup and conduct plenty of simulation and optimization works in order to achieve the further large-scale industrialization.

## 2.3 Application of SMB systems

The original application of SMB is known as the Parex process by UOP for extraction of

p-xylene from c8 aromatic mixture. SMB was mainly used in petrochemical industry before 1990s, such as the Orbex process, Parex and Ebex processes, Sarex process, and Molex process [56]. After that, SMB application was extended to sugar and pharmaceutical industry due to its high separation efficiency and low cost for some complicated systems. In recent years, this method also widely applied in some bio-products purification process. In this section, we summarized and investigated the developments and applications of SMB process in recent 10 years as shown in table 2-1[57-101].

**Table 2-1 Summary of applications of SMB technology in recent 10 years**

Substance investigated	Authors	Objectives	Description of the work	Conclusions and contributions
Paclitaxel	Mun and Wang (2008) Purdue University	Optimize the productivity of paclitaxel purification process under the constraints of product purity and zone flowrate;  Compare the simulation results between isocratic and solvent gradient SMB.	A solvent gradient SMB and an isocratic SMB for were designed and optimized;  Optimization variables: zone flow rates, switching time, and solvent concentrations in the desorbent and feed;  Optimization method: non-dominated sorting genetic algorithm with elitism and jumping genes (NSGA-II-JG) and rate model.	Paclitaxel was successfully separated from cephalomannine with the highest productivity by using a solvent gradient SMB;  In this case, the productivity of the gradient SMB can be increased to 11-fold that of the isocratic SMB.
Rolipram	Goncalves et al. (2008) University of Campinas	Purify the n-boc-Rolipram racemate by using SMB.	Experiments were carried out under diluted conditions;  Selectivity of this system: 1.26;  Henry's constants were determined.	Purification of racemic Rolipram was achieved by a laboratory 4-zone SMB unit.
Glycine and threonine	Makart et al. (2008) ETH Zurich	Integrate of a continuous SMB process and a enzyme membrane reactor;  Complete the biocatalytic production of L-allo-threonine;  Separate threonine from glycine.	Experiments were conducted on a lab-scale SMB unit under enzyme compatible conditions;  Mobile phase: aqueous eluents with minor content of organic co-solvent at neutral pH;  Stationary phase: a weak cation ex-changer, Amberlite CG-50 II.	Threonine was successfully separated from glycine;  The coupled SMB and bio-reactor shown great potential as a continuous tool;  This integration reduced possible operation points both for SMB and the reactor.

Capsaicin	Wei and Zhao (2008) Zhejiang University	Separate capsaicin from capsaicinoids by using SMB.	methanol/water (75/25, v/v) was used as mobile phase; ODS columns; Linear adsorption; Optimum operation conditions were determined by using triangle theory.	Capsaicin was separated from capsaicinoids.
Citric acid	Wu et al. (2009) Friedrich-Alexander-University	Purify the citric acid from fermentation broth; SMB simulations and design were conducted.	The hydrodynamics, thermodynamics and mass transfer characteristics in a single chromatographic column were determined; The transport dispersive model was used; SMB separation requirements: citric acid purity>99.8% and citric acid recovery>90%; The influences of the operating conditions on the SMB performance were investigated.	The TDM model showed a satisfactory prediction for this process; The 99.8% purity and 97.2% recovery were finally achieved.
Oxidative coupling of methane (OCM)	Kundu et al. (2009) University of Western Ontario	Modeling and simulation of SMBR for oxidative coupling of methane; Multi-objective optimization for this process.	Linear adsorption isotherm was used and determined by frontal analysis; Reaction kinetics parameters were obtained by fitting the literature experimental data to the kinetics model; Effects of operating parameters on the behavior of SMBR were studied; NSGA-II-JG was applied in optimization	The proposed mathematical model in SMBR demonstrated extremely good predictions of the experimental results; Performance of SMBR could be improved significantly under optimal operating conditions.

Pindolol	Zhang et al. (2009) University of Western Ontario	Multi-objective optimization of SMB and Varicol processes for separation of racemic pindolol.	Optimization variables: effect of feed concentration, eluent flow rate, column geometry, and column configuration; NSGA-II-JG was used to obtain the Pareto optimal solutions; The optimized solutions were verified experimentally.	Several two-objective optimization problems were solved simultaneously maximizing product purity and recovery for both SMB and Varicol processes.
Flurbiprofen	Ribeiro et al. (2009) University of Porto	Optimize the mobile phase composition for preparative chiral separation of flurbiprofen enantiomers.	An amylose-based chiral stationary phase (Chiralpak AD) was used; Solubility and adsorption isotherm measurements; Pulse and breakthrough experiments; Simulation works of SMB by using different mobile phase compositions were completed.	The results showed that a 10% ethanol/90% n-hexane mobile phase composition was the best choice; The modeling and simulation tools used in this work proved to be suitable for prediction.
$\beta$ -glucosidase	Sahoo et al. (2009) Lund University	Set-up an efficient SMB purification process for the separation of a cloned heat stable His-tagged $\beta$ -glucosidase.	A simplified approach based on an optimized single column protocol is used to design the open-loop SMB; Only the wash and elution are operated with columns in sequence.	$\beta$ -glucosidase was purified to almost single band purity with a purification factor of 15 and a recovery of 91%; SMB results showed reduced buffer consumption, higher purification fold, higher yield and productivity.

Ethyl lactate synthesis	Pereira et al. (2009) University of Porto	Conduct the synthesis of ethyl lactate using a simulated moving bed reactor (SMBR).	A mathematical model to describe the dynamic behaviour of the SMBR was developed and validated by experiments;  The effect of operating parameters on the SMBR performance was evaluated.	SMBR was proved a very attractive technology for the production of ethyl lactate;  The productivity of 32Kg/day and purity of 95% were achieved.
Nadolol	Lee and Wankat (2010) Purdue University	Separate a ternary mixture, nadolol isomers, by using a pseudo-simulated moving bed process.	Multi-objective optimization was carried out;  A four-objective, two-stage optimization method with PD model was used;  Design parameters, the position of step 1 and the number of port switches during step 2, were introduced.	Maximum productivity was up to 2 times higher and the minimum D/F was up to 50% lower than normal SMB;  Completely separate the ternary mixture with shorter column length.
(RS,RS)-2-(2,4-difluorophenyl)butane-1,2,3-triol	Acetti et al. (2010) ETH Zurich	Separate the (RS,RS)-2-(2,4-difluorophenyl)butane-1,2,3-triol enantiomers by using the intermittent simulated moving bed.	The effect of feed concentration on the choice of the operating conditions was presented;  The SMB experiments were designed according to triangle theory.	This is a new technology that has been demonstrated recently and is applied here for the first time to the separation of enantiomers;  Purity of 98% for both product streams, extract and raffinate, could be achieved.

Paclitaxel, 13-dehydroxybaccatin III, and 10-deacetylpaclitaxel	Kang et al. (2010) Hanyang University	Separate these three components by using a tandem simulated moving bed process.	This ternary separation was completed by using a process that consisted of two four-zone SMB units in series;  Adsorption isotherm and mass-transfer parameters were determined by a series of pulse experiments;  Standing wave design principle was applied for SMB experiments	The most optimal strategy of utilizing the tandem SMB was to recover paclitaxel in the first SMB unit and then separate the remaining two components in the second SMB unit.
Protein refolding	Freydell et al. (2010) Delft University of Technology	Refold a protein by batch size-exclusion chromatography and simulated moving bed size-exclusion chromatography (SMBSECR).	A statistical design of experiments was conducted;  A detailed model that accounts for both separation and refolding was used for analyzing the data;  The performance of SMBSECR and the SECR was compared.	Refolding yields of 50% was achieved;  The SMBSECR behaviour was correctly described by our model;  The solvent consumption was decreased.
Acetic acid	Nam et al. (2011) Hanyang University	Separate the acetic acid from biomass hydrolyzate on SMB by using Amberchrom-CG161C as the adsorbent.	The separation performance of Amberchrom-CG161C and Dowex99 was compared;  SMB optimization was conducted based on the standing wave design (SWD) method.	Amberchrom-CG161C offered higher selectivity between acetic acid and sugars than Dowex99.

Nucleoside mixture	Mun (2011) Hanyang University	Separate a ternary nucleoside mixture by using a five-zone SMB.	A ternary separation of a five-zone SMB was completed;  The effect of a partial-feeding application on the performance of a five-zone SMB was investigated.	The ternary separation performance was effectively improved by applying the partial-feeding;  Compare to the full-feeding mode, a higher throughput was achieved by partial-feeding.
Recombinant protein purification	Palani et al. (2011) Indian Institute of Technology-Madras	Select chromatographic system and determine the adsorption isotherm parameters.	The adsorption isotherms for streptokinase and a lumped impurity fraction present in an Escherichia coli cell lysate were determined by using perturbation method;	The Henry's constant of streptokinase was in a linear range;  These parameters were applied in the further SMB experiment design.
Recombinant protein purification	Gueorguieva et al. (2011) Otto von Guericke University Magdeburg	SMB experiment for recombinant protein purification was designed and validated.	A SMB process which contained a two-step salt gradient was design;  Equilibrium theory and an equilibrium stage model were applied;  A series of SMB experiments were carried out to validate the design strategy.	continuous purification of streptokinase by using a three-zone open-loop two-step gradient SMB process was achieved.  Theoretical and experimental results reached a good agreement.



Succinic acid and lactic acid	Nam et al. (2011) Kongju National University	Optimize the productivity of a SMB process for separation of succinic acid and lactic acid.	A series of single-column experiments were performed to determine the mass transfer parameters and the adsorption isotherms;  The measured data were validated by simulations;  SMB process was optimized based on the standing wave design (SWD) principle and NSGA-II-JG.	The optimal productivity was little affected by the pressure rating;  The productivity could have a 20% improvement with the elimination of the minimum switching time limit.
Phenylalanine and tryptophan	Nam et al. (2012) Hanyang University	Validate the optimization results of a solvent-gradient SMB process for separation of phenylalanine and tryptophan.	A lab-scale SG-SMB set-up was developed;  The optimization was completed by using genetic algorithm (GA);  Optimal operating conditions were obtained.	The experimental data were proved to agree closely with the modelling results.
Epigallocatechin gallate	Wang et al. (2012) University of Science & Technology Liaoning	Separate epigallocatechin gallate (EGCG) from tea polyphenol by using a two-step SMB approach.	C18-bonded silica gel and a mixture of methanol and water were used as the stationary phase and mobile phase, respectively;  Solvent gradient in zones I and II was established by the different methanol dosage;  The operating conditions of SMB were selected according to the triangle theory.	In the first step, a raffinate solution with 92.2% purity and 99.7% recovery of EGCG was collected;  In the second step, the purity and recovery of EGCG were increased to 97.8% and 99.8%.

Ethyl linoleate and ethyl oleate	Cristancho et al. (2012) Hamburg University of Technology	Separate the fatty acid ethyl esters by using a two-step supercritical fluid-simulated moving bed (SF-SMB).	Silica gel and supercritical carbon dioxide were used as the stationary phase and the mobile phase, respectively; Liner adsorption isotherms were determined and applied; A two-step SMB experiments were conducted.	Fatty acid with high commercial interest was successfully separated by using this SF-SMB approach.
$\alpha$ -Tocopherol	Wei et al. (2012) Zhejiang University	Separate the $\alpha$ -Tocopherol from its homologue mixture by using a two-feed SMB process.	The two-feed SMB was established by disconnecting section I from II and section III from IV in a four-zone SMB system; The internal concentration curve was analyzed.	$\alpha$ -Tocopherol was successfully separated from its homologue mixture; The productivity was greatly increased compared to the conventional SMB; The solvent consumption was reduced.
Influenza virus	Krober et al. (2013) Otto von Guericke University Magdeburg	Separate the influenza virus from contaminating proteins by using a open loop SMB method.	A size exclusion matrix was selected as the stationary phase; Different operating conditions were chosen and SMB experiments were conducted; Performance of SMB and single column chromatography was compared.	The productivity for this SMB process was up to 3.8 times higher than that in batch mode. The single column discontinuous chromatography could be replaced by this SMB process.

Single-chain antibody fragments	Cristancho et al. (2013) Otto von Guericke University Magdeburg	Investigate the adsorption-desorption behavior of a single-chain antibody fragment (ABF), and design a two-step pH-gradient SMB to purify this system.	A commercial immobilized metal ion affinity chromatography (IMAC) column was used; The adsorption isotherms of ABF and the impurity protein were determined by using pulse experiments; The influence of mobile phase pH was investigated; An open-loop three-zone two-step pH-gradient SMB was designed.	The complete separation conditions of this SMB process was successfully predicted by the equilibrium stage true moving bed model. SMB performed better than the batch operation.
Recombinant proteins	Wellhoefer et al. (2013) University of Natural Resources and Life Sciences Vienna	Combine the continuous inclusion body dissolution process with the refolding process based on the closed-loop SMB chromatography.	A continuous refolding process for recombinant proteins was achieved by SMB; Throughput, productivity, and buffer consumption were compared to the batch process.	The refolding and cleavage yield of proteins were increased by 10%; The refolding buffer consumption was significantly reduced.
Protein loaded nanoparticles	Satzer et al. (2014) University of Natural Resources and Life Sciences Vienna	Purify the the protein loaded nanoparticles by size exclusion chromatography using a four-zone SMB.	The operating conditions of SMB were determined by batch experiments and the triangle theory; Sephacryl300 26/70 mm column was used; switch times for BSA and beta casein were 5 min and 7 min, respectively.	In the case of BSA, 63% purity and 98% recovery of loaded nanoparticles were obtained; In the case of beta case, 89% purity and 90% recovery were achieved.

Guaifenesin enantiomers	Gong et al. (2014) University of Porto	Separate the guaifenesin enantiomers by using SMB process and Varicol process.	<p>The columns packed with cellulose tris 3,5-dimethylphenylcarbamate (Chiralcel OD) were used as the stationary phase;</p> <p>A mixture of n-hexane and ethanol was used as the mobile phase;</p> <p>Both SMB and Varicol experiments were designed and conducted.</p>	<p>Product with more than 99.0% purity was obtained in both processes;</p> <p>Productivity of SMB was 0.42 <math>\text{g}_{\text{enantiomer}}/\text{d cm}^3 \text{ CSP}</math>, and productivity of Varicol was 0.54 <math>\text{g}_{\text{enantiomer}}/\text{d cm}^3 \text{ CSP}</math>.</p>
Methionine	Fuereder et al. (2014) ETH Zuerich	Investigate the influence of the mobile phase and temperature on SMB performance.	<p>The adsorption isotherms, solubility, and column back pressure were regarded as the function of MeOH content and temperature;</p> <p>Based on this model, the optimal productivity was calculated and then the corresponding operating conditions were determined.</p>	<p>A moderate methanol content (25-35%) for this separation process was suggested;</p> <p>Higher temperature and lower back pressure were proved to perform better.</p>
Lanthanide and actinide	Sreedhar et al. (2014) Georgia Institute of Technology	Design a SMB process to separate lanthanides (Ln) and actinides (An).	<p>Reillex HPQ™ resin was used as the stationary phase, and 0.5-3.0 M nitric acid was used as the mobile phase;</p> <p>Model parameters for SMB design were measured by pulse experiments;</p> <p>A mathematical model was applied for prediction.</p>	<p>The optimal nitric acid concentration was 3.0 M.</p> <p>Product with 99.5% purity could be obtained.</p>

Cyclolinopeptides C and E extracted from flaxseed oil	Okinyo-Owiti et al. (2014) University of Saskatchewan	Separate cyclolinopeptides C and E by using a three-zone SMB.	An 8-column 3-zone SMB system comprising 3, 2, and 3 columns in zones 1, 2 and 3, respectively, was used; Absolute ethanol (100%) was used as the mobile phase.	This is the first time to use SMB in the separation of large quantities of Cyclolinopeptides; It seems SMB is a economical and high-production system for this difficult separation.
Glycol ether ester	Agrawal et al. (2014) Georgia Institute of Technology	Produce the propylene glycol methyl ether acetate by using ModiCon SMBR.	AMBERLYST™ 15 was used as a catalyst and adsorbent; The performance of the conventional SMBR and the modulation of the feed concentration (ModiCon) mode were investigated and compared; A multi-objective optimization approach was used to design the SMBR.	This is the first time to integrate ModiCon to SMBR operation; ModiCon showed a higher productivity by 12-36% than the conventional mode.
D-psicose	Wagner et al. (2015) ETH Zurich	Conduct the multi-objective optimization of SMB process for D-psicose separation.	Model parameters were measured by using the inverse method; A 2-2-2-2 lab-scale SMB set-up was prepared; Productivity and desorbent consumption were selected as the objectives in the optimization works.	The results proved the great potential of SMB method for the economic separation of the D-psicose from impurities.

Eicosapentaenoic acid and docosahexaenoic acid	Li et al. (2015) Zhejiang University	Separate the eicosapentaenoic acid and docosahexaenoic acid by using SMB method.	<p>C18 silica gel was used as the stationary phase, and the pure methanol was used as the mobile phase;</p> <p>Model parameters were measured by using pulse experiments;</p> <p>The Langmuir model was used to describe the adsorption behavior;</p> <p>SMB simulation works were completed.</p>	<p>With a feed concentration of 100 g/L, the product with 99% purity, 13.11 g/L adsorbent/h, and solvent consumption of 0.46 L/g could be obtained.</p> <p>The simulation result and the experimental data reached a good agreement.</p>
Agarose-hydrolyzate components	Kim et al. (2015) Hanyang University	Conduct a ternary separation of galactose, levulinic acid (LA), and 5-hydroxymethylfurfural (5-HMF) by using SMB.	<p>Model parameters were determined by using the frontal analysis;</p> <p>The obtained parameters were used to design the SMB experiments;</p> <p>The open-loop SMB experiments were carried out in the lab.</p>	<p>The experiment results agreed closely to the simulation predictions;</p> <p>These three components were separated with high purities, high yields, and high throughput.</p>
Sulfuric acid and sugars	Sun et al. (2016) Sichuan University	<p>Select suitable stationary phase to replace the unavailable Diaion MA03SS;</p> <p>Conduct SMB separation processes by using different kinds of resins.</p>	<p>Screening test of six kinds of resins was conducted by using pulse experiments;</p> <p>After the initial screening, Dowex 1X4 and Dowex 1X8 were selected to do the next SMB experiments.</p> <p>SMB performance of Diaion MA03SS, Dowex 1X4, and Dowex 1X8 was compared.</p>	<p>Performances of Dowex 1X8 was slightly higher than that of Diaion MA03SS and Dowex 1X4.</p>

Butanediol and propanediol	Liang et al. (2016) I-Shou University	Purify the 1, 3-propanediol (PDO) by using SMB chromatography.	Mitsubishi SP70 was used as the stationary phase; The influence of feeding concentration on separation was studied; Langmuir adsorption isotherms, kinetic parameters were determined by using pulse experiments; ASPEN was used in simulation.	Simulation results from ASPEN could reasonably fit the experimental data.
Praziquantel	Andrade Neto et al. (2016) Federal University of Rio de Janeiro	Present an adaptive control system based on a nonlinear model predictive control (NMPC) in SMB.	The main advantage of such model was described; The mathematical model, the optimization problem, and the control strategy were presented; Modeling, simulation, and optimization of SMB process were completed.	The purity of 99% and 98.6% for extract and raffinate products could be achieved; Fast responses and smooth actuation were observed.
Xylobiose	Choi et al. (2016) Hanyang University	Separate xylobiose from xylooligosaccharides by using SMB.	Dowex-50WX4 resin was selected as the stationary phase; Model parameters were determined by pulse experiments; Two sets of SMB experiments were carried out.	Xylobiose's purity of 99.5% and recovery of 92.3% were finally obtained. This method could be useful in the large scale industrial production.

Aminoglutethimide	Lin et al. (2016) University of Porto	Separate the aminoglutethimide enantiomers by using SMB and Varicol.	Cellulose tris 3,5-dimethylphenyl-carbamate was used as the stationary phase, and a mixture of n-hexane and ethanol was used as the mobile phase;  A five-column Varicol process with 1/1.5/1.5/1 configuration and a six-column SMB process with 1/2/2/1 configuration were conducted.	Final products of R-aminoglutethimide (R-AG) and S-aminoglutethimide (S-AG) with more than 99.0% purity were collected.
Glucose and fructose	Tangpromphan et al. (2018) Kasetsart University	Develop a operating strategy of the three-zone SMB process for the separation of glucose and fructose.	Decreasing both the desorbent consumption and the numbers of pump were the two main objectives;  The strategy PR-PCO-NFZIII was based on the principle of port-relocation and port-closing/opening technique.	With the PR-PCO-NFZIII in a three-zone SMB, the solvent consumption and the pumps needed were successfully decreased.
Tartronic and glyceric acids	Coelho et al. (2018) University of Porto	Separate the tartronic acid (TTA) and glyceric acid (GCA) by using SMB.	A 1-2-2-1 configuration SMB unit was used;  Dowex 50WX-2 was selected as the stationary phase;  SMB experiment, simulation, and optimization were completed.	The purity of 80% and 100% was obtained in the raffinate and extract ports, respectively;  Optimal operating conditions were obtained and could be applied in industrial process.



Fucose	Mun (2018) Hanyang University	Optimize the production rate, productivity, and product concentration of fucose in SMB separation process.	<p>The optimization was based on standing-wave-design method and genetic algorithm;</p> <p>The product concentration and pressure drop were chosen as constraints;</p> <p>Single optimization and multi-objective optimization were conducted.</p>	<p>A set of pareto optimal solutions was obtained;</p> <p>The results are useful in promoting the economically-efficient production of fucose.</p>
Betulinic, oleanolic, and ursolic acids	Aniceto et al. (2018) University of Aveiro	Separate the betulinic, oleanolic, and ursolic acids by using a two-step SMB process.	<p>Model parameters were determined by using frontal analysis;</p> <p>SMB was designed and optimized using a Design of Experiments approach combined with Response Surface Methodology (DoE-RSM), and simulated using a phenomenological rigorous model.</p>	The purities of betulinic, oleanolic, and ursolic acids at 99.4%, 99.1%, and 99.4% could be obtained.
Vanillin and syringaldehyde	Yao et al. (2018) Xiamen University	Separate vanillin from syringaldehyde by using an asynchronous 3-zone SMB.	<p>C18 was used as stationary phase and ethanol/water was used as mobile phase;</p> <p>Model parameters were determined by frontal analysis;</p> <p>The operating conditions of SMB were selected based on triangle theory;</p> <p>The results were compared to those in the conventional SMB process.</p>	<p>This asynchronous 3-zone SMB method was first reported in this paper;</p> <p>The feed flow rate was 44% higher than that of conventional SMB;</p> <p>The product purity of 97% was achieved.</p>

Fucose	Hong et al. (2019) Hanyang University	Produce fucose from the seaweed of <i>Undaria pinnatifida</i> by integrating a hydrolysis and a SMB process.	<p>A hydrolysis, and a series of pretreatment processing for decolorization and deionization were carried out;</p> <p>Single-column experiments were conducted to design the SMB;</p> <p>The resulting hydrolysate from the first step was then purified by using two sets of SMB process.</p>	<p>Fucose with purity of 99.9% was obtained;</p> <p>The overall fucose loss was kept below 23%.</p>
Aromatics/alkanes	Guo et al. (2019) Georgia Institute of Technology	Apply the concurrent approach to design a SMB process for aromatic/alkane separation.	<p>Mixture of toluene, dodecane, and cyclohexane was selected as the model system;</p> <p>A 16-column SMB mini-plant was designed and constructed;</p> <p>A concurrent approach which combined the adsorption measurements, model fitting, and SMB model predictions was developed.</p>	<p>Developed a complete SMB modelling process from isotherm to a “mini-plant” experiment for the first time.</p> <p>For some complicated systems, SMB could be conducted without the knowledge of multi-component adsorption isotherm.</p>

According to our knowledge, there is no reported literature on SSMB method, and no one conducted the numerical simulation or optimization works of SSMB process. For xylo-oligosaccharide, only Meng et al. investigated purification of XOS by using SMB experiments. However, detailed modeling and optimization are missed in their work.

## 2.4 Design strategies of SMB process

Triangle theory, standing wave concept, and separation volume analysis are the three most widely used design strategies for SMB separation. A brief description of these methods is given as below.

### 2.4.1 Triangle theory

Triangle theory, proposed by Storti et al. [102] and Mazzotti et al. [103] has been proven as a powerful tool for SMB process design. The net flow rate ratio,  $m_i$ , was introduced in order to design the SMB unit. In this theory, a triangle complete separation area is defined by a  $(m_{II}, m_{III})$  plane for the linear or non-linear isotherm with or without mass transfer resistance. Therefore, a criteria is developed to determine the value of  $m_i$  and then obtain the optimal operating conditions. The definition of  $m_i$  is as below.

$$m_i = \frac{Q_i t_s - V \varepsilon}{V(1 - \varepsilon)} \quad (2-14)$$

where  $Q_i$  is the flow rate of the fluid phase in section  $i$  of a SMB unit,  $V$  is the column volume,  $\varepsilon$  is the bed voidage, and  $t_s$  is the switching time.

#### (1) Linear isotherm

If a system with linear isotherm behavior and contains component A and B, and A is the more retained component (heavy component). Based on the mechanism of SMB chromatography, the complete separation requires the switching time larger than the retention time of component B and smaller than that of A. In this way, it ensures the

component B to be purged to the raffinate port without the pollution of impurity A. In addition, the complete recovery of B from the stationary phase avoids contaminating the extract port, and the component A remains in the stationary phase is eluted by the desorbent. Section I and IV are used for the regeneration of solid and liquid phase. Therefore, the switching time should be larger than the retention time of component A and smaller than the retention time of B, respectively. These constraints can be written as below.

$$\begin{aligned}
 t_{A,1}^R &\leq t_s \\
 t_{B,2}^R &\leq t_s \leq t_{A,2}^R \\
 t_{B,3}^R &\leq t_s \leq t_{A,3}^R \\
 t_s &\leq t_{B,4}^R
 \end{aligned} \tag{2-15}$$

Based on the definition of  $m_i$ , convert these constraints above into:

$$\begin{aligned}
 H_A &< m_I < \infty \\
 H_B &< m_{II} < H_A \\
 H_B &< m_{III} < H_A \\
 m_{IV} &< H_B
 \end{aligned} \tag{2-16}$$

An additional constraint,  $m_{II} < m_{III}$ , is required by the positive feed flow rate.

The complete separation zone defined by the the  $(m_{II}, m_{III})$  and  $(m_I, m_{IV})$  planes is shown in Figure 2-7.

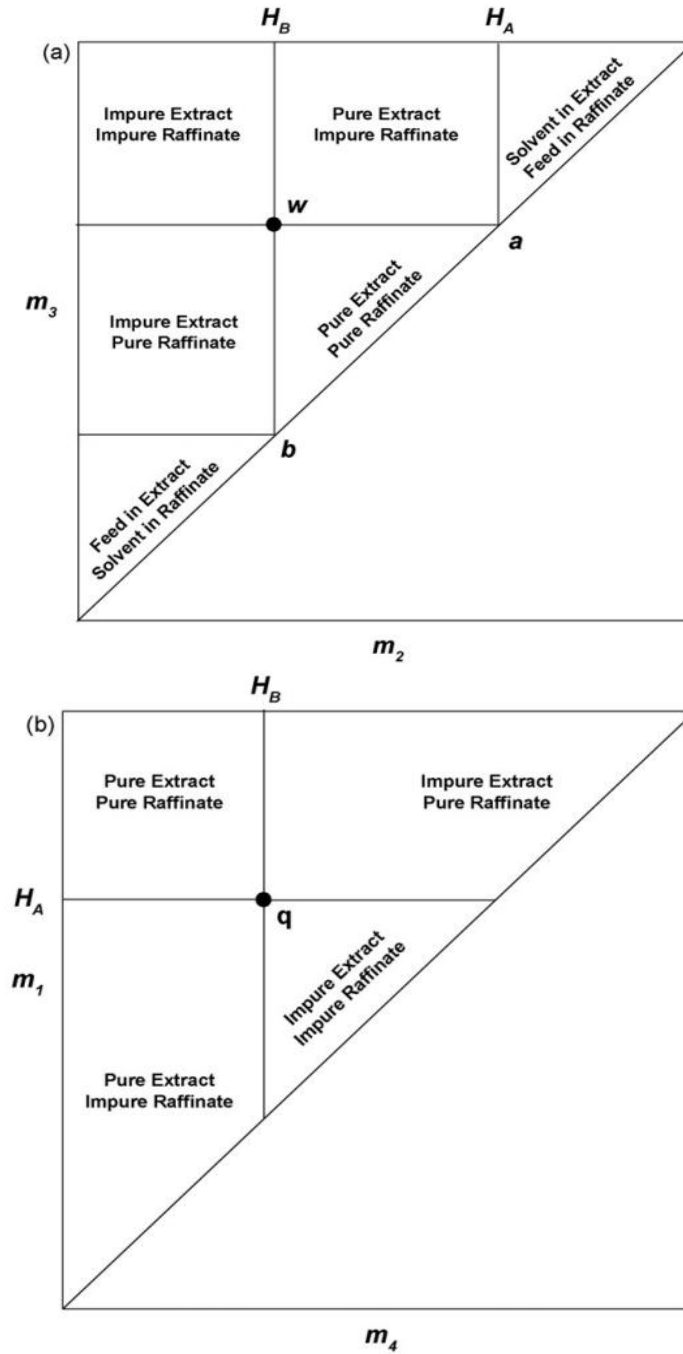


**Figure 2-7 Complete separation region and SMB operating regimes on (a) ( $m_{II}$ ,  $m_{III}$ ) plane and (b) ( $m_I$ ,  $m_{IV}$ ) plane for the binary separation of species A and B, with linear adsorption isotherm.**

## (2) Nonlinear isotherm

Triangle theory was further applied to nonlinear systems, the competitive Langmuir isotherm was chosen as an example in this section.

$$q_i = \frac{H_i c_i}{1 + \sum b_i c_i} \quad (i = A, B) \quad (2-17)$$

The following constraints were defined by Mazzotti et al. [104, 105].

$$\begin{aligned} H_A &= m_{I,\min} < m_I < \infty \\ m_{II,\min}(m_{II}, m_{III}) &< m_{II} < m_{III} < m_{III,\max}(m_{II}, m_{III}) \\ \frac{-\varepsilon_p}{1 - \varepsilon_p} &< m_{IV} < m_{IV,\max}(m_{II}, m_{III}) \\ &= \frac{1}{2} \{ H_B + m_{III} + b_B c_{B,f}(m_{III} - m_{II}) \} - \sqrt{[H_B + m_{III} + b_B c_{B,f}(m_{III} - m_{II})]^2 - 4H_B m_{III}} \end{aligned}$$

Compared with boundary of  $m_{II}$  and  $m_{III}$ , the lower bound on  $m_I$  and upper bound on  $m_{IV}$  are explicit. However, the complete separation region in the  $(m_{II}, m_{III})$  plane is still a triangle-shaped area as shown in Figure 2-8.

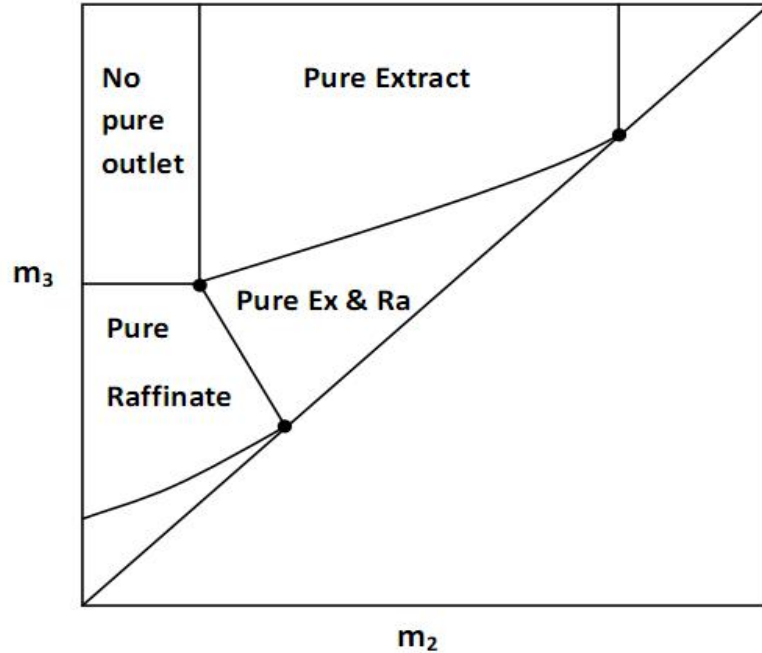


**Figure 2-8 Complete separation region and SMB operating regimes on the ( $m_{II}$ ,  $m_{III}$ ) plane for the binary separation with Langmuir adsorption isotherm.**

In addition, the shape of the triangle region is affected by the feed concentration [103]. The total area of this region will decrease with the increasing of feed concentration as shown in figure 2-9.

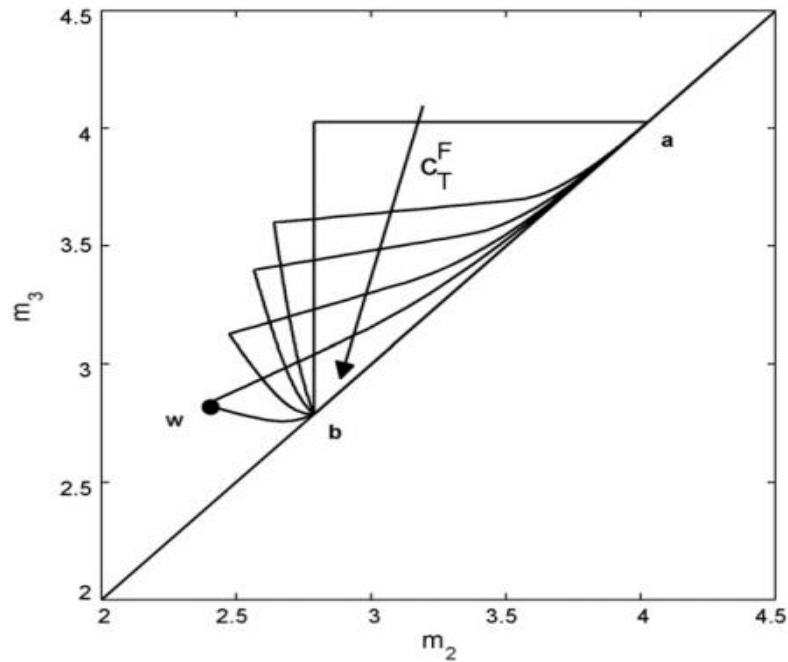


**Figure 2-9 Effect of the feed concentration on the complete separation region in the ( $m_{II}$ ,  $m_{III}$ ) plane [103]**

### 2.4.2 Standing wave concept

Standing wave analysis of chromatography was first reported by Ma et al. [106] and Mallmann et al. for linear and nonlinear systems, respectively [107]. This method contains a series of algebraic equations which effectively combine the separation performance with the axial dispersion coefficient, the length of each section in SMB, the bed movement velocity, and the velocities in the four sections. This design method is convenient, simple, and easy to implement. The optimal operating conditions could be

efficiently searched for some new SMB applications.

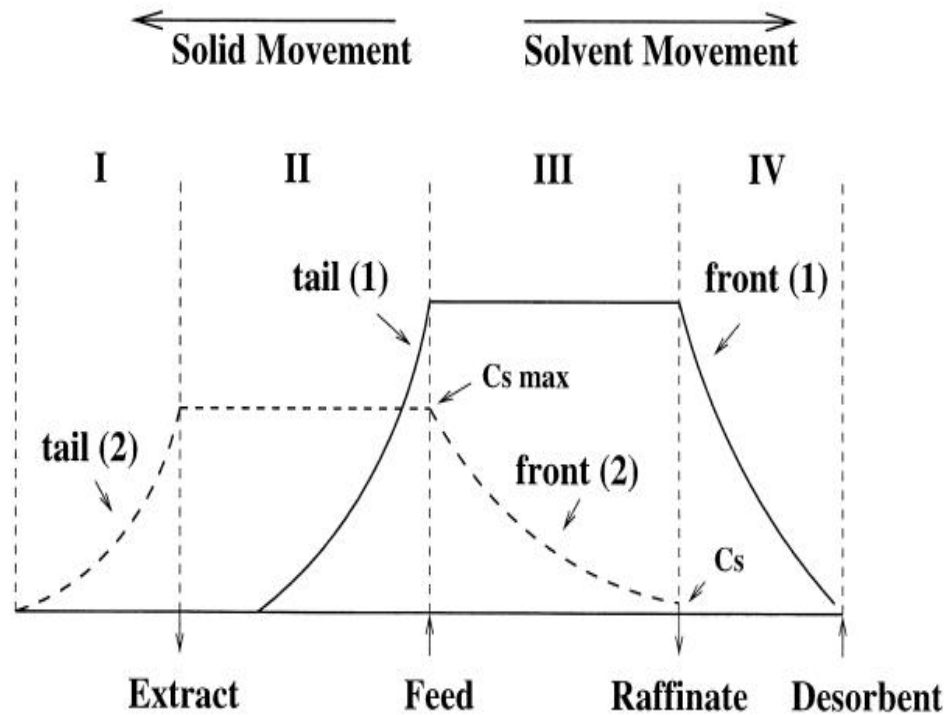


**Figure 2-10 Standing wave in a linear TMB system [108]**

For a binary system, the standing wave concept investigates the concentration waves of two components in each section. With a proper determination of the four flow rates in SMB and the solid movement velocity, the front of the light component B can be made “standing” in section IV and its desorption front standing in section II. While, the adsorption front of the more retained component A is made standing in section III and its desorption front standing in section I. In this way, the separation of component A and B is achieved as shown in figure 2-9.

To achieve high purity and recovery, according to the standing wave concept, the flow rates in the four sections must satisfy the following equations [108].



$$\begin{aligned}
(1 + P\delta_2)v - u_0^I &= -\beta_2^I \left( \frac{E_{b2}^I}{L^I} + \frac{Pv^2\delta_2^2}{K_{f2}^I L^I} \right) \\
(1 + P\delta_1)v - u_0^{II} &= -\beta_1^{II} \left( \frac{E_{b1}^{II}}{L^{II}} + \frac{Pv^2\delta_1^2}{K_{f1}^{II} L^{II}} \right) \\
(1 + P\delta_2)v - u_0^{III} &= \beta_2^{III} \left( \frac{E_{b2}^{III}}{L^{III}} + \frac{Pv^2\delta_2^2}{K_{f2}^{III} L^{III}} \right) \\
(1 + P\delta_1)v - u_0^{IV} &= \beta_1^{IV} \left( \frac{E_{b1}^{IV}}{L^{IV}} + \frac{Pv^2\delta_1^2}{K_{f1}^{IV} L^{IV}} \right)
\end{aligned} \tag{2-18}$$

$$\begin{aligned}
\frac{F^{feed}}{\varepsilon_b S} &= u_0^{III} - u_0^{II} \\
\frac{F^{des}}{\varepsilon_b S} &= u_0^I - u_0^{IV}
\end{aligned}$$

Where  $u_0$  is the interstitial velocity,  $L$  is the zone length,  $S$  is the column cross sectional area,  $E_b$  is the axial dispersion coefficient,  $K_f$  is the lumped mass-transfer coefficient,  $\delta_i = \varepsilon_p + (1 - \varepsilon_p)\alpha_i$  ( $\alpha_i$  is the partition constant between the adsorbed phase and the liquid phase for solute  $i$ ),  $P = (1 - \varepsilon_b)/\varepsilon_b$  is the bed phase ratio,  $\varepsilon_b$  is the interparticle void fraction, and  $\varepsilon_p$  is the intraparticle void fraction.  $\beta$  is related to the ratio of the highest concentration to the lowest concentration of the standing wave in the specified zone. It is always used as an index of product purity and yield. For example, the higher the  $\beta_2^{III}$  value, the higher the product purity of light solute in the raffinate.

Except for the research works above, Wu et al. and Xie et al. successfully applied this design strategy to amino acid separation by using SMB [109, 110]. In Xie et al.'s work, they extended the analysis to the SMB systems with nonlinear isotherms and mass transfer effects. Xie et al. also studied a tandem SMB process for insulin purification, and the standing wave analysis was used to obtain the optimal operating parameters [111].

### 2.4.3 Separation volume analysis

The triangle theory mainly provides a design strategy for the binary counter-current SMB separation with the neglect of mass transfer resistances and axial dispersion. However, if the mass transfer resistances are significant, the constraints are not as simple as

described in the triangle theory. The complete separation region will become narrower, and the constraints should be modified depending on the mass transfer coefficient. In order to define this new separation region, the separation volume analysis is developed [112, 113].

For the purpose of designing a SMB process, some constraints have to be satisfied as below.

$$\frac{Q_1 c_{B1}}{Q_s q_{B1}} > 1; \quad \frac{Q_2 c_{A2}}{Q_s q_{A2}} > 1 \quad \text{and} \quad \frac{Q_2 c_{B2}}{Q_s q_{B2}} < 1;$$

$$\frac{Q_3 c_{A3}}{Q_s q_{A3}} > 1 \quad \text{and} \quad \frac{Q_3 c_{B3}}{Q_s q_{B3}} < 1; \quad \frac{Q_4 c_{A4}}{Q_s q_{A4}} < 1$$

where  $Q_1, Q_2, Q_3,$  and  $Q_4$  are the volumetric liquid flow rates in each section;  $Q_s$  is the solid flow rate;  $c_{Aj}$  and  $c_{Bj}$  are the concentrations of component A and B in the liquid phase;  $q_{Aj}$ ,  $q_{Bj}$  are the concentrations of component A and B in the stationary phase in section  $j$ .

Defining the parameter  $\gamma_j = (1-\epsilon)m_j/\epsilon$  as the ratio between fluid and solid interstitial velocities in section  $j$ , the constraints become:

$$\gamma_1 > \frac{1-\epsilon}{\epsilon} \frac{q_{B1}}{c_{B1}}; \quad \frac{1-\epsilon}{\epsilon} \frac{q_{A2}}{c_{A2}} < \gamma_2 < \frac{1-\epsilon}{\epsilon} \frac{q_{B2}}{c_{B2}};$$

$$\frac{1-\epsilon}{\epsilon} \frac{q_{A3}}{c_{A3}} < \gamma_3 < \frac{1-\epsilon}{\epsilon} \frac{q_{B3}}{c_{B3}}; \quad \gamma_4 < \frac{1-\epsilon}{\epsilon} \frac{q_{A4}}{c_{A4}}$$

A higher value of  $\gamma_1$  is required in the presence of mass transfer resistances, and  $\gamma_1$  will increase with the decreasing of mass transfer coefficient. The complete separation regions will vary with different values of  $\gamma_j$ .

Azeved and Rodrigues applied this design method to a fructose-glucose SMB separation in 2001 [114]. As there was a strong mass transfer resistance presented in their system, they used this separation volume analysis in the modeling, simulation, design, and operation processes. After that, Minceva and Rodrigues determined the optimal operating

conditions for the separation of p-xylene, and proposed a two-level optimization procedure based on the concept of “separation volume” [115]. Rodrigues and Pais also extended the application of this strategy to the chiral separation design [116].

## 2.5 References

- [1] Rajendran, A., Paredes, G., and Mazzotti, M.. Simulated moving bed chromatography for the separation of enantiomers. *Journal of Chromatography A*, 2009, (1216): 709-738.
- [2] Wankat, P.C.. Large-scale adsorption and chromatography. Boca Raton, FL: CRC Press, 1986.
- [3] Juza, M., Mazzotti, M., and Morbidelli, M.. Simulated moving-bed chromatography and its application to chirotechnology. *Trends Biotechnol.*, 2000, (18): 108-118.
- [4] Mazzotti, M.. Equilibrium theory based design of simulated moving bed processes for a generalized Langmuir isotherm. *J. Chromatogr. A*, 2006, (1126): 311-322.
- [5] Broughton, D.B., and Gerhold, C.G.. Continuous sorption process employing fixed bed of sorbent and moving inlets and outlets. US Patent 2 985 589. 1961.
- [6] Schmidt-Traub, H.. Preparative chromatography. Germany: WILEY-VCH, 2005.
- [7] Guiochon, G., Golshan-Shirazi, S., and Katti, A.. Fundamentals of preparative and nonlinear chromatography. Boston: Academic Press, 1994.
- [8] Guiochon, G., and Lin, B.. Modeling for preparative chromatography. London: Academic Press, 2003.
- [9] Ruthven, D. M.. Principles of adsorption and adsorption processes. New York: John Wiley & Sons, 1984.
- [10] Seidel-Morgenstern, A., Heuer, C., and Hugo, P.. Experimental investigation and modelling of closed-loop recycling in preparative chromatography. *Chem. Eng. Sci.*,

1995, (7): 1115-1127.

[11] Lapidus, L., and Amundson, N.R. A descriptive theory of leaching: Mathematics of adsorption beds. *J. Phys. Chem.*, 1952, (56): 984-988.

[12] Van Deemter, J. J., Zuiderweg, F. J., and Klinkenberg, A.. Longitudinal diffusion and resistance to mass transfer as causes of nonideality in chromatography. *Chem. Eng. Sci.*, 1956, (5): 271-289.

[13] Zhang, Y., Hidajata, K., and Ray, A.K.. Multi-objective optimization of simulated moving bed and Varicol processes for enantio-separation of racemic pindolol. *Separation and Purification Technology*, 2009, (65): 311-321.

[14] Ahmad, T., and Guiochon, G.. Numerical determination of the adsorption isotherms of tryptophan at different temperatures and mobile phase compositions. *Journal of Chromatography A*, 2007, (2): 148-163.

[15] Yu, W.F., Hidajat, K., and Ray, A.K.. Determination of adsorption and kinetic parameters for methyl acetate esterification and hydrolysis reaction catalyzed by Amberlyst 15. *Applied Catalysis A*, 2004, (260): 191-205.

[16] Mao, S.M., Zhang, Y., Rohani, S., Ray, A.K.. Chromatographic resolution and isotherm determination of (R,S)-mandelic acid on Chiralcel-OD column. *J. Sep. Sci.*, 2012, (35): 2273-2281.

[17] Xu, J., Jiang, X.X., Guo, J.H., Chen, Y.T., Yu, W.F.. Competitive adsorption equilibrium model with continuous temperature dependent parameters for naringenin enantiomers on Chiralpak AD column. *Journal of Chromatography A*, 2015, (1422): 163-169.

[18] Li, H., Jiang, X.X., Xu, W., Chen, Y.T., Yu, W.F., and Xu, J.. Numerical determination of non-Langmuirian adsorption isotherms of ibuprofen enantiomers on Chiralcel OD column using ultraviolet-circular dichroism dual detector. *Journal of Chromatography A*, 2016, (1435): 92-99.

- [19] Jiang, X.X., Zhu, L., Yu, B., Su, Q., Xu, J., Yu, W.F.. Analyses of simulated moving bed with internal temperature gradients for binary separation of ketoprofen enantiomers using multi-objective optimization: Linear equilibria. *Journal of Chromatography A*, 2018, (1531): 131-142.
- [20] Long, N.Y.D., Le, T.H., Kim, J., Lee, J.W., and Koo, Y.M.. Separation of D-psicose and D-fructose using simulated moving bed chromatography. *J. Sep. Sci.*, 2009, (32): 1987-1995.
- [21] Vankova, K., Gramblicka, M., and Polakovic, M.. Single-component and binary adsorption equilibria of fructooligosaccharides, glucose, fructose, and sucrose on a Ca-form cation exchanger. *Journal of Chemical & Engineering Data*, 2010, (55): 405-410.
- [22] Vankova, K., and Polakovic, M.. Design of fructooligosaccharide separation using simulated moving bed chromatography. *Chem. Eng. Technol.*, 2012, (35): 161-168.
- [23] Wisniewski, L., Antosova, M., and Polakovic, M.. Simulated moving bed chromatography separation of galacto-oligosaccharides. *Acta Chimica Slovaca*, 2013, (6): 206-210.
- [24] Wisniewski, L., Pereira, C.S.M., Polakovic, M., and Rodrigues, A.E.. Chromatographic separation of prebiotic oligosaccharides. Case study: separation of galacto-oligosaccharides on a cation exchanger. *Adsorption*, 2014, (20): 483-492.
- [25] Jandera, P., Buncekova, S., Mhlbachler, K., Guiochon, G., Backovska, V., and Planeta, J.. Fitting adsorption isotherms to the distribution data determined using packed micro-columns for high-performance liquid chromatography. *Journal of Chromatography A*, 2001, (925): 19-29.
- [26] Skavrada, M., Jandera, P., Cherrak, D.E., Aced, A., and Guiochon, G.. Adsorption isotherms and retention behavior of 1,1-bis(2-naphthol) on CHIRIS AD1 and CHIRIS AD2 columns. *Journal of Chromatography A*, 2003, (1016): 143-154.
- [27] Wang, X., and Ching, C.B.. Determination of the competitive adsorption isotherms of nadolol enantiomers by an improved h-root method. *Ind. Eng. Chem. Res.*, 2003, (42):

6171-6180.

[28] Da Silva Jr., I.J., Garcia dos Santos, M.A., De Veredas, V., and Santana, C.C.. Experimental determination of chromatographic separation parameters of ketamine enantiomers on MCTA. *Separation and Purification Technology*, 2005, (43): 103-110.

[29] Zhang, Y., Hidajat, K., and Ray, A.K.. Determination of competitive adsorption isotherm parameters of pindolol enantiomers on  $\alpha_1$ -acid glycoprotein chiral stationary phase. *Journal of Chromatography A*, 2006, (1131): 176-184.

[30] Xu, J., Zhu, L., Xu, G.Q., Yu, W.F., and Ray, A.K.. Determination of competitive adsorption isotherm of enantiomers on preparative chromatographic columns using inverse method. *Journal of Chromatography A*, 2013, (1273): 49-56.

[31] Felinger, A., Zhou, D.M., and Guiochon, G.. Determination of the single component and competitive adsorption isotherms of the 1-indanol enantiomers by the inverse method. *Journal of Chromatography A*, 2003, (1005): 35-49.

[32] Ludemann-Hombourger, O., Nicoud, R.M., and Bailly, M.. The "VARICOL" process: a new multicolumn continuous chromatographic process. *Sep. Sci. Technol.*, 2000, (12): 1829-1862.

[33] Zhang, Z.Y., Hidajat, K., and Ray, A.K.. Multiobjective optimization of SMB and Varicol process for chiral separation. *AIChE Journal*, 2002, (12): 2800-2816.

[34] Subramani, H.J., Hidajat, K., and Ray, A.K.. Optimization of simulated moving bed and Varicol processes for glucose-fructose separation. *Trans IChemE*, 2003, (81): 549-567.

[35] Pais, L.S., and Rodrigues, A.E.. Design of simulated moving bed and Varicol processes for preparative separations with a low number of columns. *Journal of Chromatography A*, 2003, (1006): 33-44.

[36] Yu, W.F., Hidajat, K., and Ray, A.K.. Optimization of reactive simulated moving bed and Varicol systems for hydrolysis of methyl acetate. *Chemical Engineering Journal*,

2005, (112): 57-72.

[37] Yao, C.Y., Tang, S.K., Yao, H.M., O. Tade, M., and Xu, Y.Y.. Study on the number of decision variables in design and optimization of Varicol process. *Computers and Chemical Engineering*, 2014, (68): 114-122.

[38] Gong, R.J., Lin, X.J., Li, P., Yu, J.G., and Rodrigues, A.E.. Experiment and modeling for the separation of guaifenesin enantiomers using simulated moving bed and Varicol units. *Journal of Chromatography A*, 2014, (1363): 242-249.

[39] Kloppenburg, E. and Gilles, E.D.. A new concept for operating simulated moving-bed process. *Chem. Eng. Technol.*, 1999, (22): 813-817.

[40] Antos, D., and Seidel-Morgenstern, A.. Two-step solvent gradients in simulated moving bed chromatography: numerical study for linear equilibria. *J. Chromatogr. A*, 2002, (1): 77-91.

[41] Ziomek, G., and Antos, D.. Stochastic optimization of simulated moving bed process: sensitivity analysis for isocratic and gradient operation. *Comput. Chem. Eng.*, 2005, (7): 1577-1589.

[42] Nam, H.G., Jo, S.H., Park, C., and Mun, S.. Experimental validation of the solvent-gradient simulated moving bed process for optimal separation of phenylalanine and tryptophan. *Process Biochem.*, 2012, (3): 401-409.

[43] Jiang, C., Huang, F., and Wei, F.. A pseudo three-zone simulated moving bed with solvent gradient for quaternary separations. *J. Chromatogr. A*, 2014, (1334): 87-91.

[44] Clavier, J.Y., Nicoud, R.M., and Perrut, M.. A new efficient fractionation process: the simulated moving bed with supercritical eluent. *High Pressure Chemical Engineering*, 1996, (12): 429-434.

[45] Depta, A., Giese, T., Johannse, M., and Brunner, G.. Separation of stereoisomers in a simulated moving bed-supercritical fluid chromatography plant. *J. Chromatography A*, 1999, (865): 175-186.

- [46] Denet, F., Hauck, W., Nicoud, R.G., Giovanni, O.D., Mazzotti, M., Jaubert, J.N., and Morbidelli, M.. Enantioseparation through supercritical fluid simulated moving bed (SF-SMB) chromatography. *Industrial and Engineering Chemistry Research*, 2001, (40): 4603-4609.
- [47] Peper, S., Lubbert, M., Johannsen, M., and Brunner, G.. Separation of ibuprofen enantiomers by supercritical fluid simulated moving bed chromatography. *Separation Science and Technology*, 2002, (37): 2545-2566.
- [48] Rajendran, A., Peper, S., Johannsen, M., Mazzotti, M., Morbidelli, M., and Brunner, G.. Enantioseparation of 1-phenyl-1-propanol by supercritical fluid-simulated moving bed chromatography. *J. Chromatography A*, 2005, (1092): 55-64.
- [49] Cristancho, C.A.M., Peper, S., and Johannsen, M.. Supercritical fluid simulated moving bed chromatography for the separation of ethyl linoleate and ethyl oleate. *J. Supercritical Fluids*, 2012, (66): 129-136.
- [50] Liang, M.T., Liang, R.C., Huang, L.R., Liang, K.Y., Chien, Y.L., and Liao, J.Y.. Supercritical fluids as the desorbent for simulated moving bed—Application to the concentration of triterpenoids from *Taiwanofugus camphorata*. *Journal of the Taiwan Institute of Chemical Engineers*, 2014, (45): 1225-1232.
- [51] Lin, C.H., Lin, H.W., Wu, J.Y., Houn, J.Y., Wan, H.P., Yang, T.Y., and Liang, M.T.. Extraction of lignans from the seed of *Schisandra chinensis* by supercritical fluid extraction and subsequent separation by supercritical fluid simulated moving bed. *J. of Supercritical Fluids*, 2015, (98): 17-24.
- [52] Migliorini, C., Wendlinger, M., Mazzotti, M., and Morbidelli, M.. Temperature gradient operation of a simulated moving bed unit. *Ind. Eng. Chem. Res.*, 2001, (12): 2606-2617.
- [53] Kim, J.K., Abunasser, N., Wankat, P.C., Stawarz, A., and Koo, Y.. Thermally assisted simulated moving bed systems. *Adsorption*, 2005, (1): 579-584.



- [54] Jin, W., and Wankat, P.C.. Thermal operation of four-zone simulated moving beds. *Ind. Eng. Chem. Res.*, 2007, (22): 7208-7220.
- [55] Xu, J., Liu, Y.M., Xu, G.Q., Yu, W.F., and Ray, A.K.. Analysis of a nonisothermal simulated moving-bed reactor. *AIChE J.* 2013, (12): 4705-4714.
- [56] Ruthven, D.M., and Ching, C.B.. Counter-current and simulated counter-current adsorption separation processes. *Chemical Engineering Science*, 1989, (44): 1011-1038.
- [57] Mun, S.Y., and Wang, N.L.. Optimization of productivity in solvent gradient simulated moving bed for paclitaxel purification. *Process Biochemistry*, 2008, (43): 1407-1418.
- [58] Goncalves, C.V., Carpes, M.J.S., Correia, C.R.D., and Santana, C.C.. Purification of n-boc-Rolipram racemate on chiral stationary phase using simulated moving bed chromatography under linear conditions. *Biochemical Engineering Journal*, 2008, (40): 526-536.
- [59] Makart, S., Bechtold, M., Panke, S.. Separation of amino acids by simulated moving bed under solvent constrained conditions for the integration of continuous chromatography and biotransformation. *Chemical Engineering Science*, 2008, (63): 5347-5355.
- [60] Wei, F., and Zhao, Y.X.. Separation of capsaicin from capsaicinoids by simulated moving bed chromatography. *Journal of Chromatography A*, 2008, (1187): 281-284.
- [61] Wu, J.L., Peng, Q.J., Arlt, W., and Minceva, M.. Model-based design of a pilot-scale simulated moving bed for purification of citric acid from fermentation broth. *Journal of Chromatography A*, 2009, (1216): 8793-8805.
- [62] Kundu, P.K., Zhang, Y., and Ray, A.K.. Modeling and simulation of simulated countercurrent moving bed chromatographic reactor for oxidative coupling of methane. *Chemical Engineering Science*, 2009, (64): 5143-5152.
- [63] Kundu, P.K., Zhang, Y., and Ray, A.K.. Multi-objective optimization of simulated

countercurrent moving bed chromatographic reactor for oxidative coupling of methane. *Chemical Engineering Science*, 2009, (64): 4137-4149.

[64] Ribeiro, A.E., Graca, N.S., Pais, L.S., and Rodrigues, A.E.. Optimization of the mobile phase composition for preparative chiral separation of flurbiprofen enantiomers. *Separation and Purification Technology*, 2009, (68): 9-23.

[65] Sahoo, D., Andersson, J., and Mattiasson, B.. Immobilized metal affinity chromatography in open-loop simulated moving bed technology: Purification of a heat stable histidine tagged  $\beta$ -glucosidase. *Journal of Chromatography B*, 2009, (877): 1651-1656.

[66] Pereira, C.S.M., Zabka, M., Silva, V.M.T.M., and Rodrigues, A.E.. A novel process for the ethyl lactate synthesis in a simulated moving bed reactor (SMBR). *Chemical Engineering Science*, 2009, (64): 3301-3310.

[67] Lee, J.W., and Wankat, P.C.. Design of pseudo-simulated moving bed process with multi-objective optimization for the separation of a ternary mixture: Linear isotherms. *Journal of Chromatography A*, 2010, (1217): 3418-3426.

[68] Acetti, D., Langel, C., Brenna, E., Fuganti, C., and Mazzotti, M.. Intermittent simulated moving bed chromatographic separation of (RS,RS)-2-(2,4-difluorophenyl)butane-1,2,3-triol. *Journal of Chromatography A*, 2010, (1217): 2840-2846.

[69] Kang, S.H., Kim, J.H., and Mun, S.Y.. Optimal design of a tandem simulated moving bed process for separation of paclitaxel, 13-dehydroxybaccatin III, and 10-deacetylpaclitaxel. *Process Biochemistry*, (45): 1468-1476.

[70] Freydell, E.J., Bulsink, Y., Hateren, S., van der Wielen, L., Eppink, M., and Ottens, M.. Size-exclusion simulated moving bed chromatographic protein refolding. *Chemical Engineering Science*, 2010, (65): 4701-4713.

[71] Nam, H.G., Jo, S.H., and Mun, S.Y.. Comparison of Amberchrom-CG161C and Dowex99 as the adsorbent of a four-zone simulated moving bed process for removal of

acetic acid from biomass hydrolyzate. *Process Biochemistry*, 2011, (46): 2044-2053.

[72] Mun, S.Y.. Effect of a partial-feeding application on product purities and throughput of a five-zone simulated moving bed process for the separation of a ternary nucleoside mixture. *Process Biochemistry*, 2011, (46): 977-986.

[73] Palani, S., Gueorguieva, L., Rinas, U., Seidel-Morgenstern, A., and Jayaraman, G.. Recombinant protein purification using gradient-assisted simulated moving bed hydrophobic interaction chromatography. Part I: Selection of chromatographic system and estimation of adsorption isotherms. *Journal of Chromatography A*, 2011, (1218): 6396-6401.

[74] Gueorguieva, L., Palani, S., Rinas, U., Jayaraman, G., and Seidel-Morgenstern, A.. Recombinant protein purification using gradient-assisted simulated moving bed hydrophobic interaction chromatography. Part II: Process design and experimental validation. *Journal of Chromatography A*, 2011, (1218): 6402-6411.

[75] Nam, H.G., Han, M.G., Yi, S.C., Chang, Y.K., Mun, S.Y., and Kim, J.H.. Optimization of productivity in a four-zone simulated moving bed process for separation of succinic acid and lactic acid. *Chemical Engineering Journal*, 2011, (171): 92-103.

[76] Wang, S.Y., Liang, Y., and Zheng, S.W.. Separation of epigallocatechin gallate from tea polyphenol by simulated moving bed chromatography. *Journal of Chromatography A*, 2012, (1265): 46-51.

[77] Wei, F., Shen, B., Chen, M.J., Zhou, X.B., and Zhao, Y.X.. Separation of  $\alpha$ -Tocopherol with a two-feed simulated moving bed. *Separation Science and Engineering*, 2012, (4): 673-678.

[78] Krober, T., Wolff, M.W., Hundt, B., Seidel-Morgenstern, A., and Reichl, U.. Continuous purification of influenza virus using simulated moving bed chromatography. *Journal of Chromatography A*, 2013, (1307): 99-110.

[79] Cristancho, C.A.M., David, F., Franco-Lara, E., Seidel-Morgenstern, A.. Discontinuous and continuous purification of single-chain antibody fragments using

immobilized metal ion affinity chromatography. *Journal of Biotechnology*, 2013, (163): 233-242.

[80] Wellhoefer, M., Sprinzl, W., Hahn, R., and Jungbauer, A.. Continuous processing of recombinant proteins: Integration of inclusion body solubilization and refolding using simulated moving bed size exclusion chromatography with buffer recycling. *Journal of Chromatography A*, 2013, (1319): 107-117.

[81] Satzer, P., Wellhoefer, M., Jungbauer, A.. Continuous separation of protein loaded nanoparticles by simulated moving bed chromatography. *Journal of Chromatography A*, 2014, (1349): 44-49.

[82] Gong, R.J., Lin, X.J., Li, P., Yu, J.G., and Rodrigues, A.E.. Experiment and modeling for the separation of guaifenesin enantiomers using simulated moving bed and Varicol units. *Journal of Chromatography A*, 2014, (1363): 242-249.

[83] Fuereder, M., Majeed, I.N., Panke, S., and Bechtold, M.. Model-based identification of optimal operating conditions for amino acid simulated moving bed enantioseparation using a macrocyclic glycopeptide stationary phase. *Journal of Chromatography A*, 2014, (1346): 34-42.

[84] Sreedhar, B., Hobbs, D.T., Kawajiri, Y.. Simulated moving bed chromatography designs for lanthanide and actinide separations using Reillex HPQ™ resin. *Separation and Purification Technology*, 2014, (136): 50-57.

[85] Okinyo-Owiti, D.P., Burnett, P.G., and Reaney, M.J.T.. Simulated moving bed purification of flaxseed oil orbitides: Unprecedented separation of cyclolinopeptides C and E. *Journal of Chromatography B*, 2014, (965): 231-237.

[86] Agrawal, G., Oh, J., Sreedhar, B., Tie, S., Donaldson, M.E., Frank, T.C., Schultz, A.K., Bommarius, A.S., and Kawajiri, Y.. Optimization of reactive simulated moving bed systems with modulation of feed concentration for production of glycol ether ester. *Journal of Chromatography A*, 2014, (1360): 196-208.

- [87] Wagner, N., Hakansson, E., Wahler, S., Panke, S., and Bechtold, M.. Multi-objective optimization for the economic production of D-psicose using simulated moving bed chromatography. *Journal of Chromatography A*, 2015, (1398): 47-56.
- [88] Li, M., Bao, Z.B., Xing, H.B., Yang, Q.W., Yang, Y.W., and Ren, Q.L.. Simulated moving bed chromatography for the separation of ethylesters of eicosapentaenoic acid and docosahexaenoic acid under nonlinear conditions. *Journal of Chromatography A*, 2015, (1425): 189-197.
- [89] Kim, P.H., Nam, H.G., Park, C.H., Wang, N.H., Chang, Y.K., and Mun, S.Y.. Simulated moving bed separation of agarose-hydrolyzate components for biofuel production from marine biomass. *Journal of Chromatography A*, 2015, (1406): 231-243.
- [90] Sun, Z.Y., Ura, T., Matsuura, H., Kida, K., and Jyo, A.. Dowex 1X4 and Dowex 1X8 as substitute of Diaion MA03SS in simulated moving bed chromatographic separation of sulfuric acid and sugars in concentrated sulfuric acid hydrolysates of bamboo. *Separation and Purification Technology*, 2016, (166): 92-101.
- [91] Liang, M.T., Lin, C.H., Tsai, P.Y., Wang, H.P., Wan, H.P., and Yang, T.Y.. The separation of butanediol and propanediol by simulated moving bed. *Journal of the Taiwan Institute of Chemical Engineers*, 2016, (61): 12-19.
- [92] Andrade Neto, A.S., Secchi, A.R., Souza Jr., M.B., and Barreto Jr., A.G.. Nonlinear model predictive control applied to the separation of praziquantel in simulated moving bed chromatography. *Journal of Chromatography A*, 2016, (1470): 42-49.
- [93] Choi, J.H., Park, H., Park, C.H., Wang, N.H., and Mun, S.Y.. Highly efficient recovery of xylobiose from xylooligosaccharides using a simulated moving bed method. *Journal of Chromatography A*, 2016, (1465): 143-154.
- [94] Lin, X.J., Gong, R.J., Li, J.X., Li, P., Yu, J.G., and Rodrigues, A.E.. Enantioseparation of racemic aminogluthimide using asynchronous simulated moving bed chromatography. *Journal of Chromatography A*, 2016, (1467): 347-355.
- [95] Tangpromphan, P., Budman, H., and Jaree, A.. A simplified strategy to reduce the

desorbent consumption and equipment installed in a three-zone simulated moving bed process for the separation of glucose and fructose. *Chemical Engineering & Processing: Process Intensification*, 2018, (126): 23-37.

[96] Coelho, L.C.D., Filho, N.M.L., Faria, R.P.V., Ferreira, A.F.P., Ribeiro, A.M., Rodrigues, A.E.. Separation of tartronic and glyceric acids by simulated moving bed chromatography. *Journal of Chromatography A*, 2018, (1563): 62-70.

[97] Mun, S.Y.. Optimization of production rate, productivity, and product concentration for a simulated moving bed process aimed at fucose separation using standing-wave-design and genetic algorithm. *Journal of Chromatography A*, 2018, (1575): 113-121.

[98] Aniceto, J.P.S., Azenha, I.S., Domingues, F.M.J., Mendes, A., and Silva, C.M.. Design and optimization of a simulated moving bed unit for the separation of betulinic, oleanolic and ursolic acids mixtures: Experimental and modeling studies. *Separation and Purification Technology*, 2018, (192): 401-411.

[99] Yao, C.Y., Chen, J.L., Lu, Y.H., Tang, S.K., and Fan, E.G.. Construction of an asynchronous three-zone simulated-moving-bed chromatography and its application for the separation of vanillin and syringaldehyde. *Chemical Engineering Journal*, 2018, (331): 644-651.

[100] Hong, S.B., Choi, J.H., Chang, Y.K., and Mun, S.Y.. Production of high-purity fucose from the seaweed of *Undaria pinnatifida* through acid-hydrolysis and simulated-moving bed purification. *Separation and Purification Technology*, 2019, (213): 133-141.

[101] Guo, S.W., Vengsarkar, P., Jayachandrababu, K.C., Pereira, C., Partridge, R.D., Joshi, Y.V., Nair, S., and Kawajiri, Y.. Aromatics/Alkanes separation: Simulated moving bed process model development by a concurrent approach and its validation in a mini-plant. *Separation and Purification Technology*, 2019, (215): 410-421.

[102] Storti, G., Mazzotti, M., Morbidelli, M., and Carra, S.. Robust design of binary countercurrent adsorption separation processes. *AIChE Journal*, 1993, (3): 471-492.

[103] Mazzotti, M., Storti, G., Morbidelli, M.. Optimal operation of simulated moving

bed units for nonlinear chromatographic separations. *Journal of Chromatography A*, 1997, (769): 3-24.

[104] Mazzotti, M., Storti, G., and Morbidelli, M.. Robust design of countercurrent adsorption separation process: 2. multicomponent systems. *AIChE Journal*, 1994, (40): 1825-1842.

[105] Mazzotti, M., Storti, G., and Morbidelli, M.. Robust design of countercurrent adsorption separation process: 3. nonstoichiometric systems. *AIChE Journal*, 1996, (42): 2784-2796.

[106] Ma, Z., and Wang, N.H.L.. Standing wave analysis of SMB chromatography: Linear systems. *AIChE Journal*, 1997, (10): 2488-2508.

[107] Mallmann, T., Burris, B. D., Ma, Z., and Wang, N.H.L.. Standing wave design of nonlinear SMB systems for fructose purification. *AIChE Journal*, 1998, (12): 2628-2646.

[108] Wu, D.J., Ma, Z., and Wang, N.H.L.. Optimization of throughput and desorbent consumption in simulated moving bed chromatography for paclitaxel purification. *Journal of Chromatography A*, 1999, (855): 71-89.

[109] Wu, D.J., Xie, Y., Ma, Z., and Wang, N.H.L.. Design of simulated moving bed chromatography for amino acid separations. *Ind. Eng. Chem. Res.*, 1998, (37): 4023-4035.

[110] Xie, Y., Farrenburg, C.A., Chin, C.Y., Mun, S.Y., and Wang, N.H.. Design of SMB for a nonlinear amino acid system with mass-transfer effects. *AIChE Journal*, 2003, (11): 2850-2863.

[111] Xie, Y., Mun, S.Y., Kim, J.Y., and Wang, N.H.. Standing wave design and experimental validation of a tandem simulated moving bed process for insulin purification. *Biotechnol. Prog.*, 2002, (18): 1332-1344.

[112] Azevedo, D.C.S., and Rodrigues, A.E.. Design of a simulated moving bed in the presence of mass-transfer resistances. *AIChE Journal*, 1999, (5): 956-966.

- [113] Rodrigues, A.E., and Pais, L.S.. Design of SMB chiral separations using the concept of separation volume. *Separation Science and Technology*, 2004, (2): 245-270.
- [114] Azevedo, D.C.S., and Rodrigues, A.E.. Fructose-glucose separation in a SMB pilot unit: modeling, simulation, design, and operation. *AIChE Journal*, 2001, (9): 2042-2051.
- [115] Minceva, M., and Rodrigues, A.E.. Modeling and simulation of a simulated moving bed for the separation of p-xylene. *Ind. Eng. Chem. Res.*, 2002, (41): 3454-3461.
- [116] Minceva, M., and Rodrigues, A.E.. Two-level optimization of an existing SMB for p-xylene separation. *Computers and Chemical Engineering*, 2005, (29): 2215-2228.



## Chapter 3

### 3. Equilibrium and kinetic differences of XOS2-XOS7 in xylo-oligosaccharides and their effects on the design of simulated moving bed purification process

#### 3.1 Introduction

Xylo-oligosaccharides (XOSs) are oligomers containing various numbers of xylose molecules linked by  $\beta$  1–4 glycosidic bond [1, 2, 3]. Throughout this article, XOS refers to the mixture of XOSs with degrees of polymerization from 2 to 7. XOSN refers to XOS with degree of polymerization equal to N.

XOS is non-digestible, non-cariogenic, low caloric [2, 4] and has desired prebiotic effect [5, 6]. Compared with other oligosaccharides such as fructo-oligosaccharides (FOS) and galacto-oligosaccharides (GOS), XOS has superior acid resistance and heat stability and may therefore be more widely used in the manufacturing of functional foods [3, 4]. XOS is industrially produced by hydrolysis of xylan-rich hemicelluloses. Due to the constraints of conversion and selectivity of enzyme catalyzed hydrolysis reaction, purity of commercial raw XOS syrup is generally limited to 70% with 22% unreacted xylose and 8% by-product arabinose (ARS) as the major impurities [4, 7]. Further purification of the XOS syrup is required for the applications in food industry. Several separation techniques including membranes, enzyme, activated charcoals, zeolites and ion exchange have been investigated in literature for the purification of oligosaccharides [1, 4, 8]. Among these approaches, suitable ion exchange resins that have the advantages of nontoxicity, low cost, and mechanical, chemical, and biological stability present a promising alternative.

Separation based on ion exchange resins can be realized via adsorptive or chromatographic processes. Simulated moving bed (SMB), a cyclic chromatographic operation that is featured by enhanced unit productivity and reduced solvent consumption, has been widely applied for the purification and separation of petro-chemicals,

pharmaceuticals, food and bio-products. SMBs equipped with ion exchange resins were proven to be efficient for the purification of FOS [9-12] and GOS [13-15]. To our knowledge, the only study on XOS purification by SMB was reported by Meng et al. who enriched XOS from 69% to 91% by conducting SMB experiments [7]. However, detailed modeling and optimization are missed in their work.

A comprehensive design of SMB process essentially involves three steps: i) screening of stationary phase materials and fluid composition; ii) measurements of column voidage and determination of equilibrium and kinetic parameters; iii) optimization of operational parameters. Due to the intrinsic complicity of SMB processes, numerical simulation and optimization are necessarily involved in the last step [16, 20].

Typical SMB processes are designed for binary separations. While oligosaccharides are mixtures consisting of several components, most previous studies treated oligosaccharides as a single component and used the average equilibrium and kinetic parameters [7, 15, 21, 22]. However, the variance among the components in oligosaccharides, especially, in adsorption equilibrium, may have different effects on different zones. For example, if the impurity is preferentially adsorbed, which, as will be shown later, is the case for XOS purification, the flowrate in zone II must be large enough to purge the most adsorbed component to zone III whereas flowrate in zone IV must be small enough to retain the least adsorbed component [23]. Using averaged parameters may lead to wrongly designed operations.

The ongoing work in this research is aimed at the optimal design of SMB process for XOS purification. Systematic experiments and simulations have been carried out at the current stage to choose a suitable ion exchange resin and to acquire reliable model parameters. Effects of differences among the seven XOS components on the simulation results were also evaluated.

The article is organized as follows. After this brief introduction, chemicals, instrument and procedures of experiments will be described. Then the theories involved in SMB simulations will be presented. Experimental and simulation results are summarized and discussed in Section 4. Finally, conclusions will be given.

## 3.2 Theoretical

### 3.2.1 Transport dispersive (TD) chromatography model and parameters

Component mass balance in the SMB chromatography was described by TD model [24-26] in the following form:

$$\frac{\partial c_{i,j}}{\partial t} + \varphi \frac{\partial q_{i,j}}{\partial t} + u_j \frac{\partial c_{i,j}}{\partial z} - D_{L,j} \frac{\partial^2 c_{i,j}}{\partial z^2} = 0 \quad (3-1)$$

$$\frac{\partial q_i}{\partial t} = k_{m,i} (q_i^* - q_i) \quad (3-2)$$

where  $c$  and  $q$  are concentrations in the liquid and stationary phases, respectively,  $i$  is the index for component and  $j$  for column,  $t$  is time,  $\varphi$  is phase ratio defined as  $\varphi = (1 - \varepsilon_t) / \varepsilon_t$ ,  $\varepsilon_t$  is column voidage,  $u$  ( $= Q / \varepsilon_t / \pi r^2$ ) is interstitial mobile phase velocity,  $z$  is the axial coordinate,  $D_L$  is the axial dispersion coefficient,  $k_m$  is the mass transfer coefficient. The definite conditions associated with differential equations (3-1) and (3-2) will be discussed in the next section (2.2). An additional isotherm model is required to describe the local adsorption equilibrium and calculate  $q^*$ :

$$q_i^* = f_i(c_1, c_2, \dots) \quad (3-3)$$

TD model has three parameters, namely,  $\varphi$  (or  $\varepsilon_t$ ),  $D_L$  and  $k_m$ . An adsorptively inert tracer can be applied to directly measure  $\varepsilon_t$ .  $D_L$  and  $k_m$  are generally concentration dependent and their values at the linear range can be estimated by a series of pulse experiments carried out at various flowrates [26, 27]. Henry's constant ( $H$ ) and number of equivalent theoretical plates ( $N$ ) can be derived by peak statistical moments of the elution profile of a linear pulse [24, 26]:

$$H_i = \frac{q_i^*}{c_i} = \frac{1}{\varphi} \left( \frac{\tau_i u}{L} - 1 \right) \quad (3-4)$$

$$N_i = \frac{\tau_i^2}{\sigma_i^2} \quad (3-5)$$

where  $\tau$  and  $\sigma^2$  are the 1<sup>st</sup> and 2<sup>nd</sup> moments, respectively,

$$\tau = \frac{\int_0^\infty tc(t)dt}{\int_0^\infty c(t)dt} \quad (3-6)$$

$$\sigma^2 = \frac{\int_0^\infty t^2 c(t)dt}{\int_0^\infty c(t)dt} \quad (3-7)$$

While  $H$  is a thermodynamic constant independent of flowrate,  $N$  is correlated to  $u$  by

$$\frac{1}{N_i} = \frac{2D_{L,i}}{uL} + \frac{2u}{\phi LH_i k_{m,i}} \left( \frac{\phi H_i}{1 + \phi H_i} \right)^2 = \frac{1}{N_{L,i}} + \frac{1}{k_{m,i}} u \lambda_i \quad (3-8)$$

with  $\lambda_i = \frac{2}{\phi LH_i} \left( \frac{\phi H_i}{1 + \phi H_i} \right)^2$ . It may be proven that  $N_L$  is essentially independent of  $u$

when flowrate is in a proper range such that the band broadening effects of axial molecular diffusion are negligible [26]. Eq. (3-8) therefore provides a frame for the estimation of both  $D_L$  (or  $N_L$ ) and  $k_m$  in the linear range.

### 3.2.2 Numerical scheme

As will be shown later, a constant  $N_L$  can be used for all components involved in this work. In this case, TD model can be discretized along axial direction by Martin–Synge method, which replaces the 2<sup>nd</sup> derivative ( $\partial^2/\partial z^2$  term) in Eq. (3-1) with truncation error brought in by the 1<sup>st</sup> order backward approximation of  $\partial/\partial z$  (numerical dispersion) [28]. The discretized form of Eq. (3-1) becomes

$$\frac{dc_{i,j}^M}{dt} + \phi \frac{dq_{i,j}^M}{dt} + u_j \frac{c_{i,j}^M - c_{i,j}^{M-1}}{\Delta z} = O(\Delta z^2) \quad (3-9)$$

$$\Delta z = \frac{L}{N_L} \quad (3-10)$$

where  $M$  denotes the mesh points with  $M=0$  for the inlet and  $M=N_L$  for the outlet. Since the 2nd order derivative is eliminated from Eq. (3-1), only inlet boundary condition is retained, which is described by the node balance of a 4-zone SMB unit,

$$c_{i,j}^0 = \begin{cases} c_{i,jpre}^{N_L} & u_j \leq u_{jpre} \\ \frac{u_{jpre} c_{i,jpre}^{N_L} + (u_j - u_{jpre}) c_{i,j}^{ext}}{u_j} & u_j > u_{jpre} \end{cases} \quad (3-11)$$

where the superscript *ext* is for the external stream to an inlet port, specifically, desorbent and feed for column I and IV, respectively; *jpre* is the adjacent upstream column,

$$jpre = \begin{cases} 4 & j = I \\ j-1 & j = II, III, IV \end{cases} \quad (3-12)$$

SMB performance is evaluated at the cyclic steady state. Rigorously, cyclic conditions apply to the discretized equations.

$$c_{i,j}^k(t) = c_{i,j}^k(t + t_s) \quad (3-13)$$

$$q_{i,j}^k(t) = q_{i,j}^k(t + t_s) \quad (3-14)$$

where  $t_s$  is switching time,  $j$  and  $k$  range from I-IV and 1- $N_L$ , respectively. Due to the difficulty in numerically solving the equations with cyclic conditions, the model is converted to initial value problems (IVPs) and then integrated using DIVPAG package. The following initial conditions were used to replace Eqs (3-13) and (3-14).

$$c_{i,j}^k(t=0) = q_{i,j}^k(t=0) = 0 \quad (3-15)$$

It was found in this work that cyclic steady state can be essentially achieved in less than 10 cycles. A minimum number of 15 cycles and the following constraint on mass balance of all components were used to ensure the cyclic steady state.

$$\frac{\int_0^{t_s} (Q_E c_{i,E} + Q_R c_{i,R}) dt}{\int_0^{t_s} (Q_F c_{i,F} + Q_D c_{i,D}) dt} \times 100\% \leq 0.5\% \quad (3-16)$$

where subscripts  $D, E, F, R$  are for desorbent, extract, feed and raffinate streams, respectively. All calculations in this study were programmed in FORTRAN codes and performed on a Lenovo ThinkPad L440 personal computer equipped with a 2.30 GHz Intel core i7 processor.

### 3.2.3 Operation modes of sequential simulated moving bed (SSMB)

Continuous operation of an SMB unit is realized by periodically switching the inlet and outlet ports along the flow direction. Conventionally, the ports are synchronically switched and the flowrates of all ports are maintained constant. As such, a typical 4-zone SMB process has 5 independent operational parameters, namely, switching time and four flowrates in the 4 zones. In the last two decades, several techniques such as Varicol [29], PowerFeed [30] and ModiCon [31] have been developed to further enhance the separation performance by asynchronous switch, temporally varied feed flowrate and concentration, respectively. Sequential SMB (SSMB) that has been applied for the commercial separation of fructose and glucose, where solvent consumption is a major concern, introduces operational flexibility by dividing a switch into three steps with different flow patterns. As shown in Figure 3-1, in the 1<sup>st</sup> step, the mobile phase is circulated in the whole system, forming a closed loop; in the 2<sup>nd</sup> step, section IV is isolated and an external solvent stream is introduced at the desorbent port to purge the less adsorbed species to raffinate port; in the 3<sup>rd</sup> step, section II is also isolated and another feed stream is introduced such that preferentially and less adsorbed species are simultaneously collected at extract and raffinate ports, respectively.

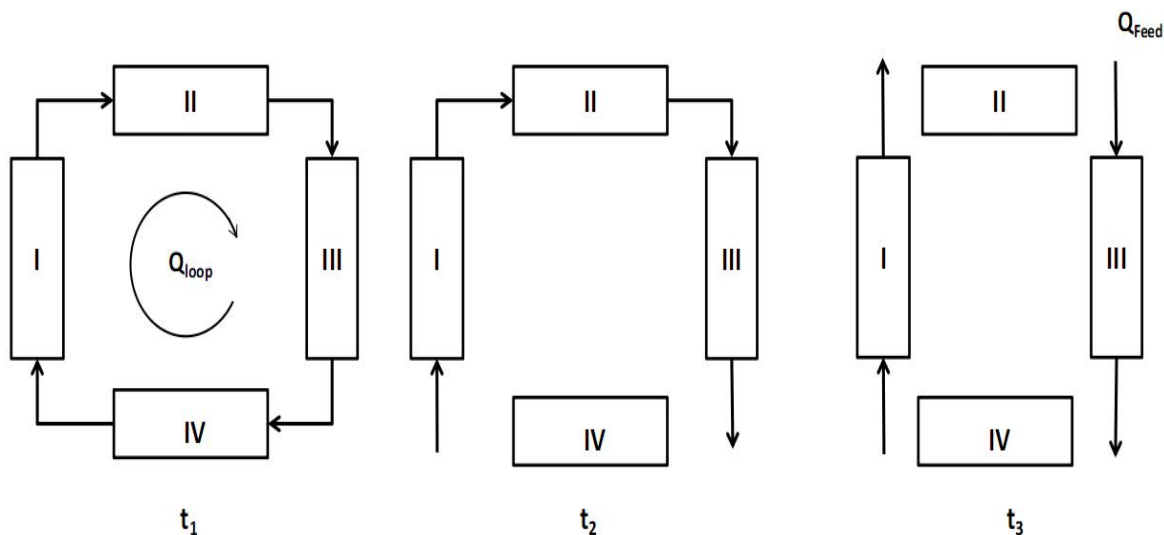


**Figure 3-1 Schematic diagram of SSMB process**

### 3.3 Experimental

#### 3.3.1 Chemicals and materials

Xylose (monohydrate), ARS (monohydrate) and XOS were obtained from Long Li (Shandong, China). Standard samples of XOS2, XOS3, XOS4, XOS5 and XOS6 were purchased from ZZBIO (Shanghai, China) while the standard of XOS7 was not available. Raw XOS syrup was prepared in the lab according to the industrial data. It contains 30 w% of dry matter that has a composition of 70% xylo-oligosaccharides, 22% xylose, and 8% arabinose. Ultrapure water (11.5 MΩ cm) was filtered through Elix advantage (US) filter and degassed. Blue Dextran solution used as an inert tracer was produced by Phamacia (Sweden).

#### 3.3.2 Instruments

An LC-3000 preparative chromatographic system (CXTH, Beijing, China) including CXTH LC-3000 pumps, an injector with a 5mL sample loop and a Shodex RI-102 refractive index (RI) detector (Shodex, Japan) was applied for determination of model

parameters. An Agilent 1100 Series (Agilent Technologies, Palo Alto, USA) high performance liquid chromatography (HPLC) system with an RI detector and a Shodex sugar KS 802 column (300\*8.0mm, 6 $\mu$ m) was used for sample analyses. A laboratory-scale SSMB system consisting of four pumps and auto-control system was provided by Hanbon, China.

Preparative glass columns (1m $\times$ 2.5cm I.D) were provided by Higang Instrument (Shanghai, China). DOWEX MONOSPHERE<sup>TM</sup> 99/310 resin (average particle size of 310 $\mu$ m) were ionized and then uniformly packed into the preparative columns using slurry-packing method. The columns were supplemented with jackets and connected to a thermostatic water bath (HW-SY21-K, Changfeng Company, China). A short preparative column (30cm $\times$ 1cm I.D) provided by Higang Instrument (Shanghai, China) was only used to measure the kinetic parameters of XOS2, XOS3, XOS4, XOS5, and XOS6. For all experiments involved in this work, the column temperature was controlled at 60 $^{\circ}$ C $\pm$ 0.5.

### 3.3.3 Procedures

As the resins with K<sup>+</sup> and Ca<sup>2+</sup> are available in the lab, an ionic form modification was completed in order to obtain the resin with Na<sup>+</sup>. At first, 5% HCL and 5% NaOH solutions were prepared, and then the column packed with Ca<sup>2+</sup> resin was flushed by using 5% HCL at a constant flowrate 5ml/min on the preparative chromatography. After 3 hours, the mobile phase was changed to water to flush the column to a neutral state. Next, 5% NaOH was used to continuously flush the column for 3 hours. Finally, water flushing was applied to keep the column at a neutral state too. The above prepared resin with Na<sup>+</sup> was compared with K<sup>+</sup> and Ca<sup>2+</sup>.

Pulse experiments of various samples, Blue dextran, XOS, xylose, ARS, and raw XOS containing XOS (70 w%), xylose (22 w%) and ARS (7 w%) were carried out to evaluate the effects of ionic form on adsorption selectivity and column efficiency [32-37]. Feed concentration, injection volume and flowrate were controlled at 25 g/L, 5 ml and 5 ml/ml, respectively.



Frontal analysis was used to determine adsorption isotherm of XOS (as a single component), xylose, and ARS [21, 38, 39, 40]. Sample solutions of concentrations from 30 to 270 g/L were prepared by volumetrically diluting the solute samples. The flowrate was maintained at 5 ml/min. Elution samples were collected at fixed time intervals and then analyzed by HPLC, which can separate XOS, xylose and arabinose and simultaneously determine their concentrations.

Pulse experiments were also applied to determine kinetic parameters [24, 26, 39]. For XOS (overall), xylose and ARS, a preparative column (1m×2.5cm I.D) was used. The sample concentration, injection volume and flowrate were controlled at 100 g/L, 5 ml and 4-12 ml/min. In the case of individual XOS2-XOS6, the short preparative column (30cm×1cm I.D) was used. The sample concentration, injection volume and flowrate were 0.5 g/L, 1 ml and 0.5-2.0 ml/min. The pre-determined flowrates were realized by programming the corresponding pumps.

Before each experiment, the whole system was purged with water for 1h, and, meanwhile, the thermostatic water bath was used to establish the desired column temperature.

## 3.4 Results and discussion

### 3.4.1 Screening of ionic form of adsorbent

In order to compare resin particles ionized with three cations, namely,  $\text{Ca}^{2+}$ ,  $\text{K}^{+}$ , and  $\text{Na}^{+}$ , they were packed in the columns under same conditions and then evaluated for XOS purification in terms of selectivity ( $\alpha = H_{\text{Xylose}}/H_{\text{XOS}}$ ) and column efficiency. For the screening of ion form, XOS was treated as a single component and the effects of ARS were neglected. According to Eqs. (3-6) and (3-7), both selectivity and column efficiency can be estimated by pulse experiments. As shown in Table 3-1,  $\text{K}^{+}$  exhibited the largest selectivity and second highest column efficiency, slightly lower than that of  $\text{Ca}^{2+}$ . Considering that the higher Henry's constant on  $\text{K}^{+}$  may lead to a higher unit production, according to triangle theory [23], the authors chose  $\text{K}^{+}$  over  $\text{Ca}^{2+}$  for further investigations.

It should be mentioned that DOWEX MONOSPHERE 99/310 resin ionized with K<sup>+</sup> performs better for XOS purification than DIAION-UBK530 Na that, according to the report by Meng et al. [7], has a selectivity of 1.71. According to the elution profile of Blue dextran, an inert component, the voidage of K<sup>+</sup> ionized column was estimated to be 0.416.

**Table 3-1 Characteristics of resins with different ionic forms**

Ion	$H(\text{XOS})$	$\alpha(\text{Xylose/XOS})$	$N(\text{XOS})$
Ca <sup>2+</sup>	0.384	2.01	67.2
K <sup>+</sup>	0.416	2.11	60.2
Na <sup>+</sup>	0.284	1.69	55.8

### 3.4.2 Frontal analysis

Breakthrough curves were measured on the K<sup>+</sup> ionized column (1m × 2.5cm I.D) by stepwisely increasing the feed concentration. The equilibrium solid phase concentration was calculated by

$$q_{i,n}^* = q_{i,n-1}^* + \frac{Q \int_0^\infty (c_{i,n} - c_i) dt}{V_{col}(1 - \varepsilon)} \quad (3-17)$$

A representative breakthrough curve is shown in Figures 3-2a. Elution profile for sample analysis and calibration curves of all components involved in this work are provided in the Supplementary Materials. Isotherms were acquired by FA up to the total concentration of 270 g/L, which is about the level of commercially available raw XOS syrup after hydrolysis reaction. As shown in Figure 3-2b, measured isotherm data for XOS, xylose, and ARS can be well captured by linear fitting with R<sup>2</sup> generally greater than 0.995. Xylose and ARS are more preferentially adsorbed than XOS.

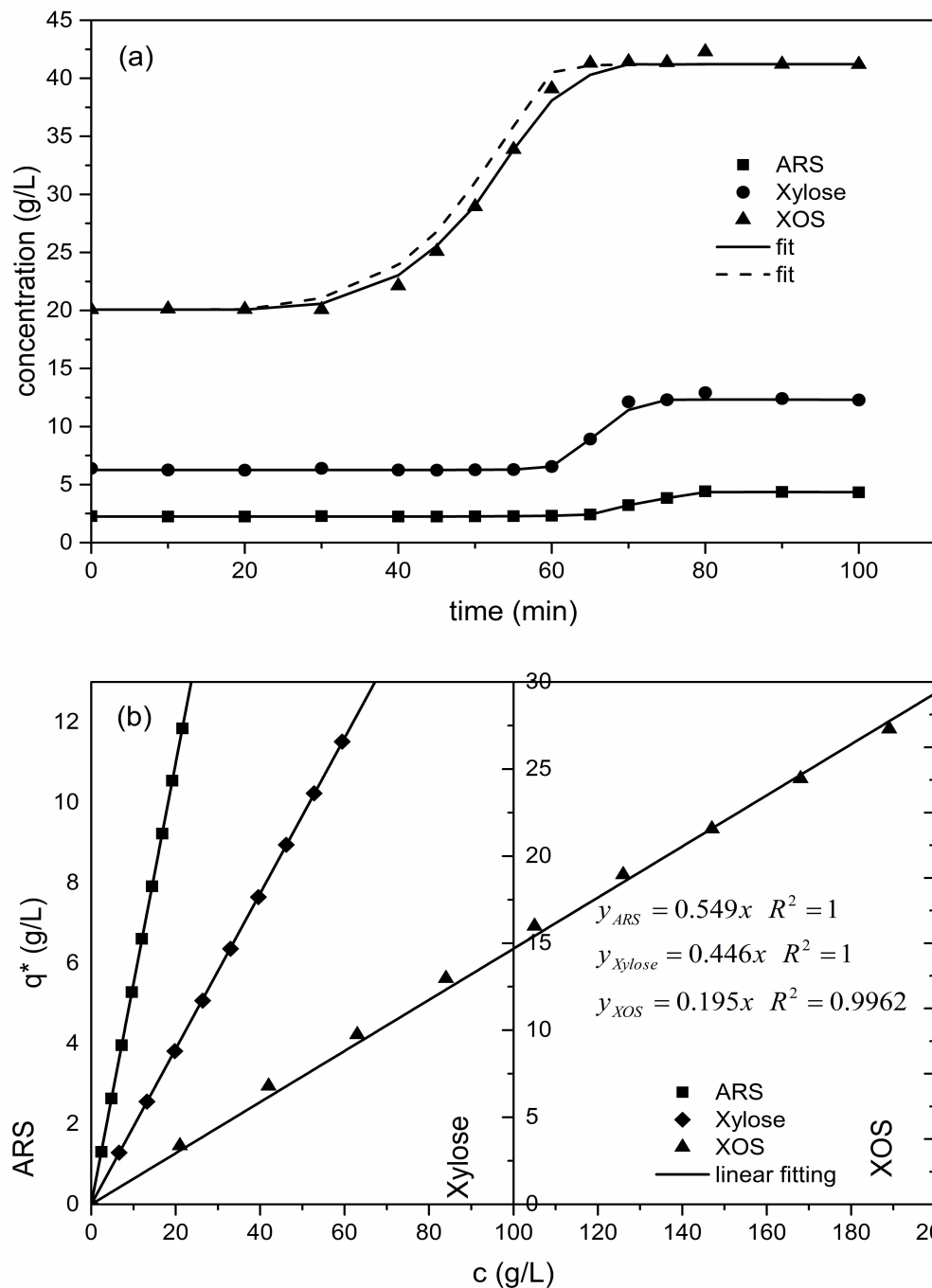


**Figure 3-2 Frontal analysis (FA) experiments. a: typical breakthrough curves (total concentration=60 g/L); b: isotherms acquired by FA. Preparative column; concentration range: 30-270 g/L; flowrate 5ml/min.**

### 3.4.3 TD model parameters by linear pulse experiments

As shown in the last section, linear equilibria apply to xylose, ARS and XOS as a single component in the concentration range of interests. In this case, pulse experiments carried out at different flowrates can be used to determine the TD model parameters as well as Henry's constant. Typical elution profiles of pulse experiments for xylose, ARS and XOS as a single component are shown in Figure 3-3a.  $H$  and  $N$  were estimated using peak statistical moments, i.e., Eqs. (3-4) and (3-5). Instead of calculating  $H$  by directly using Eq. (3-4) for each flowrate,  $\tau$  was plotted against  $L/u$ , forming a straight line for each component (Figure 3-3b). The slope of this line equals to  $(1+\phi H)$ , with  $\phi$  predetermined by Blue Dextran tracer to be 1.404. As such, only one Henry's constant is obtained by the experiments at several flowrates. Figure 3-3c shows that  $1/N$  against  $\lambda u$  also forms a straight line for each component. According to Eq. (3-8), its slope and intercept can be used to estimate  $k_m$  and  $N_L$ , respectively. In order to apply Martin-Synge method for the numerical solution of TD model that has been introduced in Section 3.2.2, a constant  $N_L$  for all components were used to fit the experimental data. As shown in Figure 3-3c, excellent fits were obtained. The results of pulse experiments for xylose, ARS and XOS as a single component are summarized in Table 3-2.

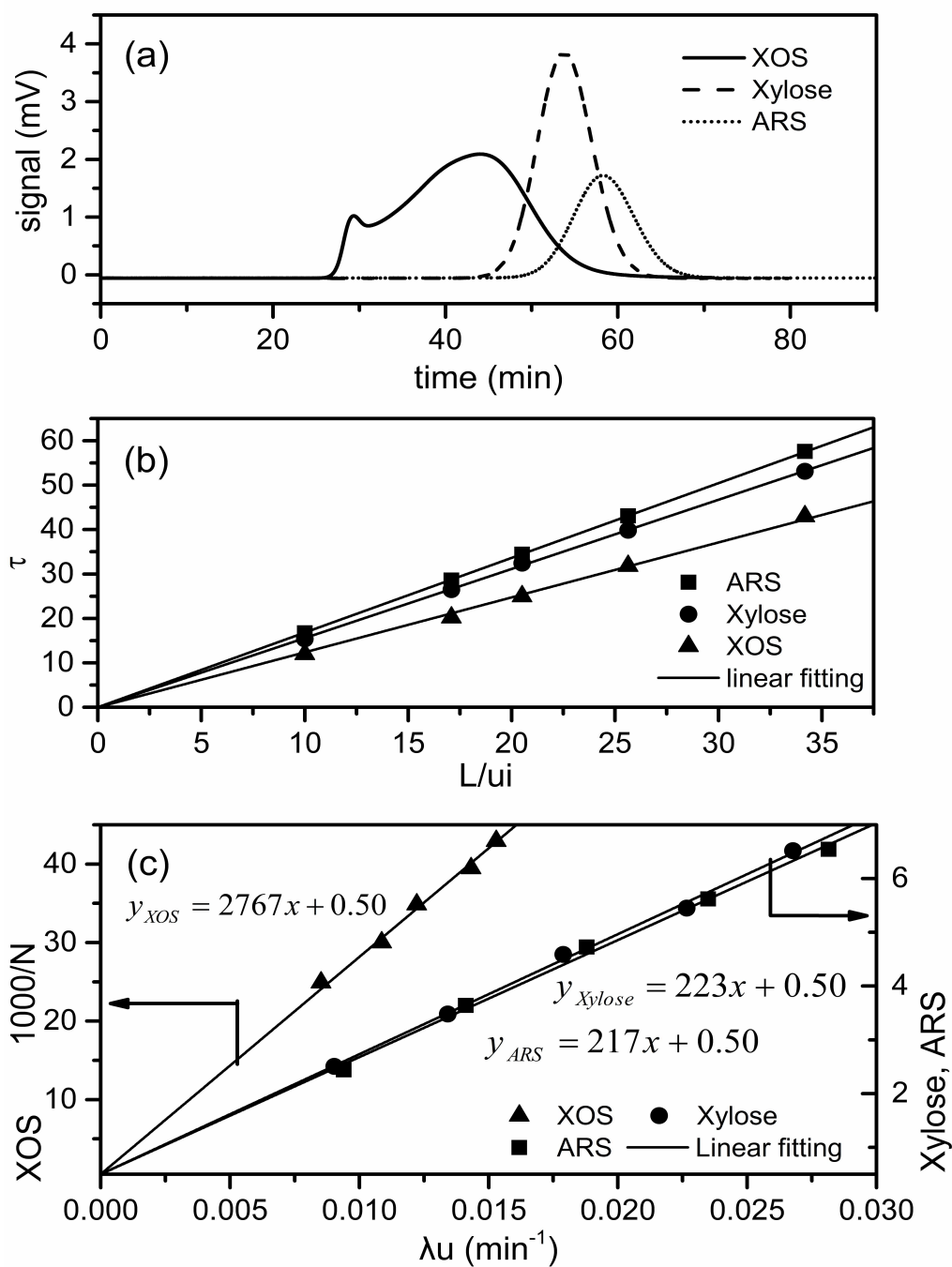


**Figure 3-3 Linear pulse experiments. a: Typical elution profiles (flowrate: 6ml/min); b: plot of  $\tau$  against  $L/u$  for the estimation of  $H$ ; c: plot of  $1/N$  against  $\lambda u$  and the fits of Eq. (3-8) with constant  $N_L$  for Xylose, ARS, and XOS. Preparative column (1m×2.5cm I.D); concentration: 100 g/L; sample size 5 mL; flowrate range: 4-12 ml/min**

**Table 3-2 Pulse experiments for xylose, ARS and XOS**

Parameter	Q (ml/min)	Species		
		xylose	ARS	XOS
$\tau$ (min)	4	80.6	86.2	75.7
	6	53.1	57.6	45.4
	8	39.8	43.1	31.8
	10	32.4	34.4	25.0
	12	26.5	28.6	20.2
$N$	4	399	410	40.1
	6	287	275	33.3
	8	218	211	28.7
	10	183	178	25.3
	12	153	153	23.3
$H$	--	0.400	0.484	0.155
$k_m$ (min <sup>-1</sup> )	--	4.48	4.60	0.361
$N_L$	--	2000		
$w\%$	--	22	8	70

Preparative column:  $L=100$  cm;  $ID=2.5$  cm;  
 $\varphi=1.404$

The above derived parameters are adequate if XOS is treated as a single component, which is a common simplification used in most previous modeling studies on SMB purification of oligosaccharides [7, 12, 14, 15, 21]. However, an important objective of the current work is to evaluate the effects of differences among various components on the separation performance. TD model parameters for individual XOSs were also determined for this purpose.

XOS sample free of xylose, and ARS was analyzed using HPLC system. As shown in Figure 3-4, a total of 6 peaks corresponding to those of XOS2-XOS6 were identified by the Shodex sugar KS 802 column and IR detector. According to the calibrations obtained for standard XOS2 - XOS6 samples, their fractions in the XOS mixture sample were estimated to be 35.8, 33.1, 18.1, 9.4, and 2.6 w%, leaving a balance of about 1.0 w%.

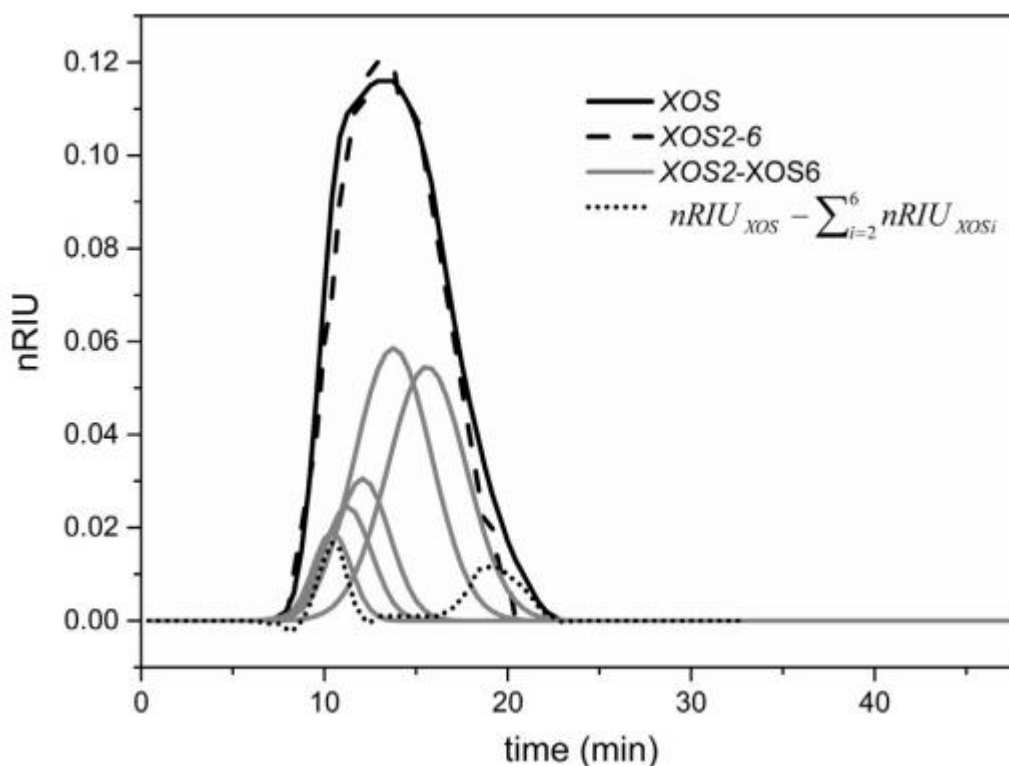


**Figure 3-4 Comparison of elution profiles on the preparative column (30cm×1cm I.D). Sample size:1mL. Flowrate: 1 ml/min. Concentration: 5 g/L XOS; 1.79, 1.655, 0.905, 0.47, 0.135 g/L XOS2 to XOS6, respectively.**

Pulse experiments on the short preparative column (30cm×1cm I.D) were carried out for individual XOS2-XOS6 following the above described procedure. Using the derived  $H$  and  $N$  values, together with the contents and calibrations, their RI responses were analytically calculated and shown in Figure 3-4 as grey curves. The superposition of these individual curves (dash black) were compared with the one for mixed XOS (solid black), showing a difference in the form of two dispersive peaks (dot black). It may be seen that one of the acquired balance peak has the similar residence time and column efficiency to those of XOS6. The same trend was also observed for other flowrates, which are omitted here for conciseness. This difference may be attributed to the existence of XOS7, of which the standard sample was not available. According to the retention time, the other peak should be recognized as some impurities in the sample.

Henry's constants and kinetic parameters of XOS2-XOS6 were determined using linear pulse experiments at various flowrates. The fits of Eq (3-8) with constant  $N_L$  to experimental data are shown in Figure 3-5. The obtained parameters required by TD model simulations are summarized in Table 3-3. Based on the observation that the calibration curves for XOS as a single component and individual XOS2-XOS6 are all highly linear, with correlation coefficients ( $R$ ) generally greater than 0.99, it may be reasonably assume that the RI responses of XOS7, of which the standard sample was not available, and its combination with XOS6 are linear as well. The similar procedure can therefore be applied to analyze aforementioned balance peak that may result from the effects of XOS7. The  $H$  and  $k_m$  acquired from these peaks measured at different flowrates are 0.0152 and 0.312 min<sup>-1</sup>, respectively. These values are very close to those determined by XOS6 sample, suggesting that XOS6 and XOS7 can be treated as a single component, assigned as XOS67 in the following discussions.



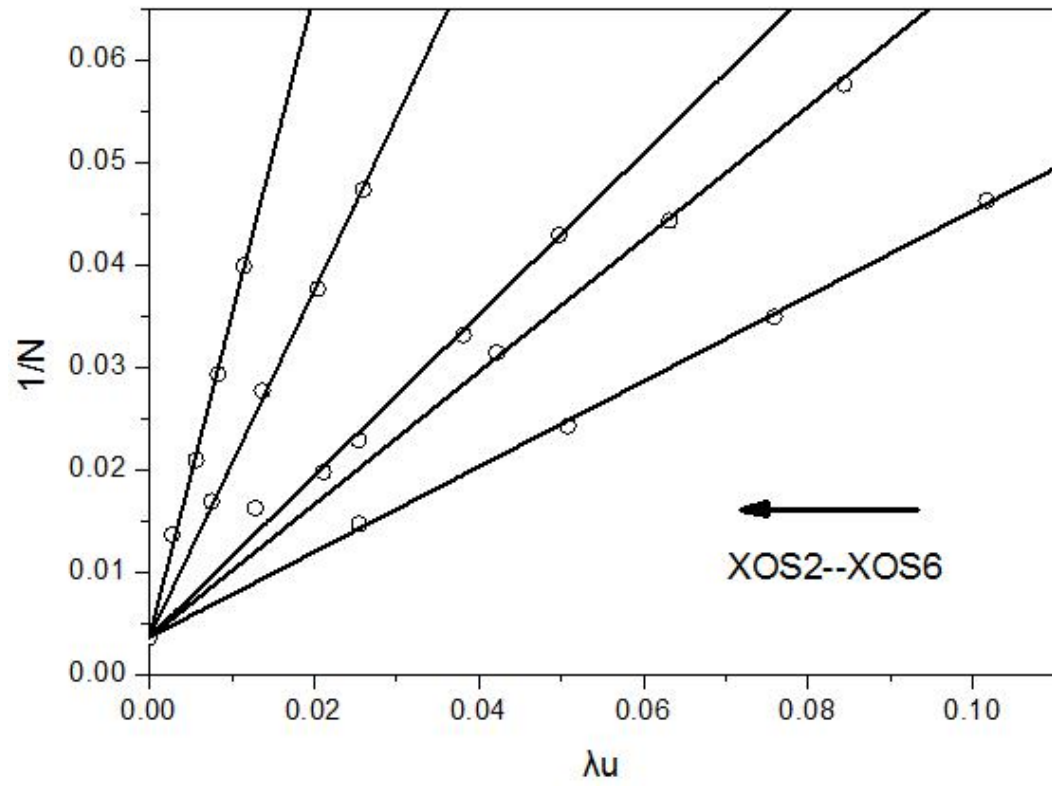


Figure 3-5 Plot  $1/N$  vs.  $\lambda u$  for XOS2-XOS6 and the fits of Eq (3-8) with constant  $N_L$

**Table 3-3 Pulse experiments for XOS2-XOS6**

Parameter	Q (ml/min)	species				
		XOS2	XOS3	XOS4	XOS5	XOS6 <sup>a</sup>
$\tau$ (min)	0.5	29.0	24.8	21.2	19.8	18.8
	1	14.5	12.4	10.6	9.81	9.40
	1.5	9.58	8.25	7.04	6.53	6.26
	2	7.23	6.19	5.26	4.88	4.70
$N$	0.5	68.1	50.7	61.6	59.3	73.4
	1	41.3	31.8	43.7	36.1	47.8
	1.5	28.6	22.6	30.2	26.6	34.1
	2	21.6	17.4	23.3	21.1	25.1
$H$	--	0.335	0.204	0.0896	0.0416	0.0155
$k_m$ (min <sup>-1</sup> )	--	2.40	1.54	1.27	0.591	0.318
$N_L$	--	278				
w% <sup>b</sup>	--	35.8	33.1	18.1	9.40	2.70

Preparative column:  $L=30$  cm;  $ID=1$  cm;

a: Results measured using XOS6. XOS6 and XOS7 treated as a single component in the chromatography modeling;

b: Percentage in XOS, not including impurities of xylose and ARS.

Assuming XOS67 accounts for 3.6 w% of total XOS, its linear calibration coefficient can be estimated from the balance between total area of XOS mixture and the summation of those for XOS2-XOS5 (see Figure 3-4). As such, the breakthrough curve in term of RI response can be calculated by

$$RI = \sum_{i=1,7} RI_i(c_i) \quad (3-18)$$

where  $c_i$  as a function of time was solved by integrating the TD model. Figure 3-2a shows the calculated breakthrough curve (solid line), which, compared with the results calculated by treating XOS as a single component and using parameters in Table 3-2 (dash line), gives better agreements to experimental measured data (dot).

### 3.4.4 SSMB simulation and experiments

SSMB simulations and experiments were carried out for a 4-column SSMB system. As shown in Figure 3-1, an SSMB process has theoretically 7 independent parameters, i.e., 3 durations and 4 flowrates. In addition, the sequence of the sub-steps within a switch can be adjusted, equivalent to another independent parameter. Systematic optimization of SSMB is therefore more involving than that of conventional SMB. The current work is aimed at obtaining reliable model parameters and investigating the feasibility of SSMB for XOS purification. For simplicity, it is assumed that  $Q_I \equiv Q_{loop}$  in all three phases is constant, which may be different from  $Q_{Feed}$  in phase 3, reducing the number of independent parameters to 5, similar to that of the regular SMB. As such, the triangle theory can be applied for the screening of operation parameters. The flowrate ratio is defined as:

$$m_j = \frac{\int_0^{t_s} Q_j dt - V\varepsilon}{V(1 - \varepsilon)} \quad (3-19)$$

Different from the conventional SMB, the flowrates of SSMB in zones II, III and IV are functions of time. Constant flowrate in zone I was arbitrarily fixed as a scaling factor, which is normally constrained by pressure drop. The other four parameters were then sequentially determined by  $m$  values:

$$t_1 = \frac{m_{IV}V(1 - \varepsilon) + V\varepsilon}{Q_{loop}} \quad (3-20)$$

$$t_2 = \frac{m_{II}V(1 - \varepsilon) + V\varepsilon}{Q_{loop}} - t_1 \quad (3-21)$$

$$t_3 = \frac{m_I V(1-\varepsilon) + V\varepsilon}{Q_{loop}} - t_1 - t_2 \quad (3-22)$$

$$Q_{Feed} = \frac{m_{III} V(1-\varepsilon) + V\varepsilon - (t_1 + t_2)Q_{loop}}{t_3} \quad (3-23)$$

According to Eq. (3-8), the contributions of axial dispersion and mass transfer to overall plate number are additive. their ratio can be defined as

$$r_i = \frac{k_{m,i}}{N_{L,i} u \lambda_i} \quad (3-24)$$

It may be seen from Figure 3-6 that in the flowrate range of interests, contribution of axial dispersion is about less than that of mass transfer by two magnitude orders. For the calculation efficiency,  $N_L$  was fixed at a relatively lower number of 300 that was obtained by the pulse experiments for individual XOSs, which is a reasonable simplification since the band broadening effect is dominated by mass transfer .

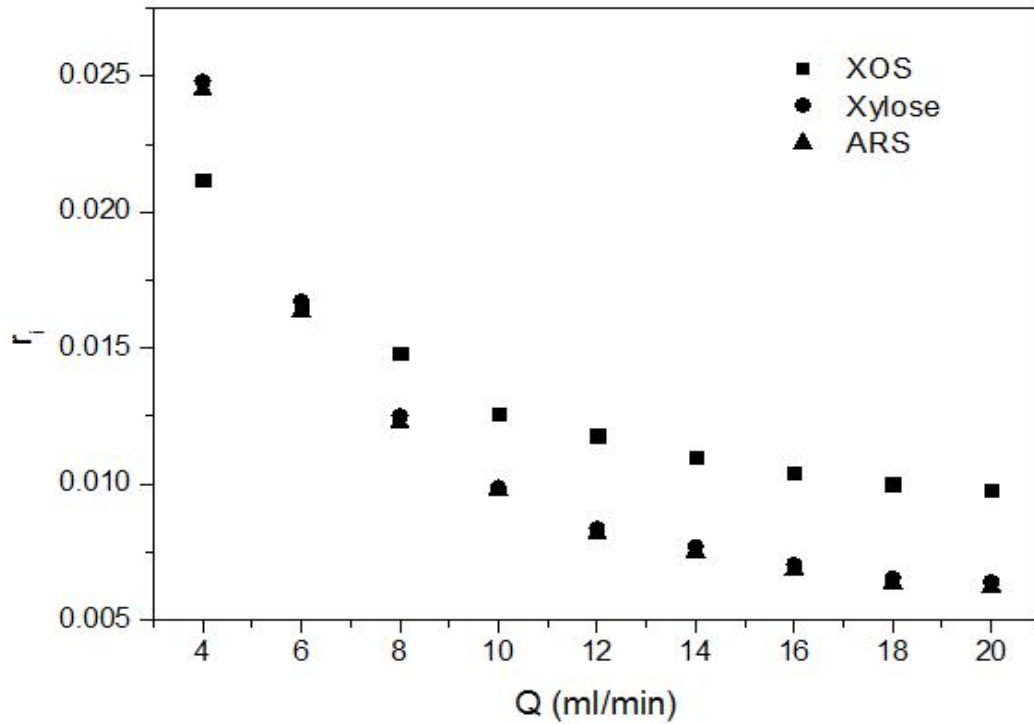


**Figure 3-6  $r_i$  as a function of flowrate for each component**

The scaling factor,  $Q_{loop}$ , was fixed at 20 mL/min. In addition,  $m_I$  and  $m_{IV}$  were fixed at 0.66 and 0.15, respectively. The value of 0.66 for  $m_I$  is significantly larger than 0.484, Henry's constant of ARS, the most preferentially adsorbed species. The value of 0.15 for  $m_{IV}$  is, however, lower than the Henry's constant by a small margin. Their effects, especially on solvent consumption, will be investigated in the future study for systematic optimization. SSMB simulations were then carried out to determine the separation zone in  $m_{II}$ - $m_{III}$  plane that satisfies practical requirements of purity and recovery defined as

$$Pur = \frac{\int_{t_0}^{t_s} \sum c_{XOS,i,Raf} Q_{Feed} dt}{\int_{t_0}^{t_s} \left( \sum c_{XOS,i,Raf} + \sum c_{impurity,i,Raf} \right) Q_{Feed} dt} \geq 0.92 \quad (3-25)$$

$$Rec = \frac{\int_{t_0}^{t_s} \sum c_{XOS,i,Raf} Q_{Feed} dt}{Q_{Feed} t_3} \geq 0.90 \quad (3-26)$$

Calculations were carried using three schemes: (a) The system is binary, consisting of XOS and impurity using parameters in Table 3-2 for XOS and algebraic average parameters of ARS and xylose for impurity; (b) XOS was treated as a single component whereas xylose and ARS were differentiated with their own parameters in Table 3-2; (c) difference among XOS2 to XOS67 were also taken into account. It may be seen from Figure 3-7 that separation zones determined by the three schemes are significantly different. For this specific system, the desired XOS is less adsorbed and, according to the Triangle Theory,  $m_{III}$  should be small enough to prevent preferentially adsorbed impurities from entering raffinate port. Under the conditions determined by scheme (a) (dot line) that uses average Henry's constant of impurities, a fraction of the relatively light component in the impurities, more specifically, xylose, may breakthrough to the raffinate port, reducing product purity. As a result, scheme (b) (dash line) that accounts for the difference between xylose and ARS, compared with scheme (a), predicts a smaller  $m_{III}$  boundary. Similarly, using average Henry's constant for XOSs may predict lower  $m_{II}$  that is insufficient to purge the relatively heavy components (XOS2 and XOS3) in XOSs to the feed port. This fraction of XOSs is carried by the stationary phase to zone I after column switching and finally exits the unit via the extract port together with impurities,

resulting in a reduced product recovery. For this reason, compared with schemes (a) and (b), scheme (c) (solid line) that accounts for variance among XOS predicts a higher  $m_{II}$  boundary. Comparison between schemes (a) and (b) shows that  $m_{III}$  determined by scheme (b) is safe to efficiently retain both xylose and ARS impurities in zone III. However, in addition to the product collected at the raffinate port, a fraction of XOSs enters zone IV. Since  $m_{IV}$  was intentionally fixed at 0.15, just slightly lower than the average Henry's constant of XOS, the relatively light components in XOSs (XOS4-XOS67) may not be sufficiently retained in zone IV. This fraction of XOSs is conveyed by the mobile phase to zone I and is purged out of the unit via the extract port. Therefore, given fixed  $m_{IV}$ ,  $m_{III}$  must be further decreased to meet the recovery constraint.

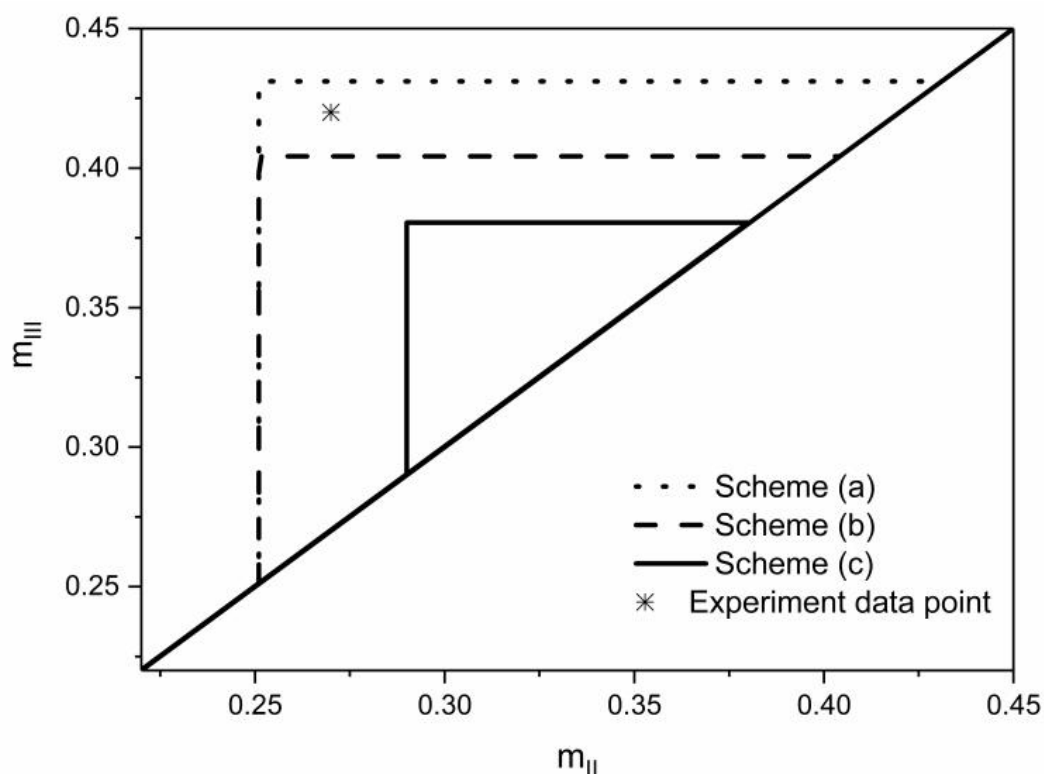


**Figure 3-7 Comparison of SSMB simulation results obtained by three schemes**

Another case with recovery constraint reduced to 0.8 was also investigated using the above mentioned three schemes. For conciseness, the results are shown in the supplementary material as Figure S3-4. Compared with the trends shown in Figure 3-7, the most significant difference is that, while  $m_{III}$  boundary determined by scheme (c) is

still lower than that by scheme (b), the  $m_{II}$  boundaries predicted by these two schemes are very close. Recall that the difference in  $m_{II}$  can be mainly attributed to the effects of relatively heavy components in XOSs, specifically, XOS2 and XOS3. Their Henry's constants are higher than the average value of 0.155 by factors of about 2.2 and 1.3. With reduced recovery requirement, this level of difference in Henry's constant can be disguised by the low value of average mass transfer coefficients, since both lead to band broadening phenomena. However, the difference in  $m_{III}$  is mainly due to relatively light components in XOSs, i.e., XOS4 to XOS67. Their Henry's constants deviate from the average value by factors of 1.7-10. This high level of difference in Henry's constants cannot be compensated with the low value of average mass transfer coefficient.

**Table 3-4 Experiment data and simulation results by using different schemes**

Objective	Experiment	Simulations		
		Scheme a	Scheme b	Scheme c
Purity %	83.2	92.0	90.4	88.7
Recovery %	85.7	90.3	88.9	86.2

SSMB with 4 preparative columns (1m×2.5cm I.D).

Operational conditions corresponding to the \* point in Figure 3-7:

$Q_{loop}=20$  ml/min;  $Q_{feed}=10$  ml/min;  $t_1=12.85$  min;  $t_2=2$  min;  $t_3=3$  min. .

SSMB experiment was carried out under the conditions corresponding to the \* point in Figure 3-7, which is inside the boundary of scheme (a) but outside the boundary of scheme (c). Experimentally measured purity and recovery of XOS are 83.2% and 85.7%, respectively. Comparison among the above mentioned three calculation schemes shows that scheme (c) gives the best agreement with experimental results. The other two schemes using average Henry's constant may overestimate the separation zone and result in unsatisfactory purity and recovery of desired XOS product. This comparison further validating the necessity to account for the variance among different species during the SMB process design for XOS purification. It should be emphasized that the experimental

condition was determined to evaluate the effects of variance among XOS2 to XOS7 rather than to achieve high performance of XOS purification. These effects should be considered during the systematic optimization of SSMB operating conditions including  $m_I$  and  $m_{IV}$ , in addition to  $m_{II}$  and  $m_{III}$ , which is beyond the scope of current study and will be pursued in the future.

### 3.5 Conclusions

Compared with  $\text{Na}^+$  and  $\text{Ca}^{2+}$ ,  $\text{K}^+$  ionized resin showed higher selectivity and was therefore chosen for further researching. Frontal analysis technique was applied to determine the adsorption isotherms of xylose, ARS and XOS as a single component. The result shows that all these components exhibit linear adsorption in the concentration range of interests. TD model parameters, namely,  $N_L$  and  $k_m$  of xylose, ARS, XOS (containing XOS2 to XOS7), as well as XOS2 to XOS6 were determined by pulse experiments performed at different flow rates. While the standard sample of XOS7 was not available, a comparison between the elution profiles for XOS (containing XOS2 to XOS7) and those for individual XOS2 to XOS6 showed that XOS7 has adsorption behaviors similar to those of XOS6.

SSMB simulations were carried out to determine operation conditions that satisfy practical constraints on XOS purity and recovery. Comparison among the results obtained by three schemes different in the treatments of XOSs and impurities shows that using average Henry's constants and TD model parameters may overestimate unit throughput and lead to unsatisfactory purity and recovery. Variance among XOSs with different degrees of polymerization may play different roles in different operation zones, which should be considered during the systematic optimization of SSMB operating conditions including  $m_I$  and  $m_{IV}$ .

The acquired Henry's constants and TD model parameters were verified by single column breakthrough and SSMB experiments. Modeling and experimental results showed that high XOS purity and recovery can be achieved using SSMB process with  $\text{K}^+$  DOWEX MONOSPHERE™ 99/310 resin as the stationary phase. The acquired



parameters can be used in futural systematic optimization towards maximum unit throughput and minimum solvent consumption.

### 3.6 References

- [1] Madhukumar, M.S., Muralikrishna, G.. Structural characterisation and determination of prebiotic activity of purified xylo-oligosaccharides obtained from Bengal gram husk (*Cicer arietinum* L.) and wheat bran (*Triticum aestivum*). *Food Chemistry*, 2010, (118): 215-223.
- [2] Takeo, K., Ohguchi, Y., Hasegawa, R., Kitamura, S.. Synthesis of(1 4)- $\beta$ -D-xylo-oligosaccharides of dp 4-10 by a blockwise approach. *Carbohydrate Research*, 1995, (278): 301-313.
- [3] Carvalho, A.F., Neto, P.O., Silva, D.F., Pastore, G.M.. Xylo-oligosaccharides from lignocellulosic materials: Chemical structure, health benefits and production by chemical and enzymatic hydrolysis. *Food Research International*, 2013, (51): 75-85.
- [4] Moure, A., Gullon, P., Dominguez, H., Carlos Parajo, J.. Advances in the manufacture, purification and applications of xylo-oligosaccharides as food additives and nutraceuticals. *Process Biochemistry*, 2006, (41): 1913-1923.
- [5] Samala, A., Srinivasan, R., Yadav, M.. Comparison of xylo-oligosaccharides production by autohydrolysis of fibers separated from ground corn flour and DDGS. *Food and Bioproducts Processing*, 2015, (94): 354-364.
- [6] Pu, J., Zhao, X., Xiao, L., Zhao, H.. Development and validation of a HILIC-ELSD method for simultaneous analysis of non-substituted and acetylated xylo-oligosaccharides. *Journal of Pharmaceutical and Biomedical Analysis*, 2017, (139): 232-237.
- [7] Meng, N., Feng, X.Y., Wang, C.F., Lu, F.P.. Study on separation of xylooligosaccharides by simulated moving bed chromatography. *Science and Technology of Food Industry*, 2011, (10): 310-313.

- [8] Nabarlatz, D., Torras, C., Garcia-Valls, R., Montane, D.. Purification of xylo-oligosaccharides from almond shells by ultrafiltration. *Separation and Purification Technology*, 2007, (53): 235-243.
- [9] Jiang, B., Wang, Z., Yang, R. J., Tang, L., Lamia, L.. Production of fructo-oligosaccharides with high purity. *China Food Additives*, 1999, (3): 1-7.
- [10] Nobre, C., Castro, C.C., Hantson, A.L., Teixeira, J.A., Rodrigues, L.R., Weireld, G.D.. Strategies for the production of high-content fructo-oligosaccharides through the removal of small saccharides by co-culture or successive fermentation with yeast. *Carbohydrate Polymers*, 2016, (136): 274-281.
- [11] Nobre, C., Teixeira, J.A., Rodrigues, L.R.. New trends and technological challenges in the industrial production and purification of fructo-oligosaccharides. *Critical Reviews in Food Science and Nutrition*, 2013, (55): 1444-1455.
- [12] Nobre, C.. Fructo-oligosaccharides recovery from fermentation processes. Portugal: Universidade do Minho, 2011.
- [13] Liu, Z.L., Wang, N.Q., Wang, M.Z., Wang, C.M., Yang, H.J.. Application of simulated moving bed chromatography in production of functional oligosaccharides. *China food additives*, 2012, (3): 200-204.
- [14] Valero, J.I.. Production of Galacto-Oligosaccharides from Lactose by Immobilized  $\beta$ -Galactosidase and Posterior Chromatographic Separation. The United States: The Ohio State University, 2009.
- [15] Wiśniewski, L., Antořová, M., Polakovič, M.. Simulated moving bed chromatography separation of galacto-oligosaccharides. *Acta Chimica Slovaca*, 2013, (2): 206-210.
- [16] Yu, W.F., Hidajat, K., Ray, A.K.. Determination of adsorption and kinetic parameters for methyl acetate esterification and hydrolysis reaction catalyzed by Amberlyst 15. *Applied Catalysis A: General*, 2004, (260): 191-205.

- [17] Yu, W.F., Hidajat, K., Ray, A.K.. Optimization of reactive simulated moving bed and Varicol systems for hydrolysis of methyl acetate. *Chemical Engineering Journal*, 2005, (112): 57-72.
- [18] Juza, M.. Development of an high-performance liquid chromatographic simulated moving bed separation from an industrial perspective. *J. Chromatogr. A*, 1999, (865): 35-49.
- [19] Coelho, M.S., Azevedo, D.C.S., Teixeira, J.A., Rodrigues, A.E.. Dextran and fructose separation on an SMB continuous chromatographic unit. *Biochemical Engineering Journal*, 2002, (12): 215-221.
- [20] Faria, R.P.V., Rodrigues, A.E.. Instrumental aspects of Simulated Moving Bed chromatography. *J. Chromatogr. A*, 2015, (1421): 82-102.
- [21] Wisniewski, L., Pereira, S. M., Polakovic, M., Rodrigues, A.E.. Chromatographic separation of prebiotic oligosaccharides. Case study: separation of galacto-oligosaccharides on a cation exchanger. *Adsorption*, 2014, (20): 483-492.
- [22] Vankova, K., Gramblicka, M., Polakovic, M.. Single-Component and Binary Adsorption Equilibria of Fructooligosaccharides, Glucose, Fructose, and Sucrose on a Ca-Form Cation Exchanger. *J. Chem. Eng. Data*, 2010, (55): 405-410.
- [23] Rajendran, A., Paredes, G., Mazzotti, M.. Simulated moving bed chromatography for the separation of enantiomers. *J. Chromatogra. A*, 2009, (1216): 709-738.
- [24] Xu, J., Jiang, X.X., Guo, J.H., Chen, Y.T., Yu, W.F.. Competitive adsorption equilibrium model with continuous temperature dependent parameters for naringenin enantiomers on Chiralpak AD column. *Journal of Chromatography A*, 2015, (1422): 163-169.
- [25] Mao, S.M., Zhang, Y., Rohani, S., Ray, A.K.. Chromatographic resolution and isotherm determination of (R,S)-mandelic acid on Chiralcel-OD column. *J. Sep. Sci.*, 2012, (35): 2273-2281.

- [26] Xu, J., Zhu, L., Xu, G.Q., Yu, W.F., Ray, A.K.. Determination of competitive adsorption isotherm of enantiomers on preparative chromatographic columns using inverse method. *J. Chromatogr. A*, 2013, (1273): 49-56.
- [27] Schmidt-Traub, H.. *Preparative Chromatography*. Germany: WILEY-VCH, 2005.
- [28] Jiang, X.X., Zhu, L., Yu, B., Su, Q., Xu, J., Yu, W.F.. Analyses of simulated moving bed with internal temperature gradients for binary separation of ketoprofen enantiomers using multi-objective optimization: Linear equilibria. *Journal of Chromatography A*, 2018, (1531): 131-142.
- [29] Pais, L.S., Rodrigues, A.E.. Design of simulated moving bed and Varicol processes for preparative separations with a low number of columns. *Journal of Chromatography A*, 2003, (1006): 33-44.
- [30] Zang, Y.F., Wankat, P.C.. SMB operation strategy-partial feed. *Ind. Eng. Chem. Res.*, 2002, (41): 2504-2511.
- [31] Schramm, H., Kienle, A., Kaspereit, M., Seidel-Morgenstern, A.. Improved operation of simulated moving bed processes through cyclic modulation of feed flow and feed concentration. *Chem. Eng. Sci.*, 2003, (58): 5217-5227.
- [32] Moravcik, J., Gramblicka, M., Wisniewski, L., Vankova, K., Polakovic, M.. Influence of the ionic form of a cation-exchange adsorbent on chromatographic separation of galacto-oligosaccharides. *Chem. Pap.*, 2012, (66): 583-588.
- [33] Rabelo, M., Pereira, C., Rodrigues, S., Rodrigues, A., Azevedo, D.. Chromatographic separation of isomalto-oligosaccharides on ion-exchange resins: effect of the cationic form. *Adsorpt. Sci. Technol.*, 2012, (30): 773-784.
- [34] Pedruzzi, I., Borges da Silva, E.A., Rodrigues, A.E.. Selection of resins, equilibrium and sorption kinetics of lactobionic acid, fructose, lactose and sorbitol. *Sep. Purif. Technol.*, 2008, (63): 600-611.

- [35] Nobre, C., Suvarov, P., Weireld, G.. Evaluation of commercial resins for fructo-oligosaccharide separation. *New Biotechnology*, 2014, (31): 55-63.
- [36] Nobre, C., Santosa, M.J., Domingueza, A., Torresa, D., Rochab, O., Peresc, A.M., Rochaa, I., Ferreira, E.C., Teixeiraa, J.A., Rodriguesa, L.R.. Comparison of adsorption equilibrium of fructose, glucose and sucrose on potassium gel-type and macroporous sodium ion-exchange resins. *Analytica Chimica Acta*, 2009, (654): 71-76.
- [37] Guiochon, G., Shirazi, S.G., Katti, A.. *Fundamentals of Preparative and Nonlinear Chromatography*. Boston: Academic Press, 1994.
- [38] Andrzejewska, A., Kaczmarek, K., Guiochon, G.. Theoretical study of the accuracy of the pulse method, frontal analysis, and frontal analysis by characteristic points for the determination of single component adsorption isotherms. *J. Chromatogr. A*, 2009, (1216): 1067-1083.
- [39] Zhang, Y., Hidajat, K., Ray, A.K.. Determination of competitive adsorption isotherm parameters of pindolol enantiomers on  $\alpha$ 1-acid glycoprotein chiral stationary phase. *J. Chromatogr. A*, 2006, (1131): 176-184.
- [40] Borges da Silva, E.A., Ulson de Souza, A.A., U. de Souza, S.G., Rodrigues, A.E.. Analysis of the high-fructose syrup production using reactive SMB technology. *Chemical Engineering Journal*, 2006, (118): 167-181.

## Chapter 4

### 4. Multi-objective optimization of sequential simulated moving bed for the purification of xylo-oligosaccharides using averaged parameters

#### 4.1 Introduction

Simulated moving bed (SMB) technique has been proven as an efficient separation method due to its enhanced productivity and purity, reduced solvent consumption, convenient operating control, and improved separation performance for some systems with low resolution and selectivity [1-6]. Industrial large scale applications of SMB include extraction of p-xylene [7, 8], corn wet milling [9], and fructose/glucose separation [10]. Recently, its applications has been extended to the separation and purification of fine chemicals, such as chiral drugs and biological components [3, 5, 11-14].

As shown in Figure 4-1a, a conventional SMB system consists of a number of series-connected packed columns, forming a closed loop. counter-current movement of liquid and solid phase with respect to the inlet and out let ports is realized by periodically switching these ports. The ports divide the columns into 4 zones that play different functional roles in the separation [6, 13-16]. Several techniques, such as Power Feed [17], Varicol [15, 16] and Gradient Operations [5, 18] have been developed to enhance SMB performances by introducing more operational flexibilities and specifically reinforcing the functional role of each individual zone. Sequential SMB (SSMB) is an alternative that divides a period of a conventional SMB into three phases (see Figure 4-1b-d). SSMB has been successfully used for fructose/glucose separation, where solvent consumption is a major concern.

A conventional isothermal and isocratic SMB with synchronous switch has 5 independent operational parameters, i.e., switching time and flowrates in the 4 zones. A widely used

theoretical approach to determine these parameters is “Triangle Theory”, which was developed based on the assumptions of instantaneous local equilibrium and negligible dispersion effects, resulting in 1<sup>st</sup> order partial differential equation. Therefore, characteristic line can be used to trace component concentrations [20]. Complete separation zone in terms of dimensionless flowrates ( $m$  values) for a binary SMB system can be analytically estimated using linear [21] or competitive [22] adsorption isotherm. Recently, the applications of Triangle Theory was remarkably extended to the case of reduced purity requirements [23]. Another theoretical method, standing wave design (SWD), was developed based on the steady-state solutions for true moving bed systems [24]. Operating parameters are correlated to separation objectives with a series of algebraic equations that can be conveniently solved. The use of SWD accounts for the mass transfer effects. A numerical alternative is multi-objective optimization (MOO) using detailed mathematical models [13]. The necessity for this more involving approach originates from the following considerations: a) in some industrial and preparative SMB processes using columns with low efficiency, for example, sugar separation and purification, mass transfer and band broadening effects may be important; b) in addition to purity and productivity, solvent consumption may be crucial for the process economy and should be taken into account; c) operational parameters may have contradicting effects on these objectives [15, 25]; d) in some modified SMB processes supplemented with sub-steps and temperature (solvent) gradients, the transient behaviors are important and the deviation from true moving bed becomes significant. The effects of these transient behaviors cannot be explained by Triangle Theory using averaged  $m$  values [5]. While MOO has been extensively used for analyses of SMB processes [26-43], to our knowledge, its application on SSMB design has not been reported in the literature.

In MOO, more than 1 objectives are simultaneously optimized by modifying the variables. Since the variables have contradicting effects on the objectives, a set of solution points considered equally good are normally obtained, called pareto solutions. A pareto set means in which when we go from any one point to another, at least one objective function becomes better and at least one worsens. Therefore, any point in a pareto set is optimal and acceptable [13, 15].

The ongoing work in this research group is aimed at developing an economic SSMB process for the purification of xylo-oligosaccharides (XOS) from industrial syrup. The desired product is XOS with degrees of polymerization from 1 to 7. The major impurities are unreacted xylose and by-product arabinose (ARS) formed in the upstream hydrolysis reaction. In a previous publication, DOWEX MONOSPHERE™ 99/310 resin ionized with  $K^+$  was examined to be a suitable stationary phase for the separation [19]. Adsorption equilibrium and kinetic parameters were also systematically determined.

The current study is focused on the identification of suitable operational conditions of SSMB for XOS purification. MOOs with various problem configurations corresponding to different requirements were performed for this purpose. At this initial stage, the system was considered binary for simplicity. The overall transport-dispersive (TD) model parameters for product (XOS 1-7) and impurity (xylose and ARS) determined in our previous work [19] were used for the modeling of SSMB process.

## 4.2 SSMB modeling

### 4.2.1 Model description

Our previous study [19] showed that transport dispersive (TD) chromatography model [4, 37, 38] together with linear isotherm can be used to describe the adsorption behaviors of XOS separation process. The model has the following form,

$$\frac{\partial c_{i,j}}{\partial t} + \phi \frac{\partial q_{i,j}}{\partial t} + u_j \frac{\partial c_{i,j}}{\partial z} - D_{L,j} \frac{\partial^2 c_{i,j}}{\partial z^2} = 0 \quad (4-1)$$

$$\frac{\partial q_i}{\partial t} = k_{m,i} (H_i c_i - q_i) \quad (4-2)$$

where  $c$  and  $q$  are concentrations in the liquid and stationary phases, respectively,  $i$  is the index for component and  $j$  for column,  $t$  is time,  $\phi$  is phase ratio defined as  $\phi = (1-\varepsilon)/\varepsilon$ ,  $\varepsilon$  is column voidage,  $u$  ( $=Q/\varepsilon/\pi r^2$ ) is interstitial mobile phase velocity,  $z$  is the axial coordinate,  $D_L$  is the axial dispersion coefficient,  $k_m$  is the mass transfer coefficient,  $H$  is



Henry's constant.

## 4.2.2 Numerical scheme for the solution of TD model

TD model can be discretized along axial direction by Martin–Synge method, which replaces the 2<sup>nd</sup> derivative ( $\partial^2/\partial z^2$  term) in Eq. (4-1) with truncation error brought in by the 1<sup>st</sup> order backward approximation of  $\partial/\partial z$  (numerical dispersion) [5]. The discretized form of Eq. (4-1) becomes

$$\frac{dc_{i,j}^M}{dt} + \varphi \frac{dq_{i,j}^M}{dt} + u_j \frac{c_{i,j}^M - c_{i,j}^{M-1}}{\Delta z} = O(\Delta z^2) \quad (4-4)$$

$$\Delta z = \frac{L}{N_L} \quad (4-5)$$

where  $M$  denotes the mesh points with  $M=0$  for the inlet and  $M=N_L$  for the outlet. Since the 2<sup>nd</sup> order derivative is eliminated from Eq. (4-1), only inlet boundary condition is retained, which is described by the node balance of a 4-zone SMB unit,

$$c_{i,j}^0 = \begin{cases} c_{i,jpre}^{N_L} & u_j \leq u_{jpre} \\ \frac{u_{jpre} c_{i,jpre}^{N_L} + (u_j - u_{jpre}) c_{i,j}^{ext}}{u_j} & u_j > u_{jpre} \end{cases} \quad (4-6)$$

where the superscript *ext* is for the external stream to an inlet port, specifically, desorbent and feed for column I and IV, respectively; *jpre* is the adjacent upstream column,

$$jpre = \begin{cases} 4 & j = I \\ j-1 & j = II, III, IV \end{cases} \quad (4-7)$$

SSMB performance is evaluated at the cyclic steady state. Rigorously, cyclic conditions apply to the discretized equations.

$$c_{i,j}^k(t) = c_{i,j}^k(t + t_s) \quad (4-8)$$

$$q_{i,j}^k(t) = q_{i,j}^k(t + t_s) \quad (4-9)$$

where  $t_s$  is switching time,  $j$  and  $k$  range from I-IV and 1- $N_L$ , respectively. Due to the difficulty in numerically solving the equations with cyclic conditions, the model is converted to initial value problems (IVPs) and then integrated using DIVPAG package. The following initial conditions were used to replace Eqs. (4-8) and (4-9).

$$c_{i,j}^k(t=0) = q_{i,j}^k(t=0) = 0 \quad (4-10)$$

It was found in this work that cyclic steady state can be essentially achieved in less than 10 cycles. A minimum number of 15 cycles (60 switches, 180 sub-phases) and relative mass balance error of both components less than 0.5% were used to ensure the steady state during SSMB simulations involved in this work.

### 4.2.3 Model parameters

Parameters for the simulations of a 4-column SSMB unit with TD model are summarized in Table 4-1. The feed concentrations were provided by COFCO Ltd., consistent with the composition of raw XOS syrup from typical the industrial processes. The column parameters were measured for a preparative SSMB unit in our lab. Equilibrium and kinetic parameters were acquired in a previous study [19].

**Table 4-1 Model parameters**

Columns	Column number	4
	d	2.5 cm
	L	100 cm
	$\varepsilon$	0.416
	$Q_{\max}$	20 ml min <sup>-1</sup>
Kinetic parameters	$N_L$	2000
	$k_{m,XOS}$	0.36 min <sup>-1</sup>
	$k_{m,impurity}$	4.54 min <sup>-1</sup>
Isotherm	$H_{XOS}$	0.167
(T=60°C)	$H_{impurity}$	0.450
Feed composition	$C_{XOS,feed}$	210 g/L
	$C_{impurity,feed}$	90 g/L

### 4.3 Variables and objectives of a binary SSMB system

As shown in Figure 4-1, an SSMB process has 7 independent operating parameters, i.e., 3 durations ( $t_1$ ,  $t_2$ ,  $t_3$ ), 4 flowrates ( $Q_{loop}$ ,  $Q_{eluent,phase1}$ ,  $Q_{eluent,phase3}$  and  $Q_{feed}$ ). For simplicity, it is assumed in this work that the flowrate in Zone I in all three phases is constant. Moreover, this constant flowrate in Zone I is fixed at the maximum flowrate limited by column pressure drop, i.e.,  $Q_{loop} = Q_{eluent} = Q_I \equiv Q_{\max}$ . As such, operating parameters of the three phases can be described as Table 4-2.

**Table 4-2 Dimensional operating parameters of SSMB**

Phase No.	duration	$Q_I$	$Q_{II}$	$Q_{III}$	$Q_{IV}$
1	$t_1$	$Q_{\max}$	0	$Q_{\text{feed}}$	0
2	$t_2$	$Q_{\max}$	$Q_{\max}$	$Q_{\max}$	$Q_{\max}$
3	$t_3$	$Q_{\max}$	$Q_{\max}$	$Q_{\max}$	0

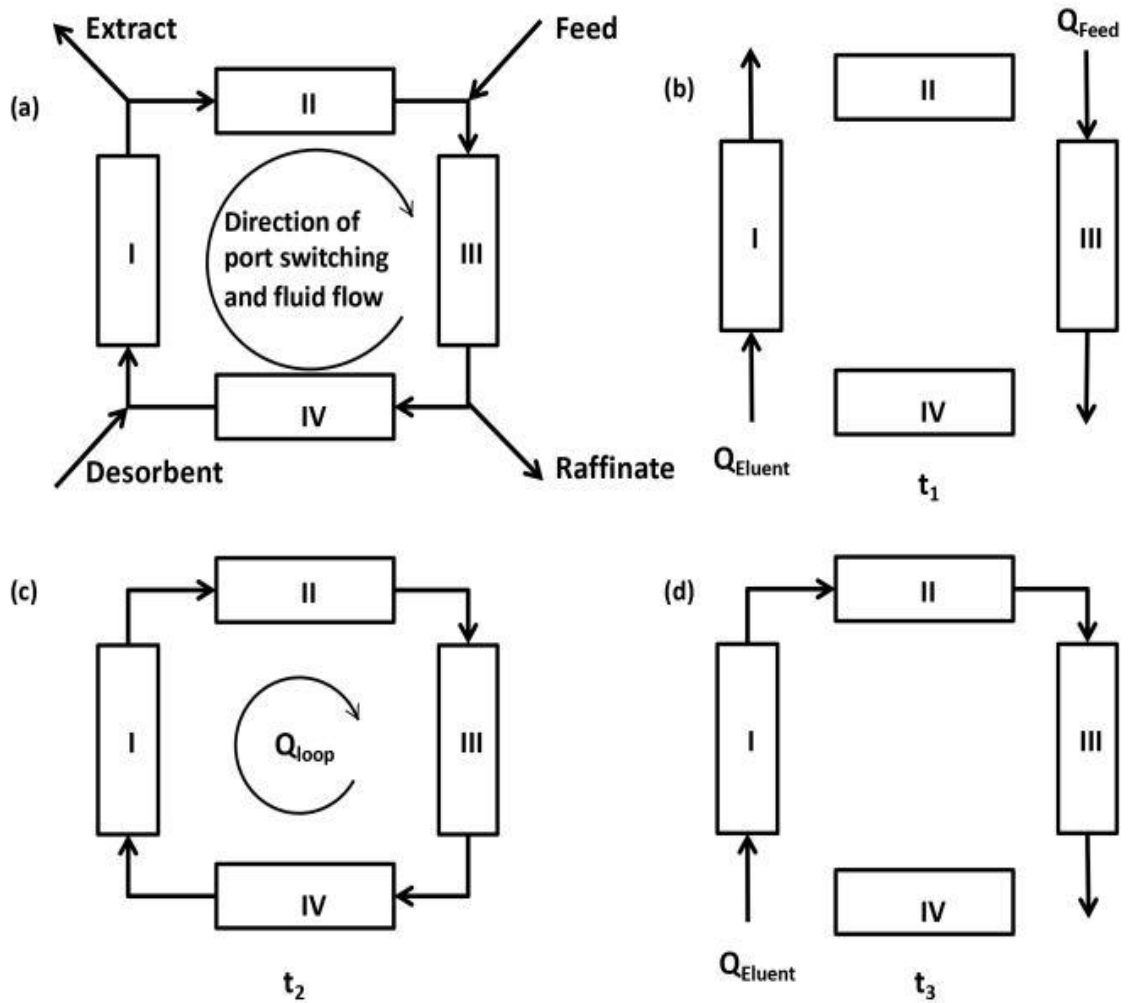


**Figure 4-1 Schematic diagrams of SMB and SSMB**

Throughout this work,  $Q_{max}$  was fixed at 20 ml/min as a scaling factor, in consistence with our previous publication. As a results, the number of independent parameters subjected to optimization is reduced to 4, similar to that of conventional SMB. While these parameters were determined by MOO in this work, Triangle Theory provides a convenient tool for the screening of suitable parameter ranges. The flowrate ratio defined below is also extensively involved in the following discussions.

$$m_j = \frac{\int_0^{t_s} Q_j dt - V\varepsilon}{V(1-\varepsilon)} \quad (4-11)$$

The 4 SSMB variables subjected to optimization can be sequentially determined from these  $m$  values :

$$t_2 = \frac{m_{IV}V(1-\varepsilon) + V\varepsilon}{Q_{max}} \quad (4-12)$$

$$t_3 = \frac{m_{II}V(1-\varepsilon) + V\varepsilon}{Q_{max}} - t_2 \quad (4-13)$$

$$t_1 = \frac{m_I V(1-\varepsilon) + V\varepsilon}{Q_{max}} - t_3 - t_2 \quad (4-14)$$

$$Q_{feed} = \frac{m_{III}V(1-\varepsilon) + V\varepsilon - (t_2 + t_3)Q_{Max}}{t_1} \quad (4-15)$$

As shown in the previous work, the desired product, XOS, is the less retained on the solid phase and is, therefore, collected at the raffinate port. The performance of SSMB processes were evaluated in terms of XOS purity (Pur) and recovery (Rec), unit throughput (UT), and water consumption (WC), which are defined in the following equations.

$$Pur = \frac{\int_0^{t_s} c_{XOS,Raf} Q_{Raf} dt}{\int_0^{t_s} (c_{XOS,Raf} + c_{impurity,Raf}) Q_{Raf} dt} \times 100\% \quad (4-16)$$

$$UT = \frac{Q_{feed}t_1}{t_s} \quad (4-17)$$

$$WC = \frac{Q_{Max}(t_1 + t_3)}{t_s} \quad (4-18)$$

$$Rec = \frac{\int_0^{t_s} c_{XOS,Raf} Q_{Raf} dt}{c_{XOS,feed} Q_{feed} t_1} \times 100\% \quad (4-19)$$

In this following discussions, two of the objectives were simultaneously optimized. Non-dominated sorting genetic algorithm (NSGA-II), which has been proven efficient to solve multi-objective optimization problems involved in various industrial chemical processes [39, 40], was applied to obtain the pareto solutions [34-36]. All calculations were programmed in FORTRAN codes and performed on a Lenovo ThinkPad L440 personal computer equipped with a 2.30 GHz Intel core i7 processor.

In total, three optimization problems with different objective functions were considered in this work. In addition, minimum requirements on purity, recovery and unit throughput may be set as constraints to limit the solutions in practically valuable range. The configurations of optimization problems are summarized in Table 4-3, together with the upper and lower bounds of operational variables, which are required by the use of NSGA II method. Numbers of population and generations, the other two key parameters for NSGA II, were both set to be 100.

**Table 4-3 Summary of optimization formulations and bounds of variables**

Case	Objectives	Constraints	Variables
1.1	Max Pur;	Pur>90%;	$0.6 < m_I < 1.2$ ; $0.15 < m_{II} < 0.35$ ;
	Max UT	Rec>90%	$0.2 < m_{III} < 0.6$ ; $0.05 < m_{IV} < 0.15$
1.2	Max Pur;	Pur>90%; Rec>90%	$0.6 < m_I < 1.2$ ; $0.15 < m_{II} < 0.35$ ;
	Max UT		$2 < Q_{feed} < 10$ ; $0.05 < m_{IV} < 0.15$
2	Max UT;	Pur>90,95,97%;	Same as 1.1
	Min WC	Rec>90%	
3	Max Rec;	Pur>90%;	$0.5 < m_I < 1.2$ ; $0.15 < m_{II} < 0.35$ ;
	Min WC	UT=2,3,4 ml/min	$0.05 < m_{IV} < 0.15$

## 4.4 Results and discussions

### 4.4.1 Case 1: simultaneous maximization of Pur and UT

Simultaneous maximization of Pur and UT was first investigated in this work. This is one of the most extensively pursued MOO problems in SMB literature and pareto solutions are normally acquired. In addition to the two objectives, minimum purity and recovery, both at practical value of 90%, were set as constraints. During the use of NSGA II, great penalty was applied if either of the constraints was not satisfied. Two groups of calculations using different variables were carried out and the results are presented below.

#### Case 1.1: Using variables of $m_I$ , $m_{II}$ , $m_{III}$ , and $m_{IV}$

As aforementioned in Section 3, four independent operational parameters of an SSMB unit are subjected to MOO. The flowrate ratios,  $m_I$ ,  $m_{II}$ ,  $m_{III}$ , and  $m_{IV}$  were first screened

in this case. The corresponding dimensional parameters,  $t_1$ ,  $t_2$ ,  $t_3$  and  $Q_{feed}$  were calculated using Eqs (4-12)-(4-15). Then, SSMB simulations were carried out using the column, equilibrium and kinetic parameters listed in Table 4-3. Simulation results in terms of objective functions and constraints were evaluated by NSGA-II, which then automatically update the operational parameters in the preset range. The optimal results obtained after 100 iterations (generations) are plotted in Figure 4-2.

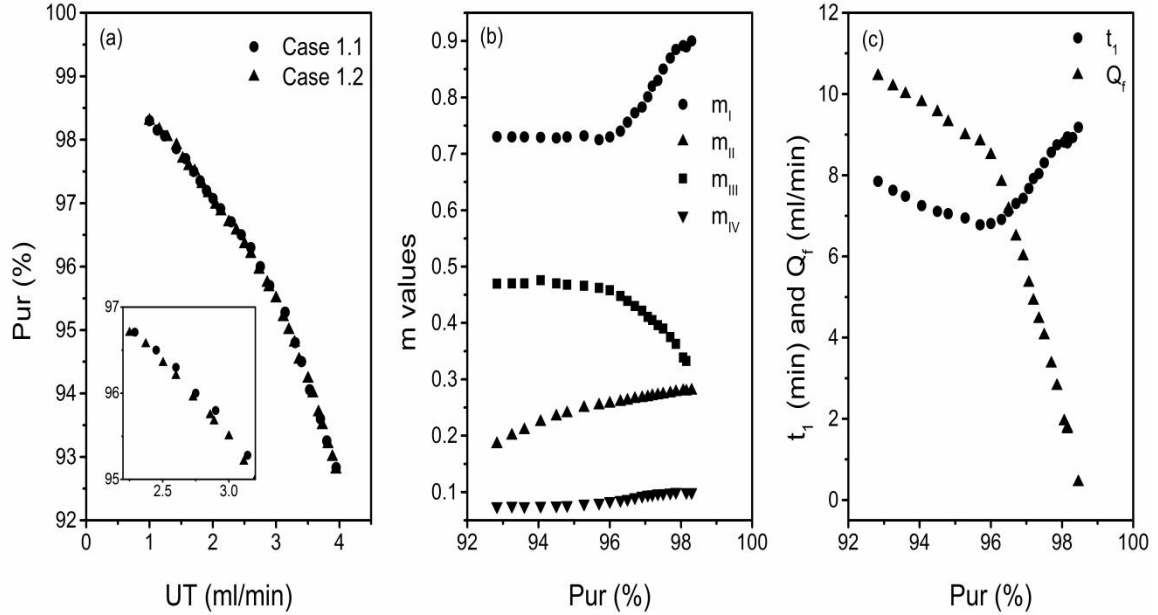


**Figure 4-2 Simultaneous maximization of unit throughput and purity. a: pareto, circle and triangle points are for Cases 1.1 and 1.2, respectively; b: corresponding optimized m values; c:  $t_1$  (min) and  $Q_f$  (ml/min) derived from the m values.**

Figure 4-2a shows that XOS's purity above 90% can be successfully achieved by properly operated SSMB, meeting the minimum commercial requirement. The maximum unit throughput decreases with the increase in XOS's purity. Any other operation in the examined parametric space (defined by the bounds in Table 4-3) gives an objective point lower than the pareto curve on (Pur-UT) plane, i.e., at least one of the objectives is worse when compared with any point on the curve. Therefore, all points on this curve are considered solutions to this optimization problem. Some of the obvious off-line points given by NSGA-II after 100 generations were manually removed.



The corresponding decision variables,  $m_I$ ,  $m_{II}$ ,  $m_{III}$ , and  $m_{IV}$ , are plotted against product purity in Figure 4-2b. Comparison with the bounds in Table 4-3 shows that all acquired optimal operation points are confined in the preset parametric range.

The trends in Figure 4-2b may be divided into two sections: (i) In the purity range lower than about 95.3%,  $m_I$ ,  $m_{III}$  and  $m_{IV}$  are essentially constant whereas  $m_{II}$  increases with increased purity; (ii)  $m_{III}$  decreases and the other three  $m$  values increases with increased purity in the higher range. These trends are compared with those of conventional SMB in Table 4-4. Pareto solutions and the corresponding decision variables for conventional SMB with the same parameters are provided in the Supplementary Materials (Figure S4-1).

**Table 4-4 Optimized  $m$  values for SSMB and SMB**

Range	Operation	Purity	UT	$m_I$	$m_{II}$	$m_{III}$	$m_{IV}$
lower	SMB	+ <sup>a</sup>	-	=	-	-	=
	SSMB	+	-	=	+	=	=
higher	SMB	+	-	+	-	-	+
	SSMB	+	-	+	+	-	+

a: +, -, = are for increase, decrease, and constant.

For a conventional SMB with a fixed flow pattern in a switch,  $m$  values of the 4 zones are individually determined by the corresponding flowrate. Therefore, based on the functional role of each zone, Triangle Theory may be applied to provide direct explanations to the trends in Table 4-4. Separation is mainly realized in Zones II and III. According to Triangle Theory, in order to increase unit throughput, flowrate in Zone II should be large to convey more light component to the feed port. On the other hand, to meet the purity requirement, the flowrate should be small to retain the heavy component. That  $m_{II}$  decreases with increased purity indicates that, the latter effect is dominant in the whole practical purity range greater than 90%. Flowrate in Zone III is limited by the breakthrough of heavy component at raffinate. Therefore,  $m_{III}$  decreases with increased

purity. The decrease in  $m_{III}$  is more significant than that in  $m_{II}$ , resulting in decreased unit throughput, which is the difference between flowrates in Zones II and III. Zone I and IV are for regeneration of stationary and mobile phases, respectively. They have negligible effects on purity in the lower range. In the higher range, both  $m_I$  and  $m_{IV}$  need to be increased to prevent retaining of heavy component that may pollute the raffinate product after column switching.

In the case of SSMB, however, the  $m$  values, as defined in Eq. (4-11), are averaged over a switch that is divided into three phases with different flow patterns. According to Eqs (4-12)-(4-15), given fixed  $Q_{max}$ , only  $m_{IV}$ , is determined by a single operating parameter,  $t_2$ . In addition,  $m_I$  is directly determined by  $t_s$ , which can be used to replace one of  $t_1$  and  $t_3$  as an independent operating parameter. However, 2 and 4 parameters are needed to determine  $m_{II}$  and  $m_{III}$ , respectively. It is on the ( $m_{II}$ - $m_{III}$ ) plane that the “Triangle” is plotted to optimize unit throughput for specified purity requirement. As a result, compared with conventional SMB, optimal SSMB operations may exhibit some different trends that cannot be directly explained by Triangle Theory with averaged  $m$  values.

As highlighted in Table 4-4, the trends of  $m_I$  and  $m_{IV}$  of SSMB are similar to those of conventional SMB whereas  $m_{II}$  and  $m_{III}$  exhibit some different features. These two values are determined by the combination of more than 1 phase with different flow patterns. As there have been few literature reports focused on SSMB, it is necessary to firstly clarify the specific role of each operational phase in a switch. For this purpose, internal concentration profiles at cyclic steady state corresponding to the optimized operation for purity of 95.8% are plotted in Figure 4-3.

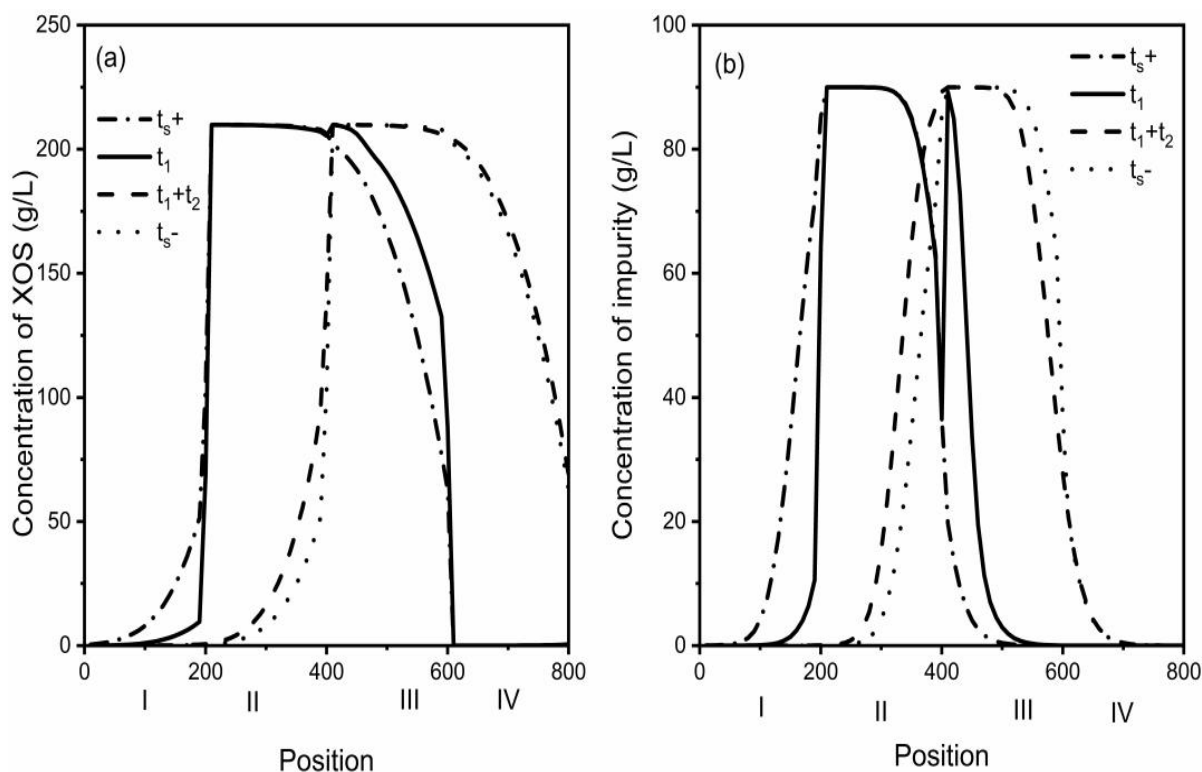


**Figure 4-3 Internal concentration profiles for 95.2% purity. a: XOS; b: impurity.**

**Corresponding  $m$  values:  $m_I=0.73$ ,  $m_{II}=0.25$ ,  $m_{III}=0.46$ ,  $m_{IV}=0.079$ .**

At the beginning of a switch ( $t_s^+$ ), XOS is almost saturated in Zone II. Its profile is extended to Zone I at lower level and to Zone III at a high level. The impurity is also mainly distributed in Zone II. A relatively large fraction is retained in Zone I and a small fraction is extended to Zone III. Zone IV is free of any components.

In the first phase, an external feed is introduced into Zone III, where previously enriched XOS is driven towards the raffinate port. Its front moves forward by about one third of the column during this phase. While impurity is also conveyed forward, the moving speed is slower due to the higher adsorption strength, they are retained in the column. The operation is switched to the next phase far before the breakthrough of impurities, which is different from conventional SMB optimized conditions (see Supplementary Materials Figure S4-2). Simultaneously, fresh water is introduced into Zone I. Previous retained impurity is purged out and collected at the extract port. Also purged out is a small fraction of XOS, diminishing the recovery. According to the description in Figure

4-1b-d, extract port is only open in phase 1. Therefore, at cyclic steady-state, the majority of impurity contained in the feed must be collected during this phase, which is similar to conventional SMB. As shown in Figure 4-3, by the end of this phase, adsorbent in Zone I is essentially regenerated, which determines the duration of  $t_I$ . During this phase, concentration profiles in isolated Zones II and IV with no mobile phase flow are not changed.

In the second phase, all inlet and outlet ports are closed. Both components are driven forward and redistributed by an internal loop that is applied to all columns. By the end of this phase, XOS is saturated in Zone III and is enriched in Zone IV. It is in this step that Zone IV is functioning in term of regeneration of mobile phase by the retaining of light component, which is similar to conventional SMB. However, since the extract port is not open and there is no outlet stream, a fraction of XOS is allowed to enter Zone I. The impurity profile is mainly distributed in Zones II and III, further separated with XOS that is about a whole column ahead.

Finally, in the last phase, fresh eluent is introduced again to convey the mobile phase in Zones I, II and III, whereas Zone IV is isolated. Only raffinate outlet is open. XOS previously saturated in Zone III is collected. Impurity breakthrough occurs during this period, reducing the overall product purity. While there is no flow in Zone IV, the concentration of XOS slightly decreases, which is due to the limited mass transfer between solid and fluid phases accounted for by TD model.

In order to explain the trends in Figure 4-2a, mass flows (MF) of component  $i$  defined below for three representative cases are plotted as functions of  $t/t_s$  in Figure 4-4.

$$MF_i = c_{i,Raf} Q_{Raf} \quad (4-20)$$

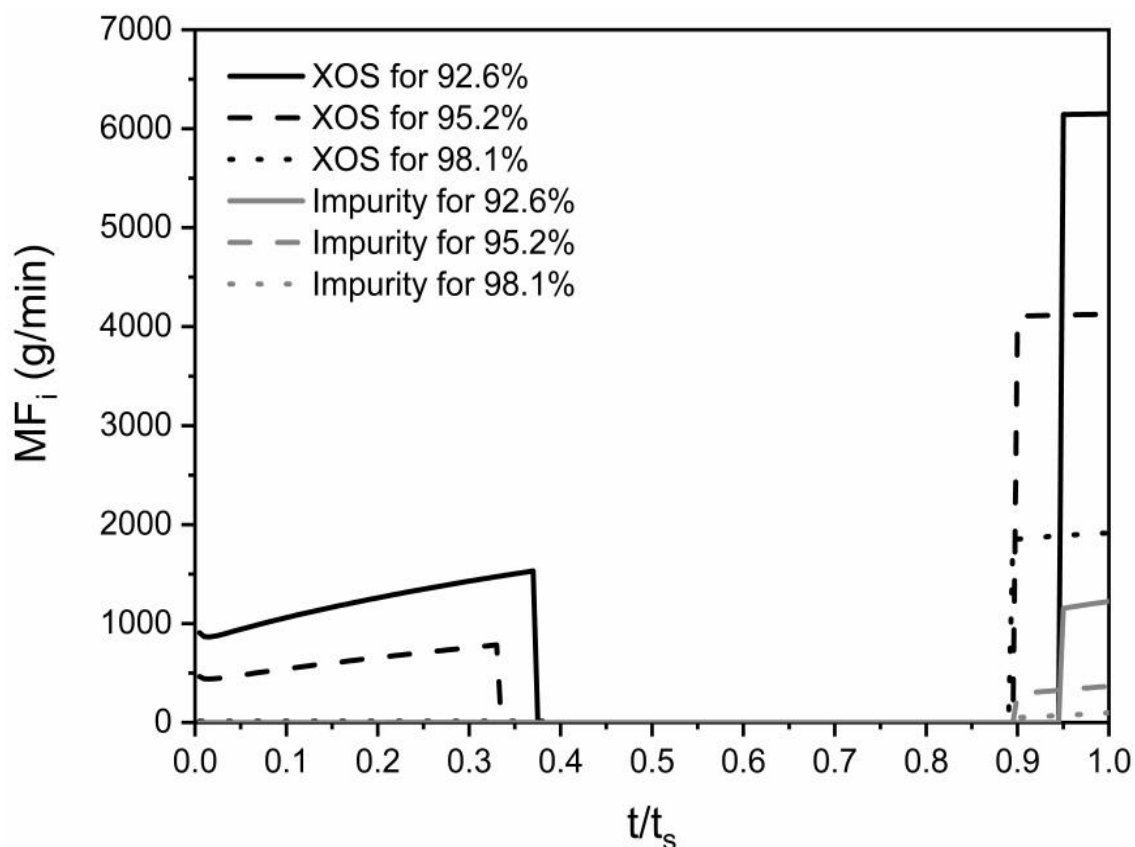


**Figure 4-4 MF plot for three representative purities. Black for XOS, gray for impurity; solid, dash and dot curves are for purities of 92.6% ( $m_I=0.73$ ,  $m_{II}=0.18$ ,  $m_{III}=0.47$ ,  $m_{IV}=0.075$ ), 95.2% ( $m_I=0.73$ ,  $m_{II}=0.25$ ,  $m_{III}=0.46$ ,  $m_{IV}=0.079$ ) and 98.1% ( $m_I=0.89$ ,  $m_{II}=0.28$ ,  $m_{III}=0.33$ ,  $m_{IV}=0.099$ ), respectively.**

The area below each curve is the averaged mass flow (AMF, g/min) of the corresponding component at the raffinate port. Calculated AMF values are summarized in Table 4-5.

**Table 4-5 The averaged mass flow values of three different cases**

Purity	Decision variables				AMF (g/min)					
	$m_I$	$m_{II}$	$m_{III}$	$m_{IV}$	XOS 1 <sup>a</sup>	XOS 3	XOS T	IMP <sup>b</sup> 1	IMP 3	IMP T
92.6%	0.73	0.1 8	0.4 7	0.07 5	445	307	752	0.408	59.5	59.9
95.2%	0.73	0.2 5	0.4 6	0.07 9	203	404	607	0	30.9	30.9
98.1%	0.89	0.2 8	0.3 3	0.09 9	2	211	213	0	4.23	4.23

a: 1, 3 and T are for phase 1, 3 and total; b: IMP is for impurity.

For the purity requirement of 95.2%, about 607 g/min XOS and 30.9 g/min impurity were collected in the raffinate port, respectively. About two third of XOS were collected in phase 3. More noticeable is that essentially all impurity is introduced in raffinate stream in phase 3.

As purity requirement is reduced to 92.6%, both  $t_I$  and  $Q_f$  increase (see Figure 4-2c), resulting in increased unit throughput. Different from the optimal operation for 95.2%, more retained heavy impurity, is driven further to the raffinate port and a breakthrough occurs by the end of the first phase. A significant larger amount of XOS is collected during  $t_I$ , with  $AMF_{XOS}$  increased from 203 to 445 g/min. Recall that, according to Eqs (4-12) and (4-14), given fixed maximum flowrate,  $m_I$  and  $m_{IV}$  are determined by total switch time and  $t_2$ , respectively. In the low purity range, constant  $m_I$  and  $m_{IV}$ , similar to those of conventional SMB, indicate that these two times are constant. Therefore,  $t_3$  consequently decreases with increased  $t_I$  at reduced purity. Accordingly, less XOS that is essentially saturated in Zone III is collected during a shortened phase 3. However, since the impurity front is driven further in previous steps, especially, in phase 1, impurity is more enriched than the case of 95.2% purity in Zone III during phase 3. The enrichment effect overcomes the decrease in  $t_3$ , and more impurity is collected in phase 3, reducing the overall purity. According to Eq (4-13), it is due to the decrease in  $t_3$  that  $m_{II}$  decreases

with decreased purity in the lower range. Effect of the decrease in  $t_3$  on  $m_{III}$  is compensated by the increased  $t_1$  and  $Q_f$ , and, as an overall result,  $m_{III}$  is kept constant for purities below 95.2%.

When the purity is increased further to 98.1%, contrary to the low purity range,  $t_1$  increases with increased purity, forming a minimum duration of phase 1 (see Figure 4-2c). Since extract port is open only in this phase, an extended duration is helpful for complete adsorbent regeneration by the purge with a fixed mobile phase flowrate in Zone I.  $Q_f$  in Zone III still decreases with improved purity, but the slope becomes sharper. An overall result is that less raw material is introduced to Zone III. Therefore, in order to drive XOS to Zone III where it will be collected in phase 3, duration of phase 2 needs to be increased. During this step, the longest among the three, an extended loop is beneficial for separation. Increased purity in the higher range does not have significant effect on  $t_3$ . Impurity collected in raffinate is mainly determined by the position of its front by the end of phase 2, which sets an upper limit of the increase in  $t_2$ . According to Eq (4-13),  $m_{II}$  increases with increased purity in the higher range is mainly attributed to the increase in  $t_2$ . On the contrary, it is recalled that, in the low purity range, the increase in  $m_{II}$  is due to increased  $t_3$ .

For conciseness, other trends that are similar to conventional SMB are not further discussed here.

### **Case 1.2: optimization with variables: $Q_{feed}$ , $m_I$ , $m_{II}$ , and $m_{IV}$ .**

The optimization problem with the same objective functions and constraints of case 1.1 were performed with one of the decision variables,  $m_{III}$ , replaced by  $Q_{feed}$ . It was found by Jiang et al. that replacing  $m_{III}$  with feed flowrate may simplify the definition of parameter boundaries and accelerate convergence during the MOO of a conventional SMB for a binary separation with relatively low selectivity [5].

The acquired pareto curve is plotted in Figure 4-2a for direct comparison. It may be seen that the two curves by different variables are almost overlapping, validating the robustness of NSGA-II and the acquired optimal solutions. A close comparison (the

insert in Figure 4-2a) in the purity range of 95-97%, which is of great industrial interests, however, shows the pareto curve obtained in Case 1.1 is slightly higher than the one in Case 1.2. Optimized decision variables for Case 1.2 are plotted in Figure 4-5. The trends are quantitatively similar to those in Figure 4-2a but the points are more scattered. For consistency,  $m$  values were used as decision variables in the following work.

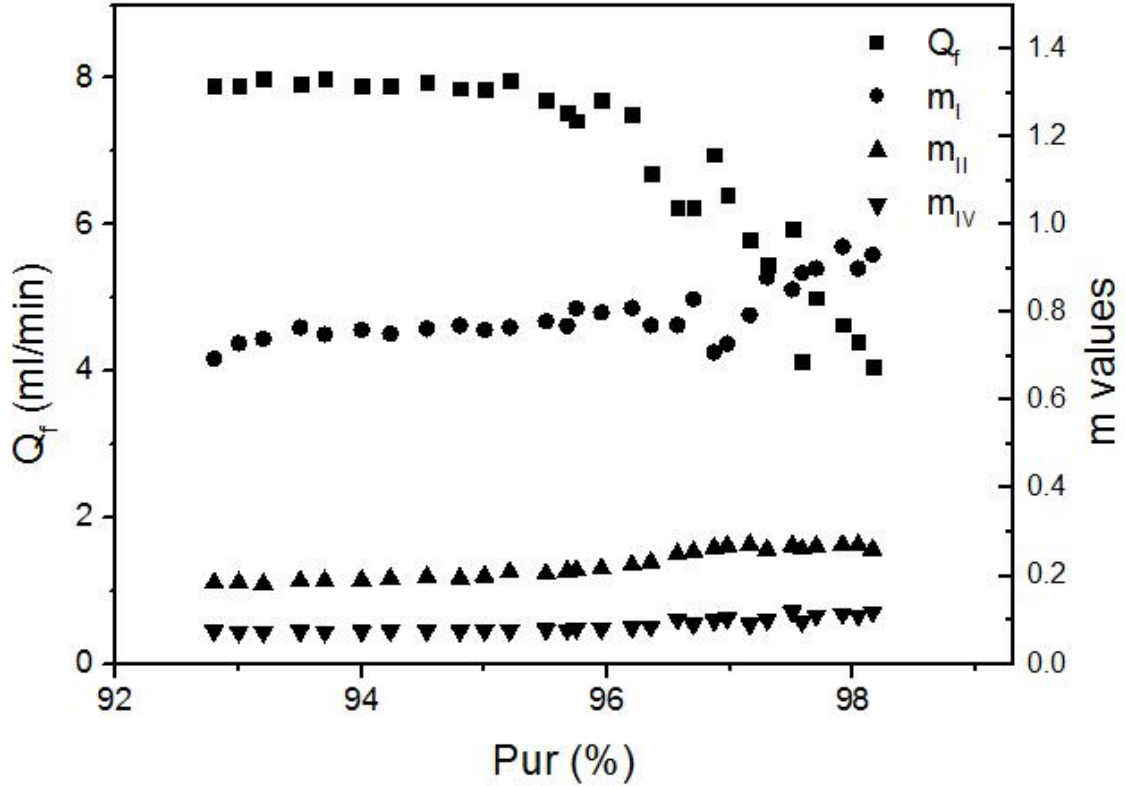


Figure 4-5 Decision variables for Case 1.2

#### 4.4.2 Case 2: maximization of unit throughput and minimization of water consumption at different XOS's purities

Solvent consumption is one of the major concerns that directly determines the cost of industrial adsorptive processes for sugar purification. In the following discussions, water consumption defined in Eq (4-18) was considered as an objective. First investigated is the simultaneous maximization of unit throughput and minimization of water consumption.



Several cases with different constraints on product purity were studied (see Table 4-2 for the problem configurations).

As shown in Figure 4-6a, for a required purity, unit throughput may be increased by the compensation of more water consumption. With increased purity, the pareto curve moves downwards.

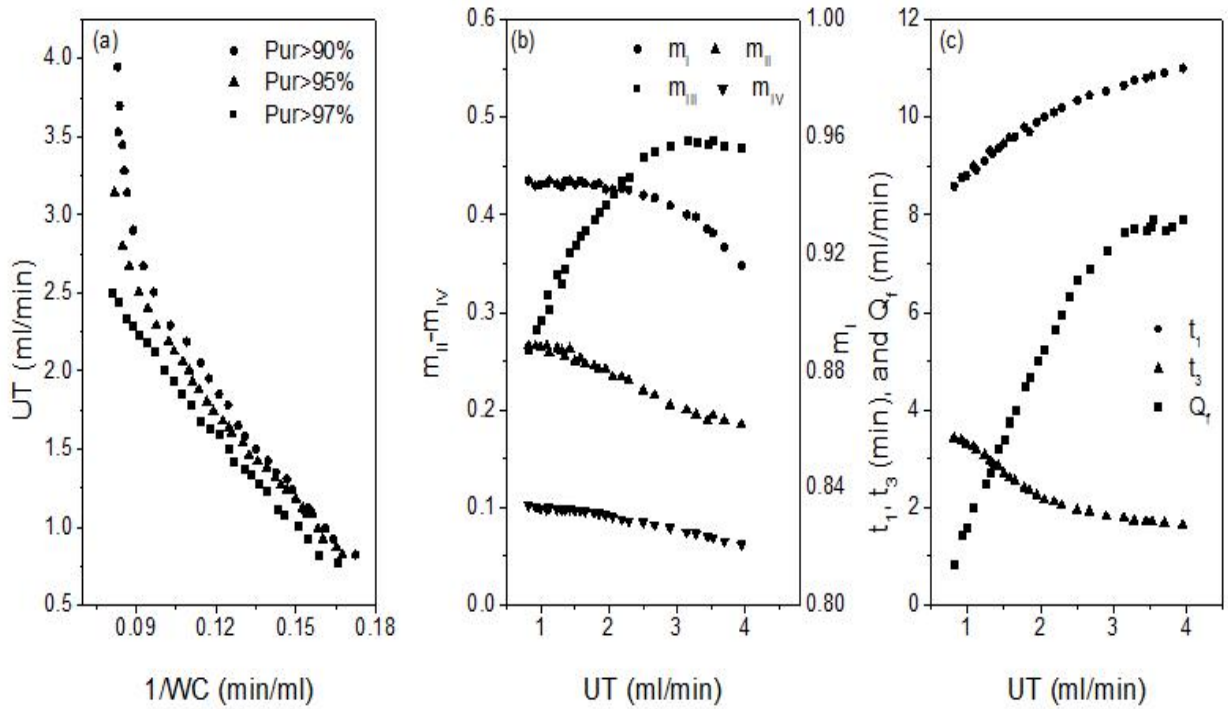


**Figure 4-6 Simultaneous maximization of unit throughput and minimization of solvent consumption at various purity requirements. a: pareto, circle, triangle, and square are for purity constraints of 90%, 95% and 97%; b: corresponding optimized  $m$  values of purity >90%; c: derived  $t_1$ ,  $t_3$ , and  $Q_f$ .**

The  $m$  values corresponding to purity greater than 90% are plotted against unit throughput in Figure 4-6b. In the low UT range,  $m_I$  is almost constant, indicating constant  $t_s$ . According to the node balance over a switch that is similar to conventional SMB, the increase in UT can be straightforwardly explained by the increased  $m_{III}$  and decreased  $m_{II}$ . The corresponding increase in WC is due to the decreased  $m_{IV}$ . In the case of conventional SMB, for a constant  $t_s$ , mobile phase flowrates in Zones II, III and IV

increases or decreases according to the corresponding  $m$  values. However, for SSMB, the qualitative trends of these  $m$  values are not sufficient to give direct guidance on how to tune all of the operating parameters. Decrease in  $m_{IV}$  suggests a decrease in  $t_2$ , duration of the loop step. According to Eq (4-13),  $m_{II}$  is affected by both  $t_2$  and  $t_3$ . Since the trend of  $m_{II}$  is in qualitative agreement with that of  $t_2$ , whether  $t_3$  increases or decreases cannot be determined. The increase in  $m_{III}$ , a function of 4 parameters defined in Eq (4-15). The trends of  $t_1$  and  $Q_f$  cannot be derived. Figure 4-6c gives optimized  $t_1$ ,  $t_3$  and  $Q_f$  as functions of UT. It may be seen that  $t_3$  actually decreases with increased UT, which has a positive effect on the decrease in  $m_{II}$  but a negative effect on the increase in  $m_{III}$ . The increase in  $m_{III}$  is therefore attributed to the increase in both  $t_1$  and  $Q_f$ . Further increase in UT requires accelerated switching time, and  $m_I$  decreases accordingly.

The  $m$  values and dimensional operating parameters corresponding to the other purity constraints are provided in Supplementary Materials (Figures S4-3 and S4-4).

#### 4.4.3 Case 3: maximization of XOS's recovery and minimization of water consumption at fixed unit throughput values

Recovery greater than 90% was used in the above cases as a constraint. In Case 3, enhancing XOS recovery and reducing water consumption were defined as the two objectives. Purity greater than 90% was set as a constraint. Three groups of optimizations were conducted with different unit throughput values. Due to the fixed unit throughput, according to the definition of Eq (4-17), the number of independent operating parameters is reduced to 3. As described in Table 4-2,  $m_I$ ,  $m_{II}$  and  $m_{IV}$  were used for this case. They were converted to  $t_1$ ,  $t_2$  and  $t_3$  using Eqs (4-12)-(4-14). Since  $m_{III}$  is not used,  $Q_f$  is calculated from Eq (4-17) for a given UT.

Figure 4-7a shows that, for each fixed UT, a pareto solution curve was obtained for simultaneous maximization of XOS recovery and minimization of water consumption. The pareto curve moves downwards on (Rec-WC) plane when the fixed UT increases. Corresponding  $m$  values for UT=2 ml/min are plotted against recovery in Figure 4-7b. It

may be seen that all three  $m$  values increase with increased recovery. Again, these trends cannot be directly interpreted. Explanations to the pareto trends involves analyses of dimensional parameters, internal concentration profiles and MF curves, which are provided in the Supplementary Materials (Figure S4-5--S4-7). The details are similar to the discussion in Case 1 and are omitted here for conciseness. In short, while there are only three independent parameters in this case, all of the four dimensionless parameters change with recovery. With increased recovery,  $t_1$ ,  $t_2$  and  $t_3$  increase whereas  $Q_f$  decreases.

In all, a switch of an SSMB is divided into three sub-steps with different functional roles. Even with number of independent operating parameters reduced to the same as conventional, SSMB is still more complicated. Specifically, product and impurity enter the raffinate stream in two separated steps and the ratio may change under different optimized conditions. The loading of raw materials in step 1 is determined by both flowrate and duration, the latter of which is should be sufficient to collect impurity in the extract stream. Averaged  $m$  values are not sufficient to give direct guidance for tuning the dimensional operating parameters. Effects of dimensional operating parameters on the objective functions and constraints are coupled and cannot be qualitatively predicted until the optimal solutions have been established. Therefore, rigorous multi-objective optimization with detailed models is necessary for the design of SSMB processes.

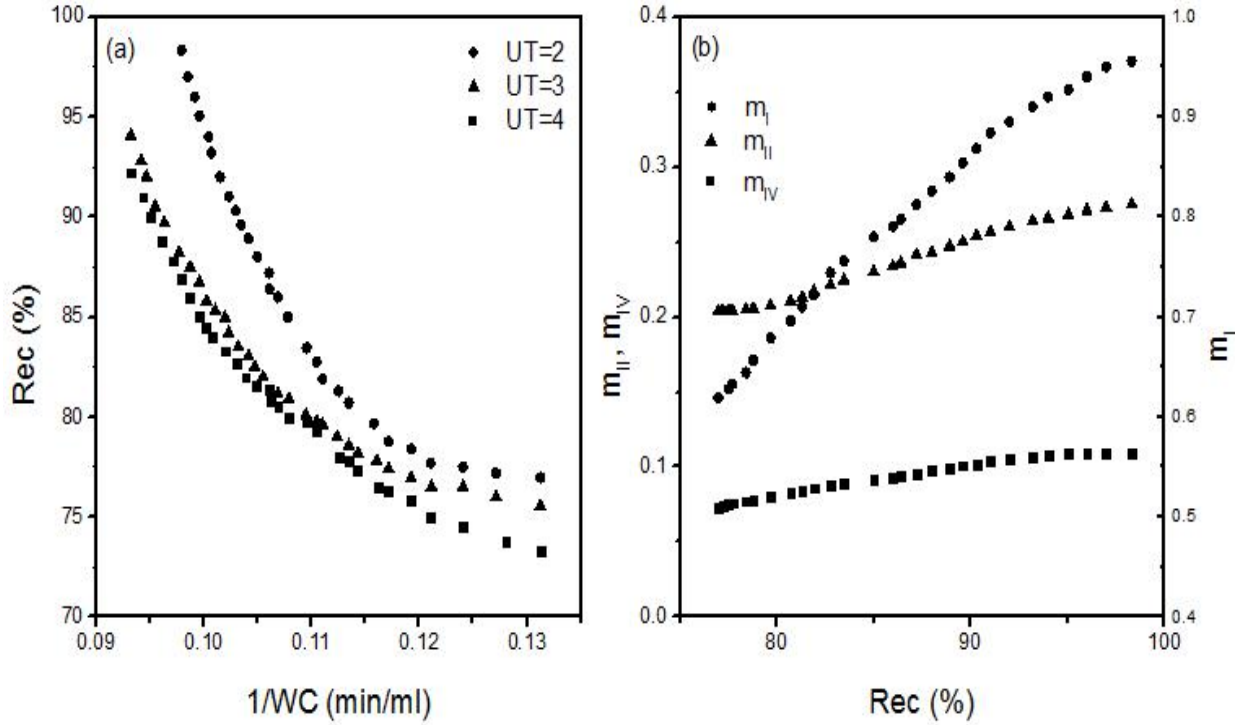


**Figure 4-7 Simultaneous maximization of XOS recovery and minimization of solvent consumption at various equipment capacities. a: pareto, circle, triangle, and square are for UT of 2, 3 and 4 ml/min; b: corresponding optimized  $m$  values of UT=2 ml/min.**

## 4.5 Conclusion

The feasibility of XOS purification by a 4 column SSMB unit was investigated using multi-objective optimizations. Transport-dispersive model with parameters determined in a previous work was used to describe the dynamic adsorption behaviors. Various optimization problems with different objective functions and constraints were solved by NSGA-II.

Results of simultaneous maximization of unit throughput and purity of XOS, the less adsorbed component, show that purity greater than 90% can be successively achieved with recovery greater than 90%. The optimal unit throughput, however, decreases with

increased purity requirement, forming a pareto curve in the (EC-PUR) plane. While the trade-off between these two objectives is generally the case for SMB separation processes, the trends of decision variables in term of  $m$  values exhibit some features qualitatively different from those of a conventional SMB. The decrease in unit throughput with increased raffinate purity is mainly attributed to a increase in  $m_{II}$  rather than a decrease in  $m_{III}$ , the latter of which is normally predicted by the extensively used Triangle Theory for a conventional SMB. These features were explained by the analyses of internal concentration profiles and mass flows at the raffinate port. Essentially, a switch of SSMB is further divided into three sub-steps with different durations and flow patterns. Each of the sub-steps has its functional role. There exists a minimum duration of step 1, corresponding to the boundary between high and low purity ranges. The increase in  $m_{II}$  with increased purity up to 95.2% is attributed to the increase in duration of step 3 with a constant flowrate in Zones I to III and isolated Zone IV. The increase in  $t_3$  is compensated with decrease of mass flow in Zone III during step 1 when Zone I and III are separately loaded with desorbent and feed, resulting in a constant  $m_{III}$ . On the other hand, with further increased purity,  $m_{II}$  increases due to the increase in duration of step 2 operated with an internal loop. As a result of sharply decreased feed flowrate,  $m_{III}$  decreases, together with increased  $m_{II}$ , accelerating the decrease in unit throughput. As a conclusion, in the case of SSMB with transient variations during a switch, averaged  $m_{II}$  and  $m_{III}$  values are determined by the combination of more than 1 dimensional operating parameters. Direct use of Triangle Theory with averaged  $m$  values may lead to wrong design and diagnosis of such processes.

Water consumption, a major concern in adsorptive sugar purification processes, was also investigated. For given requirement on purity and recovery, water consumption increases with increased unit throughput. Water consumption increases with increased purity requirement. For given requirement on purity and fixed unit throughput, enhanced recovery must be compensated with increased water consumption. The higher the unit throughput, the higher the water consumption. The trends of corresponding  $m$  values cannot be directly interpreted in these two cases. Dimensional operating parameters must be used to give the explanations based on individual functional role of the sub-steps. However, these parameters are corresponding to the optimal solutions. Therefore, multi-

objective optimization must be involved in the design of complicated SSMB processes.

## 4.6 References

- [1] Schmidt-Traub, H.. Preparative Chromatography. Germany: WILEY-VCH, 2005.
- [2] Ribeiro, A.E., Graca, N.S., Pais, L.S., and Rodrigues, A.E.. Preparative separation of ketoprofen enantiomers: Choice of mobile phase composition and measurement of competitive adsorption isotherms. *Separation and Purification Technology*, 2008, (61): 375-383.
- [3] Ribeiro, A.E., Gomes, P.S., Pais, L.S., and Rodrigues, A.E.. Chiral separation of ketoprofen enantiomers by preparative and simulated moving bed chromatography. *Separation Science and Technology*, 2011, (46): 1726-1739.
- [4] Xu, J., Jiang, X.X., Guo, J.H., Chen, Y.T., Yu, W.F.. Competitive adsorption equilibrium model with continuous temperature dependent parameters for naringenin enantiomers on Chiralpak AD column. *Journal of Chromatography A*, 2015, (1422): 163-169.
- [5] Jiang, X.X., Zhu, L., Yu, B., Su, Q., Xu, J., Yu, W.F.. Analyses of simulated moving bed with internal temperature gradients for binary separation of ketoprofen enantiomers using multi-objective optimization: Linear equilibria. *Journal of Chromatography A*, 2018, (1531): 131-142.
- [6] Rajendran, A., Paredes, G., and Mazzotti, M.. Simulated moving bed chromatography for the separation of enantiomers. *Journal of Chromatography A*, 2009, (1216): 709-738.
- [7] Minceva, M., and Rodrigues, A.E.. Modeling and simulation of a simulated moving bed for the separation of p-xylene. *Ind. Eng. Chem. Res.*, 2002, (41): 3454-3461.
- [8] Minceva, M., and Rodrigues, A.E.. Two-level optimization of an existing SMB for p-xylene separation. *Computers and Chemical Engineering*, 2005, (29): 2215-2228.
- [9] Pynnonen, B.. Simulated moving bed processing: escape from the high-cost box.

Journal of Chromatography A, 1998, (827): 143-160.

[10] Azevedo, D.C.S., and Rodrigues, A.E.. Fructose-glucose separation in a SMB pilot unit: modeling, simulation, design, and operation. AIChE J, 2001, (9): 2042-2051.

[11] Gomes, P.S., Minceva, M., and Rodrigues, A.E.. Simulated moving bed technology: old and new. Adsorption, 2006, (12): 375-392.

[12] Faria, R.P.V. and Rodrigues, A.E.. Instrumental aspects of simulated moving bed chromatography. Journal of Chromatography A, 2015, (1421): 82-102.

[13] Zhang, Y., Hidajata, K., and Ray, A.K.. Multi-objective optimization of simulated moving bed and Varicol processes for enantio-separation of racemic pindolol. Separation and Purification Technology, 2009, (65): 311-321.

[14] Pais, L.S., and Rodrigues, A.E.. Design of simulated moving bed and Varicol processes for preparative separations with a low number of columns. Journal of Chromatography A, 2003, (1006): 33-44.

[15] Zhang, Z.Y., Hidajat, K., Ray, A.K., and Morbidelli, M.. Multi-objective optimization of SMB and Varicol process for chiral separation. AIChE Journal, 2002, (12): 2800-2816.

[16] Yu, W.F., Hidajat, K., Ray, A.K.. Optimization of reactive simulated moving bed and Varicol systems for hydrolysis of methyl acetate. Chemical Engineering Journal, 2005, (112): 57-72.

[17] Wei, F., Shen, B., Chen, M.J., Zhou, X.B., and Zhao, Y.X.. Separation of  $\alpha$ -Tocopherol with a two-feed simulated moving bed. Separation Science and Engineering, 2012, (4): 673-678.

[18] Jiang, C., Huang, F., and Wei, F.. A pseudo three-zone simulated moving bed with solvent gradient for quaternary separations. J. Chromatogr. A, 2014, (1334): 87-91.

[19] Li, Y., Yu, W.F., Ding, Z.Y., Xu, J., Tong, Y., and Ray, A.K.. Equilibrium and

kinetic differences of XOS2-XOS7 in xylo-oligosaccharides and their effects on the design of simulated moving bed purification process. *Separation and Purification Technology*, 2019, (215): 360-367.

[20] Lee, E. B., and Markus, L.. *Foundations of optimal control theory*. New York: Wiley, 1967.

[21] Storti, G., Mazzotti, M., Morbidelli, M., and Carra, S.. Robust design of binary countercurrent adsorption separation processes. *AIChE Journal*, 1993, (3): 471-492.

[22] Mazzotti, M., Storti, G., Morbidelli, M.. Optimal operation of simulated moving bed units for nonlinear chromatographic separations. *Journal of Chromatography A*, 1997, (769): 3-24.

[23] Kaspereit, M., Seidel-Morgenstern, A., and Kienle, A.. Design of simulated moving bed processes under reduced purity requirements. *Journal of Chromatography A*, 2007, (1162): 2-13.

[24] Ma, Z., and Wang, N.H.L.. Standing wave analysis of SMB chromatography: linear systems. *AIChE Journal*, 1997, (10): 2488-2508.

[25] Yu, W.F., Hidajat, K., and Ray, A.K.. Modeling, simulation, and experimental study of a simulated moving bed reactor for the synthesis of methyl acetate ester. *Ind. Eng. Chem. Res.*, 2003, (26): 6743-6754.

[26] Zhang, Z.Y., Hidajat, K., Ray, A.K.. Multi-objective optimization of simulated countercurrent moving bed chromatographic reactor (SCMCR) for MTBE synthesis. *Ind. Eng. Chem. Res.*, 2002, (41): 3213-3232.

[27] Bhaskar, V., Gupta, S.K., and Ray, A.K.. Multi-objective optimization of an industrial wiped film poly (ethylene terephthalate) reactor: some further insights. *Computers and Chemical Engineering*, 2001, (25): 391-407.

[28] Tarafder, A., Rangaiah, G.P., Ray, A.K.. Multi-objective optimization of an industrial styrene monomer manufacturing process. *Chemical Engineering Science*, 2005,



(60): 347-363.

[29] Bhutani, N., Ray, A.K., and Rangaiah, G.P.. Modeling, simulation, and multi-objective optimization of an industrial hydrocracking unit. *Ind. Eng. Chem. Res.*, 2006, (45): 1354-1372.

[30] Yu, W.F., Hariprasad, J.S., Zhang, Z.Y., Hidajat, K., and Ray, A.K.. Application of multi-objective optimization in the design of SMB in chemical process industry. *J. Chin. Inst. Chem. Engrs.*, 2004, (1): 1-8.

[31] Tarafder, A., Rangaiah, G.P., and Ray, A.K.. A study of finding many desirable solutions in multi-objective optimization of chemical processes. *Computers and Chemical Engineering*, 2007, (31): 1257-1271.

[32] Agrawal, N., Rangaiah, G.P., Ray, A.K., and Gupta, S.K.. Multi-objective optimization of the operation of an industrial low-density polyethylene tubular reactor using genetic algorithm and its jumping gene adaptations. *Ind. Eng. Chem. Res.*, 2006, (45): 3182-3199.

[33] Rajesh, J.K., Gupta, S.K., Rangaiah, G.P., and Ray, A.K.. Multi-objective optimization of industrial hydrogen plants. *Chemical Engineering Science*, 2001, (56): 999-1010.

[34] Kasat, R.B., Kunzru, D., Saraf, D.N., and Gupta, S.K.. Multiobjective optimization of industrial FCC units using elitist nondominated sorting genetic algorithm. *Ind. Eng. Chem. Res.*, 2002, (41): 4765-4776.

[35] Lee, F.C., Rangaiah, G.P., and Ray, A.K.. Multi-objective optimization of an industrial penicillin V bioreactor train using non-dominated sorting genetic algorithm. *Biotechnology and Bioengineering*, 2007, (3): 586-598.

[36] Tarafder, A., Lee, B.C.S., Ray, A.K., and Rangaiah, G.P.. Multi-objective optimization of an industrial ethylene reactor using a non-dominated sorting genetic algorithm. *Ind. Eng. Chem. Res.*, 2005, (44): 124-141.

- [37] Mao, S.M., Zhang, Y., Rohani, S., Ray, A.K.. Chromatographic resolution and isotherm determination of (R,S)-mandelic acid on Chiralcel-OD column. *J. Sep. Sci.*, 2012, (35): 2273-2281.
- [38] Xu, J., Zhu, L., Xu, G.Q., Yu, W.F., Ray, A.K.. Determination of competitive adsorption isotherm of enantiomers on preparative chromatographic columns using inverse method. *J. Chromatogr. A*, 2013, (1273): 49-56.
- [39] Agrawal, N., Rangaiah, G.P., Ray, A.K., Gupta, S.K.. Design stage optimization of an industrial low-density polyethylene tubular reactor for multiple objectives using NSGA-II and its jumping gene adaptations. *Chemical Engineering Science*, 2007, (62): 2346-2365.
- [40] Nandasana, A.D., Ray, A.K., and Gupta, S.K.. Applications of the non-dominated sorting genetic algorithm (NSGA) in chemical reaction engineering. *International Journal of Chemical Reactor Engineering*, 2003, (1):1-16.
- [41] Kasat, R.B., and Gupta, S.K.. Multi-objective optimization of an industrial fluidized-bed catalytic cracking unit (FCCU) using genetic algorithm (GA) with the jumping genes operator. *Computers and Chemical Engineering*, 2003, (27): 1785-1800.
- [42] Yu, H.W., and Ching, C.B.. Optimization of a simulated moving bed based on an approximated langmuir model. *AIChE Journal*, 2002, (48): 2240-2246.
- [43] Yu, H.W., and Ching, C.B.. Modeling, simulation and operation performance of a simulated moving bed for enantioseparation of fluoxetine on new  $\beta$ -cyclodextrin columns. *Adsorption*, 2003, (9): 213-223.

## Chapter 5

### 5. A comparison between SMB and SSMB for fructose-glucose separation based on multi-objective optimization

#### 5.1 Introduction

Simulated moving bed (SMB), compared with conventional batch adsorption/desorption processes, has the advantages of continuous operation, complete separation at low selectivity, and reduced solvent consumption. As shown in Figure 5-1a, a typical SMB system consists of a number of series-connected chromatographic columns and is divided into four zones by two inlet (feed, desorbent) and two outlet (raffinate, and extract) ports. A relative counter-current movement of stationary and mobile phases with respect to the ports is realized by periodically switching these ports along the direction of mobile phase flow. Each of the four zones plays specific functional roles in the adsorptive separation [1-5].

SMB technique was firstly developed in 1960s by Universal Oil Product (UOP) for the adsorptive purification of p-xylene (PX) from C8 mixture [6]. Another large scale application of SMB is in sugar industry, especially, fructose/glucose separation [7]. More recently, the use of SMB has been extended to pharmaceutical industry to purify the chiral drugs and some biological components with high economic value [8-10].

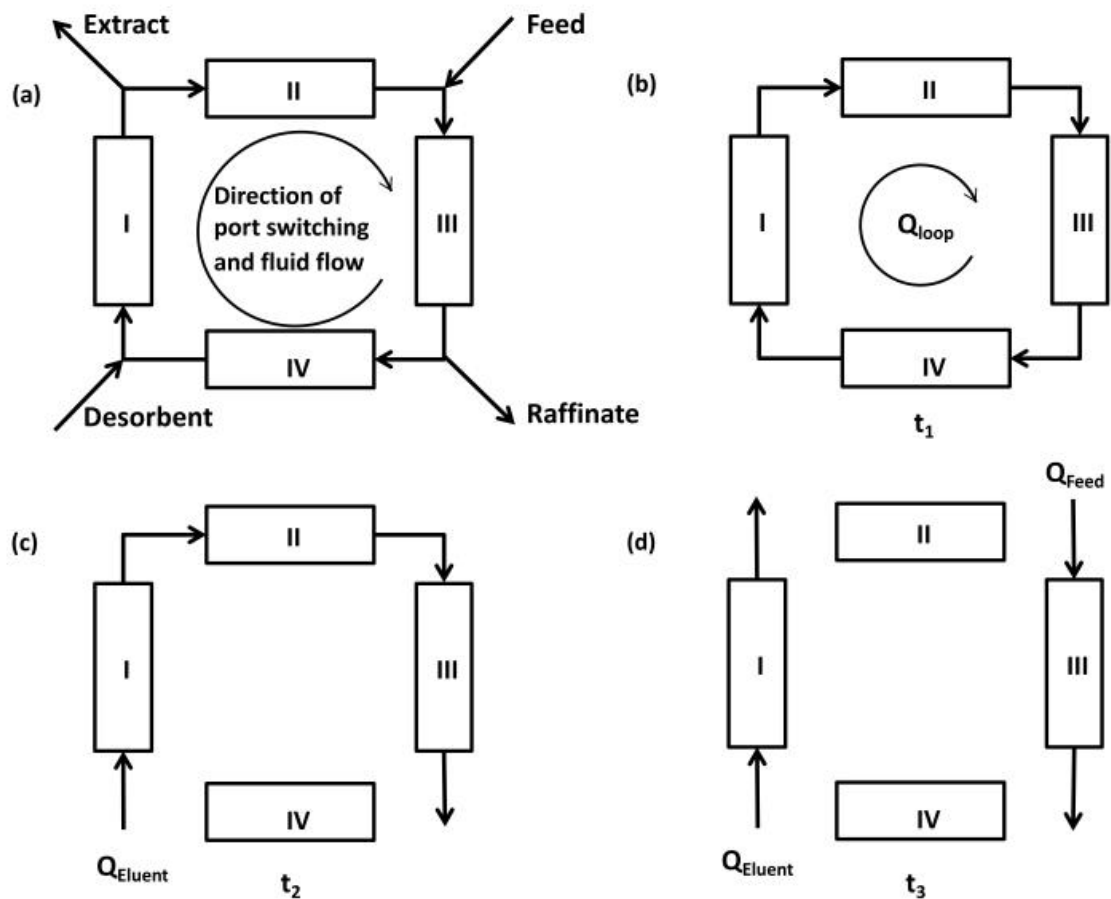


**Figure 5-1 Schematic diagrams of regular 4-zone SMB and SSMB**

Theoretical studies on SMB for fructose-glucose separation have been extensively reported. Beste et al., Azevedo et al., and Subramani et al. carried out several simulation and optimization works [11-13]. Model parameters were measured and the separation performance in terms of purity and productivity was successfully improved under the guidance of computational results. Subramani et al. performed optimization work on a varicol process, a modified SMB operation that divides a switch into several sub-steps with different column distributions among the 4 functional zones, and compared the results to those of regular SMB process [13]. However, solvent consumption, a major concern in industrial fructose-glucose separation, was not considered as an optimization objective in these works. Tangpromphan et al. reported a three-zone SMB process that can be used to reduce solvent consumption based on the port-relocation procedure [14]. Systematic optimization results were not presented in this work. Azevedo et al., Borges

da Silva et al., and Zhang et al. studied reactive SMB processes for the production of highly concentrated fructose syrup by glucose isomerization of [15-17]. In-situ adsorptive separation was used to enhance the conversion of reversible isomerization to the level beyond thermodynamic limit.

An alternative to reduce solvent consumption is sequential simulated moving bed (SSMB), a modified SMB technique. As shown in Figures 5-1b, 5-1c, and 5-1d, one switch in SSMB is divided into three sub-steps with different flow patterns. In the 1<sup>st</sup> step, the mobile phase is circulated in the whole system, forming a closed loop; in the 2<sup>nd</sup> step, zone IV is isolated and an external solvent stream is introduced at the desorbent port to purge the less adsorbed species to raffinate port; in the 3<sup>rd</sup> step, zone II is also isolated and another feed stream is introduced such that preferentially and less adsorbed species are simultaneously collected at extract and raffinate ports, respectively [18].

While SSMB has been successfully applied in industrial fructose/glucose separation for tens of years, to our knowledge, no relevant theoretical studies have been reported in the literature. In order to provide theoretical guidance to industrial design and operation, it is valuable to give a comprehensive comparison between SSMB and regular SMB processes for fructose-glucose separation. This kind of comparison should be carried out under separately optimized conditions [19].

A widely used approach to SMB optimization is Triangle Theory that determines flowrate ratios, normally referred to as  $m$  values, in the four zones using just linear or nonlinear adsorption isotherms [20, 21]. However, Triangle Theory is mainly focused on the maximization of unit throughput for given purity requirements [22]. Its application on the reduction of solvent consumption has not been verified. In addition, according to our previous study on xylo-oligosaccharides purification, due to the complicity of SSMB, effects of operating parameters on optimal unit throughput, purity, and solvent consumption cannot be qualitatively interpreted using averaged  $m$  values [23]. Quantitatively, Triangle Theory was developed based on the assumption of infinite column efficiency, which is generally not satisfied by stationary phase materials in sugar industry.

Noticing that operating parameters normally have contradicting effects on separation objectives, such as purity, recovery, productivity, and solvent consumption [2, 4], systematic multi-objective optimization studies have been carried out to determine suitable operating conditions of various SMB processes [2, 4, 24, 25]. However, multi-objective optimization of SSMB has not been reported in the literature.

The current work has been aimed at providing a comparison between SSMB and regular SMB processes for fructose-glucose separation based on multi-objective optimization results. For this purpose, multi-objective optimization with various objective functions corresponding to different process requirements were conducted for both processes. Great attentions were specially paid to solvent consumption.

## 5.2 Mathematical model

### 5.2.1 Model description

The conventional equilibrium-dispersive (ED) [2, 26-29] and linear isotherm models were applied to describe the component mass balance and adsorption behaviors of fructose-glucose separation process. The models could be written as below.

$$\frac{\partial c_{i,j}}{\partial t} + \varphi \frac{\partial q_{i,j}}{\partial t} + u_j \frac{\partial c_{i,j}}{\partial z} - D_{ap,j} \frac{\partial^2 c_{i,j}}{\partial z^2} = 0 \quad (5-1)$$

$$q_i^* = H_i c_i \quad (5-2)$$

where  $c$  and  $q$  are concentrations in the liquid and stationary phases, respectively,  $j$  is the index for column,  $t$  is time,  $\varphi$  is phase ratio defined as  $\varphi=(1-\varepsilon)/\varepsilon$ ,  $\varepsilon$  is column voidage,  $u$  ( $=Q/\varepsilon/\pi r^2$ ) is interstitial mobile phase velocity,  $z$  is the axial coordinate,  $D_{ap}$  is the apparent diffusivity,  $H$  is Henry's constant. Footnote  $i$  is component index, "glu" for glucose and "fru" for fructose.

### 5.2.2 Numerical scheme

ED model was discretized along axial direction by Martin–Synge method, which replaces the 2<sup>nd</sup> derivative ( $\partial^2/\partial z^2$  term) in Eq. (5-1) with truncation error brought in by the 1<sup>st</sup> order backward approximation of  $\partial/\partial z$  (numerical dispersion) [19]. The discretized form of Eq. (5-1) becomes

$$\frac{dc_{i,j}^M}{dt} + \varphi \frac{dq_{i,j}^M}{dt} + u_j \frac{c_{i,j}^M - c_{i,j}^{M-1}}{\Delta z} = O(\Delta z^2) \quad (5-3)$$

$$\Delta z = \frac{L}{N_L} \quad (5-4)$$

where  $M$  denotes the mesh points with  $M=0$  for the inlet and  $M=N_L$  for the outlet. Since the original 2<sup>nd</sup> order derivative in Eq. (5-1) is eliminated, only inlet boundary condition is retained, which can be described by the node balance for a 4-zone SMB unit,

$$c_{i,j}^0 = \begin{cases} c_{i,jpre}^{N_L} & u_j \leq u_{jpre} \\ \frac{u_{jpre} c_{i,jpre}^{N_L} + (u_j - u_{jpre}) c_{i,j}^{ext}}{u_j} & u_j > u_{jpre} \end{cases} \quad (5-5)$$

where the superscript *ext* is for the external stream to an inlet port, specifically, desorbent and feed for column I and IV, respectively; *jpre* is the adjacent upstream column,

$$jpre = \begin{cases} 4 & j = I \\ j-1 & j = II, III, IV \end{cases} \quad (5-6)$$

SMB and SSMB performance is evaluated at the cyclic steady state. Rigorously, cyclic conditions apply to the discretized equations.

$$c_{i,j}^k(t) = c_{i,j}^k(t + t_s) \quad (5-7)$$

where  $t_s$  is switching time,  $j$  and  $k$  range from I-IV and 1- $N_L$ , respectively. Due to the difficulty in numerically solving the equations with cyclic conditions, the model is converted to initial value problems (IVPs) and then integrated using DIVPAG package. The following initial conditions were used to replace Eqs. (5-5--5-7).

$$c_{i,j}^k(t=0)=0 \quad (5-8)$$

It was found in this work that cyclic steady state can be essentially achieved in less than 10 cycles. A minimum number of 15 cycles (60 switches, 180 sub-phases) and relative mass balance error of both components defined below were used to ensure the steady state during SMB and SSMB simulations involved in this work.

$$\frac{\int_0^{ts} (Q_E c_{i,I}^N + Q_R c_{i,III}^N) dt}{\int_0^{ts} Q_F c_{i,F} dt} \times 100\% \leq 0.5\% \quad (5-9)$$

where foot notes  $E, F, R$  stand for extract, feed, and raffinate, respectively. Similarly, an additional  $D$  is used for the other desorbent port,, which will be involved in the following sections.

### 5.2.3 Model parameters

Parameters for the simulations of 4-column SMB and SSMB units with ED model are summarized in Table 5-1. While the current work is essentially theoretical, model parameters were experimentally acquired for preparative columns packed with industrial stationary phase materials, which selectively adsorbs fructose over glucose. Industrial fructose-glucose syrup products have three standard grades, containing 42%, 55%, and 90% fructose, respectively [17]. The feed composition and concentration were provided by COFCO Ltd., corresponding to the grade of 42%. Henry's constant were measured at 60 °C, lower than industrial operating temperature normally in the range of 65-75 °C. This is due to the limitation of lab-scale instrument and should have no qualitative effects on the conclusions drawn in this work.



**Table 5-1 Model parameters**

Columns	Column distribution	1/1/1/1
	D	2.5 cm
	L	100 cm
	$\epsilon$	0.341
	$Q_{\max}$	20 ml min <sup>-1</sup>
Isotherm	$H_{\text{fructose}}$	0.538
(T=60 °C)	$H_{\text{glucose}}$	0.320
Feed composition	$C_{\text{fructose,feed}}$	325 g/L
(in water)	$C_{\text{glucose,feed}}$	448 g/L

It should be emphasized that the use of ED model and parameters in Table 5-1 were validated by comparison between model predictions and purities of both components experimentally measured on a preparative 4-column SSMB unit [30]. More details of the experiments were separately reported [30].

## 5.3 Multi-objective optimization problems

### 5.3.1 Variables and objectives of SMB

As shown in Figure 5-1a, a closed loop SMB process has 5 independent operating parameters, i.e., the switching time ( $t_s$ ) and mobile phase flowrates in the 4 zones ( $Q_I$ - $Q_{IV}$ ), or, equivalently, flowrates of the inlet and outlet streams according to

$$\begin{cases} Q_D = Q_I - Q_{IV} \\ Q_E = Q_I - Q_{II} \\ Q_F = Q_{III} - Q_{II} \\ Q_R = Q_{III} - Q_{IV} \end{cases} \quad (5-10)$$

As in general, a “scaling factor” is defined based on the restrictions of control system and pumps [4, 20]. Throughout this work, flowrate in zone I of SMB was fixed at a maximum value of 20 ml/min, corresponding to maximum column pressure. As such, the number of independent parameters subjected to optimization was reduced to 4. They were described by the following dimensionless flowrate ratios.

$$m_j = \frac{\int_0^{t_s} Q_j dt - V\varepsilon}{V(1 - \varepsilon)} \quad (5-11)$$

where  $V$  is the column volume.

Performance of SMB process was evaluated in terms of purity ( $Pur$ ) and recovery ( $Rec$ ) of glucose, unit throughput ( $UT$ ), and water consumption ratio ( $WCR$ ). They were defined in the following dimensionless form.

$$Pur_{glu} = \frac{\int_0^{t_s} c_{glu,R} dt}{\int_0^{t_s} (c_{glu,R} + c_{fru,R}) dt} \times 100\% \quad (5-12)$$

$$Pur_{fru} = \frac{\int_0^{t_s} c_{fru,E} dt}{\int_0^{t_s} (c_{glu,E} + c_{fru,E}) dt} \times 100\% \quad (5-13)$$

$$Rec_{glu} = \frac{Q_R \int_0^{t_s} c_{glu,R} dt}{c_{glu,F} Q_F t_s} \times 100\% \quad (5-14)$$

$$Rec_{fru} = \frac{Q_E \int_0^{t_s} c_{fru,E} dt}{c_{fru,F} Q_F t_s} \times 100\% \quad (5-15)$$

$$UT = Q_F \quad (5-16)$$

$$WCR = \frac{Q_D}{Q_F} \quad (5-17)$$

It should be noted that Eq. (5-17) defines  $WCR$  as a volume ratio, different from the mass ratio normally used by industrial engineers. Since the feed solution is highly concentrated in industrial processes, its density is normally greater than 1.2 g/ml, increasing with increased operating temperature [30].

### 5.3.2 SSMB process

Different from SMB, an SSMB process is more complicated and has 7 independent operating parameters, 3 durations ( $t_1, t_2, t_3$ ) and 4 flowrates ( $Q_{loop}$ ,  $Q_{eluent,phase2}$ ,  $Q_{eluent,phase3}$  and  $Q_{feed}$ ). For simplicity, it was assumed that  $Q_{loop}$  and  $Q_{eluent,phase2}$  are both fixed at the maximum flowrate ( $Q_{max}$ ). The number of independent parameters was then reduced to 5. They were described by the four  $m$  values and an additional  $\alpha$ . During the SSMB simulations, these dimensionless variables were converted to dimensional variables that are summarized in Table 5-2 using the following equations.

$$Q_{eluent,phase3} = \alpha Q_{max} \quad (5-18)$$

$$t_1 = \frac{m_{IV}V(1-\varepsilon) + V\varepsilon}{Q_{max}} \quad (5-19)$$

$$t_2 = \frac{m_{II}V(1-\varepsilon) + V\varepsilon}{Q_{max}} - t_1 \quad (5-20)$$

$$t_3 = \frac{m_I V(1-\varepsilon) + V\varepsilon - (t_1 + t_2)Q_{max}}{\alpha Q_{max}} \quad (5-21)$$

$$Q_{feed} = \frac{m_{III}V(1-\varepsilon) + V\varepsilon - (t_1 + t_2)Q_{max}}{t_3} \quad (5-22)$$

**Table 5-2 Dimensional operating parameters of SSMB**

Phase No.	duration	$Q_I$	$Q_{II}$	$Q_{III}$	$Q_{IV}$
1	$t_1$	$Q_{\max}$	$Q_{\max}$	$Q_{\max}$	$Q_{\max}$
2	$t_2$	$Q_{\max}$	$Q_{\max}$	$Q_{\max}$	0
3	$t_3$	$\alpha^*Q_{\max}$	0	$Q_{\text{feed}}$	0

Since a switch of an SSMB is divided into three sub-steps with different flow patterns, its performance parameters,  $UT$ ,  $Pur$ ,  $Rec$ , and  $WCR$ , were averaged over a whole switch.

$$Pur_{glu} = \frac{\int_0^{t_s} c_{glu,R} Q_R dt}{\int_0^{t_s} (c_{glu,R} + c_{fru,R}) Q_R dt} \times 100\% \quad (5-23)$$

$$Pur_{fru} = \frac{\int_0^{t_s} c_{fru,E} Q_E dt}{\int_0^{t_s} (c_{glu,E} + c_{fru,E}) Q_E dt} \times 100\% \quad (5-24)$$

$$Rec_{glu} = \frac{\int_0^{t_s} c_{glu,R} Q_R dt}{c_{glu,feed} Q_{feed} t_s} \times 100\% \quad (5-25)$$

$$Rec_{fru} = \frac{\int_0^{t_s} c_{fru,E} Q_E dt}{c_{fru,feed} Q_{feed} t_s} \times 100\% \quad (5-26)$$

$$UT = \frac{Q_{feed} t_3}{t_s} \quad (5-27)$$

$$WCR = \frac{Q_{Max} t_2 + \alpha Q_{Max} t_3}{Q_{feed} t_3} \quad (5-28)$$

Where  $t_s = t_1 + t_2 + t_3$

Mass flows ( $MF$ ) and averaged mass flow ( $AMF$ , g/min) defined below were introduced in a parallel work for detailed analyses of SSMB processes [23]. These values of both components at the raffinate port are extensively involved in the following discussion.

$$MF_i = c_{i,R} Q_R \quad (5-29)$$

$$AMF_i = \int_0^1 MF_i d(t/t_s) \quad (5-30)$$

### 5.3.3 Configurations of optimization problems for both processes

In this work, two of the objectives were simultaneously optimized for both SMB and SSMB processes. Since operating parameters have contradicting effects on different objectives, pareto solutions in the objective function space are normally obtained. A pareto set is defined as when one moves from one point to another, at least one objective function improves while another one worsens. Since no point in this set is superior to any other one in all objectives [15, 31], these solutions are considered equally good and provide the decision-maker valuable guidance to select and screen desired operating conditions. Non-dominated sorting genetic algorithm (NSGA-II) [2, 14], which has been proven efficient to solve multi-objective optimization problems involved in various industrial chemical processes [32-36], was applied to acquire the pareto solutions in this work. All the calculations were programmed in FORTRAN codes and performed on a Lenovo ThinkPad L440 personal computer equipped with a 2.30 GHz Intel core i7 processor.

In total, five optimization problems with different objective functions were considered in this work. In addition, minimum requirements on purity and recovery were set as constraints to limit the solutions in practically valuable range. The configurations of optimization problems are summarized in Table 5-3, together with the upper and lower bounds of operational variables, which define the parametric space for searching solutions and are required by the use of NSGA II method. Numbers of population and generations, key parameters for NSGA II, were both set to be 100. Results of the last

generation were used in the following discussion. Some of the obvious off-line points were manually removed.

**Table 5-3 Summary of optimization formulations and bounds of variables**

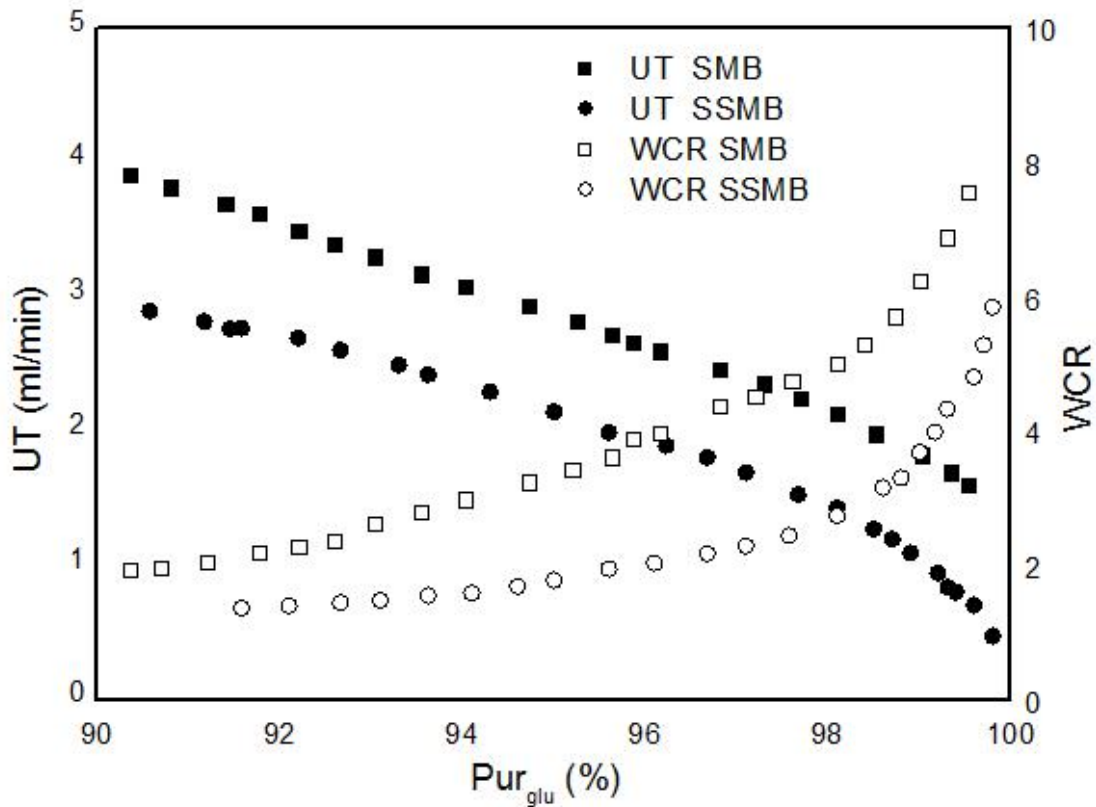
Case	Objectives	Constraints	Variables of SMB	Variables of SSMB
1	Max $Pur_{glucose}$ ;	$Pur_{glucose} > 90\%$ ;	$0.4 < m_I < 1.2$ ; $0.1 < m_{II} < 0.5$ ;	$0.4 < m_I < 1.2$ ; $0.1 < m_{II} < 0.5$ ;
	Max UT	$Pur_{fructose} > 90\%$	$0.3 < m_{III} < 0.8$ ; $0 < m_{IV} < 0.5$	$0.3 < m_{III} < 0.8$ ; $0 < m_{IV} < 0.5$ ; $0 < \alpha < 0.8$
2	Max $Pur_{glucose}$ ; Min WCR	$Rec_{glucose} > 80\%$ ; $Rec_{fructose} > 80\%$	Same as 1	Same as 1
3	Max $Pur_{glucose}$ ; Min WCR; Fix UT=3	$Rec_{glucose} > 80\%$ ; $Rec_{fructose} > 80\%$	$0.4 < m_I < 1.2$ ; $0.1 < m_{II} < 0.5$ ; $0 < m_{IV} < 0.5$	$0.4 < m_I < 1.2$ ; $0.1 < m_{II} < 0.5$ ; $0 < m_{IV} < 0.5$ ; $0 < \alpha < 0.8$
4	Max $Rec_{glucose}$ ; Min WCR	$Pur_{glucose} > 90\%$ ; $Pur_{fructose} > 90\%$	Same as 1	Same as 1
5	Max $Rec_{glucose}$ ; Min WCR; Fix UT=3	$Pur_{glucose} > 90\%$ ; $Pur_{fructose} > 90\%$	Same as 3	Same as 3

## 5.4 Results and discussions

### 5.4.1 Case 1: simultaneous maximization of $Pur_{glu}$ and UT

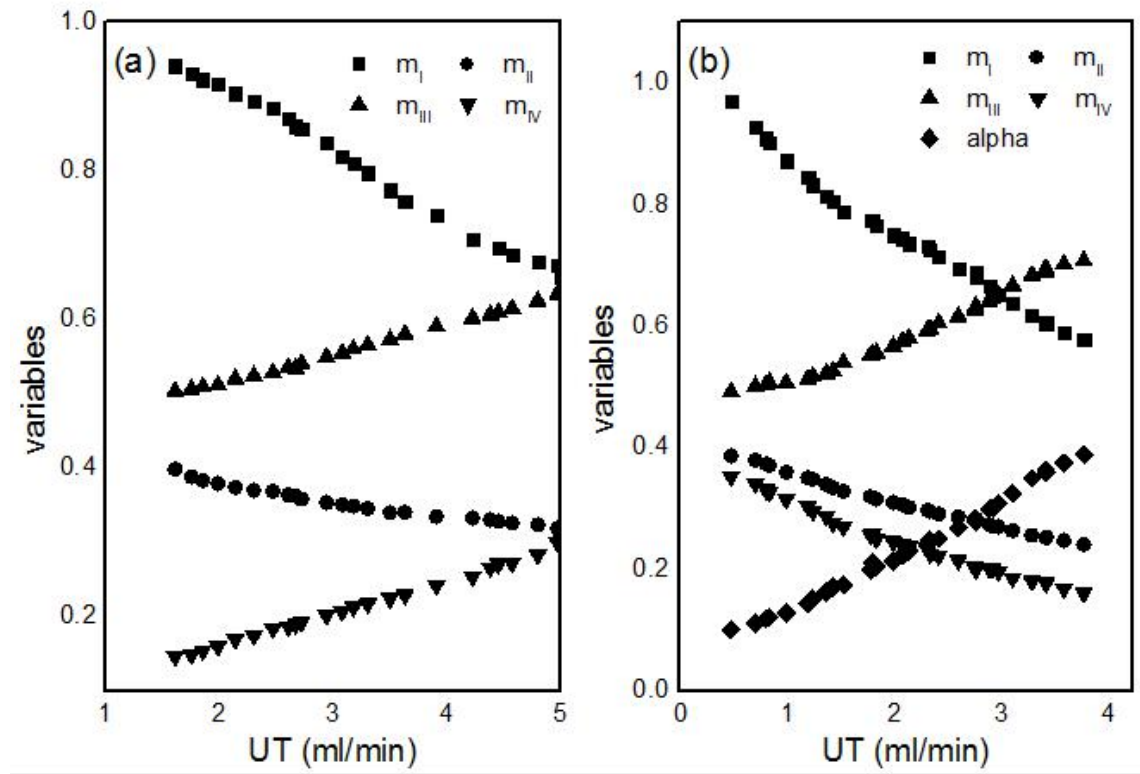
In this case, simultaneous maximization of  $Pur_{glu}$  and  $UT$  was defined as the objective for both SMB and SSMB processes. In addition, purities of both components greater than 90%, were set as constraints to limit the searching of optimal variables in a practical parametric window. Fructose purity greater than 90% is a commercial requirement for the by-product. In addition, it provides a constraint of relatively high glucose recovery for this binary system.

Figure 5-2 shows that glucose purity above 90% can be successfully achieved by properly operated units, meeting the minimum commercial requirement. Meanwhile, for both processes, maximum  $UT$  decreases with increased glucose purity. The pareto curve of SMB is generally higher than that of SSMB, i.e., for the same glucose purity requirement, the former has a higher  $UT$ .



**Figure 5-2 Comparison between pareto solutions for SMB and SSMB: Case 1**

Optimal  $m$  values corresponding to the pareto solutions are plotted against  $UT$  in Figure 5-3a and 5-3b for SMB and SSMB, respectively. Compared with the bounds in Table 5-3, the acquired optimal operation conditions are well confined in the preset parametric range. That  $m_I$  is consistently higher than  $m_{III}$  for SMB in the investigated range validates the assumption of maximum flowrate in Zone I. On the other hand,  $m_{III}$  may be greater than  $m_I$  for SSMB in the range of high  $UT$  (low purity), which is a result of higher  $Q_{III}(=Q_F)$  than  $Q_I(=\alpha Q_{max})$  during sub-step 3. Due to the possibility of  $m_{III}$  greater than  $m_I$ , it is necessary to separately optimize the two flowrates during sub-step 3.



**Figure 5-3 Optimal  $m$  values corresponding to the pareto solutions in Figure 5-2. a: SMB; b: SSMB.**

For SMB, substituting Eq. (5-11) to Eq. (5-16) and applying the assumption of maximum flowrate in Zone I gives

$$UT = Q_{\max} \frac{(m_{III} - m_{II})}{m_I + \varphi} \quad (5-31)$$



Figure 5-3a reveals that the increase in  $UT$  for an SMB unit is attributed to the combined effects of increased  $m_{III}$ , decreased  $m_{II}$ , and decreased  $m_I$ . On the other hand, with an increased  $m_{III}$ , fructose, the heavy component, may not be sufficiently retained in Zone III and enter the raffinate port, reducing glucose purity. In addition, decreased  $m_I$  may also result in insufficient purge of fructose in Zone I. A fraction of retained fructose enters Zone III after two switches and is conveyed to raffinate port. According to Figure 5-3a, an increase in  $m_{IV}$  is favorable for  $UT$ . Meanwhile, increased  $m_{IV}$  partially prevents fructose from going into the raffinate stream and is therefore also favorable for glucose purity. However, a fraction of glucose that is not be sufficiently retained in Zone IV may enter Zone I and is purged out to the extract port, reducing purity of fructose. Calculation results show that, while the constraint of 90% fructose purity was satisfied by all pareto solutions, as  $UT$  increases from 2 to 3 ml/min, fructose purity decreases from 94.5% to 91.2%. Recovery of glucose in raffinate stream decreases accordingly from 92.7% to 89.2%, as a result of material balance of this binary system. Optimization involving recovery as an objective will be discussed in section 5.4.4.

The trends of  $m$  values for SSMB are similar to those of SMB except  $m_{IV}$ , which decreases with increased  $UT$ . That trends of optimal  $m$  values of an SSMB may be opposite to those of an SMB had been observed and analyzed in a parallel study carried out in this group [23]. Dimensional operating parameters corresponding to the pareto solutions for SSMB are provided in the supplementary materials as Figure S5-1. It is seen that the decrease in  $m_{IV}$  is mainly attributed to the decrease of  $t_I$ , duration of the 1<sup>st</sup> step with an internal loop, which may be expected from Eq. (5-19).

In order to explain the superiority of SMB in terms of simultaneous maximization of  $UT$  and  $Pur_{glu}$ , an optimal point was first selected from the pareto curve of SMB ( $UT=2.66$  ml/min;  $Pur_{glucose}=95.5\%$ ) in Figure 5-2. The corresponding flowrate ratios and  $\alpha=1$  were used carry out a simulation for SSMB. As shown in Table 5-4, while SSMB, with the same  $m$  values and  $\alpha=1$ , has the same  $UT$  as SMB, which results directly from  $UT$  definitions in Eqs. (5-14) and (5-17), glucose purity of SSMB significantly drops to 89.2%. Moreover, decreasing  $\alpha$  for the same  $m$  values results in a decrease in  $UT$ , which is attributed to the increased in  $t_s$ . However, the glucose purity exhibits an apparently

random fluctuation with in the range of 88.5-90.4%, consistently lower than 95.5% for SMB (see Supplementary Materials Table S5-1). These results show that operating an SSMB with the same  $m$  values optimized for an SMB may lead to reduced product purity. It is therefore necessary to perform independent optimization during the design of an SSMB process.

**Table 5-4 Results of three simulations**

No.	Unit	Decision variables					Objectives		AMF g/min	
		$m_I$	$m_{II}$	$m_{III}$	$m_{IV}$	$\alpha$	UT ml/min	Pur <sub>glu</sub> %	Glu	Fru
1	SMB	0.856	0.358	0.541	0.193	-	2.66	95.5	1129	53.2
2	SSMB	0.856	0.358	0.541	0.193	1	2.66	89.1	1140	138.6
3	SSMB	0.714	0.290	0.605	0.222	0.25	2.00	95.5	763	35.9

$MF$  of the above two simulations for SMB and SSMB with same  $m$  values are plotted in Figure 5-4. It is seen that glucose is continuously flushed out and collected at the raffinate port during the last 80% of the whole switch. In the case of SSMB with the same  $m$  values, glucose is collected only in sub-steps 2 and 3, accounting for only about half of the switch.  $AMF$  values are provided in Table 5-4. Compared with SMB, SSMB has a similar  $AMF_{glu}$  but a much higher  $AMF_{fru}$ , explaining the reduced purity.

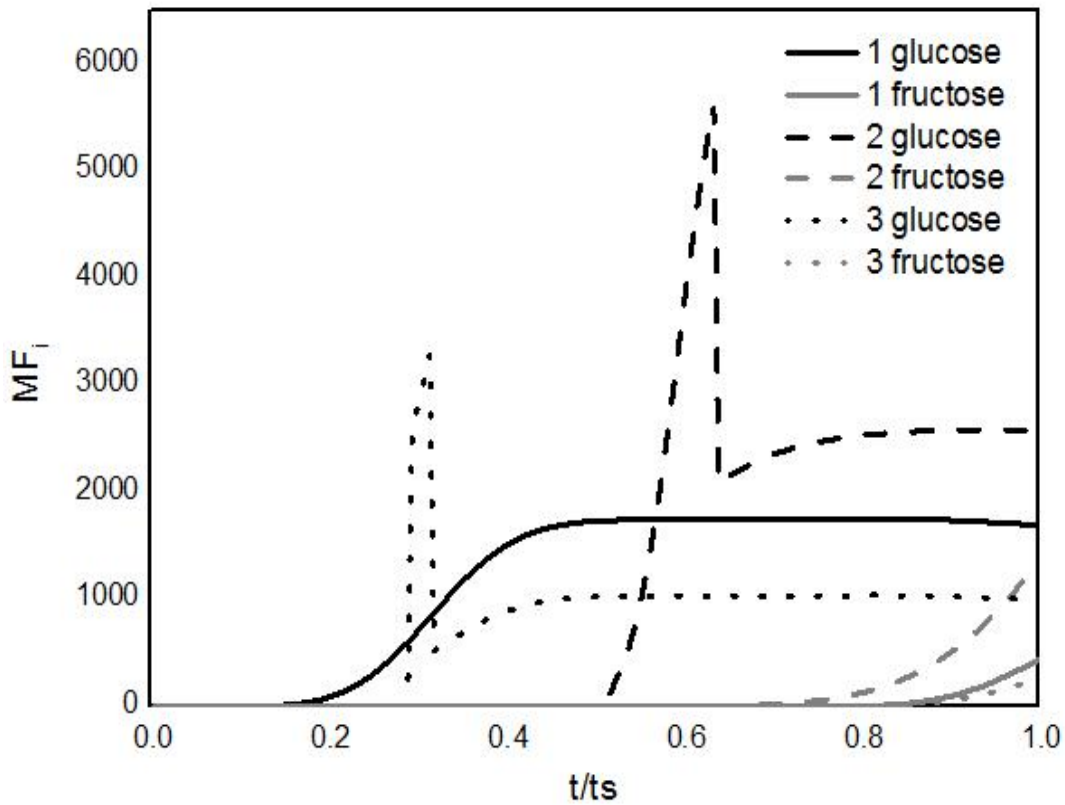


**Figure 5-4 MF plots of the three simulations in Table 5-4**

Simulation results of an SSMB process optimized at the purity of 95.5% are also provided in Table 5-4 and Figure 5-4 for additional comparison. Compared with simulation 2, SSMB with  $m$  values optimized for SMB, optimal SSMB has a shorter  $t_I$  and glucose is collected during a relatively longer fraction, about 70%, of the whole switch, still lower than that of SMB. However, the concentration of glucose at the raffinate port is significantly reduced. Compared with SMB, SSMB optimized at the same purity has  $AMF$  values of both components decreased by a factor of about 33%, corresponding to the reduced  $UT$ .

Figures 5-5 and 5-6 show concentration profiles of simulations 1 and 3 in Table 5-4. It is seen in Figure 5-5a that the profile of glucose in optimal SMB unit is expended from Zone II to Zone IV. On the other hand, for SSMB optimized at the same purity, glucose is mainly concentrated in Zone I to Zone III (Figure 5-5b). In addition, during the last two sub-steps, glucose is located in Zones III and a fraction of Zone II, barely propagating

towards the down stream because Zones II and IV are isolated. Comparison in Figure 5-6 shows the distribution of fructose for SSMB is close to that of SMB. By the end of the first sub-step, the front of fructose is at the inlet of Zone III and the tail is in the middle of Zone I. The concentration profile is driven down stream by external streams during the last two steps, different from the case of glucose. Since glucose, the light component, is distributed in a relatively narrow range during the last two steps of SSMB, the stationary phase in isolated Zones IV and II is not well utilized as in the optimized SMB system. Specifically, glucose is essentially absent in Zone IV during the whole switch of SSMB. In an SMB, a fraction of glucose is recovered in Zone IV and moved to Zone III after a switch. Furthermore, glucose in Zone II of SMB is conveyed by the mobile phase to the feed port, partially attributing to collection of glucose. These functions are not fully realized in SSMB. It is due to the relatively low utility of stationary phase in isolated Zones II and IV that SSMB has worse performance in terms of optimal  $UT$  and  $Pur_{glu}$  than SMB.

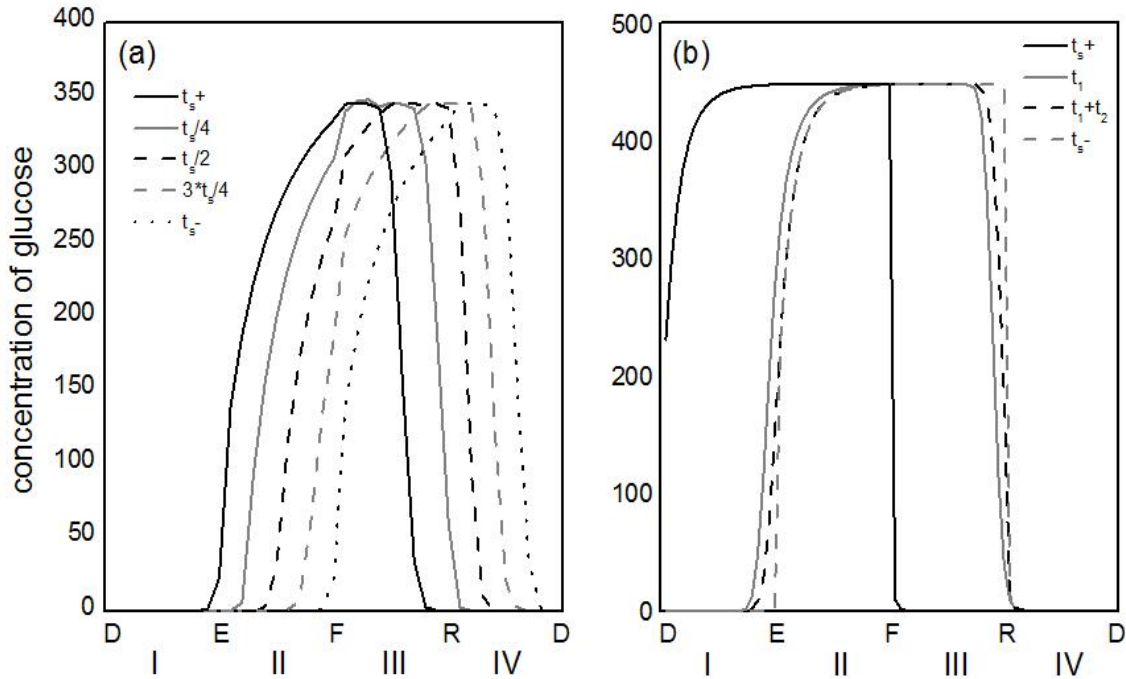


**Figure 5-5 Internal concentration profiles of glucose for SMB and SSMB with maximum  $UT$  at  $Pur_{glu}=95.5\%$**

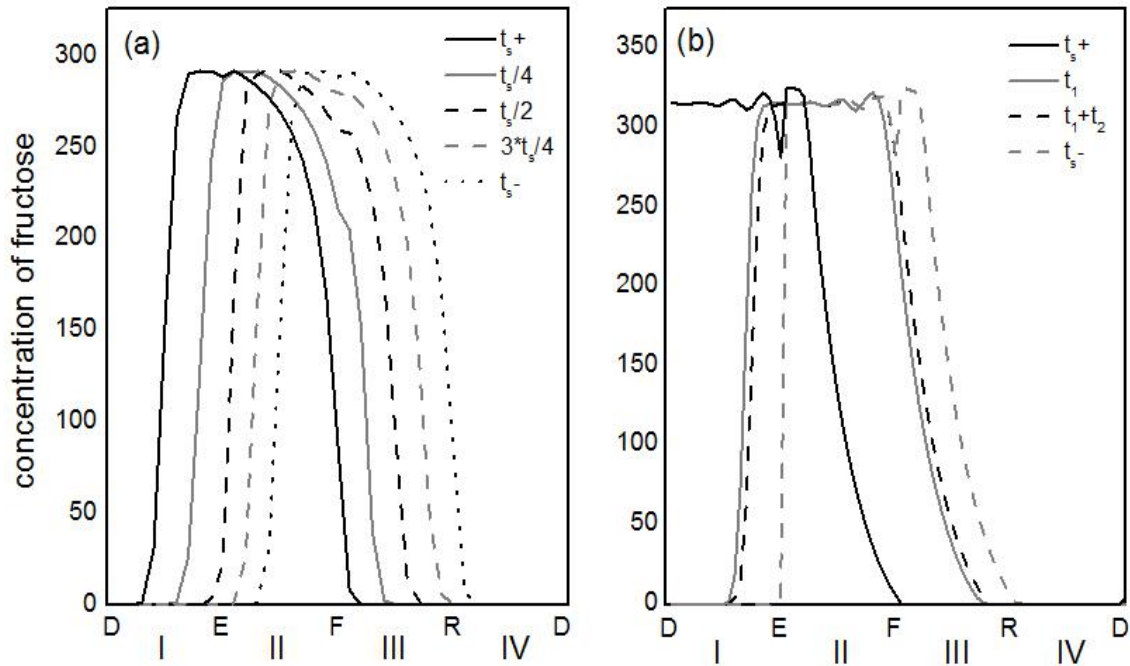


**Figure 5-6 Internal concentration profiles of fructose for SMB and SSMB with maximum UT at  $Pur_{glu}=95.5\%$**

It is also seen in Figures 5-5b and 5-6b that, in a properly operated SSMB system, a major fraction of concentration profile propagation is realized in the 1<sup>st</sup> sub-step, which is driven by an internal loop without introducing any external streams. Therefore, compared with SMB that drives mobile phase with constant external desorbent and feed streams, SSMB has a relatively high utility of mobile phase. As indicated by the comparison of hollow points in Figure 5-2, SSMB may be applied to efficiently reduce solvent consumption, which was further examined in the following cases.

#### 5.4.2 Case 2: maximization of $Pur_{glu}$ and minimization of WCR

Reducing solvent consumption is considered as the most important industrial target for glucose/fructose separation. In the following discussions, water consumption ratio (WCR) was defined as one of the optimization objectives. In this section, simultaneously

maximizing  $Pur_{glu}$  and minimizing  $WCR$  was firstly investigated. Recoveries of both components greater than 80% were set as constraints.

As shown in Figure 5-7,  $WCR$  increases with the increased purity requirement for both SMB and SSMB processes. The solution curve of SSMB is at the right side of the SMB curve, showing advantage of SSMB in this optimization problem. It is also seen from the figure that reduced  $WCR$  of SSMB is compensated with reduced  $UT$ .

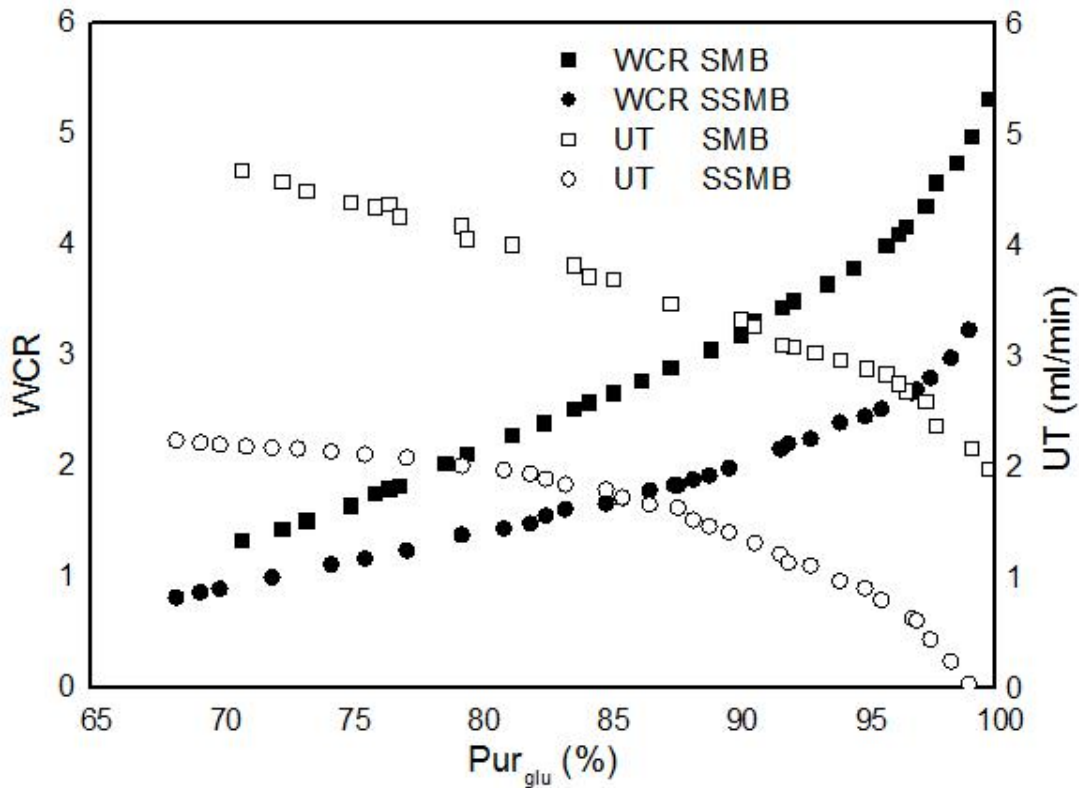


**Figure 5-7 Comparison between pareto solutions for SMB and SSMB: case 2**

Four representative points are chosen from the solution curves. The first two are for SMB and SSMB with the same  $WCR$  of 1.4 and the last two have the same  $Pur_{glu}$  of 90%.

Decision variables and objectives are summarized in Table 5-5.  $WCR$  of 1.4 is the smallest value that can be achieved by SMB and satisfies the preset constraints.  $AMF$  values calculated from  $MF$  plots in Figure 5-8 are also compiled in Table 5-5. As shown in Figure 5-8a, at the optimal conditions for SMB,  $MF$  of glucose is essentially constant, indicating that zone III is nearly saturated with glucose. Fructose breakthrough at about

half of the switch and is saturated in Zone III far before the end of a switch. Significant fraction of fructose therefore enters the raffinate stream, limiting glucose purity to 72%. With the same  $WCR$  at 1.44, optimal SSMB has an  $AMF$  of glucose less than that of SMB by about 50%. On the other hand,  $AMF$  of glucose is reduced even further by about 70%. As an overall result, the maximum glucose purity of SSMB at this  $WCR$  is increased to 81%. As shown in Figure 5-8c, at  $Pur_{glu}$  of 90%,  $MF$  plots of optimized SMB exhibit trends similar to those in Figure 5-5. At this constant purity, SSMB has  $AMF$  values about only 40% of those for SMB, indicating lower unit throughput, similar to the results obtained in the last section. However,  $WCR$  of SSMB is significantly reduced from 3.2 to 1.9.

**Table 5-5 Representative points from the solution curves for maximized  $Pur_{glu}$  and minimized  $WCR$**

No.	Unit	Decision variables					Objectives		AMF g/min	
		$m_I$	$m_{II}$	$m_{III}$	$m_{IV}$	$\alpha$	$WCR$	$Pur_{glu}$ %	Glu	Fru
a	SMB	0.752	0.391	0.682	0.383	-	1.44	72.37	1695	647
b	SSMB	0.763	0.252	0.643	0.298	0.22	1.44	80.98	808	190
c	SMB	0.868	0.354	0.585	0.231	-	3.18	90	1422	158
d	SSMB	0.827	0.280	0.589	0.250	0.28	1.99	90	574	64

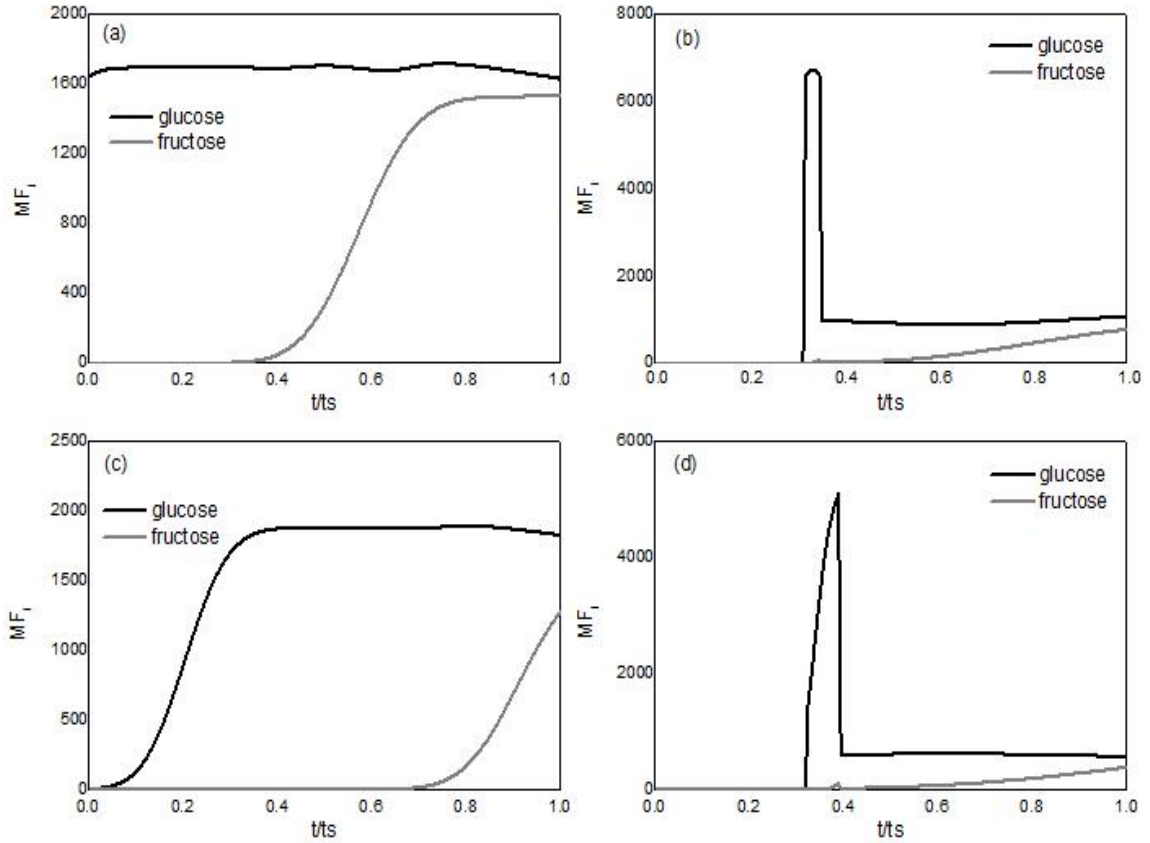


**Figure 5-8 MF plots of the four solution points in Table 5-5**

It may be derived that, for both SMB and SSMB processes,  $WCR$  is related to  $m$  values by

$$WCR = \frac{m_I - m_{IV}}{m_{III} - m_{II}} \quad (5-32)$$

$m$  values in Table 5-5 suggests that, compared with SMB optimized at the same purity, the lower  $WCR$  of SSMB is mainly attributed to lower  $m_I$  and  $m_{II}$ . Figure 5-9 shows that low  $m_I$  and  $m_{II}$  have major contribution to reduced  $WCR$  of SSMB up to the purity of about 95%. In the range of  $Pur_{glu}$  greater than 95%, higher  $m_{III}$  and  $m_{IV}$  compared with those of SMB become important factors for reduced  $WCR$  of SSMB.



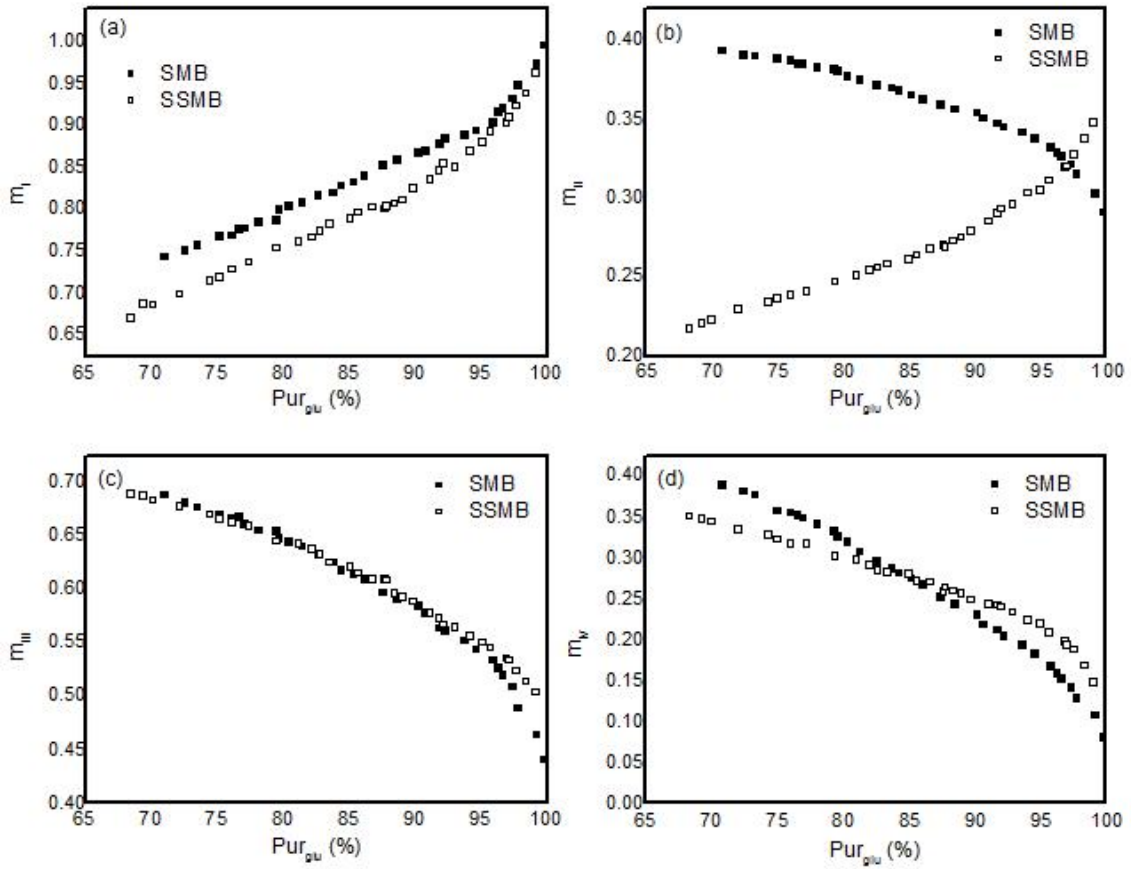


**Figure 5-9 Optimal  $m$  values of SMB and SSMB for Case 2. a:  $m_I$ ; b:  $m_{II}$ , c:  $m_{III}$ ; d:**

**$m_{IV}$**

### 5.4.3 Case 3: maximization of $Pur_{glu}$ and minimization of WCR with fixed UT

The above case for simultaneous maximization of  $Pur_{glu}$  and minimization of  $WCR$  was further investigated with a fixed  $UT$ , which is of more practical interests by the industry. For this purpose, an arbitrary  $UT$  value of 3 ml/min was fixed. Accordingly, number of independent variables should be reduced by 1. In this work,  $m_{III}$  was removed as a decision variable for both SMB and SSMB processes.

As shown in Figure 5-10, the trade-off trends between  $Pur_{glu}$  and  $WCR$  still exist. In the commercially practical range of  $Pur_{glu}$  greater than 90%, the performance of SSMB is obviously better than SMB process. In this case with fixed  $UT$ , the reduced  $WCR$  of SSMB is compensated with reduced glucose recovery.

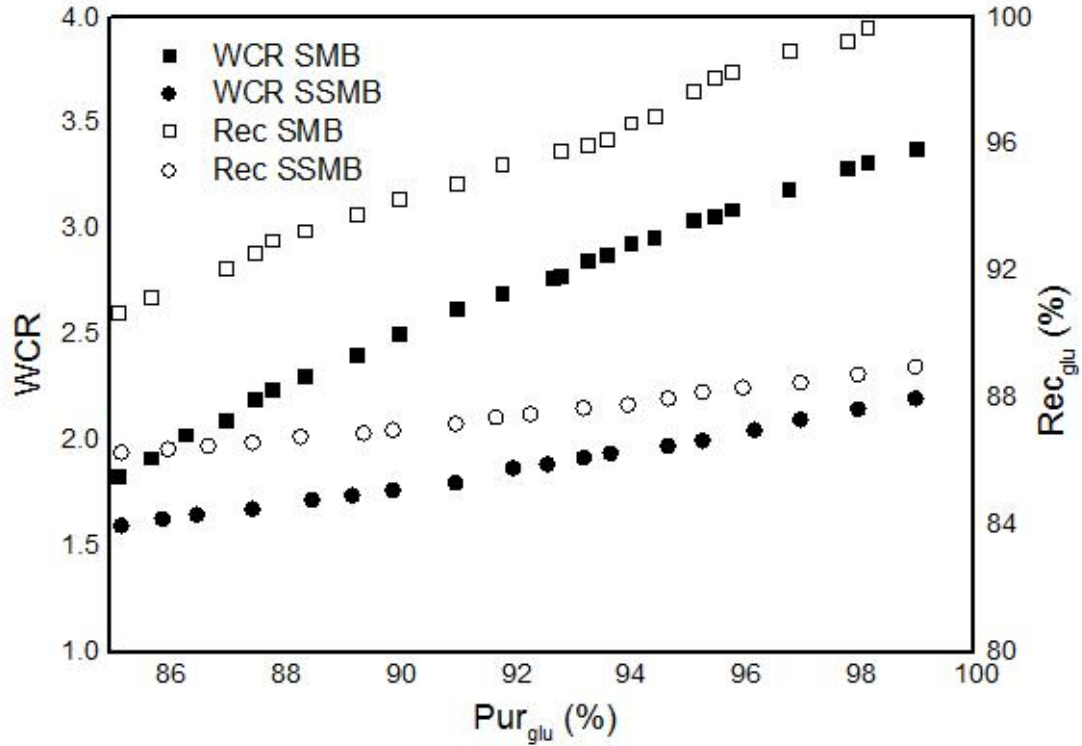


**Figure 5-10 Comparison between pareto solutions for SMB and SSMB: case 3**

Optimized  $m$  values for the two processes are compared in Figure 5-11. Substituting Eq. (5-18) to Eq. (5-22) gives the following expression of  $m_{III}$  for SSMB that was not subjected to optimization.

$$m_{III} = m_{II} + \frac{UT(m_I + \alpha m_{II} - m_{II})}{\alpha Q_{\max}} + \frac{\phi UT}{Q_{\max}} \quad (5-33)$$

In the case of SMB,  $m_{III}$  was calculated as a function of  $m_I$ ,  $m_{II}$  and  $UT$  using Eq. (5-31). Figure 5-11 shows that below the purity of around 90%, the reduced  $WCR$  of SSMB is mainly attributed to its lower  $m_{III}$ . With the increased purity, the difference in  $WCR$

between SMB and SSMB becomes more significant, which is induced by the additional  $m_I$  effect.

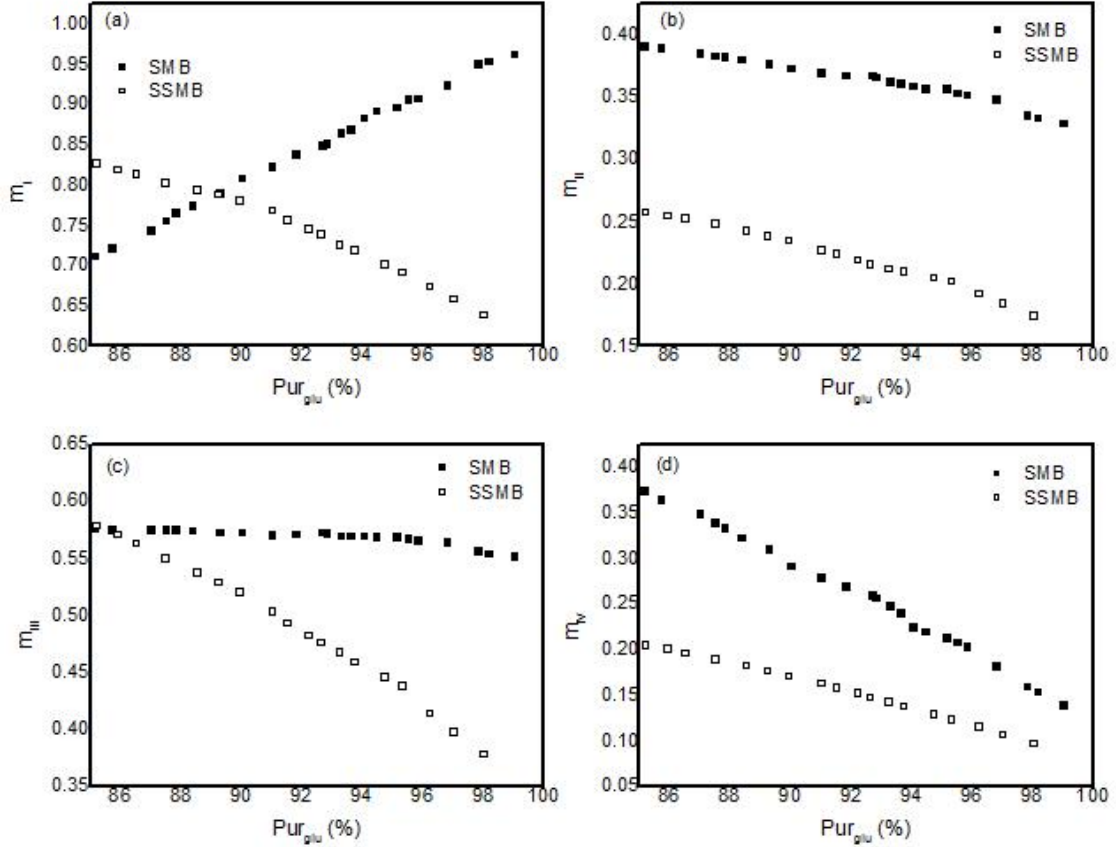


**Figure 5-11 Optimal  $m$  values of SMB and SSMB for Case 3. a:  $m_I$ ; b:  $m_{II}$ ; c:  $m_{III}$ ; d:  $m_{IV}$**

As shown in Figure 5-11, while  $m$  values optimized for SMB have trends similar to Figure 5-10, those for SSMB exhibit some significantly different features. Dimensional parameters corresponding to optimal SSMB operations for cases 2 and 3 are provided in the Supplementary Materials (Figures S5-2, S5-3) for conciseness. In case 2, the decrease of  $WCR$  with decreased  $Pur_{glu}$  of SSMB is mainly attributed to the decreased  $m_I$  and  $m_{II}$ . Figure S5-2 shows that, as purity decreases, the decrease in  $t_2$  overcomes the increase in  $t_1$ , directly resulting in decreased  $m_{II}$  according to Eq. (5-20). The decrease in  $m_I$  is, however, more complicated because it is determined by 4 dimensional parameters that have contradicting effects according to Eq. (5-21). On the other hand, in case 3, the

decrease in  $WCR$  with decreased purity is mainly attributed to the increase in  $m_{III}$  and  $m_{IV}$ . The latter results directly from increased  $t_I$  according to Eq (5-19). The former is, again, a combined result of 4 contradicting dimensional parameters according to Eq. (5-22).

It had been found in a parallel study that, due to the complicity of SSMB compared with regular SMB,  $m$  values averaged over a whole switch cannot be directly used to interpret the effects of operating parameters on the trends of multi-objective optimization results [23]. Detailed analyses generally involve the corresponding dimensional operating parameters,  $MF$  plots, and internal concentration profiles, which is beyond the scope of current work and can be found elsewhere [23].

#### 5.4.4 Case 4 and case 5: maximization of $Rec_{glu}$ and minimization of water consumption ratio

Recovery was preset as constraints in the above cases. In the last two optimization cases, glucose recovery was considered as an objective subjected to optimization together with  $WCR$ .

Similar to cases 2 and 3, cases 4 and 5 have the same objective functions but the latter has an additional constraint on fixed  $UT$  at 3 ml/min. Purity of both components greater than 90% were set as constraints. For conciseness, only the major results are summarized below.

As shown in Figures 5-12 and 5-13, with or without the constraint on  $UT$ , pareto solutions were obtained for both processes and SSMB is superior to SMB. When  $UT$  is fixed, the superiority of SSMB becomes apparently more obvious. Comparison of  $m$  values are provided in Supplementary Materials as Figures S5-4 and S5-5. In case 4, below the recovery of around 95%, the lower  $WCR$  of SSMB compared with SMB is mainly attributed to the lower  $m_{II}$ . When the recovery is higher than 95%, the combined effects of lower  $m_I$ , higher  $m_{III}$  and  $m_{IV}$  are more important. In case 5 with  $UT$  fixed at 3ml/min, the lower  $WCR$  of SSMB is due to lower  $m_{II}$  and higher  $m_{III}$  when  $Rec_{glu}$  is less than 90%. In the higher recovery range, lower  $m_I$  and higher  $m_{III}$  become the dominant factors. In case 4, reduced  $WCR$  of SSMB is compensated with lower  $UT$  (Figure 5-12).

In case 5 with fixed  $UT$ , the reduced  $WCR$  of SSMB is compensated with lower glucose purity (Figure 5-13).

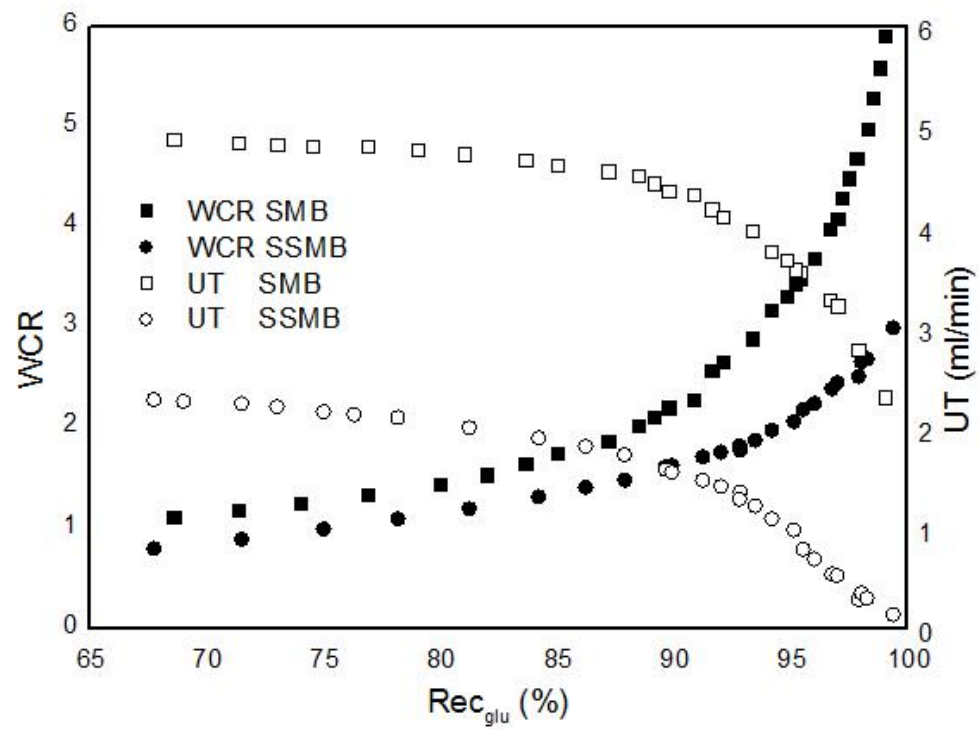
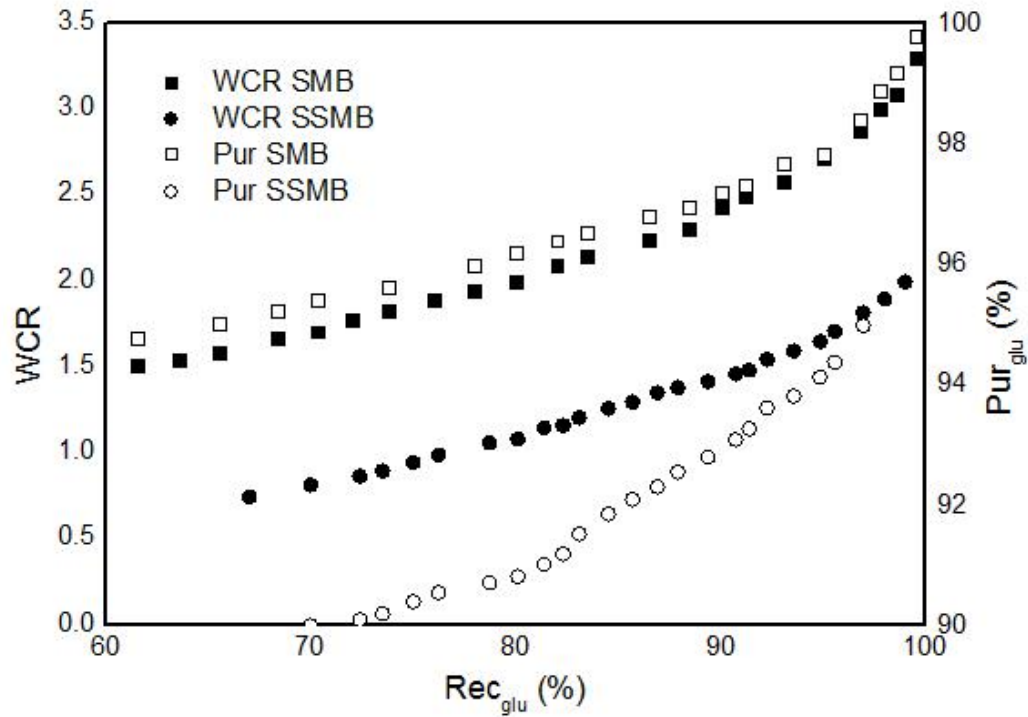


Figure 5-12 Comparison between pareto solutions for SMB and SSMB: case 4



**Figure 5-13 Comparison between pareto solutions for SMB and SSMB: case 5**

## 5.5 Conclusions and Remarks

Sequential simulated moving bed (SSMB), a modified SMB technique featured by a switch divided into 3 sub-steps with different flow patterns, has been extensively used for industrial glucose/fructose separation. In order to provide theoretical guidance to the industrial development and operation of SSMB process, it was compared with regular 4-column SMB under individually optimized conditions. A total of 5 multi-objective optimization problems with various objectives and constraints were considered.

For simultaneous maximization of unit throughput and glucose purity, the most extensively investigated multi-objective optimization problem in SMB studies, regular SMB has better performance than SSMB although the latter has a more complicated operation. As water consumption ratio, a major concern in industrial glucose/fructose separation, is simultaneously optimized with glucose purity or recovery, SSMB is

superior to SMB. However, this superiority is compensated with reduced unit throughput. In the case of fixed unit throughput, SSMB can be used to meet a purity requirement at lower water consumption ratio, which is compensated with a reduced recovery; given recovery can also be realized by SSMB at lower water consumption ratio, which is compensated with reduced purity.

Dimensionless flowrate ratios ( $m$ ), mass flow plots and internal concentration profiles were used to interpret the trends of optimization results. From the process point of view, SSMB, compared with regular SMB, has a high utility of mobile phase since a significant fraction of concentration profile propagation is realized in sub-step 1 with an internal loop and no external streams. On the other hand, stationary phase in Zones II and IV, which are isolated with no mobile phase flow during one or two of the sub-steps, are not fully utilized as in an SMB unit. The above mentioned trade-off behaviors between water consumption ratio and other performance parameters are attributed to the combined effects high mobile phase utility and low stationary phase utility of SSMB.

Water consumption can be analytically described as a same function of  $m$  values for both processes. While optimized SSMB generally has a lower water consumption ratio than SMB, the contributions of these  $m$  values vary not only with the choice of the other objective, but also with the range of the the other objective.

For all multi-objective optimization problems considered in this work, trends of some  $m$  values corresponding to pareto solutions for SSMB may be opposite to those for regular SMB. Detailed analyses on the similar observations had been reported elsewhere [23] and were not discussed in details in this article.

Throughout this article, two of the performance parameters were defined as the objectives. The presented results apparently suggest the existence of pareto solutions to optimization problems with more objectives. In addition, the optimization problems were defined with the major focus on glucose, whereas both glucose and fructose are desired products in industrial processes. Multi-objective optimization problems having more objectives and taking fructose into consideration will be pursued in the future studies.

## 5.6 References

- [1] Rajendran, A., Paredes, G., and Mazzotti, M.. Simulated moving bed chromatography for the separation of enantiomers. *Journal of Chromatography A*, 2009, (1216): 709-738.
- [2] Zhang, Y., Hidajata, K., and Ray, A.K.. Multi-objective optimization of simulated moving bed and Varicol processes for enantio-separation of racemic pindolol. *Separation and Purification Technology*, 2009, (65): 311-321.
- [3] Pais, L.S., and Rodrigues, A.E.. Design of simulated moving bed and Varicol processes for preparative separations with a low number of columns. *Journal of Chromatography A*, 2003, (1006): 33-44.
- [4] Zhang, Z.Y., Hidajat, K., Ray, A.K., and Morbidelli, M.. Multi-objective optimization of SMB and Varicol process for chiral separation. *AIChE Journal*, 2002, (12): 2800-2816.
- [5] Yu, W.F., Hidajat, K., Ray, A.K.. Optimization of reactive simulated moving bed and Varicol systems for hydrolysis of methyl acetate. *Chemical Engineering Journal*, 2005, (112): 57-72.
- [6] Broughton, D.B., and Gerhold, C.G.. Continuous sorption process employing fixed bed of sorbent and moving inlets and outlets. US Patent 2 985 589. 1961.
- [7] Broughton, D. B., Bieser, H. J., Berg, R. C., and Connel, E. D.. High purity fructose via continuous adsorptive separation. *Suc. belg.*, 1977, (96): 155-162 .



- [8] Ribeiro, A.E., Gomes, P.S., Pais, L.S., and Rodrigues, A.E.. Chiral separation of ketoprofen enantiomers by preparative and simulated moving bed chromatography. *Separation Science and Technology*, 2011, (46): 1726-1739.
- [9] Gomes, P.S., Minceva, M., and Rodrigues, A.E.. Simulated moving bed technology: old and new. *Adsorption*, 2006, (12): 375-392.
- [10] Faria, R.P.V. and Rodrigues, A.E.. Instrumental aspects of simulated moving bed chromatography. *Journal of Chromatography A*, 2015, (1421): 82-102.
- [11] Beste, Y.A., Lisso, M., Wozny, G., and Arlt, W.. Optimization of simulated moving bed plants with low efficient stationary phases: separation of fructose and glucose. *Journal of Chromatography A*, 2000, (868): 169-188.
- [12] Azevedo, D.C.S., and Rodrigues, A.E.. Fructose-glucose separation in a SMB pilot unit: modeling, simulation, design, and operation. *AIChE Journal*, 2001, (47): 2042-2051.
- [13] Subramani, H.J., Hidajat, K., and Ray, A.K.. Optimization of simulated moving bed and varicol processes for glucose-fructose separation. *Trans IChemE*, 2003, (81): 549-567.
- [14] Tangpromphan, P., Budman, H., and Jaree, A.. A simplified strategy to reduce the desorbent consumption and equipment installed in a three-zone simulated moving bed process for the separation of glucose and fructose. *Chemical Engineering & Processing: Process Intensification*, 2018, (126): 23-37.

- [15] Azevedo, D.C.S., and Rodrigues, A.E.. Design methodology and operation of a simulated moving bed reactor for the inversion of sucrose and glucose-fructose separation. *Chemical Engineering Journal*, 2001, (82): 95-107.
- [16] Borges da Silva, E.A., Ulson de Souza, A.A., U. de Souza, S.G., Rodrigues, A.E.. Analysis of the high-fructose syrup production using reactive SMB technology. *Chemical Engineering Journal*, 2006, (118): 167-181.
- [17] Zhang, Y., Hidajat, K., and Ray, A.K.. Modified reactive SMB for production of high concentrated fructose syrup by isomerization of glucose to fructose. *Biochemical Engineering Journal*, 2007, (35): 341-351.
- [18] Li, Y., Yu, W.F., Ding, Z.Y., Xu, J., Tong, Y., and Ray, A.K.. Equilibrium and kinetic differences of XOS2-XOS7 in xylo-oligosaccharides and their effects on the design of simulated moving bed purification process. *Separation and Purification Technology*, 2019, (215): 360-367.
- [19] Jiang, X.X., Zhu, L., Yu, B., Su, Q., Xu, J., Yu, W.F.. Analyses of simulated moving bed with internal temperature gradients for binary separation of ketoprofen enantiomers using multi-objective optimization: Linear equilibria. *Journal of Chromatography A*, 2018, (1531): 131-142.
- [20] Storti, G., Mazzotti, M., Morbidelli, M., and Carra, S.. Robust design of binary countercurrent adsorption separation processes. *AIChE Journal*, 1993, (3): 471-492.

- [21] Mazzotti, M., Storti, G., Morbidelli, M.. Optimal operation of simulated moving bed units for nonlinear chromatographic separations. *Journal of Chromatography A*, 1997, (769): 3-24.
- [22] Kaspereit, M., Seidel-Morgenstern, A., and Kienle, A.. Design of simulated moving bed processes under reduced purity requirements. *Journal of Chromatography A*, 2007, (1162): 2-13.
- [23] Li, Y., Xu, J., Yu, W.F., Ray, A.K.. Multi-objective optimization of sequential simulated moving bed for the purification of xylo-oligosaccharides using averaged parameters. Submitted, unpublished manuscript, 2019.
- [24] Yu, W.F., Hariprasad, J.S., Zhang, Z.Y., Hidajat, K., and Ray, A.K.. Application of multi-objective optimization in the design of SMB in chemical process industry. *J. Chin. Inst. Chem. Engrs.*, 2004, (1): 1-8.
- [25] Zhang, Z.Y., Hidajat, K., Ray, A.K.. Multi-objective optimization of simulated countercurrent moving bed chromatographic reactor (SCMCR) for MTBE synthesis. *Ind. Eng. Chem. Res.*, 2002, (41): 3213-3232.
- [26] Ahmad, T., and Guiochon, G.. Numerical determination of the adsorption isotherms of tryptophan at different temperatures and mobile phase compositions. *Journal of Chromatography A*, 2007, (2): 148-163.
- [27] Yu, W.F., Hidajat, K., and Ray, A.K.. Determination of adsorption and kinetic parameters for methyl acetate esterification and hydrolysis reaction catalyzed by Amberlyst 15. *Applied Catalysis A*, 2004, (260): 191-205.

- [28] Zhang, Y., Hidajat, K., and Ray, A.K.. Enantio-separation of racemic pindolol on  $\alpha_1$ -acid glycoprotein chiral stationary phase by SMB and Varicol. Chemical engineering science, 2007, (62): 1364-1375.
- [29] Kundu, P.K., Zhang, Y., and Ray, A.K.. Modeling and simulation of simulated countercurrent moving bed chromatographic reactor for oxidative coupling of methane. Chemical engineering science, 2009, (64): 5143-5152.
- [30] Chen, Y.T., and Yu, W.F.. Study of the separation process of fructose syrup by sequential simulated moving bed. Wenzhou: Wenzhou University, 2017.
- [31] Lode, F., Francesconi, G., Mazzotti, M., and Morbidelli, M.. Synthesis of methylacetate in a simulated moving-bed reactor: experiments and modeling. AIChE Journal, 2003, (6): 1516-1524.
- [32] Agrawal, N., Rangaiah, G.P., Ray, A.K., Gupta, S.K.. Design stage optimization of an industrial low-density polyethylene tubular reactor for multiple objectives using NSGA-II and its jumping gene adaptations. Chemical Engineering Science, 2007, (62): 2346-2365.
- [33] Nandasana, A.D., Ray, A.K., and Gupta, S.K.. Applications of the non-dominated sorting genetic algorithm (NSGA) in chemical reaction engineering. International Journal of Chemical Reactor Engineering, 2003, (1):1-16.
- [34] Kasat, R.B., Kunzru, D., Saraf, D.N., and Gupta, S.K.. Multiobjective optimization of industrial FCC units using elitist nondominated sorting genetic algorithm. Ind. Eng. Chem. Res., 2002, (41): 4765-4776.

[35] Lee, F.C., Rangaiah, G.P., and Ray, A.K.. Multi-objective optimization of an industrial penicillin V bioreactor train using non-dominated sorting genetic algorithm. *Biotechnology and Bioengineering*, 2007, (3): 586-598.

[36] Tarafder, A., Lee, B.C.S., Ray, A.K., and Rangaiah, G.P.. Multi-objective optimization of an industrial ethylene reactor using a non-dominated sorting genetic algorithm. *Ind. Eng. Chem. Res.*, 2005, (44): 124-141.

## Chapter 6

### 6. Conclusions and recommendations

A systematic study of the experimental design, simulation, and optimization for SSMB process based on xylo-oligosaccharides (XOS) was presented in this thesis. Meanwhile, in order to obtain a good understanding for the advantages and disadvantages of SSMB unit, the optimization works contain different objectives were conducted for both SMB and SSMB processes based on fructose-glucose system. In the first section, the suitable stationary phase for XOS separation was screened, and the kinetics and adsorption isotherm parameters were determined on a preparative chromatographic column. After that, the SSMB operating conditions were selected and the experiments were carried out on a lab-scale SSMB set-up. Simultaneously, the corresponding SSMB simulation works were conducted in order to verify the parameters and models. Finally, the multi-objective optimization of XOS separation by using SSMB process was completed, and diverse groups of optimal operating conditions were successfully obtained. In the second section, the target system was changed to fructose-glucose mixture, and the multi-objective optimization works by using both SMB and SSMB methods were completed and compared.

#### 6.1 Major conclusions based on XOS system

The ion exchange resin is an attractive method to purify the oligosacchrides in industry. Different types of ion form resins were investigated in this study, and the optimum one DOWEX MONOSPHERE™ 99/310 K<sup>+</sup>, was chosen for further researching. Frontal analysis technique was applied to determine the adsorption isotherms of XOS, xylose, and ARS in a XOS syrup system. The result shows that all these components follow a linear adsorption behavior. Transport-dispersive (TD) model is utilized to describe the component mass balance in the preparative column. In order to obtain the TD model parameters, the mass transfer and diffusion coefficients, several groups of pulse experiments with different flow rates were carried out. In addition, the kinetics and adsorption isotherms of XOS2-XOS7 were measured by using pulse experiments and a

simple fitting method. Adsorption equilibrium isotherms of many saccharides on polystyrene resins crosslinked with divinylbenzene were measured, but none of them included XOS and the individual XOS2, XOS3, XOS4, XOS5, XOS6, and XOS7. As the standard of XOS7 is currently not commercially available, a reasonable approach to predict the specific parameters of XOS7 was of great significance.

SMB simulations and experiments shows that the acquired parameters are authentic and can be used in the further design of preparative SMB processes. For the oligosaccharide systems, such as fructo-oligosaccharide, galacto-oligosaccharide, and xylo-oligosaccharide, always contain 5-7 different kinds of saccharides with variable molecular weight. Most researchers focused on oligosaccharides separation only studied the whole system's characteristics, in other words, only investigated the average parameters of the complicated compound and then used these parameters to conduct the SMB simulation and optimization [12, 17, 21, 22]. However, in this paper, the SMB simulation comparison between two groups provided a significant idea and a simple but reliable experimental method for the future oligosaccharides research works.

Multi-objective optimization of SSMB process for separation and purification of XOS was completed by using NSGA-II in this work. Simultaneously improving the unit throughput and the purity of XOS was firstly conducted. Results indicate that the optimal unit throughput decreases with increased purity requirement, forming a pareto curve in the (UT-Pur) plane. In SSMB, the trends of decision variables in term of  $m$  values exhibits some features qualitatively different from those of a conventional SMB, which cannot be directly explained by the Triangle Theory. These features were interpreted by the analyses of internal concentration profiles and mass flows at the raffinate port. As a conclusion, in the case of SSMB with transient variations during a switch, averaged  $m_{II}$  and  $m_{III}$  values are determined by the combination of more than 1 dimensional operating parameters. Direct use of Triangle Theory with averaged  $m$  values may lead to wrong design and diagnosis of such processes. Based on the industrial application, water consumption is the main concern in the other two optimization cases. The second case aimed at increasing the unit throughput and decreasing water consumption amount were carried out at different purity requirements. The purpose of case 3 is improving the

recovery of XOS and reducing the water consumption for a given unit throughput value. Water consumption increases with increased purity or recovery requirement. The trends of corresponding  $m$  values also cannot be directly explained in these two cases. Dimensional operating parameters must be used to give the explanations based on individual functional role of the sub-steps. All these conclusions are of great significance for industrial production in the future and provide effective guidance for SSMB simulation and optimization works not only for oligosaccharides separation but also for some extended areas.

## 6.2 Major conclusions based on fructose-glucose system

Based on the fructose-glucose system, the SSMB separation process was compared with the regular 4-column SMB process under individually optimized conditions. A total of 5 multi-objective optimization problems with various objectives and constraints were successfully conducted in this thesis.

Corresponding to the objectives of unit throughput and glucose purity, SMB performs better than SSMB. However, when the water consumption ratio, a major concern in industrial glucose/fructose separation, is considered as one optimization objective, SSMB seems superior to SMB. In order to explain these optimization results, dimensionless flowrate ratios, mass flow plots, and internal concentration profiles were introduced and analyzed in this work.

## 6.3 Recommendations for future work

Firstly, based on the XOS system, the optimization works in this thesis only focused on the binary separation process. As the XOS is very complicated and contains XOS2-XOS7, and the kinetics and adsorption isotherms of these individual components were already successfully measured in our previous work, the multi-objective optimization corresponding to XOS2-XOS7 should be properly designed and finished in the future, which will provide us several more accurate optimal operating conditions for SSMB unit.



In addition, XOS separation by using the conventional SMB process can be conducted in the future and the results also can be used to compared to those of SSMB, which would provide a better understanding for both separation techniques.

As the SSMB unit exhibits some obvious advantages over the SMB in this work, and there is no application of SSMB reported by researchers in the literature, more industrial applications about SSMB process should be explored and studied in the future.

## Appendices

### Appendix A: Supplementary information of Chapter 3

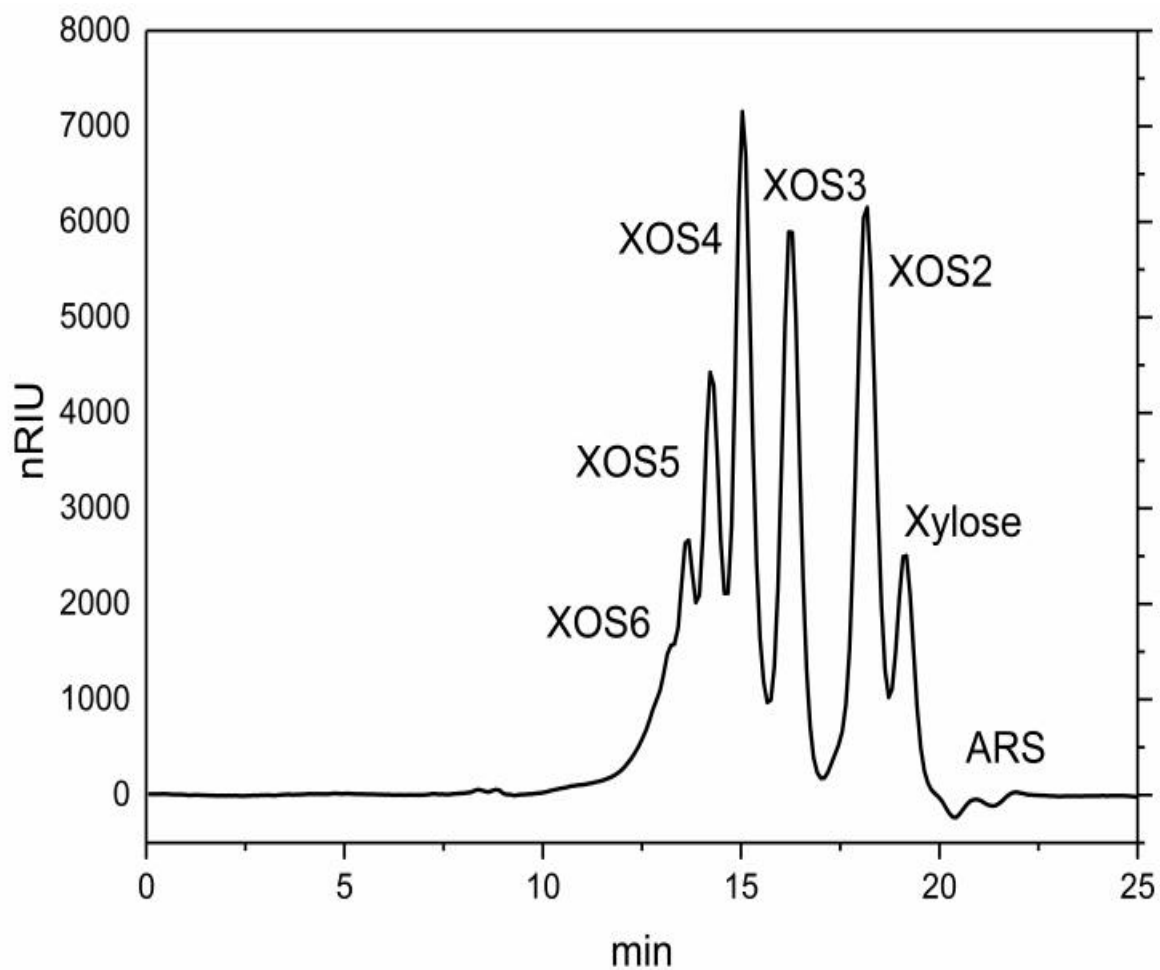


**Figure S3-1 Elution profile for sample analysis.**

The figure above is the HPLC elution curve of one typical sample collected during the Frontal Analysis experiments.

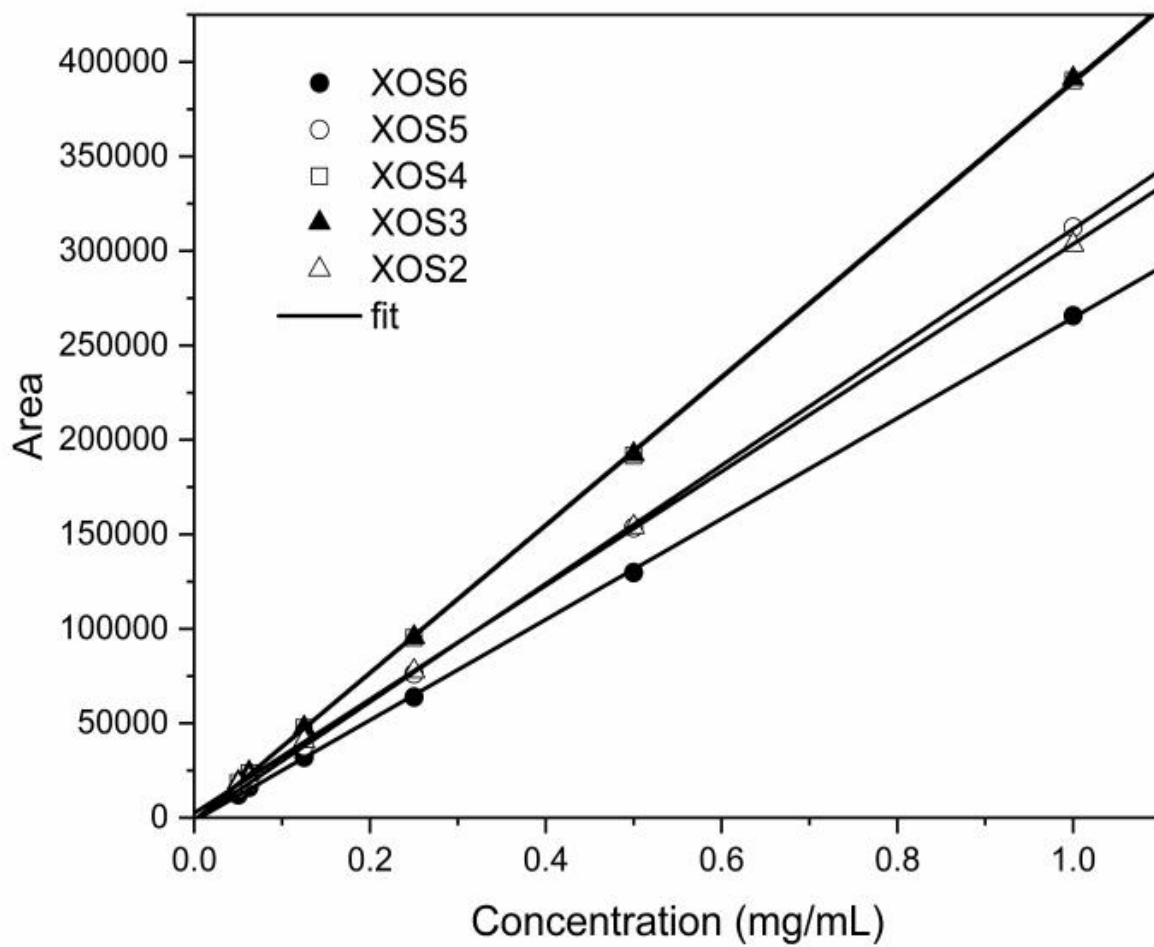
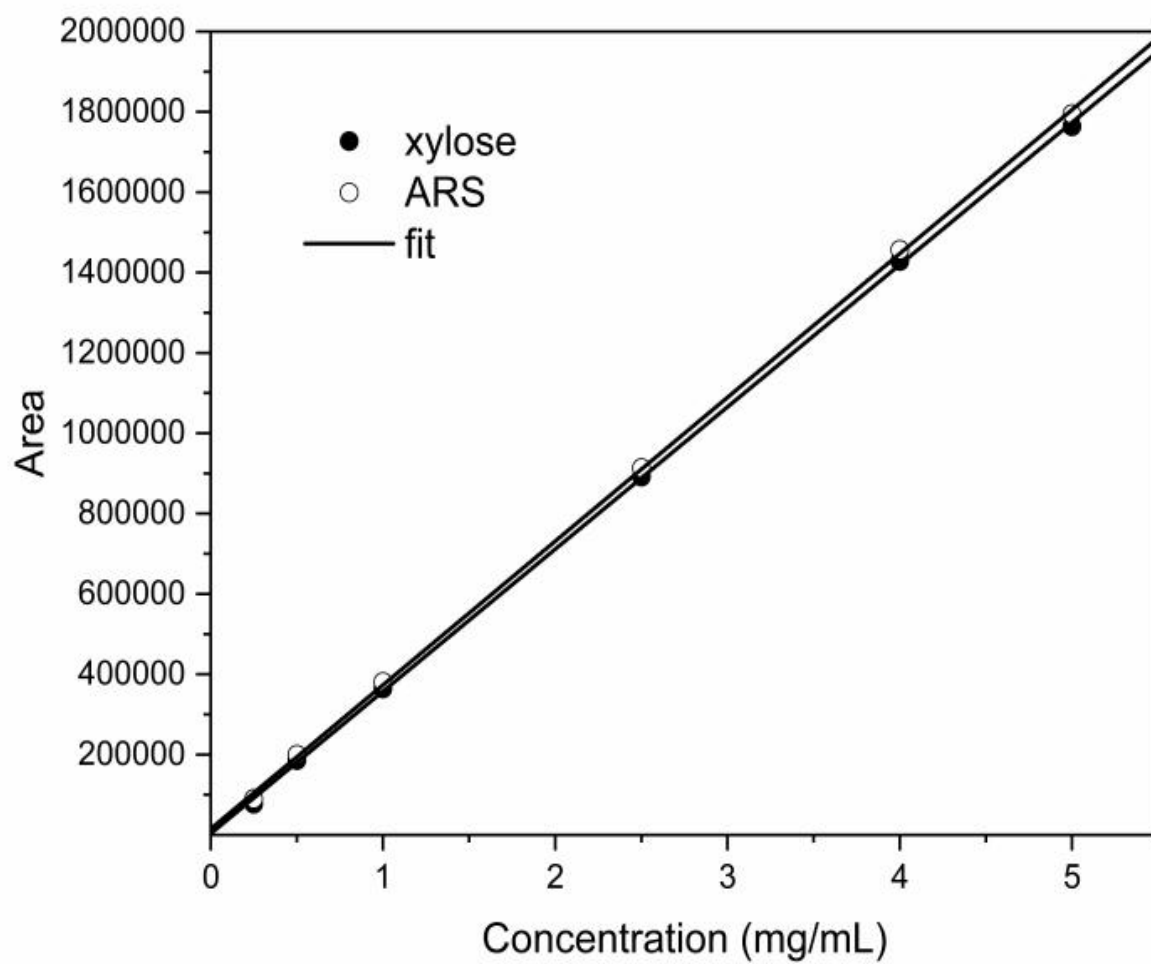
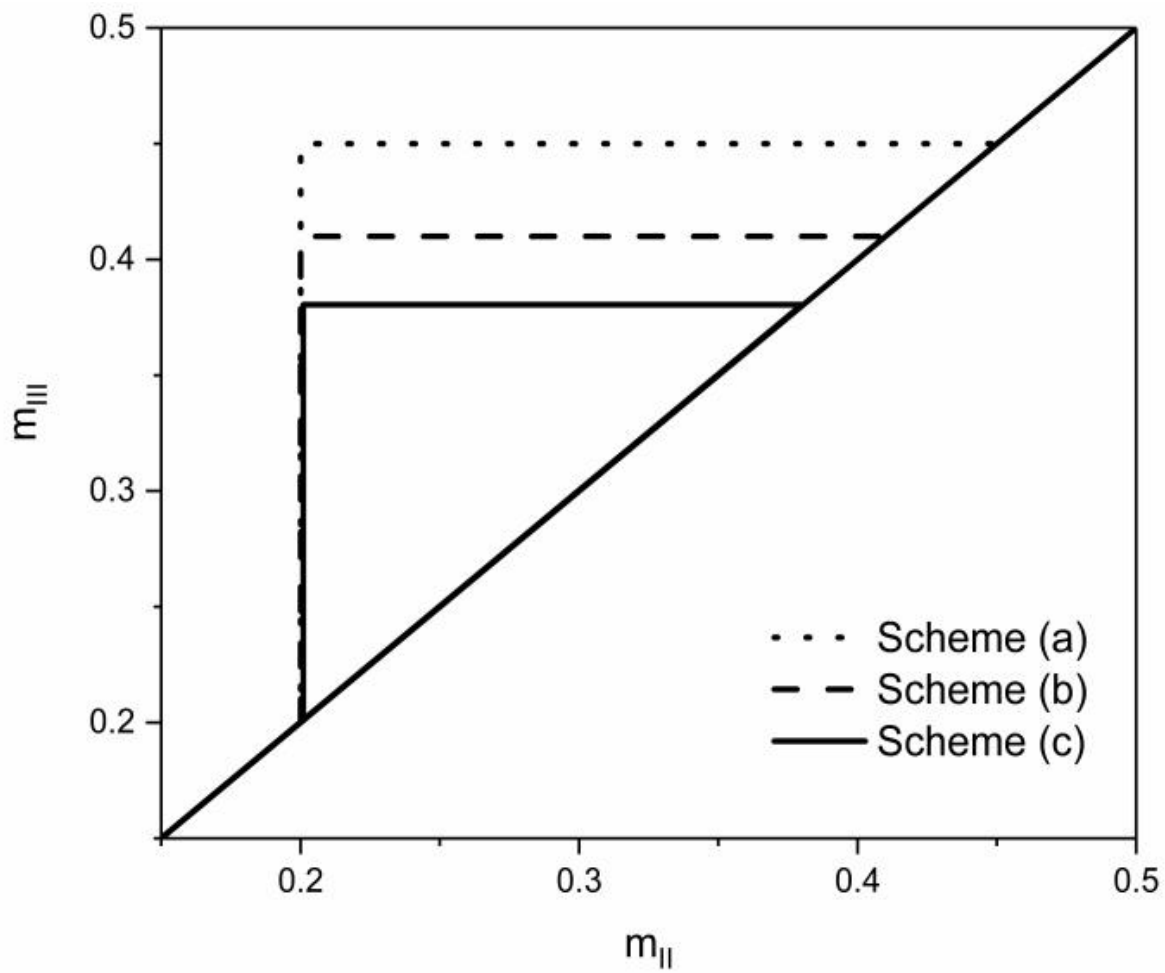


Figure S3-2 Calibration curves of XOS2-XOS6



**Figure S3-3 Calibration curves of xylose and ARS**



**Figure S3-4 SSMB simulation results of three different schemes with the recovery of 80%**

## Appendix B: Supplementary information of Chapter 4

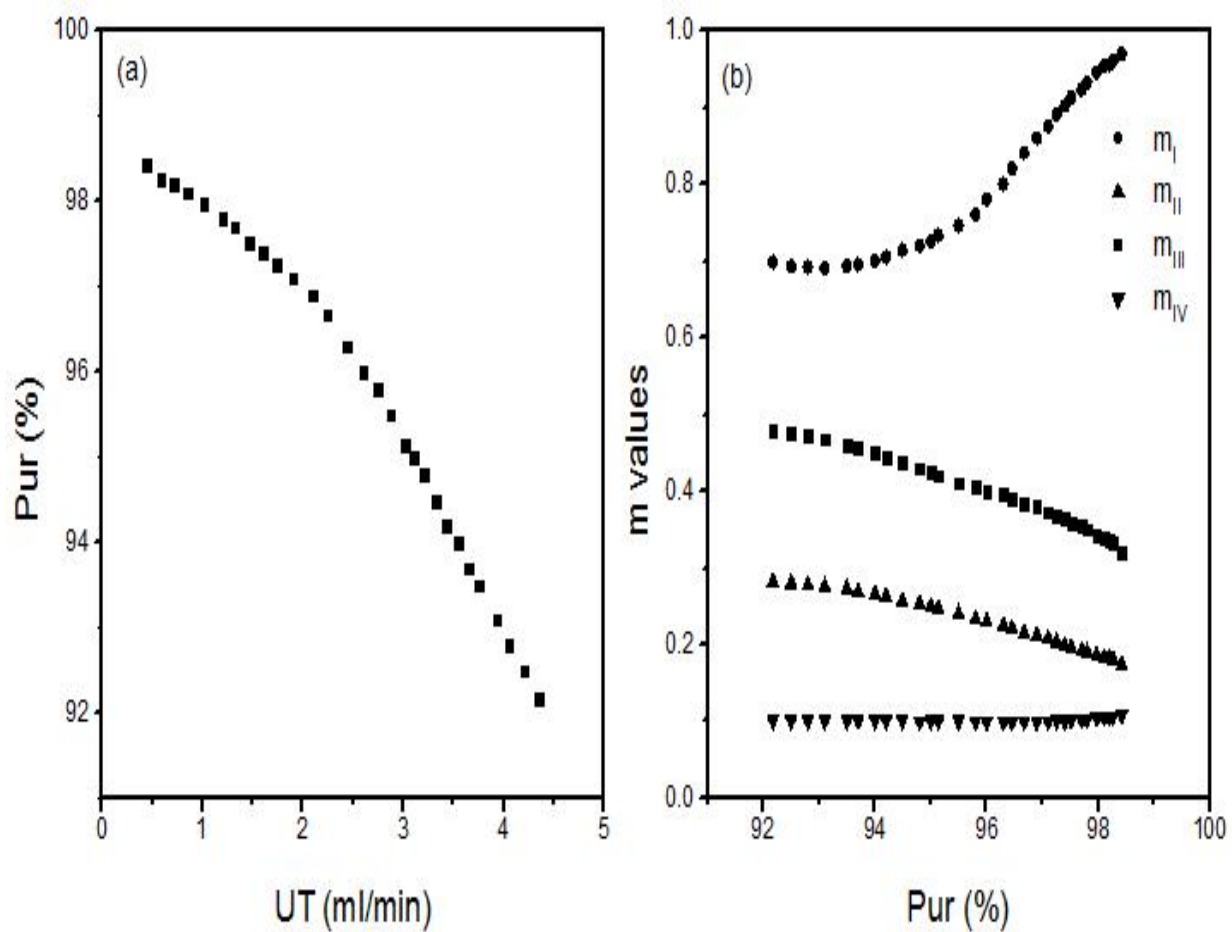


**Figure S4-1 Simultaneous maximization of unit throughput and purity for a conventional SMB. a: pareto; b: corresponding optimized  $m$  values.**

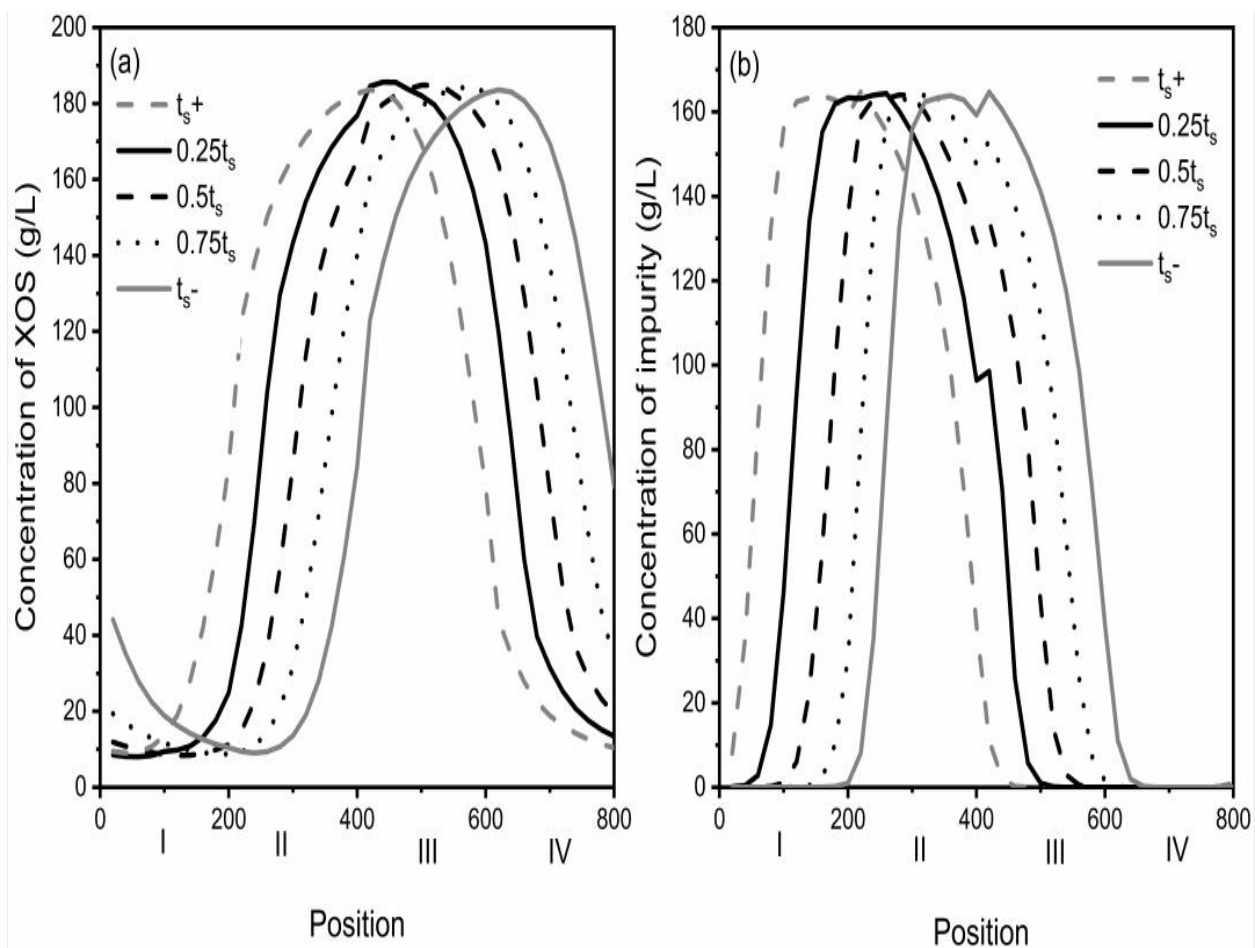


**Figure S4-2 Internal concentration profiles of a conventional SMB at optimized condition for purity of 97.76%. a: XOS; b: impurity.  $m_I=0.60$ ,  $m_{II}=0.20$ ,  $m_{III}=0.39$ ,  $m_{IV}=0.19$ .**

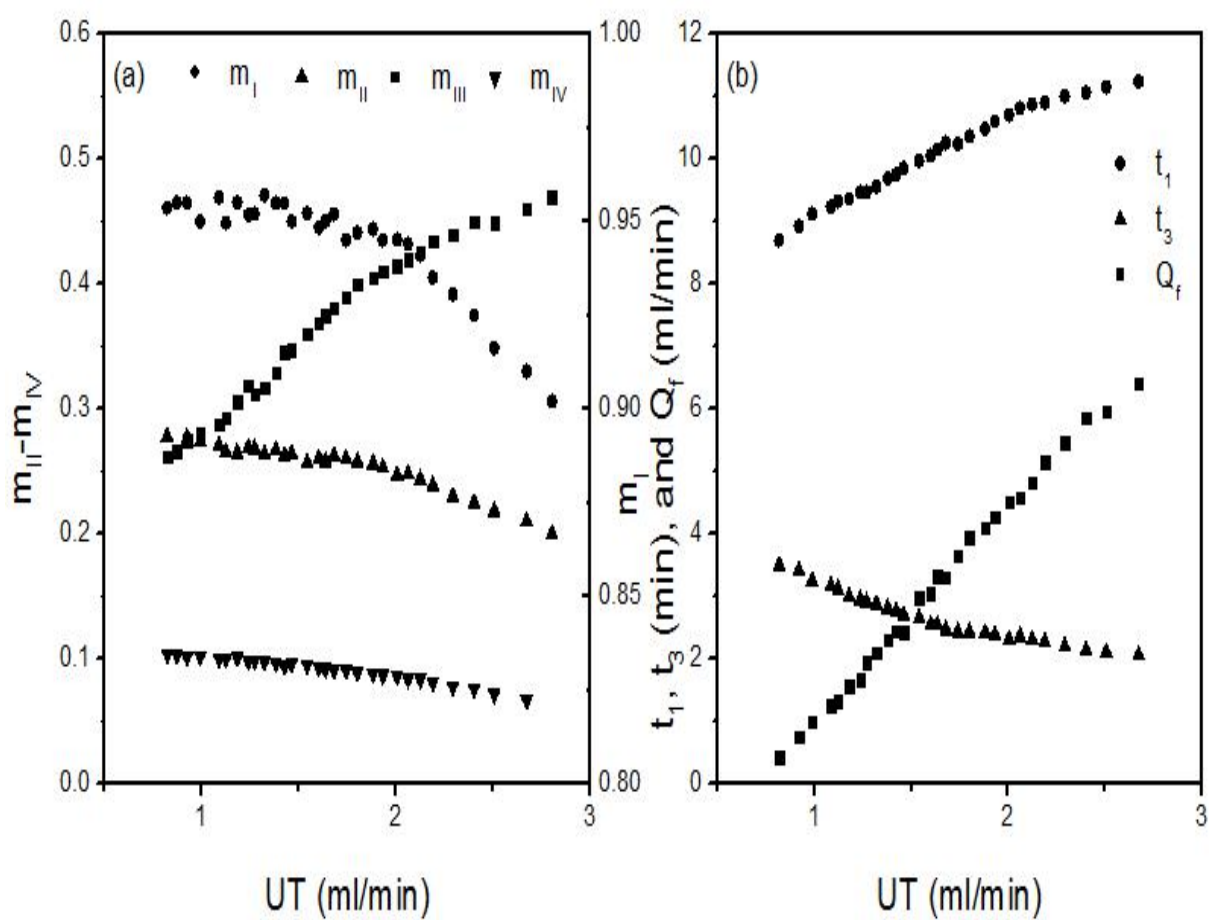


**Figure S4-3 Simultaneous maximization of unit throughput and minimization of solvent consumption at purity of 95%. a: corresponding optimized  $m$  values; b: derived  $t_1$ ,  $t_3$ , and  $Q_f$ .**



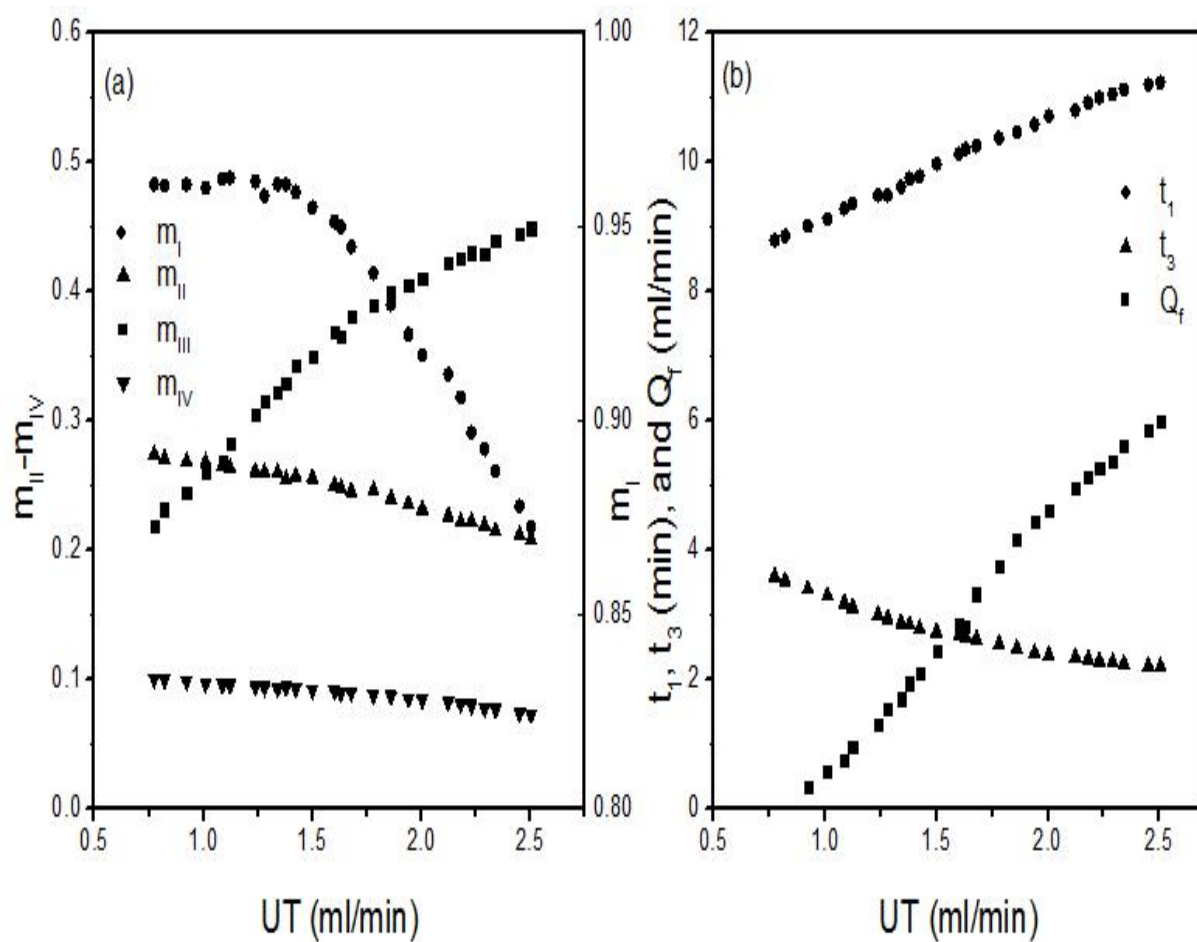


**Figure S4-4 Simultaneous maximization of unit throughput and minimization of solvent consumption at purity of 97%. a: corresponding optimized  $m$  values; b: derived  $t_1$ ,  $t_3$ , and  $Q_f$ .**

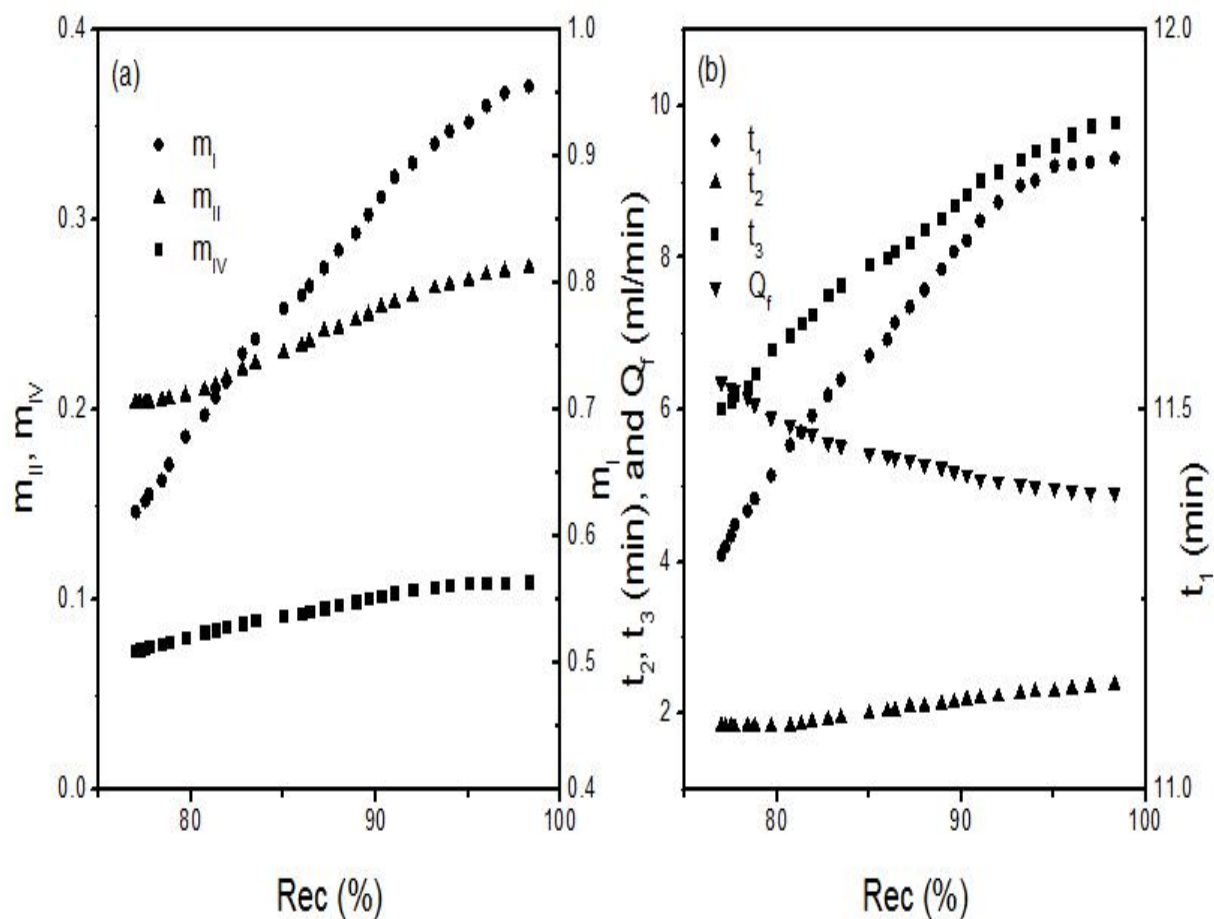


**Figure S4-5 Simultaneous maximization of XOS recovery and minimization of solvent consumption at UT=2 ml/min. a: corresponding optimized  $m$  values; b: derive  $t_1$ ,  $t_2$ ,  $t_3$ , and  $Q_f$ .**

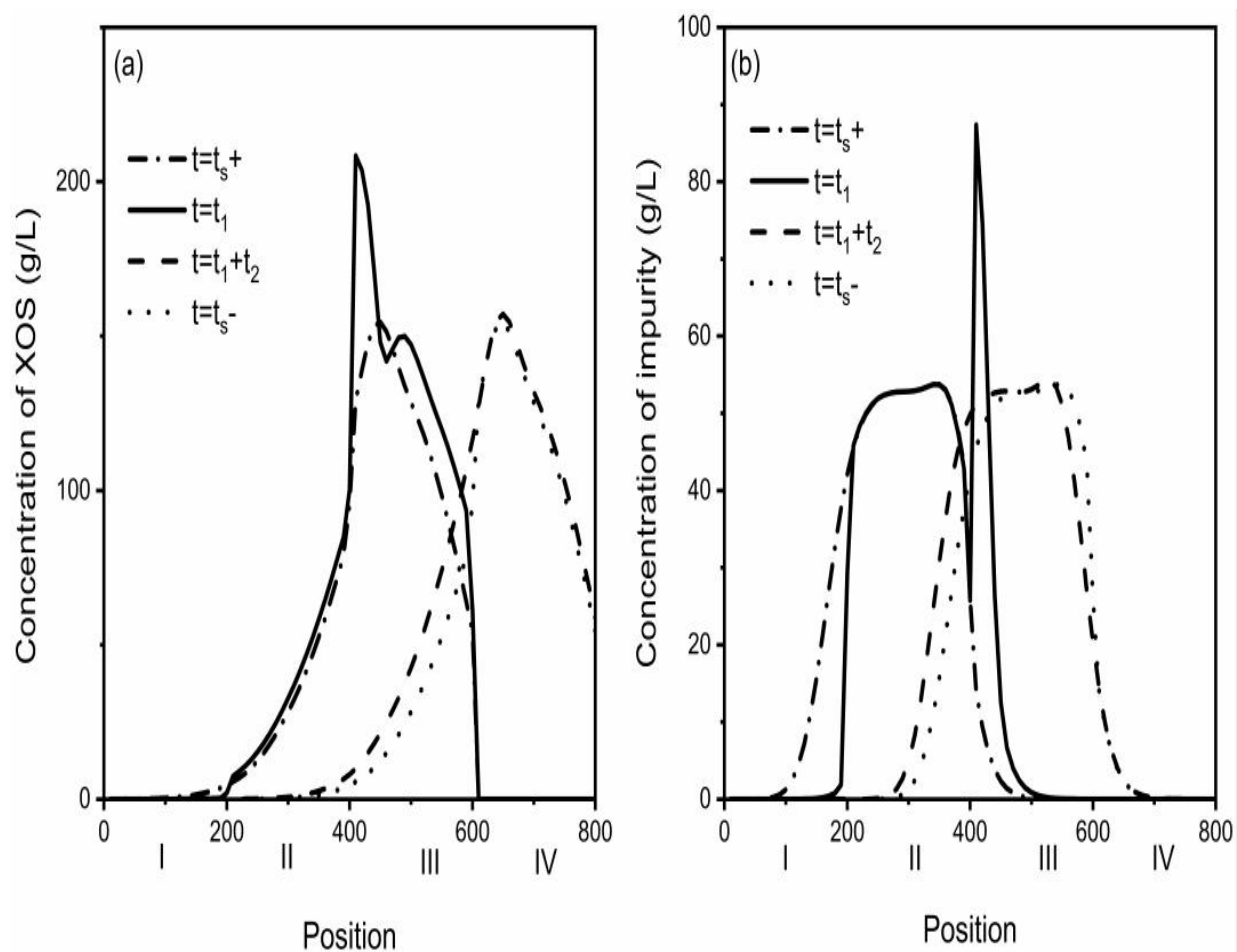


**Figure S4-6 Internal concentration profiles for  $UT=2$  ml/min. a: XOS; b: impurity.**

**Corresponding  $m$  values:  $m_I=0.88$ ,  $m_{II}=0.26$ ,  $m_{IV}=0.10$ .**

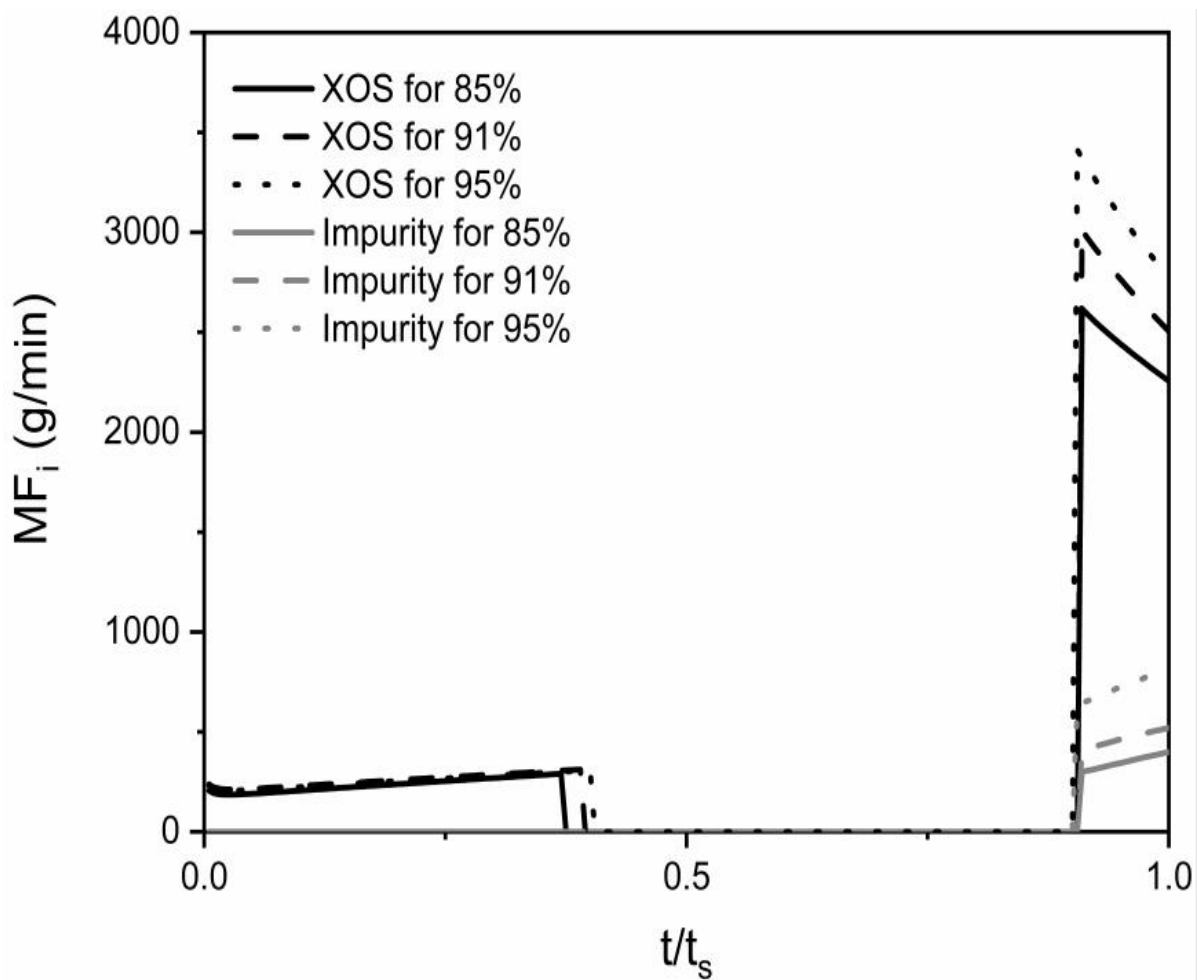


**Figure S4-7 MF plot for three representative recoveries for UT=2 ml/min. Black for XOS, gray for impurity; solid, dash and dot curves are for recoveries of 85% ( $m_I=0.78$ ,  $m_{II}=0.23$ ,  $m_{IV}=0.091$ ), 91% ( $m_I=0.88$ ,  $m_{II}=0.26$ ,  $m_{IV}=0.10$ ) and 95% ( $m_I=0.93$ ,  $m_{II}=0.27$ ,  $m_{IV}=0.11$ ), respectively.**

## Appendix C: Supplementary information of Chapter 5

**Table S5-1 Simulation results of SSMB process with the flowrate ratios  $m_I=0.856$ ,  $m_{II}=0.358$ ,  $m_{III}=0.541$ ,  $m_{IV}=0.193$  and varied  $\alpha$**

SSMB #	$t_1$	$t_2$	$t_3$	$t_s$	$Q_f$	UT	$Pur_{glu}$
	min	min	min	min	ml/min	ml/min	%
$\alpha=1$	11.54	2.68	8.09	22.31	7.35	2.66	89.17
$\alpha=0.9$	11.54	2.68	8.99	23.21	6.62	2.56	90
$\alpha=0.8$	11.54	2.68	10.11	24.33	5.88	2.44	88.9
$\alpha=0.7$	11.54	2.68	11.56	25.78	5.14	2.3	89.1
$\alpha=0.6$	11.54	2.68	13.48	27.7	4.41	2.14	88.5
$\alpha=0.5$	11.54	2.68	16.18	30.4	3.67	1.95	90.23
$\alpha=0.4$	11.54	2.68	20.22	34.44	2.94	1.73	90.4
$\alpha=0.3$	11.54	2.68	26.97	41.19	2.2	1.44	89.01

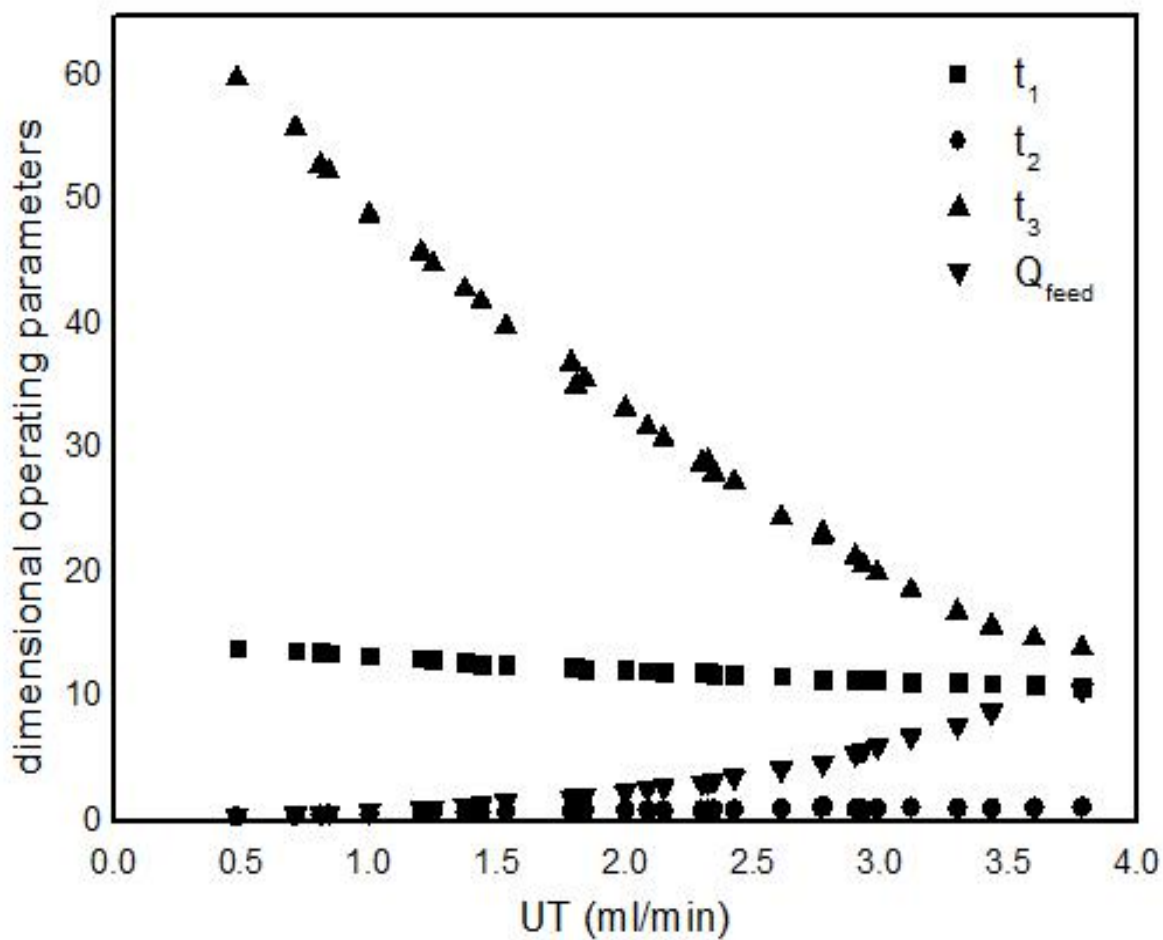


Figure S5-1 Dimensional operating parameters corresponding to optimal SSMB solutions of Case 1

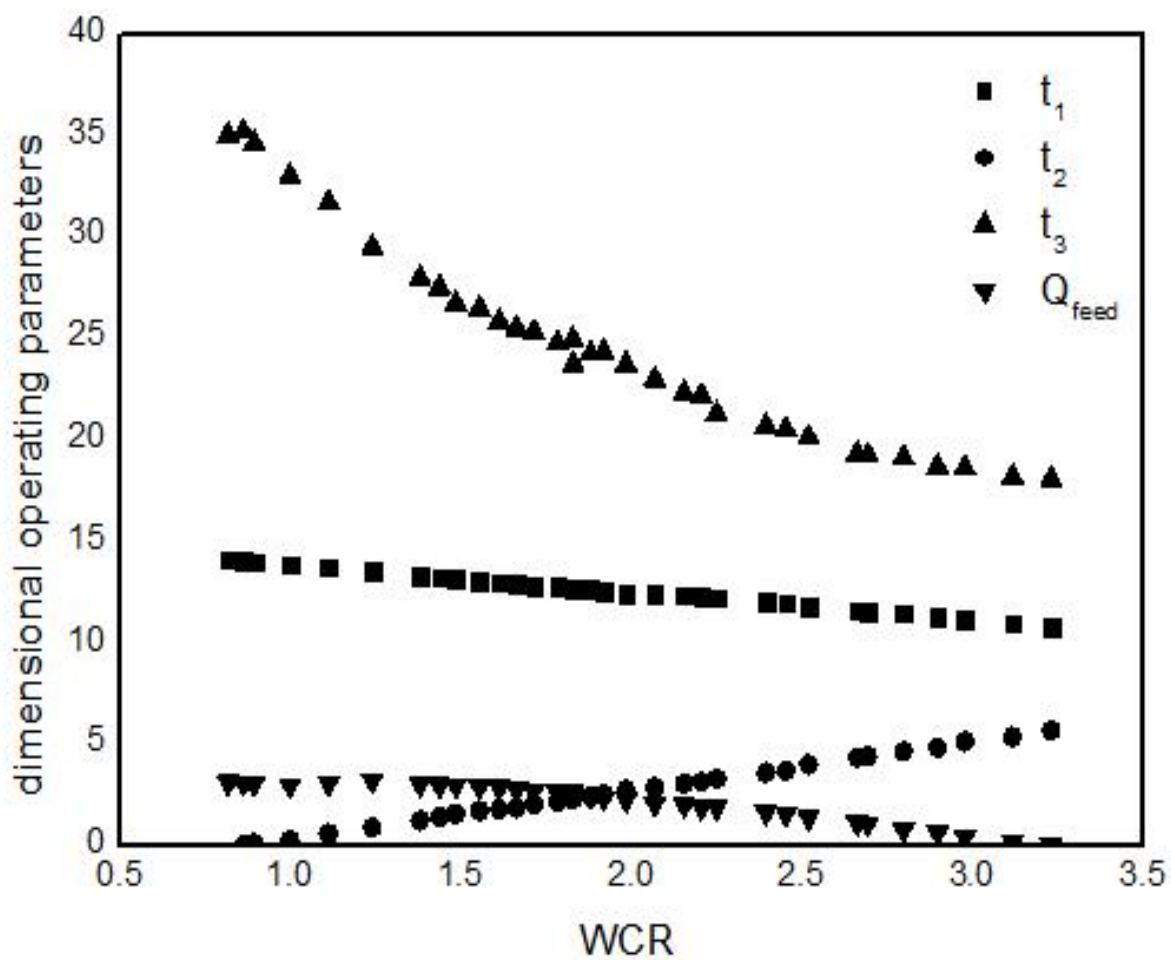


Figure S5-2 Dimensional operating parameters corresponding to optimal SSMB solutions of Case 2

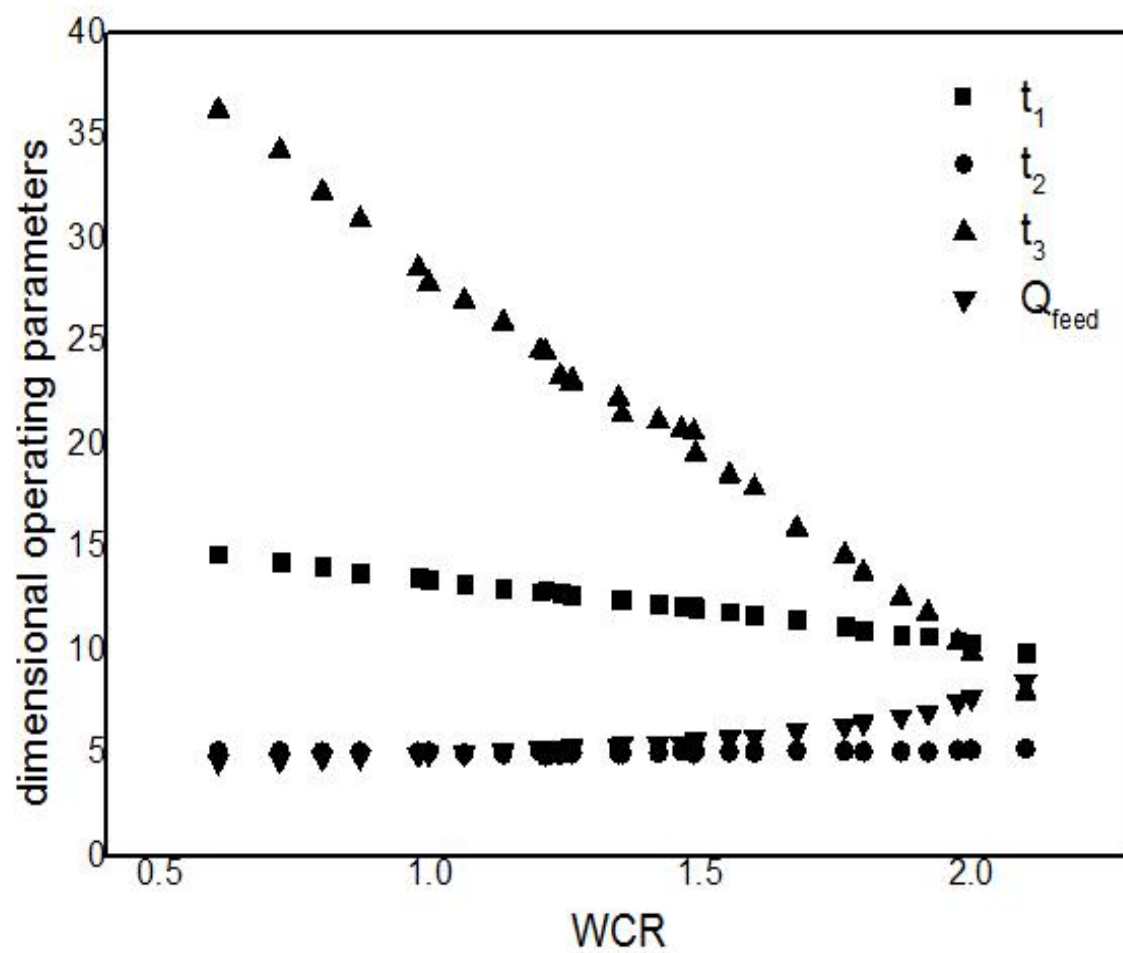
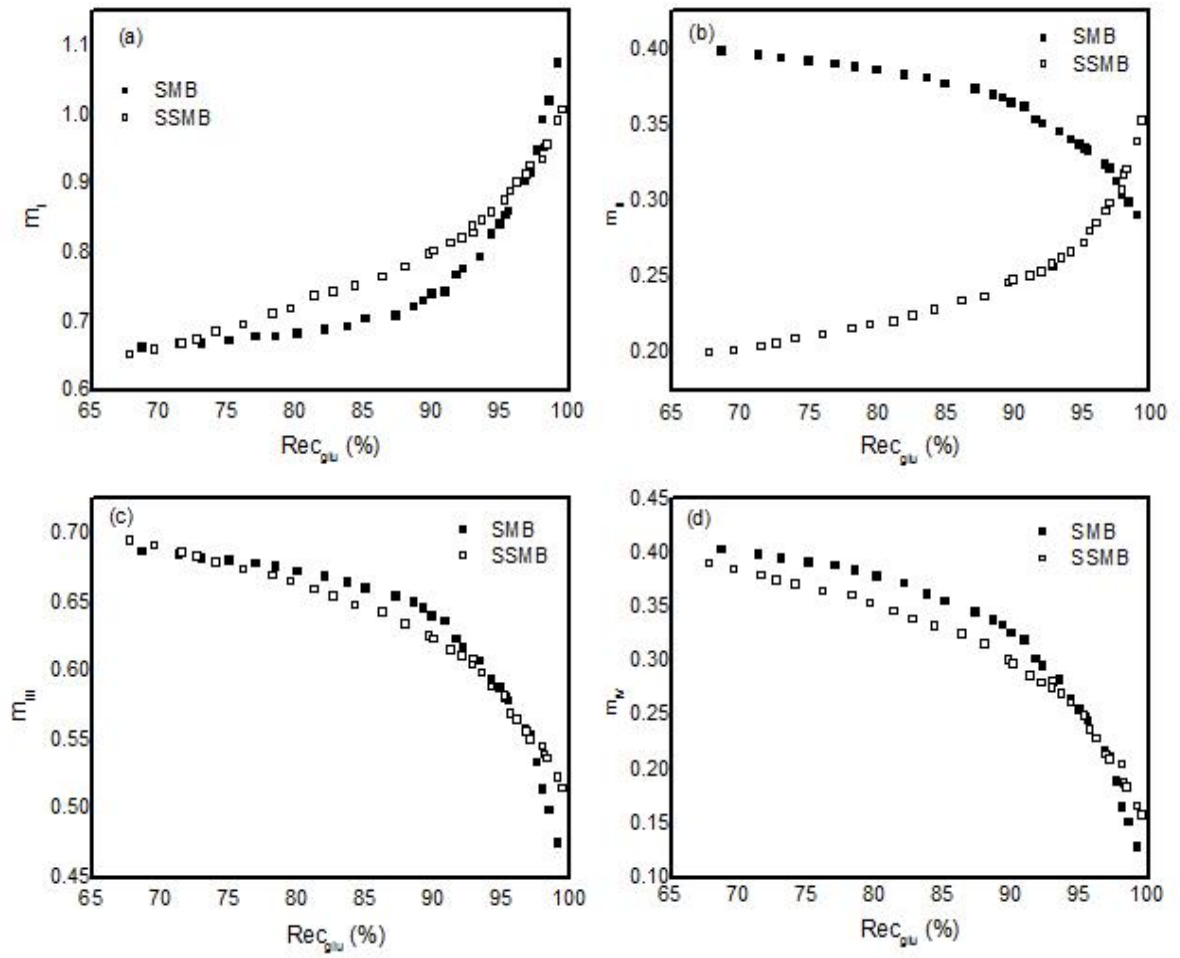
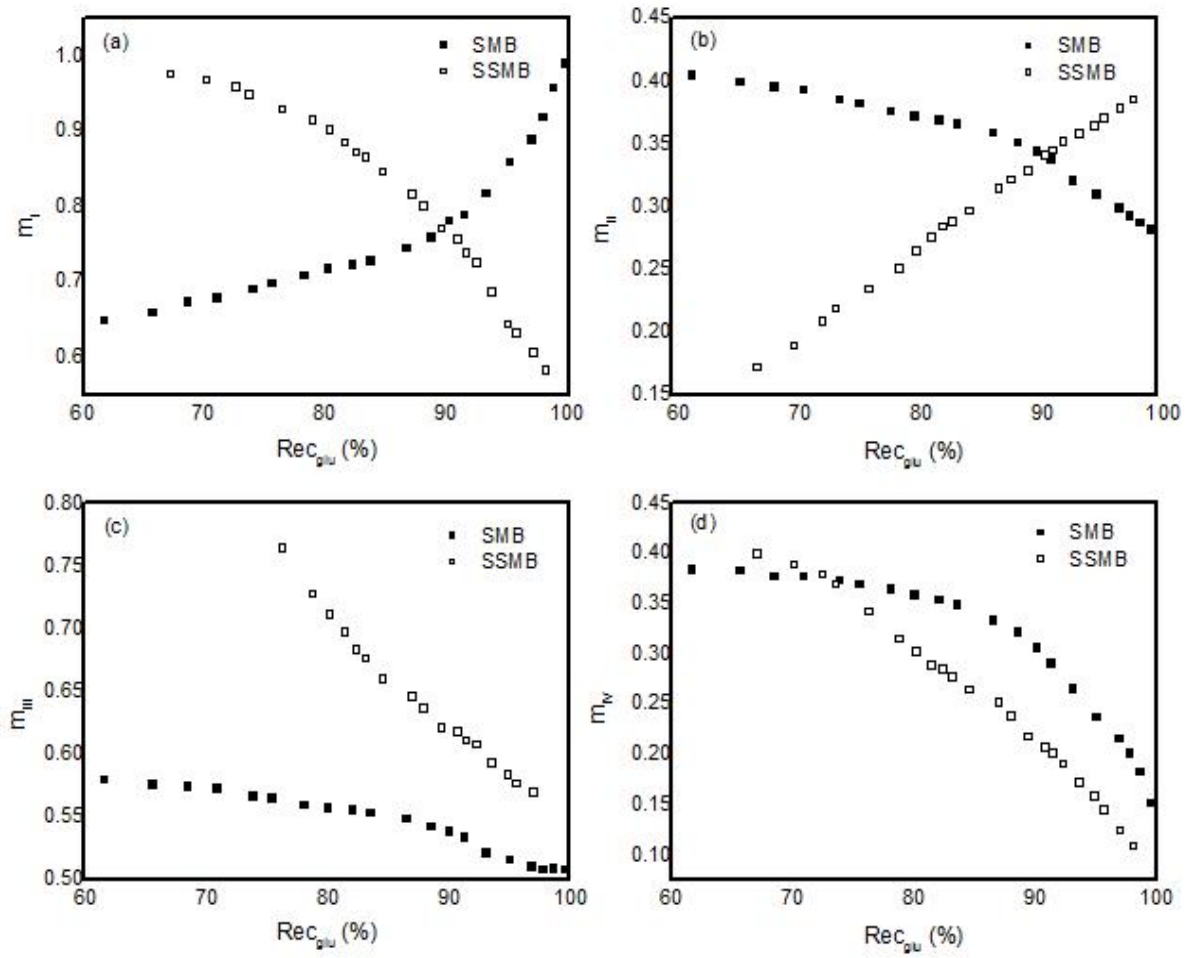


Figure S5-3 Dimensional operating parameters corresponding to optimal SSMB solutions of Case 3





**Figure S5-4 Optimal  $m$  values of SMB and SSMB for Case 4. a:  $m_I$ ; b:  $m_{II}$ ; c:  $m_{III}$ ; d:  $m_{IV}$**



**Figure S5-5 Optimal  $m$  values of SMB and SSMB for Case 5. a:  $m_I$ ; b:  $m_{II}$ ; c:  $m_{III}$ ; d:  $m_{IV}$**

# Curriculum Vitae

**Yan Li**

## **EDUCATION**

---

**Western University**; PhD, Chemical Engineering, **GPA: 91.5%**      *May 2015—Present*  
**Memorial University**; MS, Process Engineering, **GPA: A**      *Sep 2012—Sep 2014*  
**Tianjin University**; BS, Chemical Engineering, **GPA: 3.08/4.0**      *Sep 2008—Jul 2012*

## **RESEARCH PROJECTS**

---

*A comprehensive study for the sequential simulated moving bed (SSMB) and the simulated moving bed (SMB) techniques (PhD Research topic)      Sep 2015—Present*

- Xylo oligosaccharides (XOS) are claimed to have prebiotic effect; moreover, they are non-cariogenic and low caloric what makes them a versatile functional food additive
- SMB is a technique widely used to separate complicated systems; SSMB is developed due to its reduced solvent consumption and no literature reported it before
- The purity of XOS in the final product was increased to 90%
- Simulation and optimization works of the whole SSMB process were conducted and can be applied in industrial production
- Multi-objective optimization of SMB and SSMB processes was conducted based on the conventional fructose-glucose system; the advantages and disadvantages for both methods were summarized

*Adsorption isotherm and kinetic parameters determination of XOS system and the corresponding lab-scale SSMB experiments (cooperation with COFCO in China)*

*May 2016—Sep2017*

- XOS is a complicated system which contains XOS2-XOS7

- The adsorption isotherms of XOS, xylose, and arabinose were determined by using frontal analysis method; the kinetics were measured by using pulse experiments on the preparative chromatographic column
- Several groups of SSMB experiments in order to purify the XOS and validate the parameters were carried out

***Studying the dynamic influence of impurity on the crystallization process (MS***

***Research topic)***

***Dec 2013—Sep2014***

- L-Phenylalanine was chosen as the system, L-tyrosine was regarded as the impurity
- The influence of the impurity on solubility was considered first
- Discussed the impurity influence on kinetics: primary nucleation and growth, respectively

***Physicochemical and Structural Characterization of a kind of chiral drug: Tryptophan***

***(MS Research topic)***

***Jan 2013—Dec 2013***

- Built the binary melting point diagram by DSC analysis
- HPLC method was applied to measure the solubility in order to draw the ternary phase diagram
- Using powder XRD to confirm the result by comparing profiles of various mass fractions of L-tryptophan
- Added single crystal analysis to finalize the verification of the characterization

***Performance of liquid-liquid system in microchannel (BS Thesis) Dec 2011—Jun 2012***

- Butyl alcohol-succinic acid-water was chosen as the research system, and a microchannel device was designed
- The efficiency of mass transfer was compared under different conditions (different size of the microchannel, different size of drops, different flow rate).
- A microscope and camera system was used to observe the size of drops in microchannel

***Industrial production of Methanol with an annual output of 400,000 tons by distillation (IChemE Design)***

***Jul 2011—Dec 2011***

- The task was to design and simulate the whole industrial process in order to meet the requirement of product purity
- Three rectification columns were applied to refine the methanol
- Auto CAD and Aspen were used to draw the flow chart and simulate the operating process, respectively
- Some detailed designs were completed involving every column, pipeline and control element

***Extraction of silicon from oil (Internship)***

***Jul 2010—Aug 2010***

- Worked as a research assistant for several graduate students for this project in the National Engineering Research Center for Distillation Technology, Tianjin University.

## **EXPERTISE & SKILLS**

---

- Experimental skills: **SMB, HPLC, DSC, Powder x-ray analysis, UV, single crystal analysis**
- Software: **Aspen, Auto CAD, Design Expert, Matlab, Mercury, Fortran**
- Statistical packages: **Lindo, Excel, Origin**

## **TEACHING EXPERIENCE**

---

**Graduate teaching assistant**

*Western university, Department of Chemical and Biochemical Engineering (CBE)*

**Responsibilities**

- Instruction, lecturing or supervision in classes, tutorials, or laboratories
- Assist professor with curriculum development, course content, grading essays, assignments, lab reports, tutorials, quizzes, and exams, and proctoring of exams
- Facilitate workshops for undergraduate students
- Prepare materials or set-up required displays or apparatus for classes, tutorials, or laboratories

- Aid students in the resolution of multifaceted engineering problems and help in the construction of their engineering models and prototypes
- Assist undergraduate students to learn techniques in instrument handling to conduct various laboratory experiments
- Release grades and post announcements in the University Online Learning Management system

#### **Courses facilitated:**

- Chemical Engineering Thermodynamics: CBE 2224B *Jan 2019—Apr 2019*
- Reaction Engineering: CBE 3315 *Sep 2018—Dec 2018*
- Chemical Engineering Thermodynamics: CBE 2224B *Jan 2018—Apr 2018*
- Reaction Engineering: CBE 3315 *Sep 2017—Dec 2017*
- Mathematical Methods in Engineering: CBE 9170 *Sep 2016—Dec 2016*
- Process Dynamics and Control: CBE 3310 *Jan 2016—Apr 2016*
- Reaction Engineering: CBE 3315 *Sep 2015—Dec 2015*

### **VOLUNTEERING & AWARDS**

Obtained a full scholarship during PhD degree	<i>2015-2019</i>
Obtained a full scholarship during master degree	<i>2012-2014</i>
Member of the “Culture to Community” volunteer program	<i>2012-2014</i>
Building Tour guide at the Fluvarium, St. John’s, NL	<i>2013-2014</i>
Excellent Minister of the Psychological Association of Tianjin University	<i>2009-2010</i>

### **PUBLICATIONS**

Journal paper “Physicochemical and Structural Characterization of a Kind of Chiral Drug: Tryptophan” was published on Chirality. *2014*

Journal paper “Equilibrium and kinetic differences of XOS2-XOS7 in xylo-oligosaccharides and their effects on the design of simulated moving bed purification process” was published on Separation and Purification Technology. *2019*

Journal paper “Multi-objective optimization of sequential simulated moving bed for the purification of xylo-oligosaccharides using averaged parameters” was submitted to Chemical Engineering Science. *2019*

Journal paper “A comparison between SMB and SSMB for fructose-glucose separation based on multi-objective optimization” was submitted to Chemical Engineering Science.

2019

## **CERTIFICATIONS**

---

Western university certificate: WHIMIS

Western university certificate: The teaching assistant training program

Western university certificate: Language of research presentations

Western university certificate: Public speaking-giving effective presentations in grad school

## **Foreign Language Abilities**

---

Seven years study experience in Canada.